The background of the slide features a top-down view of laboratory glassware. On the left is a red pipette tip rack. In the center is a graduated cylinder containing a clear liquid, with volume markings from 100 to 900. To its right is a beaker, also containing clear liquid. In the foreground, a white pipette with a blue tip is visible. The text is overlaid on a semi-transparent grey rectangle in the lower half of the image.

Can we **ENERGISE** our metabolic health?

A deeper look into players of lipid metabolism and the regulation of fasting and cold-induced browning

Merel Defour

Propositions

1. Despite upregulation of PPAR α in white adipose tissue during cold exposure, PPAR α is not required for the browning process.
(this thesis)
2. The distinct transcriptional response of mice and humans upon fasting emphasizes the need for translational research.
(this thesis)
3. Caution should be exercised when using pharmacological compounds as tools to understand physiological processes.
4. Convincingly showing absence of an effect is more cumbersome than demonstrating the hypothesized outcomes.
5. Dutch and Belgians are very close in distance, but their communication styles could not be more apart.
6. The skill of perseverance acquired during a PhD track does not only prepare you for a career in science, it also helps you to put your baby to sleep.

Propositions belonging to the thesis, entitled

Can we ENERGISE our metabolic health?

A deeper look into players of lipid metabolism and the regulation of fasting and cold-induced browning

Merel Defour

Wageningen, October 8th, 2021

Can we ENERGISE our metabolic health?

A deeper look into players of lipid metabolism and the regulation of fasting and cold-induced browning

Merel Defour

Thesis committee

Promotor

Prof. Dr Sander Kersten
Professor of Nutrition, Metabolism and Genomics
Wageningen University & Research

Other members

Prof. Dr Renger F. Witkamp, Wageningen University and Research
Dr Eric Kalkhoven, University Medical Center Utrecht
Dr Joris Hoeks, Maastricht University
Prof. Dr Ko Willems van Dijk, Leiden University Medical Center

This thesis was conducted under the auspices of the Graduate School VLAG (Advanced studies in Food Technology, Agrobiotechnology, Nutrition and Health Sciences).

Can we ENERGISE our metabolic health?

A deeper look into players of lipid metabolism and the regulation of fasting and cold-induced browning

Merel Defour

Thesis

submitted in fulfilment of the requirements for the degree of doctor

at Wageningen University

by the authority of the Rector Magnificus,

Prof. Dr A.P.J Mol,

in the presence of the

Thesis Committee appointed by the Academic Board

to be defended in public

on Friday 8 October 2021

at 11.00 a.m in the Aula

Merel Defour

Can we ENERGISE our metabolic health?

a deeper look into players of lipid metabolism and the regulation of fasting and cold-induced browning

PhD thesis, Wageningen University, Wageningen, The Netherlands (2021)

With references, with summary in English

ISBN: 978-94-6395-857-8

DOI: 10.18174/548645

I think mice are rather nice
Their tails are long, their faces small
They haven't any chins at all.
Their ears are pink, their teeth are white
They run about the house at night.
They nibble things they shouldn't touch
And, no-one seems to like them much
But I think mice are nice.

Rose Fyleman

Table of contents

CHAPTER 1	General Introduction	9
CHAPTER 2	Hepatic ADTRP overexpression does not influence lipid and glucose metabolism	31
CHAPTER 3	Probing the role of the PPAR α regulated gene TMED5	55
CHAPTER 4	The Peroxisome Proliferator-Activated Receptor α is dispensable for cold-induced adipose tissue browning in mice	77
CHAPTER 5	Transcriptomic signature of fasting in human adipose tissue	111
CHAPTER 6	Probing metabolic memory in the hepatic response to fasting	173
CHAPTER 7	General Discussion	235
	Summary	255
	Acknowledgements/Dankwoord	259
	About the author	
	Curriculum vitae	266
	List of publications	267
	Overview of completed training activities	268

CHAPTER 1



General Introduction

Energy metabolism

Energy metabolism describes all processes of the human body needed to cope with the fluctuations in energy supply and demand. The human body's ability to store, make available, or convert nutrients at the desired time ensures that we can deal with periods of starvation, sickness, or other causes of elevated energy demand [1]. In present times, there is, however, a huge incidence of metabolic diseases, often caused by a misalignment in energy metabolism. While our bodies are very well equipped to cope with periods of low food supply, the current situation of overfeeding results in the well-known diseases of affluence such as obesity, diabetes mellitus type 2, and the metabolic syndrome.

Energy metabolism is maintained and regulated by different organs in our body. It is dependent on communication and collaboration between organs such as the liver, pancreas, muscle, brain, gut, and adipose tissue. For example, in the postprandial state when nutrients are taken up from the *gut*, the *pancreas* releases insulin. Upon this increase in insulin, the *muscle* will take up glucose from the circulation to use it as an energy substrate. Excess glucose will subsequently be converted into glycogen to store for later use, or the *liver* will convert the glucose into fatty acids which can then be esterified with glycerol to form triglycerides (TG) [2]. Since there is little need for the production of glucose after a meal, insulin also suppresses glycogenolysis and gluconeogenesis in the liver [3,4]. Excess TGs in the liver can be secreted into the circulation in the form of very low-density lipoproteins (VLDL) and be transported throughout the body. In this way, fat can be distributed to serve as an energy source for the peripheral tissues such as the *muscle*, or can be stored in the *adipose tissue*.

In order to make this multiorgan system function smoothly, a tight regulation of metabolic processes is necessary. Enzymes and other proteins play a crucial role in the regulation of these metabolic processes. Indeed, most of the regulation of metabolic pathways is mediated by the regulation of enzymatic activity.

The activity of enzymes is regulated at different levels. The first and most obvious functional regulation is via the location of the enzyme, which generally is organ and cell-type specific. As a result, specific metabolic processes only occur in certain organs. In addition, compartmentalization of enzymes inside the cell ensures that the metabolic enzymes serve their purpose in the appropriate location in the cell. Apart from being specific to a certain tissue or cell type, the activity of enzymes is also highly responsive to external stimuli. Different physiological states usually require the activity of different enzymes. For example, upon fasting there is need for rapid regulation of certain enzymes, mostly to keep the blood glucose levels within a normal range and to switch to the use of fat as the primary energy sources.

Modulation of enzymatic function can occur in two dimensions: qualitatively and quantitatively. Qualitative changes in enzymes occur rather fast, within seconds or minutes, and can be achieved by altering binding to an enzyme of an allosteric regulator or via covalent binding of a molecule such as phosphate. When regulating an enzyme allosterically, the allosteric regulator binds to a specific region of the enzyme but not to the active site and hence does not interfere with binding of the substrate. The allosteric binding results in a conformational change that can either augment or suppress the activity of the enzyme. An example of this type of regulation in energy metabolism is the allosteric inhibition of phosphofructokinase, the key enzyme of glycolysis, by high levels of ATP [5,6]. Apart from allosteric regulation, the activity of enzymes and other proteins can also be influenced by the covalent attachment of another molecule [7]. The most common covalent modification is the reversible process of (de)phosphorylation [7,8]. Phosphorylation reactions are catalyzed by a large group of different protein kinase enzymes, which themselves are subject to extensive regulation.

Alternatively, enzyme activity can be regulated by quantitative adjustments, which represents a slower but more robust regulation and which is achieved by altering the amount of active enzyme present. The most common mechanism to alter the amount of enzyme in a cell is via the stimulation or inhibition of the transcription of the gene encoding the enzyme. The transcription of genes is under direct control of transcription factors [9,10]. Specifically, transcription factors play an important role in the initiation and the regulation of transcription of DNA into mRNA. Upon their activation, transcription factors bind to specific sites on the DNA sequence: the response elements. Binding of the transcription factor to response elements on the DNA leads to the recruitment of RNA polymerase to the promoter site and subsequent induction of the transcription of the target gene [10]. Importantly, the activity of many transcription factors can be influenced by external stimuli such as certain hormones, nutrients, and metabolites, thereby linking metabolism to regulation of gene expression and vice versa [11].

Nuclear transcription factors – Peroxisome proliferator-activated receptors (PPARs)

A specific class of transcription factors are the nuclear receptors (NRs) [12,13]. These ligand-activated transcription factors are composed of a DNA-binding domain and a ligand binding domain [14,15]. NRs can be activated by different hormones and other lipophilic molecules, upon which they modulate gene expression [16,17]. Although many NRs and their subsequent target genes have been identified, many regulatory cascades still remain unknown. A subset of these NRs have been shown to play a pivotal role in the homeostasis of energy metabolism because of their capacity to sense dietary nutrients (like lipids) and their capacity of controlling the metabolism of these nutrients [11].

A particularly interesting group of NRs involved in metabolism are the peroxisome proliferator-activated receptors (PPARs). PPARs are nutrient-sensing nuclear receptors and can be activated by, amongst others, long chain fatty acids and eicosanoids [18–20]. Next to nutrients and other endogenous compounds, a list of exogenous compounds such as lipid-lowering fibrates, thiazolidinediones, and many pesticides are known ligands of the PPARs [21–23]. Upon their activation, PPARs translocate to the nucleus of the cells and function as heterodimers with another nuclear receptor: retinoid X receptor (RXR) [24]. This PPAR-RXR complex can then bind to PPAR response elements (PPRE) on the DNA and activate the transcription of a specific target gene [24,25]. To date, three PPAR isoforms have been identified: PPAR α , PPAR γ and PPAR δ (also known as PPAR β). These three isoforms of PPAR differ from each other by their tissue expression profile and have, because of their location, a distinct physiological role [26]. Many target genes of the different PPARs have been discovered in the last decades, but there is still no complete overview of all genes regulated by these transcription factors.

PPAR γ has three isoforms (γ 1, γ 2 and γ 3) and, depending on the isoform, is most common in white adipose tissue (WAT), colon, and macrophages [27–29]. Target genes of PPAR γ are often involved in adipogenesis, energy balance, and lipid biosynthesis. Furthermore, PPAR γ plays an important role in insulin sensitivity [30,31]. PPAR γ is in general important for lipid metabolism in the adipocytes by regulating genes participating in the release, transport, and storage of fatty acids such as lipoprotein lipase (*Lpl*) [32], acyl-CoA synthase (*Acs*) [33] and the fatty acid binding protein and transporter *Fabp4* and *Cd36* [34–36]. Mice lacking PPAR γ are not viable since they do not develop a functioning adipose tissue in utero, showing the importance of PPAR γ for adipogenesis [37].

PPAR δ s expression is reasonably high in many tissues and organs in the body and varies depending on health/disease state [27,28,38]. The absence of PPAR δ leads to embryonic lethality and impaired growth, implying a role for PPAR δ target genes in embryonic development [37]. Similar to the other PPARs, PPAR δ has been shown to play a role in the modulation of cellular energy consumption. PPAR δ is less well studied and less straight-forward compared to PPAR α and PPAR γ , yet also seems to be involved in lipid metabolism [39]. For example, in muscle, PPAR δ responsible for the switch from glycolysis to fatty acid oxidation [40].

PPAR α has been most extensively studied in the liver, but is also highly expressed in brown adipose tissue, kidney, skeletal muscle, and heart, which are all highly oxidizing tissues with high energy turnover [27,28]. Accordingly, many well-established targets of PPAR α are involved in many, if not all, aspects of lipid metabolism such as: 1) β -oxidation in the mitochondria e.g. *Cpt1 α* , *Cpt2*, *Pdk4* [41–44]; 2) fatty acid transport over the cell membrane e.g. *Cd36* and *Slc27a1* [36,45]; 3) intracellular fatty acid activation and binding e.g. several fatty acid binding proteins [46]; 4) fatty

acid elongation and desaturation e.g. *Fads2*, *Scd1* [47,48] and 5) ketogenesis e.g. *Hmgcs2* [42,49].

Absence of PPAR α

PPAR α is often described as the master regulator of lipid metabolism and is especially important during fasting. Fasting is a very important stressor on hepatic lipid metabolism, partly because it raises the concentrations of free fatty acids in the bloodstream. The liver is tasked with properly accommodating this high amount of FFA. One of the key metabolic events in the liver during fasting is the induction of fatty acid oxidation and ketogenesis. For both processes, PPAR α has been shown to be indispensable [50]. Whereas PPAR α ablation does not result in a strong phenotype when kept under normal feeding conditions, fasted PPAR $\alpha^{-/-}$ mice show marked lipid accumulation in the liver and heart, elevated plasma free fatty acids, and hypoketonemia, as a result of the impaired induction of FA oxidation (in both peroxisomes and mitochondria) and ketogenesis [43,49,51–53]. Moreover, fasted PPAR $\alpha^{-/-}$ mice are hypoglycemic and exhibit hypothermia. These findings demonstrate that PPAR α is activated during fasting and causes the upregulation of numerous enzymes leading to increased FA uptake and oxidation.

In addition to physiological stimuli such as fasting, PPAR α in liver may also be activated by pathological stimuli such as obesity and subsequent insulin resistance. In mice, this situation is modelled by chronic feeding of a high fat diet (HFD). Feeding a HFD leads to increased body weight and fat mass, reduced insulin sensitivity, and increased plasma FFA levels [54]. Interestingly, PPAR $\alpha^{-/-}$ mice show a smaller increase in body weight upon a HFD but have a higher liver weight, which is accompanied by marked elevation of hepatic triglyceride levels up to 15% of the total liver weight [54]. This result implies a role for PPAR α in coping with the high influx of FFA in the liver in mice fed a HFD.

Inasmuch as most of our knowledge about the importance of PPAR α is directly coupled to the function of its target genes, the identification of genes regulated by PPAR α may aid in further elucidating the role of PPAR α in vivo. A commonly used strategy to detect novel target genes for PPAR α , which we also partially apply in **chapter 2** and **chapter 3**, is via the use of PPAR $\alpha^{-/-}$ and WT mice. By comparing hepatic gene expression patterns of PPAR $\alpha^{-/-}$ and WT mice during various stimuli, new targets can be found among the genes specifically upregulated in the WT group. The most direct approach is by exposing both groups of mice to a potent PPAR α -agonist such as fenofibrate or Wy14643, following by examination of the differential gene expression between the WT and PPAR $\alpha^{-/-}$ mice. This strategy proved to be successful in the past, as it led to the revelation of *Angptl4* and more recently *Hilpda* as PPAR α targets [55][56].

Regulation of metabolism in the liver

The liver is the largest organ in our body and has a crucial role in lipid and glucose metabolism, both during excess and shortage of nutrients. It plays a pivotal role in processing and distribution of nutrients coming from the gut and the adipose tissue.

Physiology of the fed and fasted body

After a meal, the liver produces bile acids. Bile acids aid in the digestion and uptake of fat from the gut by emulsifying lipids and promoting the formation of micelles. Fatty acids are taken up by the enterocytes and re-esterified into TGs, which subsequently are packed in large lipoproteins called chylomicrons. The chylomicrons are released into the lymphatic system and reach the blood circulation at the level of the subclavian vein. By contrast, nutrients such as glucose and amino acids originating from the gut are directly transported to the liver via the portal vein. Glucose will be used as the primary energy source in the body and will be broken down to produce ATP via glycolysis. A moderate excess of glucose can be stored in the liver by converting it to glycogen via the glycogenesis. Since the storage of glycogen requires a lot of water (in proportion 1:3g) and since glucose is less energy dense than triglycerides, it is more favorable to store excess energy as fat [57]. Glucose can be converted to fatty acids in the liver via the fatty acid synthesis pathway. These fatty acids are subsequently esterified into triglycerides. The triglycerides can subsequently be stored inside the liver or secreted into the circulation packed in VLDL for transport throughout the body .

In between meals, the previously stored glycogen can be released into the bloodstream as glucose via glycogenolysis and thereby serve as fuel for peripheral organs [58]. Whereas other organs such as muscle and adipose tissue store glycogen for internal use, the liver is the only organ that can release glucose from its glycogen storage into the circulation. When the glucose generated by glycogen breakdown is not sufficient to maintain blood glucose levels—for example when the body remains in the fasted state for more than one day—the liver will synthesize glucose from other precursors such as amino acids via gluconeogenesis [58]. In this way, the body ensures the presence of glucose for the brain cells and erythrocytes, which cannot rely on lipids to produce energy.

During fasting, the concentration of glucose in the circulation become low. As a result, the levels of insulin drop and the pancreas starts to secrete glucagon [59,60]. During this shortage of nutrients, the body must react by activating the WAT to release of FFA and glycerol, prime tissues to favor the use of fat over glucose, and maintain sufficient glucose levels for glucose-dependent tissues such as the brain and erythrocytes. The drop in insulin levels result in a break on lipogenesis in the liver and the activation of the oxidation of fatty acids [61]. Simultaneously, the rise in glucagon results in the activation of glycogenolysis and ketogenesis [62,63].

During ketone body production, the liver converts adipose tissue-derived fatty acids into ketone bodies to serve as an alternative energy source for the brain.

Transcriptional regulation of fasting and feeding in the liver by nuclear receptors

The liver plays an important role in the feeding and fasting response. First, as stated above, long-chain FA entering the liver likely act as ligands for PPAR α . The increased influx of FA released by the adipose tissue is believed to lead to the activation of PPAR α during fasting, although the exact mechanism underlying the activation of hepatic PPAR α during fasting remains debated. As described before, PPAR α is crucial during fasting as it promotes gluconeogenesis, ketogenesis, and FA oxidation. By activating these processes, the body is capable of coping with a prolonged lack of nutrients.

Re-uptake of bile acids coming from the enterohepatic circulation in the fed state activates farnesoid X receptor (FXR) [64–66]. FXR regulates bile acid homeostasis and is shown to also influence other nutrient-related processes such as gluconeogenesis and lipogenesis [67–70]. FXR has been shown to be important for suppressing de novo bile acid synthesis and lipogenesis in the liver in the fed state. Upon activation of FXR, its target gene fibroblast growth factor (FGF) 15/19 is produced [71]. FGF15/19 suppresses bile acid synthesis and has a stimulatory effect on storage of nutrients such as glycogen and proteins by activating the Ras-extracellular signal-related kinase (ERK) pathway [72,73].

FXR suppresses the activation of the transcription factor liver X receptor (LXR) and LXR-induced sterol regulatory element-binding transcription factor 1c (SREBP-1c) via small heterodimer partner (SHP) activation [74–76]. SREBPs are transcription factors that play a crucial role in the regulation of (re)feeding in the liver by upregulating genes involved in cholesterol and FA biosynthetic processes. There are 3 types of SREBP: SREBP-1a, SREBP-1c (originating from the same *SREBPF-1* gene but distinct from each other due to different transcription start sites) and SREBP2 (originating from a separate gene *SREBPF-2*) [77]. SREBP-1a appears to be expressed at low levels and mainly in tissues with high cell proliferation capacity. In vivo, the predominant SREBP1 isoform is SREBP1c [78]. *Srebp-1c* expression is very high in liver and WAT, where it regulates genes involved in fatty acid and lipid production (eg. ATP citrate lyase [79,80] and fatty acid synthase [81,82]) and glucose metabolism (eg. Glucokinase [83]) [84]. The absence of *SREBP-1c* results in an impaired induction of FA synthesis upon refeeding, demonstrating the importance of *SREBP-1c* for the induction of lipogenic pathways [85]. *SREBP-1c* expression is regulated in three different ways: by the presence of insulin, by the presence of glucagon, and via LXR [75,76,86]. Insulin stimulates the liver to process excess carbohydrates by initiating fatty acid synthesis via induction of *SREBP-1c* expression [87,88]. By contrast, glucagon suppresses *SREBP-1c* expression and its lipogenic target genes

[87]. Consistent with this notion, *SREBP-1c* expression is strongly diminished during fasting and increases rapidly upon refeeding in an insulin-dependent manner [89]. Lastly, the nuclear receptor LXR, which is important for regulating efflux and clearance of cholesterol, can induce *SREBP-1c*, which is probably aimed at generating FA needed for the production of cholesterol esters [76]. Targets of SREBP-2 mainly play a role in cholesterol synthesis and include HMG-CoA synthase 1 and HMG-CoA reductase [90]. However, SREBP-2 is also capable of, at least partially, taking over the regulation of target genes of SREBP-1c when SREBP-1c is not present [85].

Not only lipid metabolism is regulated by transcription factors upon fasting. Transcription factors also regulate cholesterol, glucose and protein metabolism. As one example: hepatic gluconeogenesis is transcriptionally regulated by peroxisome proliferative activated receptor-gamma co-activator 1 (PGC-1 α) and forkhead transcription factor 1 (FoxO1) [91].

Regulation of metabolism in the adipose tissue

Adipose tissue has multiple function. It serves as an insulator, it protects the vital organs, and represents the primary storage place of energy. By taking up fatty acids from circulating TGs, the adipose tissue protects other organs from excessive fatty acids flux (fat overflow). Next to that the adipose tissue is classified as an endocrine organ via the secretion of enzymes, hormones and other proteins collectively named adipokines [92].

Adipose tissue is found all across the body. Generally, adipose tissue is distinguished into visceral adipose tissue, representing the fat around the internal organs (visceral), and subcutaneous fat, representing the fat just below the skin [93]. Visceral WAT (vWAT) is important to protect the organs as it surrounds the organs located in the peritoneum. Important depots of vWAT are classified as mesenteric, retroperitoneal, perigonadal and omental vWAT. The main subcutaneous WAT (sWAT) depot in mice is the inguinal WAT. In humans, the sWAT is primarily located around the hips, thighs and buttocks [93].

White adipocytes consist of one big lipid droplet filling almost the entire cell. The main function of WAT is to store and release energy at the appropriate times. The amount of fat stored and released depends on an equilibrium between fatty acid uptake, triglyceride synthesis, triglyceride hydrolysis (lipolysis), and fatty acid oxidation (mitochondrial β -oxidation). During mitochondrial β -oxidation, fatty acids are broken down into acetyl-CoA to generate ATP, which is mainly controlled by PPARs as described before. Lipolysis describes the hydrolysis of stored triglycerides into FA and glycerol and is carried out by different lipases inside the adipocyte, namely hormone-sensitive lipase (HSL), adipose triglyceride lipase (ATGL) and monoglyceride lipase (MGL)[94]. The process of adipose lipolysis and concomitantly

the concentrations of FFAs in the blood are regulated by hormones, with glucagon stimulating and insulin inhibiting fatty acid release from adipose tissue.

Molecular regulation of adaptation to fasting in adipose tissue

During fasting, several metabolic pathways are downregulated in the adipose tissue via hormonal changes. Some of the important pathways suppressed upon fasting are: 1) TG and FA synthesis, 2) energy generating pathways such as glycolysis, the TCA cycle and oxidative phosphorylation, 3) mitochondrial translation and 4) glycogen synthesis. At the transcriptional level, these processes are regulated by different insulin-sensitive transcription factors. The absence of insulin results in downregulation of PPAR γ and SREBP-1c, which accounts for the inhibition of TG and FA synthesis [95,96]. PPAR γ is known to regulate fatty acid metabolism and triglycerides storage in adipose tissue. Upon fasting, the drop in PPAR γ expression results in a break on lipogenesis.

In contrast to the pathways mentioned above, lipolysis is activated by fasting, which is also largely driven by hormonal changes. Specifically, the absence of insulin and the presence of glucagon leads to the activation of Forkhead box protein O1 (*FoxO1*), causing the upregulation of genes involved in lipid catabolism such as interferon regulatory factor 4 (*Irf4*) [97]. IRF4 has a direct effect on the expression of the lipases HSL and ATGL [97]. All these processes are in line with the main tasks of the adipose tissue during fasting, which is to release fatty acids and thus provide energy for the other organs.

Molecular regulation of thermogenic adaptations of the adipose tissue

Next to adipocytes with one big lipid droplet, there are also adipocytes with multiple, smaller lipid droplets. These type of adipocytes form the multilocular adipose tissue or brown adipose tissue and have their nucleus located in the center of the cell surrounded by numerous mitochondria. Instead of storing energy, the brown adipose tissue uses the lipids present in the small lipid droplets to convert into heat. The brown adipose tissue depots differ substantially between rodents and humans. In rodents, BAT is found in the upper back (interscapular, subscapular), around the kidneys (perirenal) and around the heart (periaortic), whereas in humans BAT is located in the neck area (supraclavicular), around the vertebral column (paravertebral), in the center of the upper trunk (mediastinal), and in the perirenal area [93]. BAT has been shown to be very important for temperature homeostasis in small rodents and human babies, but its relevance in the adult human body is less clear. Traditionally, it was believed that human BAT was restricted to neonatal and early childhood to prevent hypothermia. Later on, active BAT was found in adults by the use of radiolabeled glucose tracers and PET/CT ([¹⁸F]-FDG-PET/CT)scans [98–100]. The discovery of the presence of BAT in humans was thought to lead to potential therapeutic solutions to the obesity epidemic. Unfortunately, increasing energy expenditure in obese individuals by activating BAT appears to be a rather

complicated strategy since obese individuals show reduced BAT volume and activity [101,102].

Brown adipocytes possess many mitochondria and have high expression of the uncoupling protein 1 (UCP1). Mitochondria are the energy-factories of eukaryotic cells. The energy is stored as a proton gradient over the inner mitochondrial membrane. In case of energy need in a cell, adenosine triphosphate (ATP) is produced by letting the protons flow across the membrane through the enzyme ATP synthase. UCP1 is located in the inner mitochondrial membrane and catalyzes the flow of electron across this membrane without it leading to the formation of ATP. Instead, energy is dissipated as heat. To maintain homeostasis, it is important to keep the core temperature around 37 ° C. The human body has several tactics to produce heat when body temperature drops, which all are accompanied by an increase in energy expenditure: shivering thermogenesis, non-shivering thermogenesis, diet-induced thermogenesis and activity-induced thermogenesis.

White adipocytes can become thermogenically active adipocytes as a result of pharmacological [103] or environmental stimuli such as cold and exercise [104]. These adipocytes are also referred to as beige or brite (brown in white) adipocytes [105]. Upon norepinephrine release by sympathetic neurons when the skin senses cold, β_3 -adrenergic receptors are activated [106]. The activation of these β_3 -adrenergic receptors stimulates cyclic adenosine monophosphate signaling, which in turn results in enhanced transcription of genes involved in conversion of white to beige adipocytes [107]. This process is referred to as browning. The group of adipocytes undergoing browning is very heterogeneously distributed throughout the fat tissue and is mainly present in the subcutaneous inguinal fat depot in mice [108,109]. In humans, the same heterogenous distribution is detected yet the vWAT, specifically supraclavicular, seems to be the depot prone to browning [110,111]. These difference make translation of the browning phenomenon from mice to human studies challenging.

Gene expression patterns of beige and brown adipocytes are very similar, explaining the brown-like phenotype of the beige cells. The main feature is the high expression of UCP1, which is needed to uncouple the proton gradient and which is absent in white adipocytes. Next to UCP1, PRD1-BF1-RIZ1 homologous domain containing 16 (*Prdm16*) expression is high in BAT and beige AT [109,112,113]. PRDM16 seems to be pivotal for the conversion of WAT to beige AT. Interestingly, browning has been shown to be reversible. Upon a drop of PRDM16 levels in the beige adipocytes, the brown-like phenotype disappears [109]. Other genes preferentially expressed in BAT/beige AT are *Elovl3* (a transmembrane glycoprotein), *Pgc-1 α* (important for mitochondrial biogenesis), and *Ppara* [114–116].

Despite these similarities, there are also differences between the 2 cell types. Importantly, they originate from distinct cellular lineages. Brown fat cells share a similar developmental program as myocytes, which both originate from myogenic factor 5 positive cells (MYF5⁺). During the development, PRDM16 seems to play a pivotal role since expression of *Prdm16* in the precursor cells favors brown fat cell differentiation while the absence of PRDM16 leads towards a muscle cell differentiation program [112,117]. White and beige adipocytes originate from MYF5⁻ precursor cells, although recent evidence shows that MYF5⁺ cells can also develop into white adipocyte precursor cells [118]. A transcriptional cascade involving PPAR γ , SREBP-1c and CCAAT/enhancer-binding protein family members results in mature white adipocyte, with high expression of amongst others leptin and adiponectin and virtually no expression of UCP1 [119]. Upon specific stimulation of the β 3-adrenergic receptors, the mature white adipocyte can switch its non-thermogenic gene expression profile towards a more thermogenic profile including induced expression of *Ucp1*, *Prdm16*, *Cd137* and *Tmem26*, the latter being unique for beige fat cells [111]. In addition, *Ppara* expression is induced in the adipocytes upon browning [120,121]. Ablation of PPAR resulted in an attenuation of browning after CL316,246 treatment, a β 3-adrenergic agonist [122,123]. In **chapter 4** we look deeper into the role of PPAR α during the transition from white to beige adipose tissue, but now specifically in the physiological cold-induced browning.

Outline of this thesis

The aim of this thesis is to gain more insight into the transcriptional regulation of lipid metabolism in liver and adipose tissue. **Chapter 2 and Chapter 3** describe the characterization of novel targets of PPAR α , which are *Tmed5* and *Adtrp*. Targets of PPAR α very often play an important role in lipid metabolism in the liver or adipose tissues. By identifying new targets of this transcription factor, we aim to further elucidate the complex regulation of lipid metabolism in the liver. **Chapter 4** clarifies the role of PPAR α during cold-induced browning in vivo. **Chapter 5** compares the effect of fasting in the white adipose tissue of humans and mice at the level of the transcriptome. An overview of the similarities and a deeper look into the differences between both species is given. In **chapter 6**, a possible memory effect of a fasting stimulus on the liver is investigated. Does the liver respond differently the second time this stimulus occurs? Finally, in **chapter 7**, all findings will be discussed and integrated to provide a general conclusion about this thesis.

References

- [1] Smith, R.L., Soeters, M.R., Rob, C.I.W., 2018. Metabolic Flexibility as an Adaptation to Energy Resources and Requirements in Health and Disease (September 2017): 489–517, Doi: 10.1210/er.2017-00211.
- [2] Roach, P.J., Depaoli-Roach, A.A., Hurley, T.D., Tagliabracci, V.S., 2012. Glycogen and its metabolism: some new developments and old themes. *The Biochemical Journal* 441(3): 763–87, Doi: 10.1042/BJ20111416.
- [3] O'Brien, R.M., Lucas, P.C., Forest, C.D., Magnuson, M.A., Granner, D.K., 1990. Identification of a sequence in the PEPCK gene that mediates a negative effect of insulin on transcription. *Science (New York, N.Y.)* 249(4968): 533–7, Doi: 10.1126/science.2166335.
- [4] Hatting, M., Tavares, C.D.J., Sharabi, K., Rines, A.K., Puigserver, P., 2018. Insulin regulation of gluconeogenesis. *Annals of the New York Academy of Sciences* 1411(1): 21–35, Doi: 10.1111/nyas.13435.
- [5] Aragón, J.J., Sols, A., 1991. Regulation of enzyme activity in the cell: effect of enzyme concentration. *FASEB Journal : Official Publication of the Federation of American Societies for Experimental Biology* 5(14): 2945–50, Doi: 10.1096/fasebj.5.14.1752361.
- [6] Boiteux, A., Hess, B., 1981. Design of glycolysis. *Philosophical Transactions of the Royal Society of London. Series B, Biological Sciences* 293(1063): 5–22, Doi: 10.1098/rstb.1981.0056.
- [7] Berg JM, Tymoczko JL, S.L., 2002. Covalent modification is a means of regulating enzyme activity. *Biochemistry 5th Edition*. <https://www.ncbi.nlm.nih.gov/books/NBK22399/>.
- [8] Charlier, T.D., Cornil, C.A., Patte-Mensah, C., Meyer, L., Mensah-Nyagan, A.G., Balthazart, J., 2015. Local modulation of steroid action: rapid control of enzymatic activity. *Frontiers in Neuroscience* 9: 83, Doi: 10.3389/fnins.2015.00083.
- [9] Lambert, S.A., Jolma, A., Campitelli, L.F., Das, P.K., Yin, Y., Albu, M., et al., 2018. The Human Transcription Factors. *Cell* 172(4): 650–65, Doi: 10.1016/j.cell.2018.01.029.
- [10] Jones, N., 1990. Structure and function of transcription factors. *Seminars in Cancer Biology* 1(1): 5–17.
- [11] Burris, T.P., Busby, S.A., Griffin, P.R., 2012. Targeting orphan nuclear receptors for treatment of metabolic diseases and autoimmunity. *Chemistry & Biology* 19(1): 51–9, Doi: 10.1016/j.chembiol.2011.12.011.
- [12] Mangelsdorf, D.J., Thummel, C., Beato, M., Herrlich, P., Schütz, G., Umesono, K., et al., 1995. The nuclear receptor superfamily: the second decade. *Cell* 83(6): 835–9, Doi: 10.1016/0092-8674(95)90199-x.
- [13] Biddie, S.C., John, S., Hager, G.L., 2010. Genome-wide mechanisms of nuclear receptor action. *Trends in Endocrinology and Metabolism: TEM* 21(1): 3–9, Doi: 10.1016/j.tem.2009.08.006.
- [14] Bain, D.L., Heneghan, A.F., Connaghan-Jones, K.D., Miura, M.T., 2007. Nuclear receptor structure: implications for function. *Annual Review of Physiology* 69: 201–20, Doi: 10.1146/annurev.physiol.69.031905.160308.
- [15] Jin, L., Li, Y., 2010. Structural and functional insights into nuclear receptor signaling. *Advanced Drug Delivery Reviews* 62(13): 1218–26, Doi: 10.1016/j.addr.2010.08.007.
- [16] Evans, R.M., 1988. The steroid and thyroid hormone receptor superfamily. *Science (New York, N.Y.)* 240(4854): 889–95, Doi: 10.1126/science.3283939.

- [17] Weatherman, R. V., Fletterick, R.J., Scanlan, T.S., 1999. Nuclear-receptor ligands and ligand-binding domains. *Annual Review of Biochemistry* 68: 559–81, Doi: 10.1146/annurev.biochem.68.1.559.
- [18] Nakamura, M.T., Yudell, B.E., Loor, J.J., 2014. Regulation of energy metabolism by long-chain fatty acids. *Progress in Lipid Research* 53(1): 124–44, Doi: 10.1016/j.plipres.2013.12.001.
- [19] Forman, B.M., Chen, J., Evans, R.M., 1997. Hypolipidemic drugs, polyunsaturated fatty acids, and eicosanoids are ligands for peroxisome proliferator-activated receptors alpha and delta. *Proceedings of the National Academy of Sciences of the United States of America* 94(9): 4312–7, Doi: 10.1073/pnas.94.9.4312.
- [20] Green, S., Wahli, W., 1994. Peroxisome proliferator-activated receptors: finding the orphan a home. *Molecular and Cellular Endocrinology* 100(1): 149–53, Doi: [https://doi.org/10.1016/0303-7207\(94\)90294-1](https://doi.org/10.1016/0303-7207(94)90294-1).
- [21] Day, C., 1999. Thiazolidinediones: a new class of antidiabetic drugs. *Diabetic Medicine : A Journal of the British Diabetic Association* 16(3): 179–92, Doi: 10.1046/j.1464-5491.1999.00023.x.
- [22] Forman, B.M., Tontonoz, P., Chen, J., Brun, R.P., Spiegelman, B.M., Evans, R.M., 1995. 15-Deoxy-delta 12, 14-prostaglandin J2 is a ligand for the adipocyte determination factor PPAR gamma. *Cell* 83(5): 803–12, Doi: 10.1016/0092-8674(95)90193-0.
- [23] Takeuchi, S., Matsuda, T., Kobayashi, S., Takahashi, T., Kojima, H., 2006. In vitro screening of 200 pesticides for agonistic activity via mouse peroxisome proliferator-activated receptor (PPAR) alpha and PPARgamma and quantitative analysis of in vivo induction pathway. *Toxicology and Applied Pharmacology* 217(3): 235–44, Doi: 10.1016/j.taap.2006.08.011.
- [24] Juge-Aubry, C., Pernin, A., Favez, T., Burger, A.G., Wahli, W., Meier, C.A., et al., 1997. DNA Binding Properties of Peroxisome Proliferator-activated Receptor Subtypes on Various Natural Peroxisome Proliferator Response Elements. *Journal of Biological Chemistry* 272(40): 25252–9, Doi: <https://doi.org/10.1074/jbc.272.40.25252>.
- [25] Nakshatri, H., Bhat-Nakshatri, P., 1998. Multiple parameters determine the specificity of transcriptional response by nuclear receptors HNF-4, ARP-1, PPAR, RAR and RXR through common response elements. *Nucleic Acids Research* 26(10): 2491–9, Doi: 10.1093/nar/26.10.2491.
- [26] Grygiel-Górniak, B., 2014. Peroxisome proliferator-activated receptors and their ligands: nutritional and clinical implications--a review. *Nutrition Journal* 13: 17, Doi: 10.1186/1475-2891-13-17.
- [27] Auboeuf, D., Rieusset, J., Fajas, L., Vallier, P., Frering, V., Riou, J.P., et al., 1997. Tissue distribution and quantification of the expression of mRNAs of peroxisome proliferator-activated receptors and liver X receptor-alpha in humans: no alteration in adipose tissue of obese and NIDDM patients. *Diabetes* 46(8): 1319–27, Doi: 10.2337/diab.46.8.1319.
- [28] Braissant Olivier, Foufelle Fabienne, Scotto Christian, Dauca Michel, W.W., 1996. Differential Expression of Peroxisome ProliferatorActivated Receptors (PPARs): Tissue Distribution of PPAR-a, -b, and -gamma in the Adult Rat*. *Endocrinology* 137(1).
- [29] Imai, T., Takakuwa, R., Marchand, S., Dentz, E., Bornert, J.-M., Messaddeq, N., et al., 2004. Peroxisome proliferator-activated receptor gamma is required in mature white and brown adipocytes for their survival in the mouse. *Proceedings of the National Academy of Sciences of the United States of America* 101(13): 4543–7, Doi: 10.1073/pnas.0400356101.

- [30] Lehmann, J.M., Moore, L.B., Smith-Oliver, T.A., Wilkison, W.O., Willson, T.M., Kliewer, S.A., 1995. An antidiabetic thiazolidinedione is a high affinity ligand for peroxisome proliferator-activated receptor gamma (PPAR gamma). *The Journal of Biological Chemistry* 270(22): 12953–6, Doi: 10.1074/jbc.270.22.12953.
- [31] Vidal-Puig, A., Jimenez-Liñan, M., Lowell, B.B., Hamann, A., Hu, E., Spiegelman, B., et al., 1996. Regulation of PPAR gamma gene expression by nutrition and obesity in rodents. *The Journal of Clinical Investigation* 97(11): 2553–61, Doi: 10.1172/JCI118703.
- [32] Schoonjans, K., Peinado-Onsurbe, J., Lefebvre, A.M., Heyman, R.A., Briggs, M., Deeb, S., et al., 1996. PPARalpha and PPARgamma activators direct a distinct tissue-specific transcriptional response via a PPRE in the lipoprotein lipase gene. *The EMBO Journal* 15(19): 5336–48.
- [33] Schoonjans, K., Staels, B., Grimaldi, P., Auwerx, J., 1993. Acyl-CoA synthetase mRNA expression is controlled by fibric-acid derivatives, feeding and liver proliferation. *European Journal of Biochemistry* 216(2): 615–22, Doi: 10.1111/j.1432-1033.1993.tb18181.x.
- [34] Motojima, K., Passilly, P., Peters, J.M., Gonzalez, F.J., Latruffe, N., 1998. Expression of putative fatty acid transporter genes are regulated by peroxisome proliferator-activated receptor alpha and gamma activators in a tissue- and inducer-specific manner. *The Journal of Biological Chemistry* 273(27): 16710–4, Doi: 10.1074/jbc.273.27.16710.
- [35] Memon, R.A., Tecott, L.H., Nonogaki, K., Beigneux, A., Moser, A.H., Grunfeld, C., et al., 2000. Up-regulation of peroxisome proliferator-activated receptors (PPAR-alpha) and PPAR-gamma messenger ribonucleic acid expression in the liver in murine obesity: troglitazone induces expression of PPAR-gamma-responsive adipose tissue-specific genes in the l. *Endocrinology* 141(11): 4021–31, Doi: 10.1210/endo.141.11.7771.
- [36] Martin, G., Schoonjans, K., Lefebvre, A.M., Staels, B., Auwerx, J., 1997. Coordinate regulation of the expression of the fatty acid transport protein and acyl-CoA synthetase genes by PPARalpha and PPARgamma activators. *The Journal of Biological Chemistry* 272(45): 28210–7, Doi: 10.1074/jbc.272.45.28210.
- [37] Rees, W.D., McNeil, C.J., Maloney, C.A., 2008. The Roles of PPARs in the Fetal Origins of Metabolic Health and Disease. *PPAR Research* 2008: 459030, Doi: 10.1155/2008/459030.
- [38] Magadam, A., Engel, F.B., 2018. PPAR β/δ : Linking Metabolism to Regeneration. *International Journal of Molecular Sciences* 19(7), Doi: 10.3390/ijms19072013.
- [39] Tanaka, T., Yamamoto, J., Iwasaki, S., Asaba, H., Hamura, H., Ikeda, Y., et al., 2003. Activation of peroxisome proliferator-activated receptor delta induces fatty acid beta-oxidation in skeletal muscle and attenuates metabolic syndrome. *Proceedings of the National Academy of Sciences of the United States of America* 100(26): 15924–9, Doi: 10.1073/pnas.0306981100.
- [40] Muoio, D.M., MacLean, P.S., Lang, D.B., Li, S., Houmard, J.A., Way, J.M., et al., 2002. Fatty acid homeostasis and induction of lipid regulatory genes in skeletal muscles of peroxisome proliferator-activated receptor (PPAR) alpha knock-out mice. Evidence for compensatory regulation by PPAR delta. *The Journal of Biological Chemistry* 277(29): 26089–97, Doi: 10.1074/jbc.M203997200.
- [41] Cherkaoui-Malki, M., Meyer, K., Cao, W.Q., Latruffe, N., Yeldandi, A. V., Rao, M.S., et al., 2001. Identification of novel peroxisome proliferator-activated receptor alpha (PPARalpha) target genes in mouse liver using cDNA microarray analysis. *Gene Expression* 9(6): 291–304, Doi: 10.3727/00000001783992533.

- [42] Cheon, Y., Nara, T.Y., Band, M.R., Beever, J.E., Wallig, M.A., Nakamura, M.T., 2005. Induction of overlapping genes by fasting and a peroxisome proliferator in pigs: evidence of functional PPAR α in nonproliferating species. *American Journal of Physiology-Regulatory, Integrative and Comparative Physiology* 288(6): R1525–35, Doi: 10.1152/ajpregu.00751.2004.
- [43] Kersten, S., Seydoux, J., Peters, J.M., Gonzalez, F.J., Desvergne, B., Wahli, W., 1999. Peroxisome proliferator – activated receptor α mediates the adaptive response to fasting 103(11): 1489–98.
- [44] Motojima, K., Seto, K., 2003. Fibrates and Statins Rapidly and Synergistically Induce Pyruvate Dehydrogenase Kinase 4 mRNA in the Liver and Muscles of Mice. *Biological and Pharmaceutical Bulletin* 26(7): 954–8, Doi: 10.1248/bpb.26.954.
- [45] Teboul, L., Febbraio, M., Gaillard, D., Amri, E.Z., Silverstein, R., Grimaldi, P.A., 2001. Structural and functional characterization of the mouse fatty acid translocase promoter: activation during adipose differentiation. *The Biochemical Journal* 360(Pt 2): 305–312, Doi: 10.1042/0264-6021:3600305.
- [46] Kaikaus, R.M., Chan, W.K., Ortiz de Montellano, P.R., Bass, N.M., 1993. Mechanisms of regulation of liver fatty acid-binding protein. *Molecular and Cellular Biochemistry* 123(1–2): 93–100, Doi: 10.1007/BF01076479.
- [47] Tang, C., Cho, H.P., Nakamura, M.T., Clarke, S.D., 2003. Regulation of human delta-6 desaturase gene transcription: identification of a functional direct repeat-1 element. *Journal of Lipid Research* 44(4): 686–95, Doi: 10.1194/jlr.M200195-JLR200.
- [48] Miller, C.W., Ntambi, J.M., 1996. Peroxisome proliferators induce mouse liver stearyl-CoA desaturase 1 gene expression. *Proceedings of the National Academy of Sciences of the United States of America* 93(18): 9443–8, Doi: 10.1073/pnas.93.18.9443.
- [49] Le May, C., Pineau, T., Bigot, K., Kohl, C., Girard, J., Pégurier, J.-P., 2000. Reduced hepatic fatty acid oxidation in fasting PPAR α null mice is due to impaired mitochondrial hydroxymethylglutaryl-CoA synthase gene expression. *FEBS Letters* 475(3): 163–6, Doi: [https://doi.org/10.1016/S0014-5793\(00\)01648-3](https://doi.org/10.1016/S0014-5793(00)01648-3).
- [50] Kersten, S., Stienstra, R., 2017. The role and regulation of the peroxisome proliferator activated receptor alpha in human liver. *Biochimie* 136: 75–84, Doi: 10.1016/j.biochi.2016.12.019.
- [51] Hashimoto, T., Cook, W.S., Qi, C., Yeldandi, A. V., Reddy, J.K., Rao, M.S., 2000. Defect in peroxisome proliferator-activated receptor ??-inducible fatty acid oxidation determines the severity of hepatic steatosis in response to fasting. *Journal of Biological Chemistry* 275(37): 28918–28, Doi: 10.1074/jbc.M910350199.
- [52] Leone, T.C., Weinheimer, C.J., Kelly, D.P., 1999. A critical role for the peroxisome proliferator-activated receptor α (PPAR α) in the cellular fasting response: The PPAR α -null mouse as a model of fatty acid oxidation disorders. *Proceedings of the National Academy of Sciences of the United States of America* 96(13): 7473–8, Doi: 10.1073/pnas.96.13.7473.
- [53] Lee, S.S.T., Chan, W.-Y., Lo, C.K.C., Wan, D.C.C., Tsang, D.S.C., Cheung, W.-T., 2004. Requirement of PPAR α in maintaining phospholipid and triacylglycerol homeostasis during energy deprivation. *Journal of Lipid Research* 45(11): 2025–37, Doi: <https://doi.org/10.1194/jlr.M400078-JLR200>.
- [54] Patsouris, D., Reddy, J.K., Mu, M., Kersten, S., 2006. Peroxisome Proliferator-Activated Receptor α Mediates the Effects of High-Fat Diet on Hepatic Gene Expression 147(3): 1508–16, Doi: 10.1210/en.2005-1132.

- [55] Kersten, S., Mandard, S., Tan, N.S., Escher, P., Metzger, D., Chambon, P., et al., 2000. Characterization of the fasting-induced adipose factor FIAF, a novel peroxisome proliferator-activated receptor target gene. *The Journal of Biological Chemistry* 275(37): 28488–93, Doi: 10.1074/jbc.M004029200.
- [56] Mattijssen, F., Georgiadi, A., Andasarie, T., Szalowska, E., Zota, A., Kronen-Herzig, A., et al., 2014. Hypoxia-inducible Lipid Droplet-associated (HILPDA) is a novel Peroxisome Proliferator-activated Receptor (PPAR) target involved in hepatic triglyceride secretion. *Journal of Biological Chemistry* 289(28): 19279–93, Doi: 10.1074/jbc.M114.570044.
- [57] Kreitzman, S.N., Coxon, A.Y., Szaz, K.F., 1992. Glycogen storage: illusions of easy weight loss, excessive weight regain, and distortions in estimates of body composition. *The American Journal of Clinical Nutrition* 56(1 Suppl): 292S-293S, Doi: 10.1093/ajcn/56.1.292S.
- [58] Han, H.-S., Kang, G., Kim, J.S., Choi, B.H., Koo, S.-H., 2016. Regulation of glucose metabolism from a liver-centric perspective. *Experimental & Molecular Medicine* 48(3): e218, Doi: 10.1038/emm.2015.122.
- [59] Göke, B., 2008. Islet cell function: alpha and beta cells--partners towards normoglycaemia. *International Journal of Clinical Practice. Supplement* (159): 2–7, Doi: 10.1111/j.1742-1241.2007.01686.x.
- [60] Sutherland, E.W., de Duve, C., 1948. ORIGIN AND DISTRIBUTION OF THE HYPERGLYCEMIC-GLYCOGENOLYTIC FACTOR OF THE PANCREAS. *Journal of Biological Chemistry* 175(2): 663–74, Doi: [https://doi.org/10.1016/S0021-9258\(18\)57183-0](https://doi.org/10.1016/S0021-9258(18)57183-0).
- [61] Röder, P. V., Wu, B., Liu, Y., Han, W., 2016. Pancreatic regulation of glucose homeostasis. *Experimental & Molecular Medicine* 48(3): e219, Doi: 10.1038/emm.2016.6.
- [62] McGarry, J., Wright, P.H., Foster, D.W., 1975. Hormonal control of ketogenesis. Rapid activation of hepatic ketogenic capacity in fed rats by anti-insulin serum and glucagon. *The Journal of Clinical Investigation* 55(6): 1202–9, Doi: 10.1172/JCI108038.
- [63] Gerich, J.E., Lorenzi, M., Bier, D.M., Schneider, V., Tsalikian, E., Karam, J.H., et al., 1975. Prevention of human diabetic ketoacidosis by somatostatin. Evidence for an essential role of glucagon. *The New England Journal of Medicine* 292(19): 985–9, Doi: 10.1056/NEJM197505082921901.
- [64] Wang, H., Chen, J., Hollister, K., Sowers, L.C., Forman, B.M., 1999. Endogenous bile acids are ligands for the nuclear receptor FXR/BAR. *Molecular Cell* 3(5): 543–53, Doi: 10.1016/s1097-2765(00)80348-2.
- [65] Parks, D.J., Blanchard, S.G., Bledsoe, R.K., Chandra, G., Consler, T.G., Kliewer, S.A., et al., 1999. Bile acids: natural ligands for an orphan nuclear receptor. *Science (New York, N.Y.)* 284(5418): 1365–8, Doi: 10.1126/science.284.5418.1365.
- [66] Makishima, M., Okamoto, A.Y., Repa, J.J., Tu, H., Learned, R.M., Luk, A., et al., 1999. Identification of a nuclear receptor for bile acids. *Science (New York, N.Y.)* 284(5418): 1362–5, Doi: 10.1126/science.284.5418.1362.
- [67] Kok, T., Hulzebos, C. V., Wolters, H., Havinga, R., Agellon, L.B., Stellaard, F., et al., 2003. Enterohepatic circulation of bile salts in farnesoid X receptor-deficient mice: efficient intestinal bile salt absorption in the absence of ileal bile acid-binding protein. *The Journal of Biological Chemistry* 278(43): 41930–7, Doi: 10.1074/jbc.M306309200.

- [68] Zhang, Y., Lee, F.Y., Barrera, G., Lee, H., Vales, C., Gonzalez, F.J., et al., 2006. Activation of the nuclear receptor FXR improves hyperglycemia and hyperlipidemia in diabetic mice. *Proceedings of the National Academy of Sciences of the United States of America* 103(4): 1006–11, Doi: 10.1073/pnas.0506982103.
- [69] Ma, K., Saha, P.K., Chan, L., Moore, D.D., 2006. Farnesoid X receptor is essential for normal glucose homeostasis. *The Journal of Clinical Investigation* 116(4): 1102–9, Doi: 10.1172/JCI25604.
- [70] Matsukuma, K.E., Bennett, M.K., Huang, J., Wang, L., Gil, G., Osborne, T.F., 2006. Coordinated control of bile acids and lipogenesis through FXR-dependent regulation of fatty acid synthase. *Journal of Lipid Research* 47(12): 2754–61, Doi: 10.1194/jlr.M600342-JLR200.
- [71] Song, K.-H., Li, T., Owsley, E., Strom, S., Chiang, J.Y.L., 2009. Bile acids activate fibroblast growth factor 19 signaling in human hepatocytes to inhibit cholesterol 7 α -hydroxylase gene expression. *Hepatology (Baltimore, Md.)* 49(1): 297–305, Doi: 10.1002/hep.22627.
- [72] Inagaki, T., Choi, M., Moschetta, A., Peng, L., Cummins, C.L., McDonald, J.G., et al., 2005. Fibroblast growth factor 15 functions as an enterohepatic signal to regulate bile acid homeostasis. *Cell Metabolism* 2(4): 217–25, Doi: 10.1016/j.cmet.2005.09.001.
- [73] Kir, S., Beddow, S.A., Samuel, V.T., Miller, P., Previs, S.F., Suino-Powell, K., et al., 2011. FGF19 as a postprandial, insulin-independent activator of hepatic protein and glycogen synthesis. *Science (New York, N.Y.)* 331(6024): 1621–4, Doi: 10.1126/science.1198363.
- [74] Watanabe, M., Houten, S.M., Wang, L., Moschetta, A., Mangelsdorf, D.J., Heyman, R.A., et al., 2004. Bile acids lower triglyceride levels via a pathway involving FXR, SHP, and SREBP-1c. *The Journal of Clinical Investigation* 113(10): 1408–18, Doi: 10.1172/JCI21025.
- [75] Repa, J.J., Liang, G., Ou, J., Bashmakov, Y., Lobaccaro, J.M., Shimomura, I., et al., 2000. Regulation of mouse sterol regulatory element-binding protein-1c gene (SREBP-1c) by oxysterol receptors, LXR α and LXR β . *Genes & Development* 14(22): 2819–30, Doi: 10.1101/gad.844900.
- [76] Schultz, J.R., Tu, H., Luk, A., Repa, J.J., Medina, J.C., Li, L., et al., 2000. Role of LXRs in control of lipogenesis. *Genes & Development* 14(22): 2831–8, Doi: 10.1101/gad.850400.
- [77] Eberlé, D., Hegarty, B., Bossard, P., Ferré, P., Foufelle, F., 2004. SREBP transcription factors: master regulators of lipid homeostasis. *Biochimie* 86(11): 839–48, Doi: <https://doi.org/10.1016/j.biochi.2004.09.018>.
- [78] Shimomura, I., Shimano, H., Horton, J.D., Goldstein, J.L., Brown, M.S., 1997. Differential expression of exons 1a and 1c in mRNAs for sterol regulatory element binding protein-1 in human and mouse organs and cultured cells. *The Journal of Clinical Investigation* 99(5): 838–45, Doi: 10.1172/JCI119247.
- [79] Moon, Y.A., Lee, J.J., Park, S.W., Ahn, Y.H., Kim, K.S., 2000. The roles of sterol regulatory element-binding proteins in the transactivation of the rat ATP citrate-lyase promoter. *The Journal of Biological Chemistry* 275(39): 30280–6, Doi: 10.1074/jbc.M001066200.
- [80] Sato, R., Okamoto, A., Inoue, J., Miyamoto, W., Sakai, Y., Emoto, N., et al., 2000. Transcriptional regulation of the ATP citrate-lyase gene by sterol regulatory element-binding proteins. *The Journal of Biological Chemistry* 275(17): 12497–502, Doi: 10.1074/jbc.275.17.12497.
- [81] Griffin, M.J., Sul, H.S., 2004. Insulin regulation of fatty acid synthase gene transcription: roles of USF and SREBP-1c. *IUBMB Life* 56(10): 595–600, Doi: 10.1080/15216540400022474.

- [82] Casado, M., Vallet, V.S., Kahn, A., Vaulont, S., 1999. Essential role in vivo of upstream stimulatory factors for a normal dietary response of the fatty acid synthase gene in the liver. *The Journal of Biological Chemistry* 274(4): 2009–13, Doi: 10.1074/jbc.274.4.2009.
- [83] Kim, S.-Y., Kim, H., Kim, T.-H., Im, S.-S., Park, S.-K., Lee, I.-K., et al., 2004. SREBP-1c mediates the insulin-dependent hepatic glucokinase expression. *The Journal of Biological Chemistry* 279(29): 30823–9, Doi: 10.1074/jbc.M313223200.
- [84] Eberlé, D., Hegarty, B., Bossard, P., Ferré, P., Foufelle, F., 2004. SREBP transcription factors: master regulators of lipid homeostasis. *Biochimie* 86(11): 839–48, Doi: <https://doi.org/10.1016/j.biochi.2004.09.018>.
- [85] Liang, G., Yang, J., Horton, J.D., Hammer, R.E., Goldstein, J.L., Brown, M.S., 2002. Diminished hepatic response to fasting/refeeding and liver X receptor agonists in mice with selective deficiency of sterol regulatory element-binding protein-1c. *The Journal of Biological Chemistry* 277(11): 9520–8, Doi: 10.1074/jbc.M111421200.
- [86] Horton, J.D., Goldstein, J.L., Brown, M.S., 2002. SREBPs: activators of the complete program of cholesterol and fatty acid synthesis in the liver. *The Journal of Clinical Investigation* 109(9): 1125–31, Doi: 10.1172/JCI15593.
- [87] Foretz, M., Pacot, C., Dugail, I., Lemarchand, P., Guichard, C., Le Lièvre, X., et al., 1999. ADD1/SREBP-1c is required in the activation of hepatic lipogenic gene expression by glucose. *Molecular and Cellular Biology* 19(5): 3760–8, Doi: 10.1128/mcb.19.5.3760.
- [88] Ferré, P., Foretz, M., Azzout-Marniche, D., Bécard, D., Fougelle, F., 2001. Sterol-regulatory-element-binding protein 1c mediates insulin action on hepatic gene expression. *Biochemical Society Transactions* 29(Pt 4): 547–52, Doi: 10.1042/bst0290547.
- [89] Gosmain, Y., Dif, N., Berbe, V., Loizon, E., Rieusset, J., Vidal, H., et al., 2005. Regulation of SREBP-1 expression and transcriptional action on HKII and FAS genes during fasting and refeeding in rat tissues. *Journal of Lipid Research* 46(4): 697–705, Doi: 10.1194/jlr.M400261-JLR200.
- [90] Amemiya-Kudo, M., Shimano, H., Hasty, A.H., Yahagi, N., Yoshikawa, T., Matsuzaka, T., et al., 2002. Transcriptional activities of nuclear SREBP-1a, -1c, and -2 to different target promoters of lipogenic and cholesterologenic genes. *Journal of Lipid Research* 43(8): 1220–35.
- [91] Puigserver, P., Rhee, J., Donovan, J., Walkey, C.J., Yoon, J.C., Oriente, F., et al., 2003. Insulin-regulated hepatic gluconeogenesis through FOXO1-PGC-1 α interaction. *Nature* 423(6939): 550–5, Doi: 10.1038/nature01667.
- [92] Fasshauer, M., Blüher, M., 2015. Adipokines in health and disease. *Trends in Pharmacological Sciences* 36(7): 461–70, Doi: 10.1016/j.tips.2015.04.014.
- [93] Park, A., Kim, W.K., Bae, K.-H., 2014. Distinction of white, beige and brown adipocytes derived from mesenchymal stem cells. *World Journal of Stem Cells* 6(1): 33–42, Doi: 10.4252/wjsc.v6.i1.33.
- [94] Bolsoni-Lopes, A., Alonso-Vale, M.I.C., 2015. Lipolysis and lipases in white adipose tissue - An update. *Archives of Endocrinology and Metabolism* 59(4): 335–42, Doi: 10.1590/2359-3997000000067.
- [95] Kim, J.B., Spiegelman, B.M., 1996. ADD1/SREBP1 promotes adipocyte differentiation and gene expression linked to fatty acid metabolism. *Genes & Development* 10(9): 1096–107, Doi: 10.1101/gad.10.9.1096.

- [96] Palou, M., Sánchez, J., Priego, T., Rodríguez, A.M., Picó, C., Palou, A., 2010. Regional differences in the expression of genes involved in lipid metabolism in adipose tissue in response to short- and medium-term fasting and refeeding. *The Journal of Nutritional Biochemistry* 21(1): 23–33, Doi: <https://doi.org/10.1016/j.jnutbio.2008.10.001>.
- [97] Eguchi, J., Wang, X., Yu, S., Kershaw, E.E., Chiu, P.C., Dushay, J., et al., 2011. Transcriptional control of adipose lipid handling by IRF4. *Cell Metabolism* 13(3): 249–59, Doi: 10.1016/j.cmet.2011.02.005.
- [98] Aaron M. Cypess, M.D., Ph.D., M.M.Sc., Sanaz Lehman, M.B., B.S., Gethin Williams, M.B., B.S., Ph.D., Ilan Tal, Ph.D., Dean Rodman, M.D., Allison B. Goldfine, M.D., Frank C. Kuo, M.D., Ph.D., Edwin L. Palmer, M.D., Yu-Hua Tseng, Ph.D., Alessandro Doria, M., M., 2009. Identification and Importance of Brown Adipose Tissue in Adult Humans. *N Engl J Med.*, Doi: 10.3816/CLM.2009.n.003.Novel.
- [99] Nedergaard, J., Bengtsson, T., Cannon, B., 2007. Unexpected evidence for active brown adipose tissue in adult humans. *American Journal of Physiology. Endocrinology and Metabolism* 293(2): E444–52, Doi: 10.1152/ajpendo.00691.2006.
- [100] Chakraborty, D., Bhattacharya, A., Mittal, B.R., 2015. Patterns of brown fat uptake of 18F-fluorodeoxyglucose in positron emission tomography/computed tomography scan. *Indian Journal of Nuclear Medicine : IJNM : The Official Journal of the Society of Nuclear Medicine, India* 30(4): 320–2, Doi: 10.4103/0972-3919.164147.
- [101] Kozak, L.P., 2010. Brown Fat and the Myth of Diet-Induced Thermogenesis. *Cell Metabolism* 11(4): 263–7, Doi: <https://doi.org/10.1016/j.cmet.2010.03.009>.
- [102] Hanssen, M.J.W., van der Lans, A.A.J.J., Brans, B., Hoeks, J., Jardon, K.M.C., Schaart, G., et al., 2016. Short-term Cold Acclimation Recruits Brown Adipose Tissue in Obese Humans. *Diabetes* 65(5): 1179–89, Doi: 10.2337/db15-1372.
- [103] Himms-Hagen, J., Cui, J., Danforth, E., Taatjes, D.J., Lang, S.S., Waters, B.L., et al., 1994. Effect of CL-316,243, a thermogenic beta 3-agonist, on energy balance and brown and white adipose tissues in rats. *The American Journal of Physiology* 266(4 Pt 2): R1371–82.
- [104] Herz, C.T., Kiefer, F.W., 2019. Adipose tissue browning in mice and humans. *The Journal of Endocrinology* 241(3): R97–109, Doi: 10.1530/JOE-18-0598.
- [105] Cousin, B., Cinti, S., Morroni, M., Raimbault, S., Ricquier, D., Pénicaud, L., 1992. Occurrence of brown adipocytes in rat white adipose tissue: molecular and morphological characterization. *Journal of Cell Science* 103(Pt 4): 931–42.
- [106] Young, J.B., Saville, E., Rothwell, N.J., Stock, M.J., Landsberg, L., 1982. Effect of diet and cold exposure on norepinephrine turnover in brown adipose tissue of the rat. *The Journal of Clinical Investigation* 69(5): 1061–71, Doi: 10.1172/jci110541.
- [107] Reverte-Salisa, L., Sanyal, A., Pfeifer, A., 2019. Role of cAMP and cGMP Signaling in Brown Fat. *Handbook of Experimental Pharmacology* 251: 161–82, Doi: 10.1007/164_2018_117.
- [108] Gustafson, B., Smith, U., 2015. Regulation of white adipogenesis and its relation to ectopic fat accumulation and cardiovascular risk. *Atherosclerosis* 241(1): 27–35, Doi: 10.1016/j.atherosclerosis.2015.04.812.
- [109] Seale, P., Conroe, H.M., Estall, J., Kajimura, S., Frontini, A., Ishibashi, J., et al., 2011. Prdm16 determines the thermogenic program of subcutaneous white adipose tissue in mice. *The Journal of Clinical Investigation* 121(1): 96–105, Doi: 10.1172/JCI44271.

- [110] Harms, M., Seale, P., 2013. Brown and beige fat: development, function and therapeutic potential. *Nature Medicine* 19(10): 1252–63, Doi: 10.1038/nm.3361.
- [111] Wu, J., Boström, P., Sparks, L.M., Ye, L., Choi, J.H., Giang, A.H., et al., 2012. Beige adipocytes are a distinct type of thermogenic fat cell in mouse and human. *Cell* 150(2): 366–76, Doi: 10.1016/j.cell.2012.05.016.
- [112] Seale, P., Bjork, B., Yang, W., Kajimura, S., Chin, S., Kuang, S., et al., 2008. PRDM16 controls a brown fat/skeletal muscle switch. *Nature* 454(7207): 961–7, Doi: 10.1038/nature07182.
- [113] Seale, P., Kajimura, S., Yang, W., Chin, S., Rohas, L.M., Uldry, M., et al., 2007. Transcriptional control of brown fat determination by PRDM16. *Cell Metabolism* 6(1): 38–54, Doi: 10.1016/j.cmet.2007.06.001.
- [114] Gorla-Bajszczak, A., Siegrist-Kaiser, C., Boss, O., Burger, A.G., Meier, C.A., 2000. Expression of peroxisome proliferator-activated receptors in lean and obese Zucker rats. *European Journal of Endocrinology* 142(1): 71–8, Doi: 10.1530/eje.0.1420071.
- [115] Barberá, M.J., Schlüter, A., Pedraza, N., Iglesias, R., Villarroya, F., Giral, M., 2001. Peroxisome proliferator-activated receptor α activates transcription of the brown fat uncoupling protein-1 gene. A link between regulation of the thermogenic and lipid oxidation pathways in the brown fat cell. *Journal of Biological Chemistry* 276(2): 1486–93, Doi: 10.1074/jbc.M006246200.
- [116] Westerberg, R., Månsson, J.-E., Golozoubova, V., Shabalina, I.G., Backlund, E.C., Tvrdik, P., et al., 2006. ELOVL3 is an important component for early onset of lipid recruitment in brown adipose tissue. *The Journal of Biological Chemistry* 281(8): 4958–68, Doi: 10.1074/jbc.M511588200.
- [117] Mulya, A., Kirwan, J.P., 2017. Brown and Beige Adipose Tissue: Therapy for obesity and its comorbidities? 21(2): 129–39, Doi: 10.1016/j.ecl.2016.04.010.Brown.
- [118] Torres, N., Tovar, A.R., 2016. Adipose Tissue : White Adipose Tissue Structure and Function. 1st ed., Elsevier Ltd.
- [119] Rosen, E.D., MacDougald, O.A., 2006. Adipocyte differentiation from the inside out. *Nature Reviews. Molecular Cell Biology* 7(12): 885–96, Doi: 10.1038/nrm2066.
- [120] Rachid, T.L., Penna-de-Carvalho, A., Bringham, I., Aguila, M.B., Mandarim-de-Lacerda, C.A., Souza-Mello, V., 2015. Fenofibrate (PPAR α agonist) induces beige cell formation in subcutaneous white adipose tissue from diet-induced male obese mice. *Molecular and Cellular Endocrinology* 402: 86–94, Doi: 10.1016/j.mce.2014.12.027.
- [121] Hondares, E., Rosell, M., Díaz-Delfin, J., Olmos, Y., Monsalve, M., Iglesias, R., et al., 2011. Peroxisome proliferator-activated receptor α (PPAR α) induces PPAR γ coactivator 1 α (PGC-1 α) gene expression and contributes to thermogenic activation of brown fat: Involvement of PRDM16. *Journal of Biological Chemistry* 286(50): 43112–22, Doi: 10.1074/jbc.M111.252775.
- [122] Barquissau, V., Beuzelin, D., Pisani, D.F., Beranger, G.E., Mairal, A., Montagner, A., et al., 2016. White-to-brite conversion in human adipocytes promotes metabolic reprogramming towards fatty acid anabolic and catabolic pathways. *Molecular Metabolism* 5(5): 352–65, Doi: 10.1016/j.molmet.2016.03.002.
- [123] Li, P., Zhu, Z., Lu, Y., Granneman, J.G., 2005. Metabolic and cellular plasticity in white adipose tissue II: role of peroxisome proliferator-activated receptor- α . *American Journal of Physiology. Endocrinology and Metabolism* 289(4): E617-26, Doi: 10.1152/ajpendo.00010.2005.



CHAPTER 2



Hepatic ADTRP overexpression does not influence lipid and glucose metabolism

Merel Defour, Michel van Weeghel, Jill Hermans, and Sander Kersten

ABSTRACT

The peroxisome proliferator-activated receptors (PPARs) are a group of transcription factors belonging to the nuclear receptor superfamily. Since most target genes of PPARs are implicated in lipid and glucose metabolism, regulation by PPARs could be used as a screening tool to identify novel genes involved in lipid or glucose metabolism. Here, we identify *Adtrp*, a serine hydrolase enzyme that was reported to catalyze the hydrolysis of fatty acid esters of hydroxy fatty acids (FAHFAs), as a novel PPAR-regulated gene. *Adtrp* was significantly upregulated by PPAR α activation in mouse primary hepatocytes, liver slices, and whole liver. In addition, *Adtrp* was upregulated by PPAR γ activation in 3L3-L1 adipocytes and in white adipose tissue. CHIP-SEQ identified a strong PPAR binding site in the immediate upstream promoter of the *Adtrp* gene. Adenoviral-mediated hepatic overexpression of *Adtrp* in diet-induced obese mice caused a modest increase in plasma non-esterified fatty acids but did not influence diet-induced obesity, liver triglyceride levels, liver lipidomic profiles, liver transcriptomic profiles, and plasma cholesterol, triglycerides, glycerol, and glucose levels. Moreover, hepatic *Adtrp* overexpression did not lead to significant changes in FAHFA levels in plasma or liver and did not influence glucose and insulin tolerance. Finally, hepatic overexpression of *Adtrp* did not influence liver triglycerides and levels of plasma metabolites after a 24h fast. Taken together, our data suggest that despite being a PPAR-regulated gene, hepatic *Adtrp* does not seem to play a major role in lipid and glucose metabolism and does not regulate FAHFA levels.

INTRODUCTION

The peroxisome proliferator-activated receptors (PPARs) are a group of nuclear receptors that play an important role in the regulation of lipid metabolism in the liver and other tissues [1]. PPARs function as ligand-activated transcription factors and alter the transcription of genes by binding to specific loci on the DNA called PPAR response elements (PPREs). The transcriptional activity of PPARs is induced by different types of ligands, including environmental contaminants, food components, drugs, and endogenous lipids [2–4]. In particular, fatty acids and compounds derived from fatty acids such as eicosanoids and endocannabinoids have been shown to serve as endogenous ligands of PPARs.

Three different PPARs can be distinguished: PPAR α (Nr1c1), PPAR δ (Nr1c2), and PPAR γ (Nr1c3). The different PPARs are characterized by very different tissue expression profiles. While PPAR α is shown to be the master regulator of lipid metabolism in the liver, PPAR γ is mainly expressed in the adipose tissue where it plays a critical role in adipocyte differentiation [5]. Compared to the other PPARs, the PPAR δ subtype is the most ubiquitously expressed throughout the body.

Many genes involved in lipid metabolism are known to be under direct transcriptional control of PPARs. For example, *Pdk4*, *Cpt1a*, *Hmgcs2* and *Acox1* are well established PPAR α targets in the liver and are known to play a pivotal role in hepatic lipid metabolism. Target genes of PPAR γ in adipose tissue include *Cd36*, *Slc2a4* (GLUT4), *Gpd1*, *Pck1*, and *Lpl*. These genes are involved in critical steps in the storage of fat in adipose tissue. In brown adipose tissue—where expression of both PPAR α and PPAR γ is high—it has been shown that many target genes are mutually and interchangeably regulated by PPAR α and PPAR γ [6]. Since most target genes of either PPAR α or PPAR γ are implicated in lipid and glucose metabolism, regulation by PPARs could be used as a screening tool to identify novel genes involved in lipid metabolism.

Fatty acid esters of hydroxy fatty acids have been identified as a potential insulin-sensitizing class of lipids [7,8]. FAHFAs are composed of a fatty acid esterified to the hydroxyl group of a hydroxy fatty acid. One of the enzymes that catalyzes the hydrolysis of FAHFAs has been identified as ADTRP. The other enzyme is AIG1 (androgen induced gene 1) [9]. ADTRP has been the subject of a limited number of studies [10]. ADTRP derives its name Androgen-Dependent TFPI Regulating Protein from its ability to regulate the Tissue Factor Pathway Inhibitor (TFPI). TFPI is a single-chain polypeptide that functions as an endogenous coagulation inhibitor [11]. Here we screened for novel genes regulated by PPARs and describe the further characterization of the *Adtrp* gene.

METHODS AND MATERIALS

Cell experiments

Hepatocytes were isolated from mice from 6 different strains; NMRI, SV129, BALB/C, C57BL/6J (male) and FVB and DBA (female) by two-step collagenase perfusion and plated on collagen-coated plates as described previously [12]. Mice were euthanized via cervical dislocation. Cells were suspended in William's E medium (Lonza Bioscience, Verviers, Belgium) supplemented with 10% (v/v) fetal calf serum, 20 milliunits/ml insulin, 50 nM dexamethasone, 100 units/ml penicillin, 100 g/ml streptomycin, 0.25 g/ml fungizone, and 50 g/ml gentamycin. The next day, cells were incubated in fresh medium supplemented with Wy14643 (5 μ M) dissolved in DMSO or with pure DMSO for 24 h.

3T3-L1 preadipocytes (#CL-173) were obtained from ATCC (Manassas, VA, USA). Cells were cultured in DMEM (Gibco, Life Technologies, Blijswijk, the Netherlands) supplemented with 10% FCS and 1% penicillin/streptomycin (Lonza, Verviers, Belgium) in a humidified chamber at 37°C with 5% CO₂. During differentiation, 3T3-L1 cells were cultured in 6-wells plate until 2 days post-confluency. At 2 days post-confluency the induction medium was added (0.5mM IBMX, 5ug/ml insulin, 1 μ M dexamethasone) for 3 days. Induction medium was replaced with insulin medium (5 μ g/ml of insulin and 1 μ M of rosiglitazone). The medium was subsequently changed every 3 days, and no further insulin was added after 6 days. Dharmacon ON-TARGETplus SMARTpool small interfering RNAs (siRNAs) against *Pparg* and non-targeting control small interfering RNAs (siCtrls) were purchased from Thermo Fisher Scientific. siRNAs were diluted in Dharmacon 1 \times siRNA buffer [final concentration 20 mM KCl, 6 mM HEPES (pH 7.5), and 0.2 mM MgCl₂]. Transfections were performed with Lipofectamine RNAiMAX transfection reagent (Life Technologies, Bleiswijk, The Netherlands). To silence *Pparg* in mature 3T3-L1 adipocytes, cells were washed with phosphate-buffered saline (PBS), trypsinized, and collected in PBS or DMEM. After centrifugation at 400g for 5 minutes, cells were strained over a 70 μ M cell strainer and plated to 70% confluency. siRNAs were added 2 hours later in a concentration of 40 nM siRNA and 2 μ L transfection reagent for a 12-well plate and experiments were carried out after an additional 48 to 72 hours of incubation.

FAO cells were cultured in DMEM (Gibco, Life Technologies, Blijswijk, the Netherlands) supplemented with 10% FCS and 1% penicillin/streptomycin (Lonza, Verviers, Belgium) in a humidified chamber at 37°C with 5% CO₂. Cells were treated with Wy14643 (10 μ M) for 0, 1, 2, 3, 4 or 5 hours. After treatment cells were washed with PBS and snap frozen until further analysis.

Liver Slices

Precision cut liver slices obtained from male C57BL/6J mice were prepared as described previously [13]. In short, 5 mm cylindrical liver cores were prepared with a surgical biopsy punch and sectioned to 200 μm slices using a Krumdieck tissue slicer (Alabama Research and Development, Munford, AL, USA) filled with carbonated Krebs-Henseleit buffer (pH 7.4, supplemented with 25 mM glucose). The precision cut liver slices were incubated in William's E Medium (Lonza, Verviers, Belgium) supplemented with pen/strep in 6-well plates at 37°C/5% CO₂/80% O₂ under continuous shaking (70 rpm). After 1 h, the medium was replaced by fresh William's E Medium containing 0.1% DMSO or 20 μM Wy14643. After incubation for 24 hours the liver slices were snap frozen in liquid nitrogen and stored until further analysis.

Recombinant adeno-associated viruses (AAVs)

AAVs expressing *Adtrp* were generated by Vector Biolabs (Malvern, PA, USA). In short, mouse *Adtrp* cDNA was inserted into pAAV-ALBp-3iALB, a vector containing a modified albumin promoter flanked by two AAV2-derived inverted terminal repeats [13]. The construct was verified by sequencing. The same amount of AAV2/AAV8 hybrid virus expressing GFP was injected to serve as a control.

Mouse studies

PPAR α knock out experiments

Male wild-type and PPAR α ^{-/-} mice on an Sv129 background were obtained from the Jackson Laboratory (Bar Harbor, ME). All mice were maintained on a 12-h light-dark cycle with ad libitum access to chow and water. For PPAR α agonist treatment, five-month-old wild-type and PPAR α ^{-/-} mice were fed a diet containing Wy14643 (0.1% w/w of feed) for 5 days (n=5 mice per group). For the fasting experiment, five-month-old wild-type and PPAR α ^{-/-} mice were fasted for different durations for a maximum of 24 h (n=5 mice per group). At the end of each study, blood was collected via orbital puncture under isoflurane anesthesia into EDTA tubes. Mice were euthanized via cervical dislocation, after which tissues were collected and snap frozen in liquid nitrogen.

Hepatic Adtrp overexpression experiments

Male 8-week-old C57BL/6J mice were purchased from Harlan and maintained on a 12-h light-dark cycle with ad libitum access to chow and water. The AAVs were administered in a volume of 100 μl via the tail vein. Animals were injected intravenously with different amounts of AAV-*Adtrp*, ranging from 2.5*10¹⁰, 1*10¹¹, 2.5*10¹¹ and 6*10¹¹ genomic copies to determine the dose required for a significant increase in hepatic *Adtrp* expression. Male wild-type C57BL/6J mice (9–12 weeks

old) were injected with 2.5×10^{11} genomic copies of AAV-*Gfp* or AAV-*Adtrp* (n=12 mice per group). Two weeks after injection, mice were fed a high fat diet containing 60 energy percent fat (D12492, Research Diets, Inc., New Brunswick, USA) for 7 weeks. After 5 weeks of high fat diet, an intraperitoneal glucose tolerance test and after 6 weeks an intraperitoneal insulin tolerance test was performed. After 7 weeks on this high fat diet, the mice were anaesthetized with isoflurane and blood was collected via orbital puncture in tubes containing EDTA (Sarstedt, Nümbrecht, Germany). Immediately thereafter, mice were euthanized by cervical dislocation, after which tissues were excised, weighed, and frozen in liquid nitrogen or prepared for histology. Frozen samples were stored at -80°C . Of the AAV-*Adtrp* group, 4 mice were removed from analysis because of a lack of *Adtrp* overexpression. For the fasting experiment, male wild-type C57BL/6J animals (9–12 weeks old) were injected with 6×10^{11} genomic copies of AAV-*Gfp* or AAV-*Adtrp* (n = 12 mice per group). Three weeks after injection, mice were fasted for 24 hours or remained on an ad libitum chow diet. The mice were anaesthetized with isoflurane and blood was collected via orbital puncture in tubes containing EDTA (Sarstedt, Nümbrecht, Germany). Immediately thereafter, mice were euthanized by cervical dislocation, after which tissues were excised, weighed, and frozen in liquid nitrogen or prepared for histology. Frozen samples were stored at -80°C . All animal experiments were approved by the local animal welfare committee of Wageningen University (2016.W-0093.012, 2016038, 2016049).

ChIP-SEQ

Chromatin immunoprecipitation coupled to sequencing (ChIP-SEQ) data from mouse liver (GSE113157) [21], from 3T3-L1 cells (GSE13511) [14] and mouse eWAT and BAT, either whole tissue (GSE43763) [15] or primary in vitro differentiated adipocytes (GSE41481) [16], were obtained from the Gene Expression Omnibus database. PPAR γ peaks in mouse adipocytes were identified with default settings and scanned for the presence of known motifs using HOMER [17]. The University of California, Santa Cruz, genome browser [18] or Integrative Genome Viewer [19] was used for visualization.

RNA isolations and qPCR

Mouse liver slices and tissues were homogenized in TRIzol[®] (Invitrogen) using the Qiagen TissueLyser II and stainless steel beads. Total RNA was isolated using the RNeasy Micro kit from Qiagen (Venlo, The Netherlands). Subsequently, 500 nanogram RNA was used to synthesize cDNA using iScript cDNA synthesis kit (Bio-Rad Laboratories, Veenendaal, The Netherlands). Messenger RNA levels of *Adtrp* were determined by reverse transcription quantitative PCR using SensiMix (Bioline; GC Biotech, Alphen aan den Rijn, The Netherlands) on a CFX384 real-time PCR detection system (Bio-Rad Laboratories, Veenendaal, the Netherlands). The housekeeping

gene *36b4* was used for normalization. Primers were synthesized by Eurogentec (Seraing, Belgium). Primer sequences for Adtrp were TCACATCCCACAGATTGGAAGG (forward primer) and AATGGCCTGCAAGAGCAGATT (reverse primer).

Microarray analysis

For microarray analysis, RNA was isolated as described above. RNA integrity and quality was analyzed with RNA 6000 Nano chips on the Agilent 2100 Bioanalyzer (Agilent Technologies, Amsterdam, The Netherlands). Purified RNA (100 ng) was labeled with the Ambion WT expression kit (Invitrogen) and hybridized to an Affymetrix Mouse Gene 2.1 ST array plate (Affymetrix, Santa Clara, CA). Hybridization, washing, and scanning were carried out on an Affymetrix GeneTitan platform, and readouts were processed and analyzed according to the manufacturer's instructions. Normalized expression estimates were obtained from the raw intensity values applying the robust multi-array analysis preprocessing algorithm available in the Bioconductor library AffyPLM with default settings [20,21]. Probe sets were defined according to Dai et al. [22]. In this method, probes are assigned to Entrez IDs as a unique gene identifier using the Entrez Gene database, build 37, version 1 (remapped CDF v22). P values were calculated using an intensity-based moderated T-statistic (IBMT). Microarray data were submitted to Gene Expression Omnibus (accession number pending).

Protein isolations and western blot

Liver samples and T37i cells were lysed in a mild RIPA-like lysis buffer (25 mM Tris-HCl pH 7.4, 150 mM NaCl, 1 mM EDTA, 1% NP-40 and 5% glycerol; Thermo Scientific) with protease and phosphatase inhibitors (Roche). Protein concentration was determined using a Pierce BCA kit (Thermo Scientific), and equal amounts of protein were diluted with 2× Laemmli sample buffer. Protein lysates were loaded on a 8–16% gradient Criterion gel (Bio-Rad) and separated by SDS gel electrophoresis. Proteins were transferred to a PVDF membrane by means of a Transblot Turbo System (Bio-Rad). Antibodies against ADTRP (1:500; Santa Cruz biotechnology, catalog no. sc-139309 (Y-14) and sc-139310 (I-12)), HSP90 (1:5000; Cell Signaling Technology, Inc., catalog no. 4874), and goat anti-rabbit (1:10.000; Jackson ImmunoResearch, catalog no. 111-035-003) were diluted in 5% (w/v) Tris-buffered saline, pH 7.5, with 0.1% Tween-20 (TBS-T) and 5% dry milk. Primary antibodies were applied overnight at 4 °C, and secondary antibody was applied for 1 h at room temperature. Blots were visualized using the ChemiDoc MP system (Bio-Rad) and Clarity ECL substrate (Bio-Rad).

Lipidomics

Lipidomics analysis was performed as described (Herzog, 2016). The HPLC system consisted of an Ultimate 3000 binary HPLC pump, a vacuum degasser, a column temperature controller, and an autosampler (Thermo Fisher Scientific). The column temperature was maintained at 25°C. The lipid extract was injected onto a “normal phase column” LiChrospher 2x250-mm silica-60 column, 5 µm particle diameter (Merck) and a “reverse phase column” Acquity UPLC HSS T3, 1.8 µm particle diameter (Waters, Milford, MA, USA). A Q Exactive Plus Orbitrap (Thermo Fisher Scientific) mass spectrometer was used in the negative and positive electrospray ionization mode. Nitrogen was used as the nebulizing gas. The spray voltage used was 2500 V, and the capillary temperature was 256°C. S-lens RF level: 50, auxiliary gas: 11, auxiliary temperature 300°C, sheath gas: 48, sweep cone gas: 2. In both the negative and positive ionization mode, mass spectra of the lipid species were obtained by continuous scanning from m/z 150 to m/z 2000 with a resolution of 280,000 full width at half maximum (FWHM). Data was analyzed using R programming language (<https://www.r-project.org>).

FAHFA analysis

Methods for FAHFA measurement were based on previous literature [23]. In short, for lipid extraction from liver tissue, 150mg tissue was homogenized in 3mL 1:1 methanol/PBS and 3mL chloroform. The mixture was then centrifuged at 14000rpm, 5 min at 4°C. For lipid extraction from plasma 200 µL was added to a mixture of 1.5mL methanol, 1.3mL PBS and 3mL chloroform. After shaking, the mixture was homogenized and centrifuged at 14000rpm for 5min at 4°C. The organic phase of the extracts were transferred to a new vial and dried down under a gentle stream of nitrogen and stored at -20°C. Solid phase extraction (SPE) was performed using a vacuum manifold SPE system to push solvents through a Strata® SI-1 Silica (55 µm, 70 Å), 500 mg / 3 mL Tubes, 50/Pk (Phenomex 8B-S012-HBJ-T). The SPE cartridge was first prewashed with 6 mL of ethyl acetate and then conditioned with 6 mL hexane. Previously extracted lipids were reconstituted in 200 µL chloroform and then applied to the cartridge. Neutral lipids were removed using 6 mL 5% ethyl in hexane, followed by elution of FAHFAs using 4 mL ethyl acetate. The FAHFA fraction was dried down under a gentle stream of nitrogen. Subsequently, the FAHFAs were dissolved in 40 µL of methanol before injection. FAHFAs were measured on an Waters Acquity UPLC coupled to a TQ-XS mass spectrometer (Waters, Milford, Massachusetts, USA) using Multiple Reaction Monitoring (MRM) in negative ionization mode with individually optimized cone voltage and collision energies (Supplemental table 1, <https://doi.org/10.6084/m9.figshare.14617662>). The following MS source parameters were used: spray voltage, 2.0 kV; desolvation temperature, 325°C; source temperature, 150 °C; desolvation gas flow, 900 L/Hr; gas flow cone, 150 L/Hr; and nebulizer, 7.0

Bar. An Acquity UPLC BEH C18 column (1.7 μm , 2.1 mm \times 100 mm, Waters) was used for separation of FAHFAs.

Plasma analysis

Blood from the various mouse studies described previously was collected into EDTA tubes (Sarstedt, Numbrecht, Germany) and spun down for 10 minutes at 2000 g at 4°C. Plasma was aliquoted and stored at -80°C until further measurements. Plasma concentrations of non-esterified fatty acids (Wako Chemicals, Neuss, Germany; HR(2) Kit), triglycerides (Instruchemie, Delfzijl, the Netherlands), glucose (Sopachem, Ochten, the Netherlands) and glycerol (Sigma–Aldrich, Houten, the Netherlands) were determined following the manufacturers' instructions.

Hepatic triglycerides

Liver pieces of ~50 mg were homogenized to a 5% lysate (for high fat diet) or 10% (for fasting) (m/v) containing 10 mM Tris-HCl, 1 mM EDTA, 250 mM sucrose, pH 7.5. Liver triglyceride levels were determined using a commercially available kit from Instruchemie (Delfzijl, The Netherlands).

Statistical Analysis

Data are presented as mean \pm SEM. Comparisons between two groups were made using two-tailed Student's t-test or by two-way ANOVA. $P < 0.05$ was considered as statistically significant.

RESULTS

PPAR α activation upregulates *Adtrp* expression in mouse liver

In order to identify novel target genes of PPAR α , we treated primary mouse hepatocytes with the PPAR α agonist Wy14643 and performed transcriptome analysis [12]. Apart from many well-known PPAR α target genes, one of the genes that was significantly induced by PPAR α activation was *Adtrp* (Figure 1A,B). Expression of *Adtrp* was also significantly induced by PPAR α activation in mouse liver slices (Figure 1C). In addition, treatment of rat hepatoma FAO cells with Wy14643 for different durations significantly increased *Adtrp* expression (Figure 1D). To examine the regulation of *Adtrp* by PPAR α *in vivo*, we treated mice with Wy14643 for 5 days. Treatment with Wy14643 significantly increased *Adtrp* mRNA levels in livers of wildtype mice but not in PPAR α ^{-/-} mice (Figure 1E). A similar strong induction by Wy14643 was observed in ADTRP protein levels using two different antibodies (Figure 1F). To examine the physiological regulation of *Adtrp*, mice were exposed to fasting for different periods of time. A modest increase of hepatic *Adtrp* mRNA levels

was seen in wildtype mice after 6 hours and 12 hours of fasting but not after 24 hours of fasting (Figure 1G). Importantly, *Adtrp* mRNA levels were consistently lower in the livers of PPAR α ^{-/-} mice. To study if *Adtrp* may be directly regulated by PPAR α , ChIP-SEQ data from mouse liver were analyzed to detect possible binding sites for PPAR α in the *Adtrp* promoter region (Figure 1H) [24]. The most prominent peak was located in intron 1 in the region immediately upstream of the transcriptional start site of *Adtrp* transcript variant 2. Multiple PPRES could be identified in this binding site. Collectively, these data show that *Adtrp* expression is upregulated by PPAR α in mouse liver.

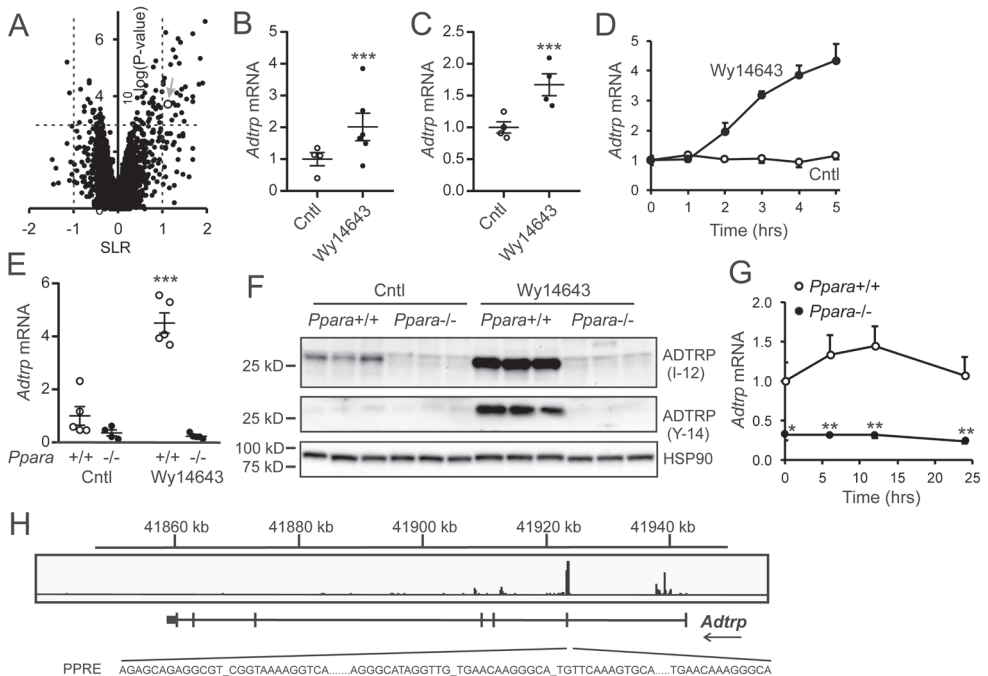


Figure 1. Hepatic *Adtrp* expression is induced by PPAR α
 A) Volcano plot showing the relation between mean signal log ratio ($^2\log[\text{fold change}]$, x-axis) and the $^{-10}\log$ of the P value (y-axis) for the effect of Wy14643 treatment (10 μM , 24h) on the transcriptome of mouse primary hepatocytes. *Adtrp* is indicated by the arrow. mRNA levels of *Adtrp* in mouse primary hepatocytes (n = 4-6 per group) (B) and liver slices (n = 4 per group) (C) incubated with Wy14643 (10 μM , 24h). D) mRNA levels of *Adtrp* in rat FAO hepatoma cells incubated with Wy14643 (10 μM , filled circles) or vehicle (open circles) for increasing duration (n = 3 per group). *Adtrp* mRNA (E) and protein (F) levels in livers of wild-type and *Ppara*^{-/-} mice fed chow containing 0 or 0.1% Wy14643 for 5 days (n = 4-5 per group). G) *Adtrp* mRNA in liver of wild-type (open circles) and *Ppara*^{-/-} mice (filled circles) fasted for different durations. (n = 5 per group). H) Screenshot of the mouse *Adtrp* locus showing ChIP-SEQ profiles of PPAR α in mouse liver. The presence of several PPAR α binding sites within the major PPAR α binding site is indicated. Error bars represent SEM. Asterisks mark a significant effect of Wy14643 compared to control treatment or of *Ppara*^{-/-} compared to wild-type according to Student's T test (* $P < 0.05$; ** $P < 0.01$; *** $P < 0.001$).

***Adtrp* is upregulated by PPAR γ activation in mouse adipocytes**

To learn more about the possible regulation of *Adtrp* by PPARs in other tissues, we explored the tissue expression pattern of *Adtrp*. The highest mRNA levels of *Adtrp* were found in liver and brown adipose tissue (BAT), followed by small intestine and kidney. These tissues are all characterized by a relatively high PPAR α expression. Lower *Adtrp* expression levels were found in white adipose tissue (WAT) (Figure 2A). To study the possible regulation of *Adtrp* by PPAR γ in adipocytes, we first measured *Adtrp* mRNA expression during 3T3-L1 adipogenesis, which is driven by PPAR γ . Expression of *Adtrp* gradually increased during adipogenesis, which was paralleled by an marked increase in expression of *Pparg* as well as the PPAR γ target *Fabp4* (Figure 2B). To study the effect of PPAR γ activation on *Adtrp* expression in differentiated adipocytes, we silenced *Pparg* by siRNA or activated PPAR γ using rosiglitazone. Silencing of *Pparg* in 3T3-L1 adipocytes using siRNA reduced *Pparg* expression by about 90% and *Adtrp* expression by about 50% (Figure 2C), whereas activation of PPAR γ by rosiglitazone increased *Adtrp* expression by about 4-fold (Figure 2D). Transcriptome analysis indicated that in mouse adipose tissue, *Adtrp* was among the 30 most highly induced genes by rosiglitazone treatment (Figure 2E). As for PPAR α , we analyzed CHIP-SEQ data for possible binding sites of PPAR γ in the *Adtrp* promoter region. Multiple PPAR γ binding sites were detected in 3T3-L1 adipocytes, primary adipocytes from WAT and BAT, and WAT and BAT tissues in mice. The most prominent peak was in the same location as found for PPAR α (Figure 2F). Taken together, these data suggest that *Adtrp* expression is upregulated by PPAR γ in mouse adipocytes.

2

Hepatic overexpression of *Adtrp* does not influence diet-induced obesity

In order to elucidate the functional role of ADTRP specifically in the liver, hepatocyte-specific overexpression was achieved via the use of an adeno-associated virus (AAV). Mice were intravenously injected with AAV expressing *Adtrp* (AAV-*Adtrp*) or *Gfp* (AAV-*Gfp*) under the control of the albumin promoter. Based on the results of pilot experiments (Figure 3A), we decided on a dose of AAV of 2.5×10^{11} genomic copies to be used in the rest of the experiments.

Even though high fat feeding did not influence *Adtrp* mRNA in levels in liver and white adipose tissue (Figure 3B), we reasoned that the possible effects of *Adtrp* overexpression on metabolism may be accentuated by high fat feeding, which promotes obesity and associated fatty liver. Mice were given a HFD containing 60 energy% of fat starting 2 weeks after injection of AAV-*Gfp* and AAV-*Adtrp*. Body weight increased upon the switch to a HFD, but no significant differences in weight gain were observed between the two groups of mice (Figure 3C). Also, weight of gWAT and iWAT (Figure 3D), as well as liver weight (Figure 3E) were not significantly

different between the *AAV-Gfp* or *AAV-Adtrp* mice. To examine the effect of ADTRP overexpression on metabolic parameters, we determined plasma levels of cholesterol, glucose, NEFA (non-esterified fatty acids), triglycerides and glycerol. Interestingly, plasma NEFA levels were modestly but statistically significantly higher in *AAV-Adtrp* mice compared to *AAV-Gfp* mice (Figure 3F). By contrast, plasma cholesterol, glucose, triglycerides, and glycerol were not significantly different between the two group of mice (Figure 3F).

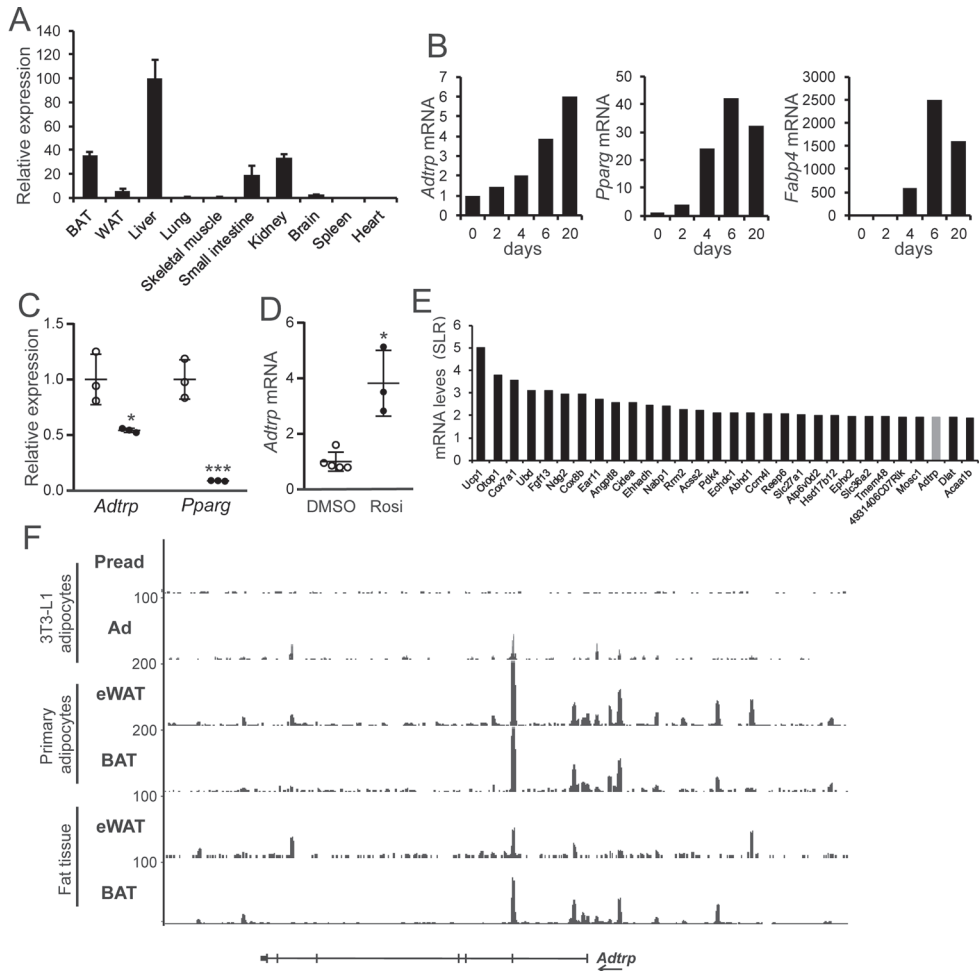


Figure 2. *Adtrp* is induced during adipocyte differentiation and is regulated by PPAR γ

A) mRNA levels of *Adtrp* across various mouse tissues (n = 3). B) mRNA levels of *Adtrp*, *Pparg* and *Fabp4* during differentiation of mouse 3T3-L1 adipocytes. C) mRNA levels of *Adtrp* and *Pparg* in mature 3T3-L1 adipocytes treated with siRNA for *Pparg* or control siRNA (n = 3 replicates). D) *Adtrp* mRNA in mature 3T3-L1 adipocytes treated with Rosiglitazone (5 μ M) for 24h (n = 3-5 replicates). E) The 30 most highly induced genes by 1 week Rosiglitazone treatment (0.01% w/w in feed) in wildtype mice fed a high fat diet for 20 weeks according to transcriptome analysis. SLR, signal log ratio. Error bars represent SEM. Asterisks mark a significant difference compared to control treatment according to Student's T test (*P < 0.05; ***P < 0.001). F) Screenshot of the mouse *Adtrp* locus showing ChIP-SEQ profiles of PPAR γ in 3T3-L1 (pre)adipocytes, primary adipocytes, and whole tissue from mouse WAT and BAT. Ad, adipocytes; Pread, preadipocytes.

Next, we zoomed in on the possible effects of ADTRP overexpression on the liver. Gene expression analysis indicated about 10-fold higher *Adtrp* mRNA levels in the AAV-*Adtrp* mice compared to AAV-*Gfp* mice (Figure 4A). Western blot analysis confirmed a marked induction in ADTRP protein in the AAV-*Adtrp* mice (Figure 4B). To assess the effect of ADTRP overexpression on hepatic gene expression, we performed transcriptome analysis. Strikingly, the only gene that met the statistical significance threshold ($P < 0.001$, $SLR > 1$ or < -1) was *Adtrp* itself (Figure 4C). These data indicate that ADTRP overexpression does not influence hepatic gene expression.

To further examine the metabolic consequences of ADTRP overexpression, we assessed hepatic lipid levels. Total liver triglyceride levels were not significantly different between the AAV-*Gfp* and AAV-*Adtrp* mice (Figure 4D). Semi-targeted lipidomics analysis also did not reveal any significant differences in the total pool of triglycerides, cholesteryl-esters, diacylglycerols, and phosphatidylcholine (Figure 4E). As shown in the Volcano plot, none of the specific lipids met the statistical significance threshold ($P < 0.001$, $SLR > 1$ or < -1) (Figure 4F). These data show that ADTRP overexpression does not influence hepatic lipid levels.

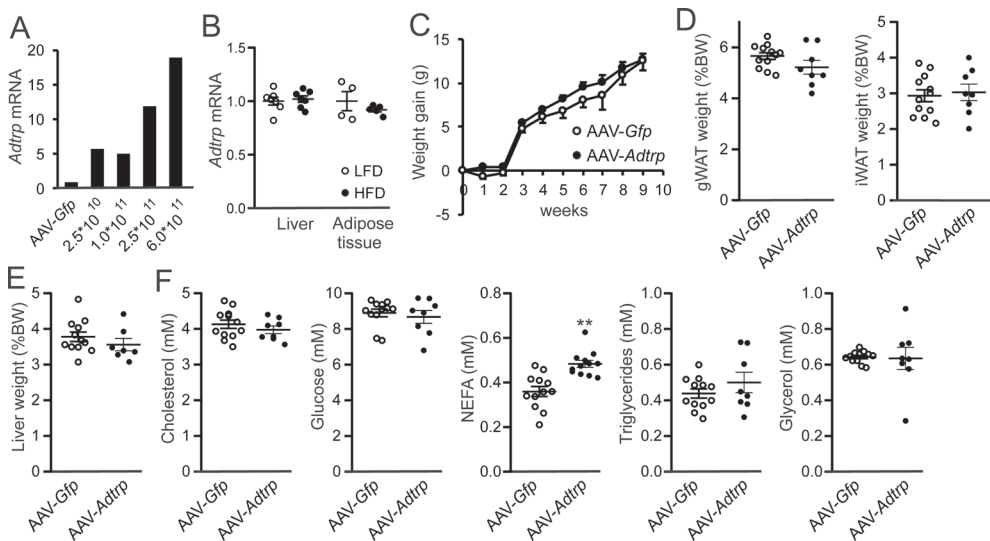


Figure 3. Hepatic overexpression of *Adtrp* combined with high fat feeding does not result in a clear metabolic phenotype

A) Hepatic expression levels of *Adtrp* in mice injected with 2.5×10^{10} , 1.0×10^{11} , 2.5×10^{11} or 6.0×10^{11} genomic copies of AAV expressing *Adtrp* ($n=3$ per group). B) *Adtrp* mRNA levels in liver and adipose tissue of wildtype C57BL/6 mice fed a low fat diet or high fat diet for 20 weeks ($n=4-8$ per group). C) Body weight of mice injected with 2.5×10^{11} genomic copies of AAV-*Gfp* and AAV-*Adtrp* ($n=8-12$ per group) followed two weeks later by a switch to a high fat diet for 7 weeks. D) Weight of gonadal and inguinal adipose tissue depots. E) Liver weight. F) Plasma levels of cholesterol, glucose, non-esterified fatty acids, triglycerides, and glycerol. Error bars represent SEM. Asterisk marks a significant difference compared to control treatment according to Student's T test (** $P < 0.01$).

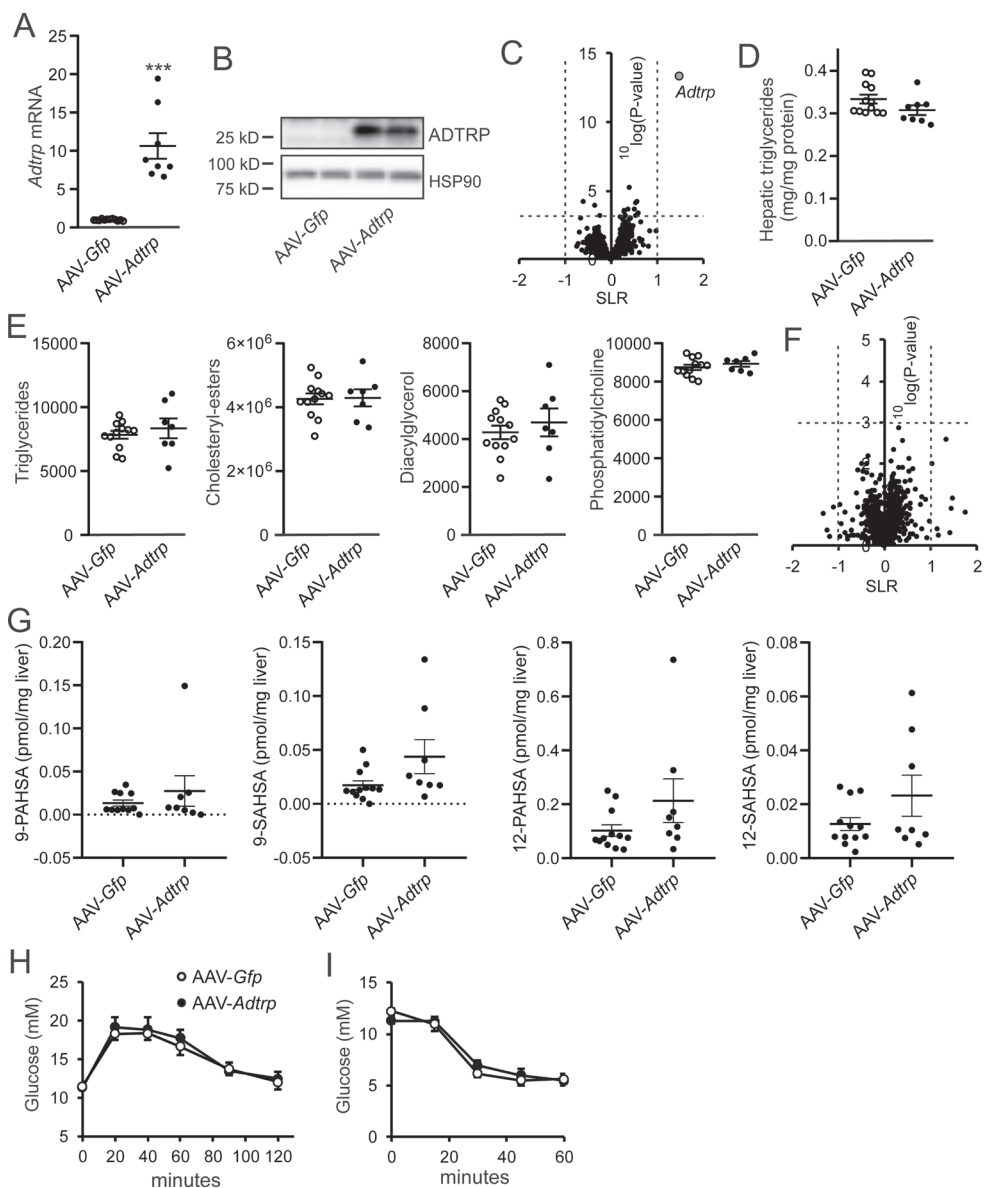


Figure 4. Hepatic overexpression of *Adtrp* combined with high fat feeding does not result in changes in liver transcriptome or liver lipidome.

Mice were injected with 2.5×10^{11} genomic copies of AAV-Gfp and AAV-Adtrp ($n=8-12$ per group) followed three weeks later by a switch to a high fat diet for 7 weeks. Hepatic *Adtrp* mRNA (A) and protein (B) levels. C) Volcano plot showing the relation between mean signal log ratio ($^2\log[\text{fold change}]$, x-axis) and the $^{-10}\log$ of the P value (y-axis) for the comparison of the liver transcriptome between AAV-Gfp and AAV-Adtrp mice. Only *Adtrp* is significantly upregulated (in grey) ($n=8$ per group). D) Liver triglyceride levels. E) Liver levels of the major lipid classes according to lipidomics analysis. F) Volcano plot showing the relation between mean signal log ratio ($^2\log[\text{fold change}]$, x-axis) and the $^{-10}\log$ of the P value (y-axis) for the comparison of the liver lipidome between AAV-Gfp and AAV-Adtrp mice ($n=8-12$ per group). G) Liver levels of selected FAHFs as determined by LCMS ($n=8-12$ per group). Intra-peritoneal glucose (H) and insulin (I) tolerance tests in AAV-Gfp (open circles) and AAV-Adtrp mice (closed circles) ($n=8-12$ per group). Error bars represent SEM. Asterisk indicates significantly different from AAV-Gfp according to the Student's T test (** $P < 0.001$).

ADTRP has been proposed to serve as a hydrolase for a specific class of lipids named FAHFAs [9,25]. Accordingly, we determined the levels of different types of FAHFAs in the liver and plasma of the AAV-*Gfp* and AAV-*Adtrp* mice by LCMS (Figure 4G and Supplemental figure 1). Levels of FAHFAs in the liver were quite variable between animals. No significant differences were observed between AAV-*Gfp* and AAV-*Adtrp* mice for any of the FAHFAs measured in either liver tissue or plasma. Since FAHFAs have been linked to improvements in insulin sensitivity [7,26], we also performed intraperitoneal glucose and insulin tolerance tests. As shown in figures 4H and 4I, neither of these tests showed any significant differences between the AAV-*Gfp* and AAV-*Adtrp* mice. Overall, the data indicate that hepatic overexpression of ADTRP does not cause any detectable metabolic alterations in diet-induced obese mice and does not significantly alter liver and plasma FAHFA levels.

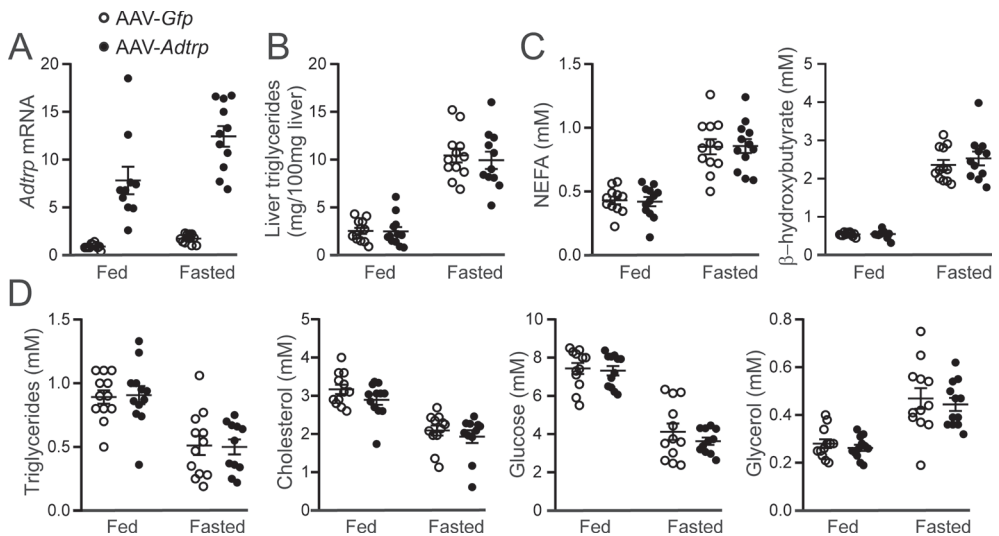


Figure 5. Hepatic *Adtrp* overexpression in the fed and fasted state does not influence plasma metabolite and liver triglyceride levels.

A) Hepatic *Adtrp* mRNA in ad libitum fed or 24 fasted mice 3 weeks post-injection with 2.5×10^{11} genomic copies of AAV-*Gfp* or AAV-*Adtrp* ($n = 12$ per group). B) Liver triglycerides. C) Plasma non-esterified fatty acids (NEFA) and β -hydroxybutyrate. D) Plasma levels of triglycerides, cholesterol, glucose and glycerol. Error bars represent SEM. Two-way ANOVA showed a significant effect of fasting on all parameters and a significant interaction between fasting and genotype for *Adtrp* mRNA ($P < 0.05$).

Hepatic overexpression of *Adtrp* does not influence the hepatic response to fasting

To further investigate the possible functional role of ADTRP in liver metabolism, we studied the effect of ADTRP overexpression under conditions of fasting. To that end, mice were injected with AAV-*Gfp* or AAV-*Adtrp* mice and 3 weeks later the mice were euthanized in the ad libitum fed state or after a 24-hour fast. Injection with AAV-*Adtrp* led to a marked increase in hepatic *Adtrp* mRNA levels (Figure 5A). Fasting caused a marked increase in hepatic triglyceride levels. However, no significant differences were observed between AAV-*Gfp* and AAV-*Adtrp* mice (Figure 5B). Plasma NEFA and β -hydroxybutyrate levels were also increased by fasting but were not significantly different between AAV-*Gfp* and AAV-*Adtrp* mice (Figure 5C). All other plasma metabolites, including cholesterol, triglycerides, glucose, and glycerol showed the typical responses following fasting but were not significantly different between AAV-*Gfp* and AAV-*Adtrp* mice (Figure 5D). Overall, these data indicate that ADTRP overexpression was not associated with any detectable metabolic perturbations in ad libitum fed or fasted mice.

DISCUSSION

Here we provide evidence that *Adtrp* is a novel PPAR γ - and PPAR α -induced gene in adipocytes and liver, respectively. Hepatic overexpression of ADTRP in mice using adeno-associated virus did not lead to any major metabolic abnormalities, either after high fat feeding or after 24 hours of fasting. Notably, glucose tolerance was not significantly affected by ADTRP overexpression. In addition, ADTRP overexpression did not influence the hepatic transcriptome and lipidome. Our data do not support a major role of hepatic ADTRP in lipid and glucose metabolism.

In 2016, Parson et al. showed that ADTRP is a serine hydrolase that catalyzes the hydrolysis of FAHFAs [9]. These FAHFAs were previously detected in serum and tissues of mice and were suggested to confer an insulin-sensitizing effect [7,8]. The most abundant FAHFA is 9-PAHSA, which consists of palmitate linked to hydroxystearate via an ester bond [7,8]. Human serum FAHFA concentrations were found to be positively correlated with insulin sensitivity. In addition, administration of PAHSAs to mice stimulated insulin and GLP-1 secretion, improved glucose tolerance, and reduced adipose tissue inflammation [7]. Subsequent studies found that a diet high in 9-PAHPA and 9-OAHPA increased insulin sensitivity and basal metabolic rate, yet had no effect on glucose tolerance [27,28]. Strikingly, depending on the diet, mice administered 9-PAHPA and 9-OAHPA were also found to develop hepatic steatosis and fibrosis and elevated liver enzyme activity [27][29]. Whether the effects of these pharmacological doses of FAHFAs have any bearing on the role of endogenous FAHFAs is unknown.

In our study, we used an overexpression strategy to study the role of ADTRP. By contrast, others have investigated the effect of targeted ADTRP inactivation. Newborn mice deficient in ADTRP exhibited marked vascular malformations in the low-pressure vasculature, including increased dilation and permeability, leading to reduced viability [30]. In contrast, Ertunc et al. did not observe any differences in viability, supposedly due to a different knockout strategy. Deficiency of ADTRP was associated with increased levels of FAHFAs in WAT and BAT but not in liver. Also, plasma levels of FAHFAs were not altered by ADTRP deficiency [25]. These data confirm the role of ADTRP as FAHFA hydrolyzing enzyme but also suggest that hepatic ADTRP may not be involved in FAHFA hydrolysis. Consistent with this notion, we found that liver-specific overexpression of ADTRP did not significantly alter FAHFA levels in liver and plasma. Intriguingly, ADTRP deficiency had no significant impact on body weight or glucose homeostasis assessed by intraperitoneal glucose tolerance test, oral glucose tolerance tests, or insulin tolerance tests, which might be related to the lack of change in plasma FAHFAs upon ADTRP deficiency [25]. In our study, we found that hepatic overexpression of ADTRP did not significantly influence glucose homeostasis either, nor did ADTRP overexpression influence various other (lipid) metabolic parameters. The only statistically significant parameter was plasma NEFA, levels of which were increased by ADTRP overexpression in mice fed a high fat diet. By contrast, plasma NEFA levels were unaltered by ADTRP overexpression in fasted mice. Collectively, these data do not suggest a major role of hepatic ADTRP in the regulation of glucose and lipid homeostasis.

Since ADTRP has been demonstrated to hydrolyze FAHFAs, we measured FAHFAs in the livers of mice overexpressing ADTRP. FAHFA levels in liver were very low with high inter-sample variation, which is consistent with other studies [7,8,25]. Combined with the relatively high hepatic expression of *Adtrp*, the findings further raise the question whether the enzymatic FAHFA hydrolase activity is the primary function of ADTRP in the liver.

It should be noted that the increase in tissue FAHFAs observed in ADTRP-deficient mice was insufficient to confer protection against glucose intolerance and insulin resistance induced by high fat diet. Accordingly, whereas pharmacological doses of FAHFAs enhance insulin sensitivity in mice, the role of endogenous FAHFAs in the regulation of glucose and lipid metabolism remains ambiguous.

In our study, we show that *Adtrp* is highly expressed in liver, BAT, small intestine, kidney and WAT. This is consistent with the levels of ADTRP protein determined by Ertunc and colleagues [25], who found ADTRP to be highly expressed in liver, BAT, kidney and intestine and to a lesser extent WAT. *ADTRP* has also been shown to be expressed in circulating mononuclear cells and in human atherosclerotic plaque macrophages [31]. In human macrophages, *ADTRP* expression was diminished upon treatment with *PPARG* siRNA and induced upon treatment with a PPAR γ agonist,

marking *ADTRP* as a potential PPAR γ target gene [31]. Regulation of *ADTRP* by PPAR γ is in line with the observed effects of *Pparg* silencing and activation on *Adtrp* mRNA in 3T3-L1 cells. In addition, CHIP-SEQ showed prominent binding of PPAR γ to the promoter region immediately upstream of the transcriptional start site of *Adtrp* transcript variant 2, an area that contains multiple PPREs. Collectively, these data suggest that *Adtrp* may be a direct PPAR γ target gene.

Our study has a number of limitations. First, to study the role of ADTRP in liver we used an overexpression model. It is possible that genetic inactivation of ADTRP more effectively reveals the metabolic role of ADTRP. However, recent studies in ADTRP-deficient mice do not show a metabolic phenotype either [10,25,30]. Second, ADTRP-overexpressing mice were studied after fasting or chronic high fat feeding. It is possible that other metabolic challenges, such as physical exercise, cold exposure, or a ketogenic diet, more clearly reveal the metabolic role of ADTRP. Third, the analysis of the phenotype of ADTRP-overexpressing mice was concentrated on metabolic outcomes. It is possible that the primary role of ADTRP is in vascular biology.

The collective evidence on ADTRP leads to the following conclusions: 1) *Adtrp* is most highly expressed in fast oxidizing tissues, such as liver, brown adipose tissue, kidney and intestine, which mirrors the expression pattern of PPAR α . 2) *Adtrp* is upregulated by PPAR α and PPAR γ . 3) ADTRP hydrolyses FAHFAs in adipose tissue but not in liver, despite higher ADTRP expression levels in liver. 4) Neither hepatic overexpression nor deficiency of ADTRP results in a clear metabolic phenotype. Taken together, our study does not support a major role of hepatic ADTRP in glucose and lipid metabolism.

Acknowledgements

We acknowledge the support from the Netherlands Cardiovascular Research Initiative: an initiative with support of the Dutch Heart Foundation (CVON2014-02 ENERGISE).

Competing interests

None declared

Author contribution

M.D. and S.K. conceived and planned the research and experiments. M.D. carried out all mouse studies. M.D. performed the experiments and analyzed the data. M.v.W. and J.H. optimized and performed the FAHFA and lipidomics analysis. M.D. and S.K. performed the statistical analyses. M.D. and S.K. wrote the manuscript. All authors provided critical feedback and helped to shape the manuscript.

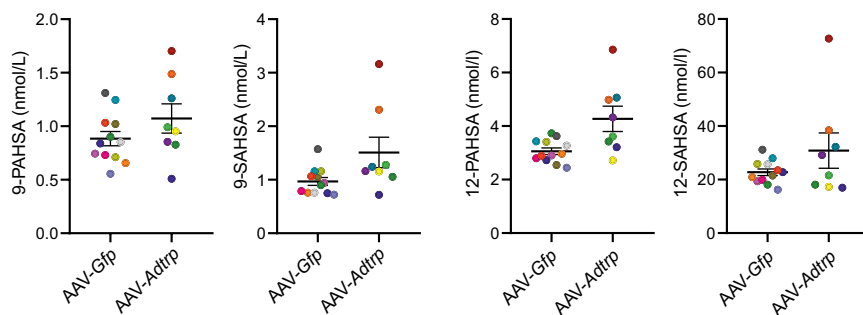
References

- [1] Green, S., Wahli, W., 1994. Peroxisome proliferator-activated receptors: finding the orphan a home. *Molecular and Cellular Endocrinology* 100(1): 149–53, Doi: [https://doi.org/10.1016/0303-7207\(94\)90294-1](https://doi.org/10.1016/0303-7207(94)90294-1).
- [2] Lehmann, J.M., Moore, L.B., Smith-Oliver, T.A., Wilkison, W.O., Willson, T.M., Kliewer, S.A., 1995. An antidiabetic thiazolidinedione is a high affinity ligand for peroxisome proliferator-activated receptor gamma (PPAR gamma). *The Journal of Biological Chemistry* 270(22): 12953–6, Doi: [10.1074/jbc.270.22.12953](https://doi.org/10.1074/jbc.270.22.12953).
- [3] Day, C., 1999. Thiazolidinediones: a new class of antidiabetic drugs. *Diabetic Medicine : A Journal of the British Diabetic Association* 16(3): 179–92, Doi: [10.1046/j.1464-5491.1999.00023.x](https://doi.org/10.1046/j.1464-5491.1999.00023.x).
- [4] Forman, B.M., Chen, J., Evans, R.M., 1997. Hypolipidemic drugs, polyunsaturated fatty acids, and eicosanoids are ligands for peroxisome proliferator-activated receptors alpha and delta. *Proceedings of the National Academy of Sciences of the United States of America* 94(9): 4312–7, Doi: [10.1073/pnas.94.9.4312](https://doi.org/10.1073/pnas.94.9.4312).
- [5] Rakhshandehroo, M., Knoch, B., Müller, M., Kersten, S., 2010. Peroxisome Proliferator-Activated Receptor Alpha Target Genes. *PPAR Research* 2010: 612089, Doi: [10.1155/2010/612089](https://doi.org/10.1155/2010/612089).
- [6] Shen, Y., Su, Y., Silva, F.J., Weller, A.H., Sostre-Colón, J., Titchenell, P.M., et al., 2020. Shared PPAR α / γ Target Genes Regulate Brown Adipocyte Thermogenic Function. *Cell Reports* 30(9): 3079-3091.e5, Doi: <https://doi.org/10.1016/j.celrep.2020.02.032>.
- [7] Yore, M.M., Syed, I., Moraes-Vieira, P.M., Zhang, T., Herman, M.A., Homan, E.A., et al., 2014. Discovery of a class of endogenous mammalian lipids with anti-diabetic and anti-inflammatory effects. *Cell* 159(2): 318–32, Doi: [10.1016/j.cell.2014.09.035](https://doi.org/10.1016/j.cell.2014.09.035).
- [8] Zhu, Q.-F., Yan, J.-W., Gao, Y., Zhang, J.-W., Yuan, B.-F., Feng, Y.-Q., 2017. Highly sensitive determination of fatty acid esters of hydroxyl fatty acids by liquid chromatography-mass spectrometry. *Journal of Chromatography. B, Analytical Technologies in the Biomedical and Life Sciences* 1061–1062: 34–40, Doi: [10.1016/j.jchromb.2017.06.045](https://doi.org/10.1016/j.jchromb.2017.06.045).
- [9] Parsons, W.H., Kolar, M.J., Kamat, S.S., Cognetta, A.B. 3rd., Hulce, J.J., Saez, E., et al., 2016. AIG1 and ADTRP are atypical integral membrane hydrolases that degrade bioactive FAHFAs. *Nature Chemical Biology* 12(5): 367–72, Doi: [10.1038/nchembio.2051](https://doi.org/10.1038/nchembio.2051).
- [10] Lupu, C., Patel, M.M., Lupu, F., 2021. Insights into the Functional Role of ADTRP (Androgen-Dependent TFPI-Regulating Protein) in Health and Disease. *International Journal of Molecular Sciences* 22(9), Doi: [10.3390/ijms22094451](https://doi.org/10.3390/ijms22094451).
- [11] Lupu, C., Zhu, H., Popescu, N.I., Wren, J.D., Lupu, F., Dc, W., 2013. Novel protein ADTRP regulates TFPI expression and function in human endothelial cells in normal conditions and in response to androgen 118(16): 4463–71, Doi: [10.1182/blood-2011-05-355370](https://doi.org/10.1182/blood-2011-05-355370).
- [12] Rakhshandehroo, M., Hooiveld, G., Müller, M., Kersten, S., 2009. Comparative analysis of gene regulation by the transcription factor PPAR α between mouse and human. *PLoS ONE* 4(8), Doi: [10.1371/journal.pone.0006796](https://doi.org/10.1371/journal.pone.0006796).
- [13] Mattijssen, F., Georgiadi, A., Andasarie, T., Szalowska, E., Zota, A., Kronen-Herzig, A., et al., 2014. Hypoxia-inducible Lipid Droplet-associated (HILPDA) is a novel Peroxisome Proliferator-activated Receptor (PPAR) target involved in hepatic triglyceride secretion. *Journal of Biological Chemistry* 289(28): 19279–93, Doi: [10.1074/jbc.M114.570044](https://doi.org/10.1074/jbc.M114.570044).

- [14] Nielsen, R., Pedersen, T.A., Hagenbeek, D., Moulos, P., Siersbaek, R., Megens, E., et al., 2008. Genome-wide profiling of PPAR γ :RXR and RNA polymerase II occupancy reveals temporal activation of distinct metabolic pathways and changes in RXR dimer composition during adipogenesis. *Genes & Development* 22(21): 2953–67, Doi: 10.1101/gad.501108.
- [15] Rajakumari, S., Wu, J., Ishibashi, J., Lim, H.-W., Giang, A.-H., Won, K.-J., et al., 2013. EBF2 determines and maintains brown adipocyte identity. *Cell Metabolism* 17(4): 562–74, Doi: 10.1016/j.cmet.2013.01.015.
- [16] Siersbæk, M.S., Loft, A., Aagaard, M.M., Nielsen, R., Schmidt, S.F., Petrovic, N., et al., 2012. Genome-wide profiling of peroxisome proliferator-activated receptor γ in primary epididymal, inguinal, and brown adipocytes reveals depot-selective binding correlated with gene expression. *Molecular and Cellular Biology* 32(17): 3452–63, Doi: 10.1128/MCB.00526-12.
- [17] Heinz, S., Benner, C., Spann, N., Bertolino, E., Lin, Y.C., Laslo, P., et al., 2010. Simple combinations of lineage-determining transcription factors prime cis-regulatory elements required for macrophage and B cell identities. *Molecular Cell* 38(4): 576–89, Doi: 10.1016/j.molcel.2010.05.004.
- [18] Kent, W.J., Sugnet, C.W., Furey, T.S., Roskin, K.M., Pringle, T.H., Zahler, A.M., et al., 2002. The human genome browser at UCSC. *Genome Research* 12(6): 996–1006, Doi: 10.1101/gr.229102.
- [19] Robinson, J.T., Thorvaldsdóttir, H., Winckler, W., Guttman, M., Lander, E.S., Getz, G., et al., 2011. Integrative genomics viewer. *Nature Biotechnology*: 24–6, Doi: 10.1038/nbt.1754.
- [20] Bolstad, B.M., Irizarry, R.A., Astrand, M., Speed, T.P., 2003. A comparison of normalization methods for high density oligonucleotide array data based on variance and bias. *Bioinformatics (Oxford, England)* 19(2): 185–93, Doi: 10.1093/bioinformatics/19.2.185.
- [21] Irizarry, R.A., Bolstad, B.M., Collin, F., Cope, L.M., Hobbs, B., Speed, T.P., 2003. Summaries of Affymetrix GeneChip probe level data. *Nucleic Acids Research* 31(4): e15, Doi: 10.1093/nar/gng015.
- [22] Dai, M., Wang, P., Boyd, A.D., Kostov, G., Athey, B., Jones, E.G., et al., 2005. Evolving gene/transcript definitions significantly alter the interpretation of GeneChip data. *Nucleic Acids Research* 33(20): e175, Doi: 10.1093/nar/gni179.
- [23] Kolar, M.J., Nelson, A.T., Chang, T., Ertunc, M.E., Christy, M.P., Ohlsson, L., et al., 2018. Faster Protocol for Endogenous Fatty Acid Esters of Hydroxy Fatty Acid (FAHFA) Measurements. *Analytical Chemistry* 90(8): 5358–65, Doi: 10.1021/acs.analchem.8b00503.
- [24] Liang, N., Damdimopoulos, A., Goñi, S., Huang, Z., Vedin, L.-L., Jakobsson, T., et al., 2019. Hepatocyte-specific loss of GPS2 in mice reduces non-alcoholic steatohepatitis via activation of PPAR α . *Nature Communications* 10(1): 1684, Doi: 10.1038/s41467-019-09524-z.
- [25] Eriksi Ertunc, M., Kok, B.P., Parsons, W.H., Wang, J.G., Tan, D., Donaldson, C.J., et al., 2020. AIG1 and ADTRP are endogenous hydrolases of fatty acid esters of hydroxy fatty acids (FAHFAs) in mice. *The Journal of Biological Chemistry* 295(18): 5891–905, Doi: 10.1074/jbc.RA119.012145.
- [26] Moraes-Vieira, P.M., Saghatelian, A., Kahn, B.B., 2016. GLUT4 Expression in Adipocytes Regulates De Novo Lipogenesis and Levels of a Novel Class of Lipids With Antidiabetic and Anti-inflammatory Effects. *Diabetes* 65(7): 1808–15, Doi: 10.2337/db16-0221.

- [27] Benlebna, M., Balas, L., Bonafos, B., Pessemesse, L., Fouret, G., Vigor, C., et al., 2020. Long-term intake of 9-PAHPA or 9-OAHPA modulates favorably the basal metabolism and exerts an insulin sensitizing effect in obesogenic diet-fed mice. *European Journal of Nutrition*, Doi: 10.1007/s00394-020-02391-1.
- [28] Benlebna, M., Balas, L., Bonafos, B., Pessemesse, L., Vigor, C., Grober, J., et al., 2020. Long-term high intake of 9-PAHPA or 9-OAHPA increases basal metabolism and insulin sensitivity but disrupts liver homeostasis in healthy mice. *The Journal of Nutritional Biochemistry* 79: 108361, Doi: 10.1016/j.jnutbio.2020.108361.
- [29] Rychtrmoc, D., Staňková, P., Kučera, O., Červinková, Z., 2020. Comparison of two anti-diabetic monoestolides regarding effects on intact murine liver tissue. *Archives of Physiology and Biochemistry*: 1–8, Doi: 10.1080/13813455.2020.1743322.
- [30] Patel, M.M., Behar, A.R., Silasi, R., Regmi, G., Sansam, C.L., Keshari, R.S., et al., 2018. Role of ADTRP (Androgen-Dependent Tissue Factor Pathway Inhibitor Regulating Protein) in Vascular Development and Function. *Journal of the American Heart Association* 7(22): e010690, Doi: 10.1161/JAHA.118.010690.
- [31] Chinetti-Gbaguidi, G., Copin, C., Derudas, B., Vanhoutte, J., Zawadzki, C., Jude, B., et al., 2015. The coronary artery disease-associated gene C6ORF105 is expressed in human macrophages under the transcriptional control of PPAR γ . *FEBS Letters* 589(4): 461–6, Doi: 10.1016/j.febslet.2015.01.002.

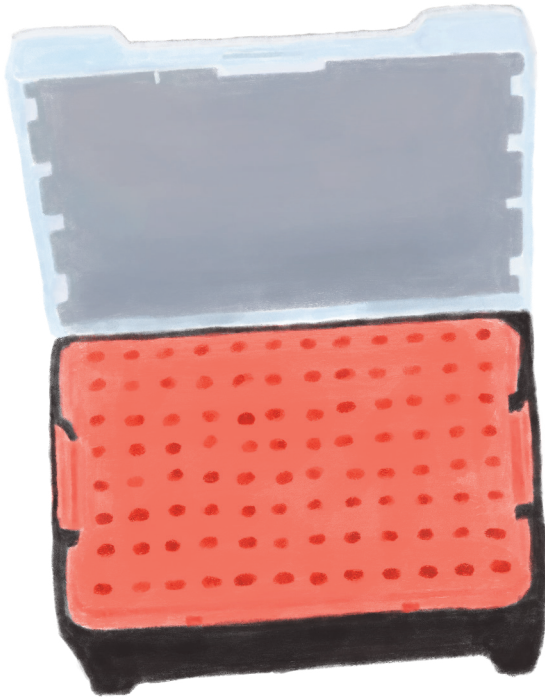
Supplemental materials



Supplemental figure 1. Plasma levels of the most abundant FAHFAs as determined by LCMS. 9-PAHSA: palmitic-acid-9-hydroxy-stearic-acid, 9-SAHSAs: stearic-acid-9-hydroxy-stearic-acid, 12-PAHSA: palmitic-acid-9-hydroxy-stearic-acid, 12-SAHSAs: stearic-acid-9-hydroxy-stearic-acid

Supplemental table 1 Transitions, cone voltage and collision energy used for the FAHFA measurements.

	Q1 [M-H]-	Q3 FA	Q3 HFA	Q3 HFA-H ₂ O	Cone voltage (V)	Collision energy (eV)
9/12 PAHSA	537.5	255.2	-	281.2	52	28
9/12 POHSA	535.23	253.13	299.06	281.03	60	30
9/12 OAHSA	563.25	281.09	299.18	-	80	32
9/12 SAHSA	565.28	282.86	299.12	-	60	30



CHAPTER 3



Probing the role of the PPAR α regulated gene TMED5

Merel Defour and Sander Kersten

ABSTRACT

The peroxisome proliferator activated receptors (PPARs) are a group of transcription factors belonging to the nuclear receptor superfamily. Since most target genes of either PPARs are implicated in lipid and glucose metabolism, regulation by PPARs could be used as a screening tool to identify novel genes involved in lipid or glucose metabolism. Here, we identify *Tmed5* as a novel PPAR-regulated gene. *Tmed5* was significantly upregulated by PPAR α activation in mouse primary hepatocytes, liver slices, and whole liver. In addition, *Tmed5* was upregulated by PPAR γ activation in 3L3-L1 adipocytes and in white adipose tissue. CHIP-SEQ identified a strong PPAR binding site in the immediate upstream promoter of the *Tmed5* gene. Adenoviral-mediated hepatic overexpression of *Tmed5* in diet-induced obese mice did not influence diet-induced obesity, liver triglyceride levels, and plasma cholesterol, triglycerides, glycerol, and glucose levels. Finally, hepatic overexpression of *Tmed5* did not influence liver triglycerides and levels of plasma metabolites in fasted mice. Taken together, our study reveals TMED5 to be a PPAR α target but overexpression of *Tmed5* does not support a major role of hepatic TMED5 in glucose and lipid metabolism.

INTRODUCTION

The liver is a key organ in the control of lipid metabolism. After a meal, the liver produces bile acids that aid in the digestion and absorption of dietary lipids. In addition, the liver takes up the chylomicron remnants produced by the processing of chylomicrons. In the fasted state, the liver serves as a sink for the circulating free fatty acids released from the adipose tissue. In the liver, these fatty acids are either oxidized for energy, partially oxidized and converted into ketone bodies, or esterified into triglycerides. The triglycerides are stored in the liver in lipid droplets or are secreted into the bloodstream as part of very low-density lipoprotein to be used as fuel by other tissues. The ketone bodies are also secreted into the bloodstream and serve as fuel for various organs, including the heart, skeletal muscles, and the brain.

The changes in lipid metabolism in the liver during feeding and fasting are largely driven by changes in the plasma levels of key metabolic hormones such as insulin and glucagon, which in turn stimulate or inhibit the activity of key enzymes through regulation at the transcriptional, translational, and post-translational level. An important group of transcription factors involved in the regulation of lipid metabolism in the liver are the nuclear hormone receptors. Within the group of nuclear receptors, a subgroup of nuclear receptors that play a critical role in the regulation of lipid metabolism in liver and other tissues are the peroxisome proliferator-activated receptors (PPARs) [1]. Three different PPARs can be distinguished: PPAR α (*Nr1c1*), PPAR δ (*Nr1c2*), and PPAR γ (*Nr1c3*). PPARs are ligand-activated transcription factors that can be induced by a variety of different compounds, including environmental contaminants, food components, and drugs, as well as by endogenous lipids [2–4]. In particular, fatty acids and compounds derived from fatty acids such as eicosanoids and endocannabinoids have been shown to serve as endogenous ligands of PPARs.

Expression of PPAR γ is the highest in mature adipocytes. In addition, PPAR γ is abundant in colonocytes and macrophages. PPAR γ is mainly known as the master regulator for adipogenesis by upregulating the expression of numerous genes involved in adipocyte differentiation, glucose and lipid uptake, and lipid storage [5–8]. In contrast to PPAR γ , PPAR δ expression is relatively stable and much more widespread. The role of PPAR δ is best described in heart and skeletal muscle, where it promotes fatty acid oxidation [5,6,8]. The expression of PPAR α is highest fast-oxidizing tissues such as liver, brown adipose tissue, heart and kidney [5,6]. In the liver, PPAR α stimulates the expression of numerous genes involved in nearly every branch of lipid metabolism, including fatty acid uptake, fatty acid (de)activation, mitochondrial and peroxisome fatty acid oxidation, ketogenesis, and the synthesis and degradation of triglycerides and lipid droplets [9,10]. The role of PPAR α in hepatic lipid metabolism is most important during fasting when large quantities of fatty acids are taken up by the liver. Consistent with this notion, mice deficient in PPAR α mainly show metabolic perturbations in the fasted state, including hepatic

steatosis, hypoglycemia, hypoketonemia, and elevated plasma free fatty acids. Inasmuch as many target genes of PPAR α are implicated in hepatic lipid metabolism, regulation by PPAR α could be used as a screening tool to identify novel genes involved in hepatic lipid metabolism. Here we screened for novel genes regulated by PPAR α and describe the identification and characterization of the TMED5 gene.

METHODS AND MATERIALS

Cell experiments

Hepatocytes

Hepatocytes were isolated by two-step collagenase perfusion and plated on collagen-coated plates. Cells were suspended in William's E medium (Lonza Bioscience, Verviers, Belgium) supplemented with 10% (v/v) fetal calf serum, 20 milliunits/ml insulin, 50 nM dexamethasone, 100 units/ml penicillin, 100 g/ml streptomycin, 0.25 g/ml fungizone, and 50 g/ml gentamycin. The next day, cells were incubated in fresh medium supplemented with Wy14643 (5 μ M) dissolved in DMSO or with pure DMSO for 24 h.

3T3-L1 preadipocytes

3T3-L1 preadipocytes (#CL-173) were obtained from ATCC (Manassas, VA, USA). Cells were cultured in DMEM (Gibco, Life Technologies, Blijswijk, the Netherlands) supplemented with 10% FCS and 1% penicillin/streptomycin (Lonza, Verviers, Belgium) in a humidified chamber at 37°C with 5% CO₂. During differentiation, 3T3-L1 cells were cultured in 6-wells plate until 2 days post-confluency. At 2 days post-confluency the induction medium was added (0.5mM IBMX, 5 μ g/ml insulin, 1 μ M dexamethasone) for 3 days. Induction medium was replaced with insulin medium (5 μ g/ml of insulin and 1 μ M of rosiglitazone). The medium was subsequently changed every 3 days, and no further insulin was added after 6 days.

T37i cells

T37i cells were cultured in DMEM (Gibco, Life Technologies, Blijswijk, the Netherlands), supplemented with 10% FBS and 1% P/S. Two days post-confluency, the medium was supplemented with insulin (112 ng/mL) and T3 (2 nM, Sigma-Aldrich) to induce differentiation. After 7 days of differentiation, cells were switched back to regular medium.

Liver Slices

Precision cut liver slices were prepared as described previously [11]. In short, 5 mm cylindrical liver cores were prepared with a surgical biopsy punch and sectioned to 200 μ m slices using a Krumdieck tissue slicer (Alabama Research and Development, Munford, AL, USA) filled with carbonated Krebs-Henseleit buffer (pH 7.4,

supplemented with 25 mM glucose). The precision cut liver slices were incubated in William's E Medium (Lonza, Verviers, Belgium) supplemented with pen/strep in 6-well plates at 37°C/5% CO₂/80% O₂ under continuous shaking (70 rpm). After 1 h, the medium was replaced by fresh William's E Medium containing 0.1% DMSO or 20 μM Wy14643. After incubation for 24 hours the liver slices were snap frozen in liquid nitrogen and stored until further analysis.

Recombinant adeno-associated viruses (AAVs)

AAVs containing *Tmed5* were generated by Vector Biolabs (Philadelphia, PA) and were used for tail-vein injection into mice. In short, mouse *Tmed5* cDNA was inserted in pAAV-ALBP-3iALB, a vector containing a modified albumin promoter flanked by two AAV2-derived inverted terminal repeats [11]. The same amount of AAV2/AAV8 hybrid virus expressing GFP was injected to serve as a control.

Mouse studies

PPARα knock out experiments

Male wild-type and PPARα^{-/-} mice on an Sv129 background were obtained from the Jackson Laboratory (Bar Harbor, ME). All mice were maintained on a 12-h light-dark cycle with ad libitum access to chow and water. For PPARα agonist treatment, five-months of age wild-type and PPARα^{-/-} mice were fed a diet containing Wy14643 (0.1% w/w of feed) for 5 days. For the fasting experiment, five-month-old wild-type and PPARα^{-/-} mice were fasted for 24 h. At the end of each study blood was collected via orbital puncture under isoflurane anesthesia into EDTA tubes. Mice were euthanized via cervical dislocation, after which tissues were collected and snap frozen in liquid nitrogen.

Hepatic Tmed5 overexpression experiments

Male 8-week-old C57BL/6J mice were purchased from Charles River Laboratories (Sulzfeld, Germany) and maintained on a 12-h light-dark cycle with ad libitum access to chow and water. Adeno-associated viruses were administered in a volume of 100 μl via the tail vein. Animals were injected intravenously with different amounts of AAV, ranging from 2.5*10¹⁰, 1*10¹¹, 2.5*10¹¹ and 6*10¹¹ genomic copies, to determine the dose required for a significant increase in hepatic *Tmed5* expression. Male wild-type C57BL/6 mice (9–12 weeks old) were injected with 6*10¹¹ genomic copies of AAV-*Gfp* or AAV-*Tmed5*. Three weeks after injection, mice were fed a high fat diet containing 60 energy percent fat (Research Diets Services, Wijk bij Duurstede, The Netherlands) for 12 weeks. After 12 weeks on this high fat diet, plasma and tissues were collected, snap frozen and stored for later analysis. For the fasting experiment, male wild-type C57BL/6 animals (9–12 weeks old) were injected with 6*10¹¹ genomic copies of AAV-*Gfp* or AAV-*Tmed5*. Three weeks after injection, mice were fasted for 24 hours or remained on an ad libitum chow diet.

After the fasting period, plasma and tissues were collected, snap frozen and stored for subsequent analysis. All animal experiments were approved by the local animal welfare committees of Wageningen.

ChIP-SEQ

Chromatin immunoprecipitation coupled to sequencing (ChIP-SEQ) data sets from 3T3-L1 cells (GSE13511) [12] and mouse eWAT and BAT, either whole tissue (GSE43763) [13] or primary in vitro differentiated adipocytes (GSE41481) [14], were obtained from the Gene Expression Omnibus database. PPAR γ peaks in mouse adipocytes were identified with default settings and scanned for the presence of known motifs using HOMER [15]. The University of California, Santa Cruz, genome browser [16] was used for visualization.

RNA isolations and qPCR

Mouse liver slices and tissues were homogenized in TRIzol[®] (Invitrogen) using the Qiagen TissueLyser II and stainless steel beads. Total RNA was isolated using the RNeasy Micro kit from Qiagen (Venlo, The Netherlands). Subsequently, 500 nanogram RNA (for whole tissues) and 1 microgram (for liver slices) was used to synthesize cDNA using iScript cDNA synthesis kit (Bio-Rad Laboratories, Veenendaal, The Netherlands) for tissues and First Strand cDNA synthesis kit (Thermo Scientific) for liver slices. Messenger RNA levels of *Tmed5* were determined by reverse transcription quantitative PCR using SensiMix (Bioline; GC Biotech, Alphen aan den Rijn, The Netherlands) on a CFX384 real-time PCR detection system (Bio-Rad Laboratories, Veenendaal, the Netherlands). The housekeeping gene *36b4* was used for normalization. Primers were synthesized by Eurogentec (Seraing, Belgium). Primer sequence for *Tmed5* were GCTTTGATAACACATTGAGCACC (forward primer) and CCACTTTTGCTTAGTCTGGACTT (reverse primer).

Microarray analysis

For microarray analysis, RNA was isolated as described above. RNA integrity and quality was analyzed with RNA 6000 Nano chips on the Agilent 2100 Bioanalyzer (Agilent Technologies, Amsterdam, The Netherlands). Purified RNA (100 ng) was labeled with the Ambion WT expression kit (Invitrogen) and hybridized to an Affymetrix Mouse Gene 1.1 ST array plate (Affymetrix, Santa Clara, CA). Hybridization, washing, and scanning were carried out on an Affymetrix GeneTitan platform, and readouts were processed and analyzed according to the manufacturer's instructions. Normalized expression estimates were obtained from the raw intensity values applying the robust multi-array analysis preprocessing algorithm available in the Bioconductor library AffyPLM with default settings [17,18]. Probe sets were defined according to Dai et al. [19]. In this method, probes are assigned to Entrez

IDs as a unique gene identifier using the Entrez Gene database, build 37, version 1 (remapped CDF v22). P-values were calculated using an intensity-based moderated T-statistic (IBMT). Microarray data were submitted to Gene Expression Omnibus (accession number pending).

Protein isolations and western blot

Liver samples and T37i cells were lysed in a mild RIPA-like lysis buffer (25 mM Tris-HCl pH 7.4, 150 mM NaCl, 1 mM EDTA, 1% NP-40 and 5% glycerol; Thermo Scientific) with protease and phosphatase inhibitors (Roche). Protein concentration was determined using a Pierce BCA kit (Thermo Scientific), and equal amounts of protein were diluted with 2× Laemmli sample buffer. Protein lysates were loaded on a 8–16% gradient Criterion gel (Bio-Rad) and separated by SDS gel electrophoresis. Proteins were transferred to a PVDF membrane by means of a Transblot Turbo System (Bio-Rad). Antibodies against TMED5 (1:2000; Santa cruz Biotechnology, catalog no. sc-138688), HSP90 (1:5000; Cell Signaling Technology, Inc., catalog no. 4874), and goat anti-rabbit (1:10.000; Jackson ImmunoResearch, catalog no. 111-035-003) were diluted in 5% (w/v) Tris-buffered saline, pH 7.5, with 0.1% Tween-20 (TBS-T) and 5% dry milk. Primary antibodies were applied overnight at 4 °C, and secondary antibody was applied for 1 h at room temperature. Blots were visualized using the ChemiDoc MP system (Bio-Rad) and Clarity ECL substrate (Bio-Rad).

Plasma analysis

Plasma concentrations of non-esterified fatty acids (Wako Chemicals, Neuss, Germany; HR(2) Kit), triglycerides (InstruChemie, Delfzijl, the Netherlands), glucose (Sopachem, Ochten, the Netherlands) and glycerol (Sigma–Aldrich, Houten, the Netherlands) were determined following the manufacturers' instructions.

Hepatic triglycerides

Liver pieces of ~50 mg were homogenized to a 5% lysate (for high fat diet) or 10% (for fasting) (m/v) containing 10 mM Tris-HCl, 1 mM EDTA, 250 mM sucrose, pH 7.5. Liver triglyceride levels were determined using a commercially available kit from InstruChemie (Delfzijl, The Netherlands).

Statistical Analysis

Data are presented as mean ± SEM. Comparisons between two groups were made using two-tailed Student's t-test or by two-way ANOVA. $P < 0.05$ was considered as statistically significant.

RESULTS

Tmed5 expression in the liver is regulated by PPAR α both ex vivo and in vivo

In order to elucidate novel genes regulated by PPAR α in human liver cells, two microarray datasets were analyzed. In the first dataset, human precision cut liver slices were treated with the PPAR α -agonist Wy14643. In the second dataset, human HepaRG hepatoma cells were treated with the PPAR α -agonist GW7647. Statistical analysis revealed that 113 genes were significantly upregulated by Wy14643 in the liver slices (FDR q value<0.001), while 53 genes were significantly upregulated by GW7647 in the HepaRG cells (Figure 1A). Sixteen genes were commonly induced by PPAR α activation in the liver slices and HepaRG cells, which included many well-known PPAR α target genes such as *PLIN2*, *ANGPTL4*, *CPT1A*, *PDK4*, *ACAA2* and *ACADVL*, as well as a poorly characterized gene named *TMED5*. The induction of *TMED5* by PPAR α activation in human liver slices was confirmed by qPCR and was further observed in primary human hepatocytes (Figure 1B and Figure 1C). These data indicate that the expression of *TMED5* is upregulated by PPAR α in human liver cells.

To further examine the regulation of *TMED5* expression by PPAR α , *Tmed5* mRNA and protein levels were measured in wildtype and PPAR α ^{-/-} mice treated for 5 days with Wy14643. Supporting the in vivo regulation of *TMED5* by PPAR α , mRNA (Figure 1D) and protein (Figure 1E) levels of *Tmed5* were markedly induced by Wy14643 in the livers of wildtype but not PPAR α ^{-/-} mice. Since PPAR α is activated physiologically during fasting, we also studied the regulation of *TMED5* by PPAR α in the fed and fasted state. Resembling the expression profile observed upon Wy14643 treatment, mRNA (Figure 1F) and protein (Figure 1G) levels of *Tmed5* were markedly induced by fasting in the livers of wildtype but not PPAR α ^{-/-} mice.

PPARs activate gene expression by binding to specific DNA elements near target genes. ChIP-SEQ data from mouse liver were analyzed to detect possible binding sites for PPAR α in the *Tmed5* promoter region (Figure 1H) [20]. A prominent PPAR α binding site was found around the transcriptional start site and at the start of the first intron of the mouse *Tmed5* gene. Collectively, these data show that *TMED5* is regulated by PPAR α in mouse liver.

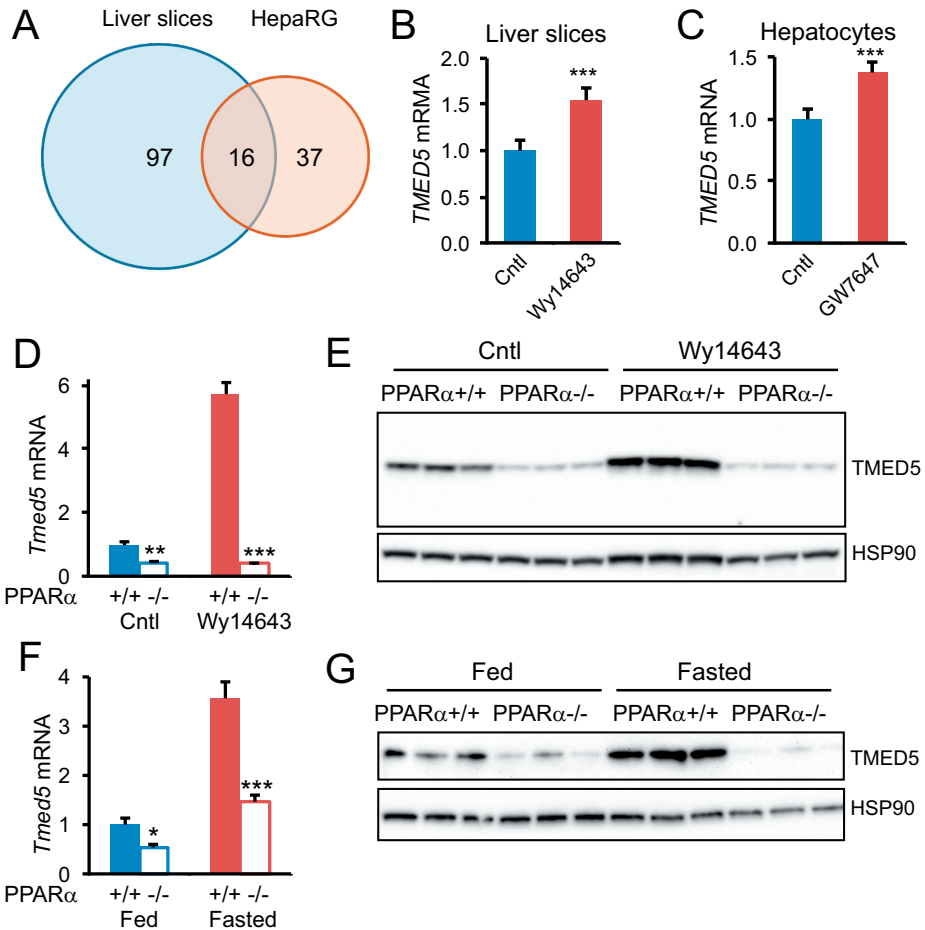


Figure 1. Hepatic *Tmed5* expression is induced by PPAR α

Venn diagram showing amount of overlapping genes induced by PPAR α agonists Wy14643 or GW7647 in liver slices and HepaRG cells (A). mRNA level of *Tmed5* in liver slices incubated with Wy14643 (B) and hepatocytes incubated with GW7647 (C). *Tmed5* mRNA (D) and protein (E) levels in livers of wild-type and *Ppara*^{-/-} mice fed chow containing 0 or 0.1% Wy14643 for 5 days. *Tmed5* mRNA (F) and protein (G) levels in livers of wild-type and *Ppara*^{-/-} mice in fed or fasted state. Screenshot of the mouse *Tmed5* locus showing ChIP-SEQ profiles of PPAR α in mouse liver (H). Error bars represent SE. Asterisks mark a significant effect compared to control treatment according to Student's T test (* P < 0.05, ** P < 0.01; *** P < 0.001).

Tmed5 expression is high in liver and adipose tissue and is induced during fat cell differentiation

Currently, very little is known about TMED5. For this reason, we explored the tissue expression pattern of TMED5 at the gene and protein level. The highest mRNA and protein levels of TMED5 were found in liver and brown adipose tissue (BAT), followed by white adipose tissue (WAT) (figure 2A and 2B).

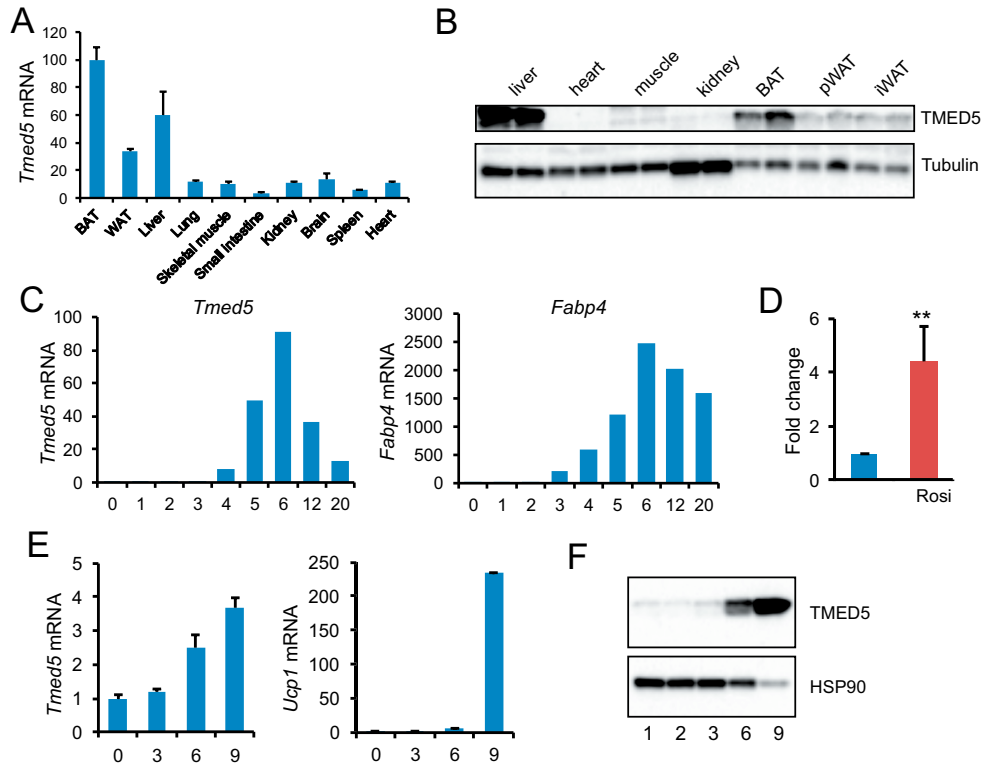
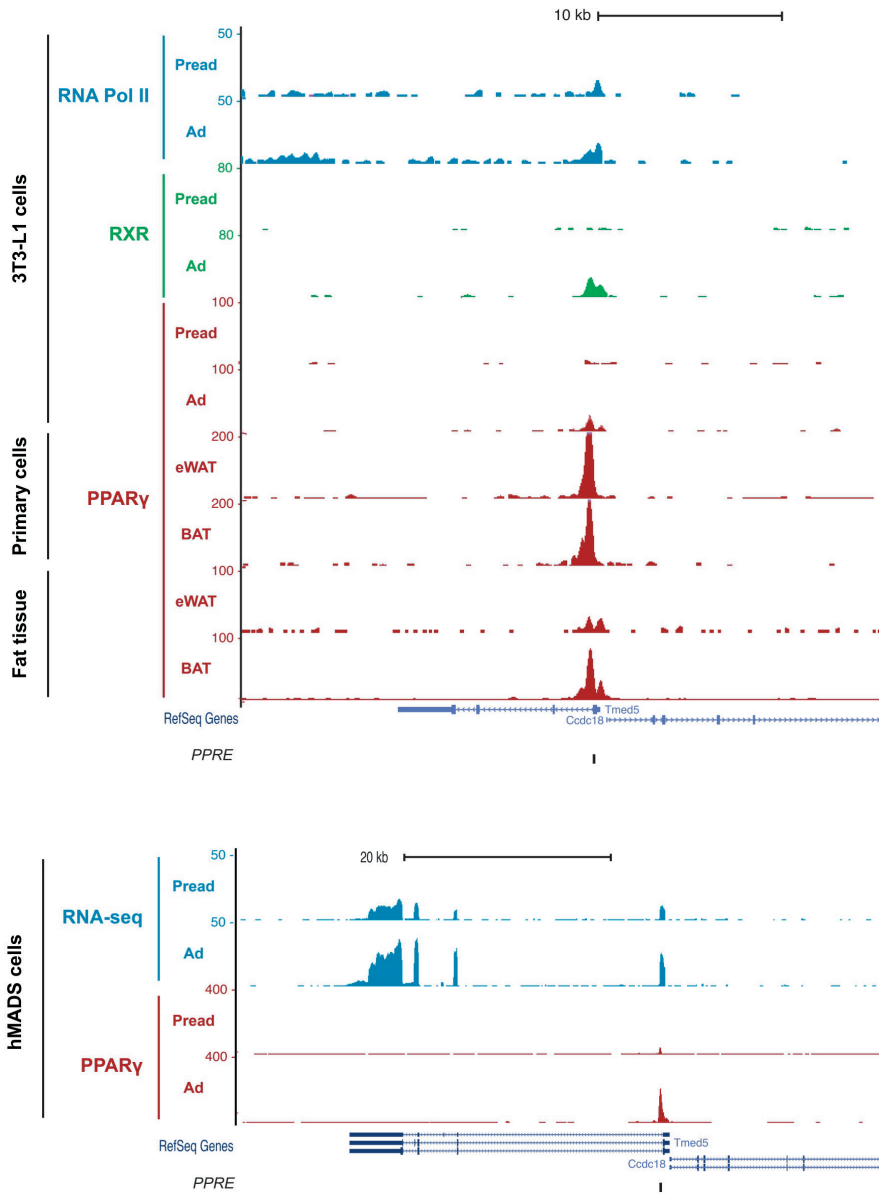


Figure 2. *Tmed5* expression in adipose tissue and during adipocyte differentiation

mRNA (A) and protein (B) levels of *Tmed* across various mouse tissues. C) mRNA levels of *Tmed5* and *Fabp4* during differentiation of mouse 3T3-L1 adipocytes. D) *Tmed5* mRNA in mature 3T3-L1 adipocytes treated with Rosiglitazone (5 μ M) for 24h. E) mRNA levels of *Tmed5* and *UCP1* during differentiation of mouse T37i adipocytes. F) protein levels of TMED5 during differentiation of mouse T37i adipocytes. Error bars represent SE. Asterisks mark a significant difference compared to control treatment according to Student's T test (**P < 0.01).



3

Figure 3. ChIP-SEQ analysis reveals a possible binding site for PPARγ on *Tmed5*

Screenshot of the mouse *Adtrp* locus showing ChIP-SEQ profiles of PPARγ in 3T3-L1 (pre)adipocytes, primary adipocytes, and whole tissue from mouse WAT and BAT. Ad, adipocytes; Pread, preadipocytes.

PPAR α is highly expressed in the liver and BAT, but weakly expressed in WAT. By contrast, PPAR γ is highly expressed in WAT, where it drives adipocyte differentiation. Interestingly, expression of *Tmed5* markedly increased during 3T3-L1 mouse adipocyte differentiation, resembling the PPAR γ target gene *Fabp4* (Figure 2C). Consistent with the upregulation of *Tmed5* by PPAR γ , expression of *Tmed5* in 3T3-L1 adipocytes was induced by treatment with the PPAR γ agonist rosiglitazone (Figure 2D). *Tmed5* mRNA levels also increased upon differentiation of mouse T37i cells, which differentiate towards a brown adipocyte phenotype characterized by the expression of UCP1. Differentiation of T37i towards brown adipocytes was also associated with a marked increase in TMED5 protein (Figure 2E and 2F). These data indicate that *Tmed5* expression is induced by adipocyte differentiation and hint at a possible regulation of TMED5 by PPAR γ .

TMED5 is a direct PPAR γ target

Using CHIP-SEQ data of genomic binding of PPAR γ from mouse 3T3-L1 adipocytes, mouse primary epididymal WAT- and BAT-derived adipocytes, we found strong binding of PPAR γ and to a lesser extent RXR to a binding site at the start of the first intron of the mouse *Tmed5* gene. The strongest PPAR γ binding to this site was observed in primary mouse adipocytes from the epididymal fat pad. This binding site was retained in human MADS adipocytes (Figure 3). These data suggest that *Tmed5* may be a direct PPAR γ target gene in mouse and human adipocytes.

Hepatic overexpression of *Tmed5* has no influence on lipid metabolism in diet-induced obese mice

Inasmuch of *Tmed5* expression is under control of PPAR α and PPAR γ in liver and adipose tissue, respectively, we reasoned that TMED5 may play a role in lipid metabolism. To investigate the functional role of TMED5, we overexpressed *Tmed5* specifically in the liver of mice via injection of an adeno-associated virus expressing *Tmed5* (AAV-*Tmed5*) or GFP (AAV-*Gfp*) under the influence of a modified albumin promoter. First, we tested the optimal dose for a physiologically relevant overexpression by injecting incremental doses of AAV-*Tmed5*. *Tmed5* expression increased about 2-fold at the low and intermediate doses, but went up about 5-fold at the highest dose (Figure 4A). Since this level of induction resembles the effect of fasting in mouse liver, we chose the highest dose for the rest of our experiments.

To study the effect of *Tmed5* overexpression on lipid metabolism and diet-induced obesity, mice were injected with 6×10^{11} GC of either AAV-*Gfp* or AAV-*Tmed5*. Three weeks after the injection, the mice were placed on a high fat (60% fat) diet for 11 weeks. The body weight increased rapidly after the switch from chow to the high fat diet. However, no differences in body weight were observed between the two groups (Figure 4B). Also, food intake was similar in the two groups (Figure 4C). As

observed in the pilot study, *Tmed5* mRNA levels were about 4-5 fold higher in the AAV-*Tmed5* mice compared to the AAV-*Gfp* mice (Figure 4D). The overexpression of *Tmed5* in the AAV-TMED5 group was confirmed at the protein level (Figure 4E).

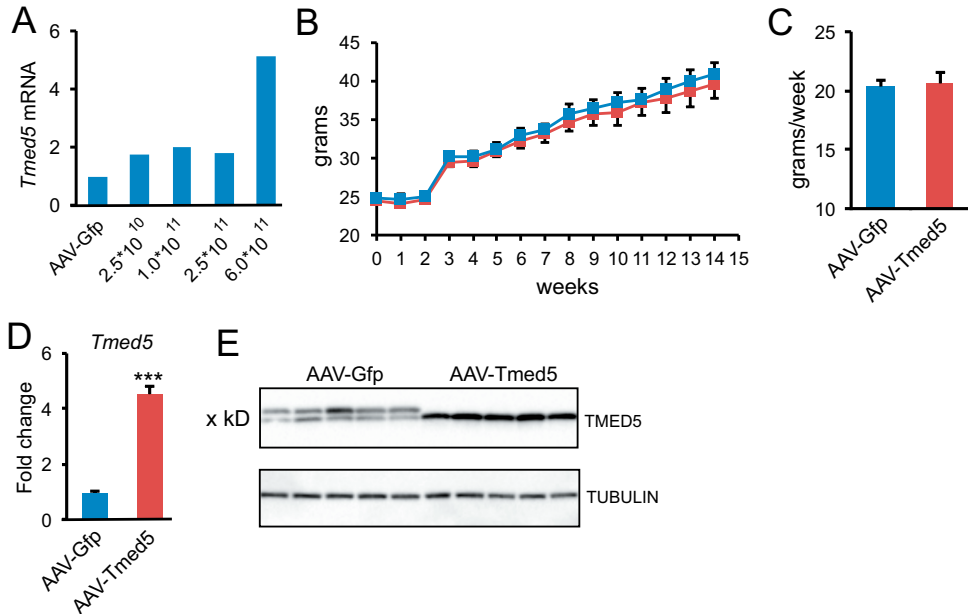


Figure 4. Hepatic overexpression of *Tmed5* combined with high fat feeding does not result in changes in body weight or food intake

A) Hepatic expression levels of *Tmed5* in mice injected with 2.5×10^{10} , 1.0×10^{11} , 2.5×10^{11} or 6.0×10^{11} genomic copies of AAV expressing *Tmed5* (n=3 per group). Body weight (B) and food intake (C) of mice injected with 6×10^{11} genomic copies of AAV-*Gfp* and AAV-*Adtrp* (n=12 per group) followed two weeks later by a switch to a high fat diet for 11 weeks. Hepatic *Tmed5* mRNA (D) and protein (E) levels. Error bars represent SE. Asterisk marks a significant difference compared to control treatment according to Student's T test (***P < 0.001).

Overexpression of *Tmed5* did not influence the weight of liver, gonadal fat pad, inguinal fat pad or perirenal fat pad (Figure 5A). Also, plasma levels of cholesterol, glucose, free fatty acids, triglycerides and glycerol levels were not significantly different between AAV-*Tmed5* and AAV-*Gfp* mice (Figure 5B). To further explore the possible role of TMED5, we performed transcriptomics analysis on the livers of AAV-*Tmed5* and AAV-*Gfp* mice. Strikingly, the only gene that met the statistical significance threshold (P<0.001, SLR>1 or <-1) was *Tmed5* itself (Figure 5C).

Rather than looking at individual genes, we performed gene set enrichment analysis (GSEA) to gain insight into whole pathways that may be altered by *Tmed5* overexpression. Interestingly, most of the positively enriched pathways were related to mitochondria, including mitochondrial translation and the electron transport chain (Figure 5D). The enrichment plot for the pathway WP295 electron

transport chain is shown in figure 5E. These data hint at a potential effect of *Tmed5* overexpression on mitochondrial function.

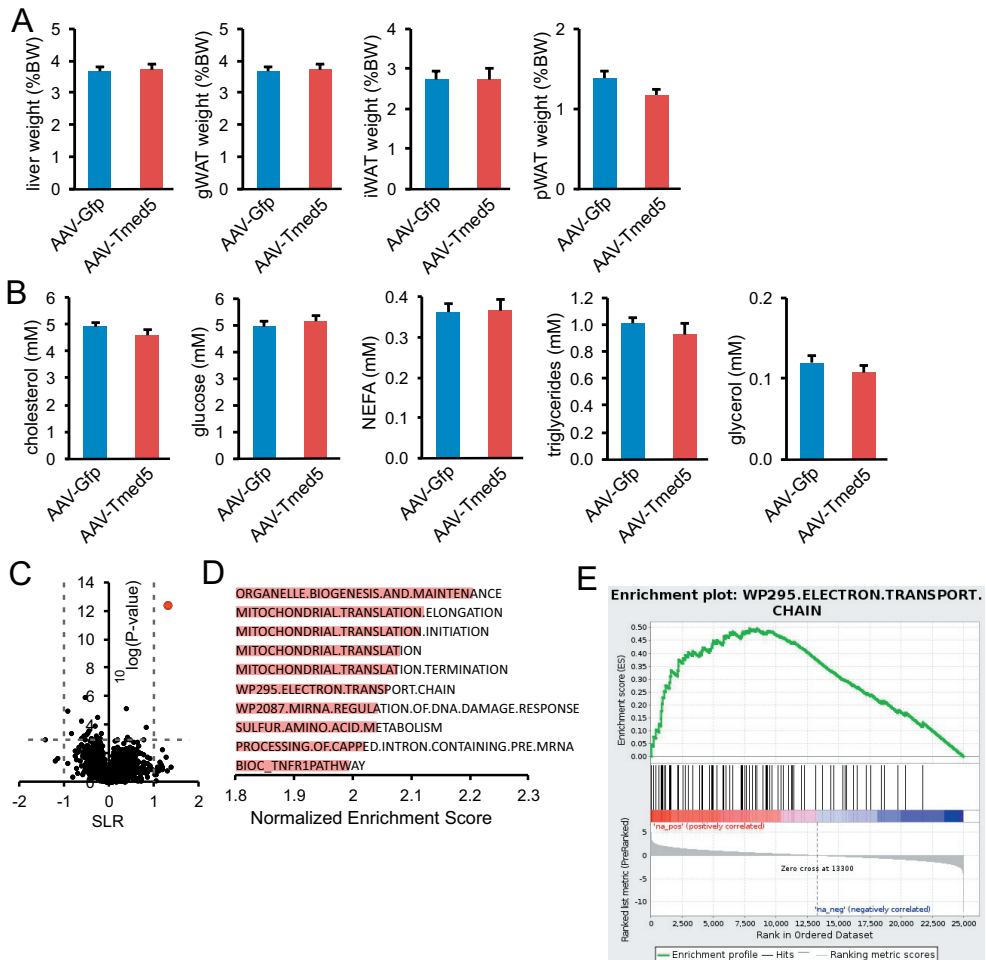


Figure 5. Hepatic overexpression of *Tmed5* combined with high fat feeding does not result in a specific phenotype on physiological parameters

A) Weight of liver and gonadal, inguinal and perirenal adipose tissue depots. B) Plasma levels of cholesterol, glucose, non-esterified fatty acids, triglycerides, and glycerol. C) Volcano plot showing the relation between mean signal log ratio (2log[fold change], x-axis) and the $-10\log$ of the P value (y-axis) for the comparison of the liver transcriptome between AAV-Gfp and AAV-Tmed5 mice. Only *Tmed5* is significantly upregulated (in red) (n=8 per group). D) Positively enriched pathways based on gene set enrichment analysis (GSEA). E) Enrichment plot of the electron transport chain. Error bars represent SE.

Since hepatic *Tmed5* expression is induced by fasting, we next aimed to study the influence of *Tmed5* overexpression on lipid metabolism during fasting. To that end, mice were injected with the highest dose of AAV-*Tmed5* or AAV-*Gfp* and after three weeks the mice were euthanized in the ad libitum fed state or after a 24-hour-fast. The elevation of *Tmed5* mRNA by injection of AAV-*Tmed5* was very similar to the effect of fasting on *Tmed5* mRNA (Figure 6A). As expected, fasting causes a marked increase in liver triglyceride storage. However, no significant difference in hepatic triglycerides was observed between the AAV-*Tmed5* and AAV-*Gfp* mice (Figure 6B). Plasma NEFA and β -hydroxybutyrate levels were also increased by fasting but were not significantly different between AAV-*Gfp* and AAV-*Tmed5* mice (Figure 5C). In addition, fasting caused the expected changes in plasma triglycerides, cholesterol, glucose, and glycerol, but again, no significant differences were observed between the AAV-*Tmed5* and AAV-*Gfp* mice (Figure 6D). Taken together, our data do not support a major effort of *Tmed5* overexpression on metabolic parameters.

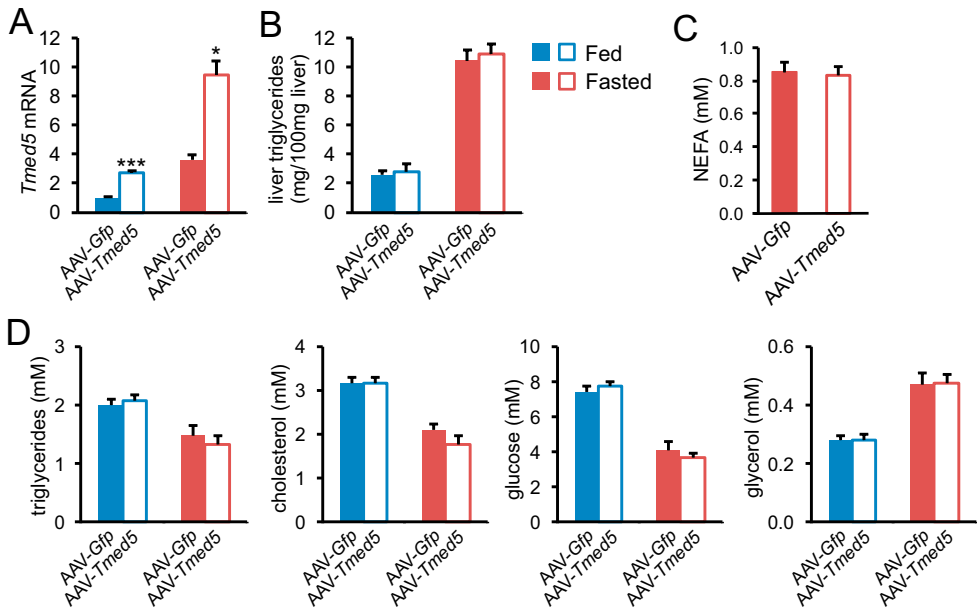


Figure 6. Hepatic *Tmed5* overexpression in the fed and fasted state does not influence plasma metabolite and liver triglyceride levels

A) Hepatic *Tmed5* mRNA in ad libitum fed or 24h fasted mice 3 weeks post-injection with 6×10^{11} genomic copies of AAV-*Gfp* or AAV-*Tmed5* ($n = 12$ per group). B) Liver triglycerides. C) Plasma non-esterified fatty acids (NEFA) and β -hydroxybutyrate. D) Plasma levels of triglycerides, cholesterol, glucose and glycerol. Error bars represent SE. Two-way ANOVA showed a significant effect of fasting on all parameters and a significant interaction between fasting and genotype for *Tmed5* mRNA (* $P < 0.05$, *** $P < 0.001$).

DISCUSSION

In this paper, we identified and characterize a novel putative PPAR α target: transmembrane emp24 domain-containing protein 5 (TMED5). Our data clearly show regulation of *Tmed5* by PPAR α agonists *in vitro* and *in vivo*, and upon fasting. Additionally, we propose a PPAR binding site at the start of the first intron of the mouse and human *Tmed5* gene. Combined, we show *Tmed5* to be a PPAR α target. Subsequently, we performed experiments in mice overexpressing TMED5 specifically in liver. Here we reveal no major alterations in the response to a HFD or fasting.

To this date, little is known about TMED5. TMED5, also referred to as p28, p24 γ 2, and CGI-100, is shown to be part of the p24 protein family. Different functions are attributed to the various members of this p24 protein family, all believed to be part of the early secretory pathway [21]. First, the family members are proposed to serve as cargo receptors, transporting proteins from the ER to the Golgi. Secondly, p24 proteins are shown to be part of COPII- and COPI-coated vesicles [22–24]. TMED5 specifically is shown to be localized to the perinuclear region and to punctate structures in the cell, which colocalize with Golgi markers and COPII coat components [25]. TMED5 is referred to as an ERGIC/cis Golgi protein and depletion of *Tmed5* via siRNA perturbs Golgi organization, indicating its necessity for the formation of the Golgi ribbon [25]. Additionally, knock down of TMED5 in mice impaired the transport of Glycosylphosphatidylinositol-anchored proteins (GPI-AP) [26]. GPI-anchored proteins are directed to the ER and subsequently, via the secretory pathway, with help of vesicles to the Golgi and finally to the plasma membrane where cleavage by phospholipases will result in controlled release of the protein [27,28]. Many GPI-anchored proteins are known to play key roles in biological processes [27].

Based on the literature and our own findings, we know that TMED5 is A) present in the Golgi and in vesicle like structures, B) is probably involved in lipid metabolism C) is present in fast oxidizing tissues like liver, brown and white adipose tissue, kidney and intestine, D) is highly upregulated upon fasting and E) possibly transports a GPI-anchored protein to the cell membrane.

Speculation about the possible proteins transported by TMED5 leads us towards proteins linked to lipid metabolism, proposed to be extracellularly and expressed in liver and BAT, such as, but not exclusively, retinoic acid receptor responder 2 (*Rarres2*, encoding for the protein Chimerin), selenoprotein P (*Sepp1*), paraoxonase 3 (*Pon3*), retinol binding protein 4 (*Rbp4*) and apolipoprotein C1 (*ApoC1*) [29–34]. Although these proteins are not proposed to be GPI-AP as predicted by PredGPI [28]. Hepatic *Tmed5* expression goes up significantly during fasting. In general, processes activated in the liver during fasting are ketogenesis, gluconeogenesis,

lipolysis and fatty acid oxidation. Metabolites and proteins being transported out of the liver, but are not exclusive to the liver, during these processes should be considered as possibly being transported via TMED5.

Based on this knowledge, future research should focus more on protein instead of RNA levels. By performing (untargeted) proteomic analysis in medium of primary hepatocytes overexpressing *Tmed5* via for example mass spectrometry, possible differences in excreted proteins can be detected. Furthermore, developing a good antibody and subsequently performing Co-Immunoprecipitation experiments may reveal proteins transported by TMED5.

Our study has a number of limitations. In order to unravel TMED5s function, we used adeno-associated viruses to overexpress *Tmed5* specifically in the liver. It is possible that genetic inactivation of *Tmed5* more effectively reveals the metabolic role of TMED5. Secondly, a tissue specific approach limits possible crosstalk of organs. Using a whole body approach may help unravel the function of TMED5. Thirdly, TMED5-overexpressing mice were studied after chronic high fat feeding and fasting. It is possible that other metabolic challenges, such as physical activity, cold exposure, or a different diet, more clearly reveal the metabolic role of TMED5.

Taken together, our study reveals TMED5 to be a PPAR α target. Overexpression of *Tmed5* does not support a major role of hepatic TMED5 in glucose and lipid metabolism on gene level. Future studies should perhaps concentrate on changes in protein level or can use a knock out system.

Acknowledgements

We acknowledge the support from the Netherlands Cardiovascular Research Initiative: an initiative with support of the Dutch Heart Foundation (CVON2014-02 ENERGISE)

Competing interests

None declared

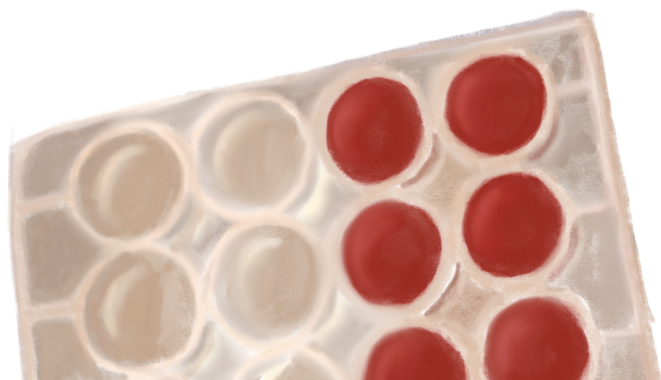
References

- [1] Green, S., Wahli, W., 1994. Peroxisome proliferator-activated receptors: finding the orphan a home. *Molecular and Cellular Endocrinology* 100(1): 149–53, Doi: [https://doi.org/10.1016/0303-7207\(94\)90294-1](https://doi.org/10.1016/0303-7207(94)90294-1).
- [2] Lehmann, J.M., Moore, L.B., Smith-Oliver, T.A., Wilkison, W.O., Willson, T.M., Kliewer, S.A., 1995. An antidiabetic thiazolidinedione is a high affinity ligand for peroxisome proliferator-activated receptor gamma (PPAR gamma). *The Journal of Biological Chemistry* 270(22): 12953–6, Doi: 10.1074/jbc.270.22.12953.
- [3] Day, C., 1999. Thiazolidinediones: a new class of antidiabetic drugs. *Diabetic Medicine : A Journal of the British Diabetic Association* 16(3): 179–92, Doi: 10.1046/j.1464-5491.1999.00023.x.
- [4] Forman, B.M., Chen, J., Evans, R.M., 1997. Hypolipidemic drugs, polyunsaturated fatty acids, and eicosanoids are ligands for peroxisome proliferator-activated receptors alpha and delta. *Proceedings of the National Academy of Sciences of the United States of America* 94(9): 4312–7, Doi: 10.1073/pnas.94.9.4312.
- [5] Braissant Olivier, Fougelle Fabienne, Scotto Christian, Dauca Michel, W.W., 1996. Differential Expression of Peroxisome Proliferator Activated Receptors (PPARs): Tissue Distribution of PPAR-a, -b, and -gamma in the Adult Rat*. *Endocrinology* 137(1).
- [6] Auboeuf, D., Rieusset, J., Fajas, L., Vallier, P., Frering, V., Riou, J.P., et al., 1997. Tissue distribution and quantification of the expression of mRNAs of peroxisome proliferator-activated receptors and liver X receptor-alpha in humans: no alteration in adipose tissue of obese and NIDDM patients. *Diabetes* 46(8): 1319–27, Doi: 10.2337/diab.46.8.1319.
- [7] Janani, C., Ranjitha Kumari, B.D., 2015. PPAR gamma gene--a review. *Diabetes & Metabolic Syndrome* 9(1): 46–50, Doi: 10.1016/j.dsx.2014.09.015.
- [8] Han, L., Shen, W.-J., Bittner, S., Kraemer, F.B., Azhar, S., 2017. PPARs: regulators of metabolism and as therapeutic targets in cardiovascular disease. Part II: PPAR-β/δ and PPAR-γ. *Future Cardiology* 13(3): 279–96, Doi: 10.2217/fca-2017-0019.
- [9] Kersten, S., Seydoux, J., Peters, J.M., Gonzalez, F.J., Desvergne, B., Wahli, W., 1999. Peroxisome proliferator-activated receptor alpha mediates the adaptive response to fasting. *Journal of Clinical Investigation* 103(11): 1489–98, Doi: 10.1172/JCI6223.
- [10] Wang, Y., Nakajima, T., Gonzalez, F.J., Tanaka, N., 2020. PPARs as Metabolic Regulators in the Liver: Lessons from Liver-Specific PPAR-Null Mice. *International Journal of Molecular Sciences* 21(6), Doi: 10.3390/ijms21062061.
- [11] Mattijssen, F., Georgiadi, A., Andasarie, T., Szalowska, E., Zota, A., Krones-Herzig, A., et al., 2014. Hypoxia-inducible Lipid Droplet-associated (HILPDA) is a novel Peroxisome Proliferator-activated Receptor (PPAR) target involved in hepatic triglyceride secretion. *Journal of Biological Chemistry* 289(28): 19279–93, Doi: 10.1074/jbc.M114.570044.
- [12] Nielsen, R., Pedersen, T.A., Hagenbeek, D., Moulos, P., Siersbaek, R., Megens, E., et al., 2008. Genome-wide profiling of PPARgamma:RXR and RNA polymerase II occupancy reveals temporal activation of distinct metabolic pathways and changes in RXR dimer composition during adipogenesis. *Genes & Development* 22(21): 2953–67, Doi: 10.1101/gad.501108.

- [13] Rajakumari, S., Wu, J., Ishibashi, J., Lim, H.-W., Giang, A.-H., Won, K.-J., et al., 2013. EBF2 determines and maintains brown adipocyte identity. *Cell Metabolism* 17(4): 562–74, Doi: 10.1016/j.cmet.2013.01.015.
- [14] Siersbæk, M.S., Loft, A., Aagaard, M.M., Nielsen, R., Schmidt, S.F., Petrovic, N., et al., 2012. Genome-wide profiling of peroxisome proliferator-activated receptor γ in primary epididymal, inguinal, and brown adipocytes reveals depot-selective binding correlated with gene expression. *Molecular and Cellular Biology* 32(17): 3452–63, Doi: 10.1128/MCB.00526-12.
- [15] Heinz, S., Benner, C., Spann, N., Bertolino, E., Lin, Y.C., Laslo, P., et al., 2010. Simple combinations of lineage-determining transcription factors prime cis-regulatory elements required for macrophage and B cell identities. *Molecular Cell* 38(4): 576–89, Doi: 10.1016/j.molcel.2010.05.004.
- [16] Kent, W.J., Sugnet, C.W., Furey, T.S., Roskin, K.M., Pringle, T.H., Zahler, A.M., et al., 2002. The human genome browser at UCSC. *Genome Research* 12(6): 996–1006, Doi: 10.1101/gr.229102.
- [17] Bolstad, B.M., Irizarry, R.A., Astrand, M., Speed, T.P., 2003. A comparison of normalization methods for high density oligonucleotide array data based on variance and bias. *Bioinformatics (Oxford, England)* 19(2): 185–93, Doi: 10.1093/bioinformatics/19.2.185.
- [18] Irizarry, R.A., Bolstad, B.M., Collin, F., Cope, L.M., Hobbs, B., Speed, T.P., 2003. Summaries of Affymetrix GeneChip probe level data. *Nucleic Acids Research* 31(4): e15, Doi: 10.1093/nar/gng015.
- [19] Dai, M., Wang, P., Boyd, A.D., Kostov, G., Athey, B., Jones, E.G., et al., 2005. Evolving gene/transcript definitions significantly alter the interpretation of GeneChip data. *Nucleic Acids Research* 33(20): e175, Doi: 10.1093/nar/gni179.
- [20] Liang, N., Damdimopoulos, A., Goñi, S., Huang, Z., Vedin, L.-L., Jakobsson, T., et al., 2019. Hepatocyte-specific loss of GPS2 in mice reduces non-alcoholic steatohepatitis via activation of PPAR α . *Nature Communications* 10(1): 1684, Doi: 10.1038/s41467-019-09524-z.
- [21] Jenne, N., Frey, K., Brügger, B., Wieland, F.T., 2002. Oligomeric State and Stoichiometry of p24 Proteins in the Early Secretory Pathway*. *Journal of Biological Chemistry* 277(48): 46504–11, Doi: <https://doi.org/10.1074/jbc.M206989200>.
- [22] Schimmöller, F., Singer-Krüger, B., Schröder, S., Krüger, U., Barlowe, C., Riezman, H., 1995. The absence of Emp24p, a component of ER-derived COPII-coated vesicles, causes a defect in transport of selected proteins to the Golgi. *The EMBO Journal* 14(7): 1329–39, Doi: <https://doi.org/10.1002/j.1460-2075.1995.tb07119.x>.
- [23] Stamnes, M.A., Craighead, M.W., Hoe, M.H., Lampen, N., Geromanos, S., Tempst, P., et al., 1995. An integral membrane component of coatamer-coated transport vesicles defines a family of proteins involved in budding. *Proceedings of the National Academy of Sciences* 92(17): 8011–5, Doi: 10.1073/pnas.92.17.8011.
- [24] Muñiz, M., Nuoffer, C., Hauri, H.-P., Riezman, H., 2000. The Emp24 Complex Recruits a Specific Cargo Molecule into Endoplasmic Reticulum-Derived Vesicles. *Journal of Cell Biology* 148(5): 925–30, Doi: 10.1083/jcb.148.5.925.
- [25] Koegler, E., Bonnon, C., Waldmeier, L., Mitrovic, S., Halbeisen, R., Hauri, H.-P., 2010. p28, a novel ERGIC/cis Golgi protein, required for Golgi ribbon formation. *Traffic (Copenhagen, Denmark)* 11(1): 70–89, Doi: 10.1111/j.1600-0854.2009.01009.x.

- [26] Theiler, R., Fujita, M., Nagae, M., Yamaguchi, Y., Maeda, Y., Kinoshita, T., 2014. The α -helical region in p24y2 subunit of p24 protein cargo receptor is pivotal for the recognition and transport of glycosylphosphatidylinositol-anchored proteins. *The Journal of Biological Chemistry* 289(24): 16835–43, Doi: 10.1074/jbc.M114.568311.
- [27] Paulick, M.G., Bertozzi, C.R., 2008. The glycosylphosphatidylinositol anchor: a complex membrane-anchoring structure for proteins. *Biochemistry* 47(27): 6991–7000, Doi: 10.1021/bi8006324.
- [28] Pierleoni, A., Martelli, P.L., Casadio, R., 2008. PredGPI: a GPI-anchor predictor. *BMC Bioinformatics* 9(1): 392, Doi: 10.1186/1471-2105-9-392.
- [29] Krautbauer, S., Wanninger, J., Eisinger, K., Hader, Y., Beck, M., Kopp, A., et al., 2013. Chemerin is highly expressed in hepatocytes and is induced in non-alcoholic steatohepatitis liver. *Experimental and Molecular Pathology* 95(2): 199–205, Doi: <https://doi.org/10.1016/j.yexmp.2013.07.009>.
- [30] Bozaoglu, K., Bolton, K., McMillan, J., Zimmet, P., Jowett, J., Collier, G., et al., 2007. Chemerin Is a Novel Adipokine Associated with Obesity and Metabolic Syndrome. *Endocrinology* 148(10): 4687–94, Doi: 10.1210/en.2007-0175.
- [31] Burk, R.F., Hill, K.E., 2005. SELENOPROTEIN P: An Extracellular Protein with Unique Physical Characteristics and a Role in Selenium Homeostasis. *Annual Review of Nutrition* 25(1): 215–35, Doi: 10.1146/annurev.nutr.24.012003.132120.
- [32] Shih, D.M., Xia, Y.-R., Yu, J.M., Lusic, A.J., 2010. Temporal and tissue-specific patterns of Pon3 expression in mouse: in situ hybridization analysis. *Advances in Experimental Medicine and Biology* 660: 73–87, Doi: 10.1007/978-1-60761-350-3_8.
- [33] Steinhoff, J.S., Lass, A., Schupp, M., 2021. Biological Functions of RBP4 and Its Relevance for Human Diseases. *Frontiers in Physiology* 12: 659977, Doi: 10.3389/fphys.2021.659977.
- [34] Fuior, E. V., Gafencu, A. V., 2019. Apolipoprotein C1: Its Pleiotropic Effects in Lipid Metabolism and Beyond. *International Journal of Molecular Sciences* 20(23), Doi: 10.3390/ijms20235939.

CHAPTER 4



The Peroxisome Proliferator-Activated Receptor α is dispensable for cold-induced adipose tissue browning in mice

Merel Defour, Wieneke Dijk, Philip Ruppert, Emmani B.M. Nascimento, Patrick Schrauwen, Sander Kersten

ABSTRACT

Objective: Chronic cold exposure causes white adipose tissue (WAT) to adopt features of brown adipose tissue, a process known as browning. Previous studies have hinted at a possible role for the transcription factor Peroxisome Proliferator-Activated Receptor alpha (PPAR α) in cold-induced browning. Here we aimed to investigate the importance of PPAR α in driving transcriptional changes during cold-induced browning in mice.

Methods: Male wildtype and PPAR α ^{-/-} mice were housed at thermoneutrality (28°C) or cold (5°C) for 10 days. Whole genome expression analysis was performed on inguinal WAT. In addition, other analyses were carried out. Whole genome expression data of livers of wildtype and PPAR α ^{-/-} mice fasted for 24 hours served as positive control for PPAR α -dependent gene regulation.

Results: Cold exposure increased food intake, and decreased weight of BAT and WAT to a similar extent in wildtype and PPAR α ^{-/-} mice. Except for plasma non-esterified fatty acids, none of the cold-induced changes in plasma metabolites were dependent on PPAR α genotype. Histological analysis of inguinal WAT showed clear browning upon cold but did not reveal any morphological differences between wildtype and PPAR α ^{-/-} mice. Transcriptomics analysis of inguinal WAT showed a marked effect of cold on overall gene expression, as revealed by principle component analysis and hierarchical clustering. However, wildtype and PPAR α ^{-/-} mice clustered together, even after cold exposure, indicating a similar overall gene expression profile in the two genotypes. Pathway analysis revealed that cold upregulated pathways involved in energy usage, oxidative phosphorylation, and fatty acid β -oxidation to a similar extent in wildtype and PPAR α ^{-/-} mice. Furthermore, cold-mediated induction of genes related to thermogenesis such as *Ucp1*, *Elovl3*, *Cox7a1*, *Cox8*, and *Cidea*, as well as many PPAR target genes, was similar in wildtype and PPAR α ^{-/-} mice. Finally, pharmacological PPAR α activation had a minimal effect on expression of cold-induced genes in murine WAT.

Conclusion: Cold-induced changes in gene expression in inguinal WAT are unaltered in mice lacking PPAR α , indicating that PPAR α is dispensable for cold-induced browning.

INTRODUCTION

Cold exposure in mice causes specific white adipose tissue (WAT) depots to adopt features of brown adipose tissue (BAT), a process known as browning [1]. Browning is characterized by the appearance of adipocytes with multiple lipid droplets and by the acquisition of a thermogenic capacity, the latter of which is dependent on an increase in uncoupling protein (UCP) 1 [2]. Concurrent with the changes in cell morphology, the transcription of numerous genes involved in thermogenesis and lipid catabolism is strongly activated [3]. Recently, it was shown that human white adipose tissue is also capable of browning under condition of prolonged and severe adrenergic stress [4]. Nowadays, browning is considered as a potential molecular target to promote weight loss and improve metabolic risk factors, prompting investigation into the molecular mechanisms that drive browning.

One of the transcription factors that has been implicated in browning is PPAR α [5]. PPAR α is a member of the family of Peroxisome Proliferator-Activated Receptors, which play key roles in the regulation of lipid homeostasis and oxidative metabolism [6-8]. Three different PPAR subtypes exist in mammals: PPAR α , PPAR δ (also referred to as PPAR β), and PPAR γ , each with a distinct tissue expression profile and set of functions. PPARs regulate gene expression in response to binding small lipophilic ligands and function as a heterodimeric complex with the retinoid X receptor RXR [9-11]. The ligands for PPARs include a variety of synthetic and endogenous compounds ranging from industrial chemicals to specific drug classes, fatty acids, eicosanoids, and other lipid species [12].

The PPAR α subtype is expressed in several tissues, with the highest expression levels in mice found in brown adipose tissue and liver, followed by kidney, heart, skeletal muscle and intestine [13, 14]. At the physiological level, PPAR α is mainly known as the master regulator of lipid metabolism in the liver during fasting. This notion is based on the finding that fasted whole-body or liver-specific PPAR α ^{-/-} mice have a severe metabolic phenotype characterized by hypoglycemia, hypoketone mia, elevated plasma non-esterified fatty acids (NEFAs), and a fatty liver [15-17]. These metabolic defects are rooted in reduced expression of hundreds of genes involved in numerous metabolic pathways covering nearly every aspect of hepatic lipid metabolism [18].

The PPAR γ subtype is predominantly expressed in colonocytes, macrophages, and adipocytes [13]. It is mainly known as the target for the insulin-sensitizing thiazolidinedione drugs [19]. In addition, PPAR γ is essential for the differentiation of brown and white adipocytes [20]. In mice, loss of PPAR γ fails to yield viable offspring [21], while in humans homozygosity for loss-of-function mutations in PPAR γ leads to a form of lipodystrophy [22].

Both PPAR α and PPAR γ have been implicated in browning [5]. With respect to PPAR γ , treatment of mice with synthetic PPAR γ agonists promotes adipose tissue browning, as shown by the appearance of multilocular adipocytes and the increased expression of thermogenic genes such as *Ucp1*, triggering thermogenic capacity in WAT [23-25]. Conversely, mice carrying a functionally impaired mutant form of PPAR γ have reduced adipose tissue browning and an impaired thermogenic capacity after treatment with the β 3-adrenergic agonist CL316,243 [26]. Furthermore, activation of PPAR γ in human pre-adipocytes and adipocytes increased expression of *UCP1* and other browning-related genes [27, 28].

The role of PPAR α in browning is less clear. Although a number of studies have implicated PPAR α in CL316,243-induced browning [27, 29], no studies have carefully examined the transcriptional role of PPAR α during cold-induced browning. Based on the reported attenuation of browning by PPAR α ablation after CL316,243 treatment [27, 29], and considering the marked induction of PPAR α mRNA and protein during cold-induced browning [30, 31], we hypothesized that PPAR α is essential for stimulating gene expression in inguinal WAT in response to cold. The objective of this study was to verify this hypothesis and investigate the importance of PPAR α in cold-induced browning in mice.

METHODS

Animals and diet

Male and female wildtype and PPAR α ^{-/-} mice that had been backcrossed on a pure C57Bl/6J background for more than 10 generations were acquired from Jackson Laboratories (no. 000664 and 008154, respectively). The mice were further bred at the animal facility of Wageningen University under specific pathogen free conditions to generate the number of mice necessary for the experiments. For the chronic cold experiment, forty three- to four-month-old male wildtype and PPAR α ^{-/-} mice were placed at thermo-neutral temperature (28°C) for 5 weeks. Thereafter, 20 wildtype and 20 PPAR α ^{-/-} mice were randomly distributed across 2 groups: half of the mice of each genotype were kept at thermo-neutral temperature and half of the mice of each genotype was placed at 21°C for one week followed by a period of 10 days at in the cold (5°C) (n=10 per group). For cold exposure, mouse cages were placed in a cold cabinet that was kept at 5°C (ELDG800, VDW Coolsystems, Geldermalsen). Mice had ad libitum access to chow feed and water. Body weight and body temperature were monitored daily during the cold exposure period. Body temperature of the cold-exposed mice was monitored via read-out of transponders (IPTT-300) that were injected subcutaneously prior to the experiment (Bio Medic Data Systems, Seaford, USA). For the acute cold experiment, three- to four-month-old male wildtype and PPAR α ^{-/-} mice were placed at thermo-neutral temperature (28°C) for 5 weeks. Thereafter, the mice were placed in the cold (5°C) for 24 hours

(n=10 per group). For the fasting experiment, three- to four-month-old male wildtype and PPAR α ^{-/-} mice were either fasted for 24 hours or had food available ad libitum (n=10-11 per group). For PPAR agonist treatment, Sv129 male mice were placed on a high fat diet (formula D12451 Research Diets, Inc., manufactured by Research Diet Services, Wijk bij Duurstede) for 21 weeks with the addition of Wy14,643 (0.1% w/w of feed) or rosiglitazone (0.01% w/w of feed) during the last week. All mice were housed at the animal facility of Wageningen University. Mice were housed in individual cages with normal bedding and cage enrichment on a 12 hour light-dark cycle. They had visual and auditory contact with littermates. At the end of the study, between 9.00h and 11.00h, blood was collected via orbital puncture under isoflurane anesthesia into EDTA tubes. Mice were euthanized via cervical dislocation, after which tissues were excised and directly frozen in liquid nitrogen or prepared for histology. All studies were approved by the Animal Ethics Committee of Wageningen University and by the Central Animal Testing Committee (CCD, AVD104002015236).

RNA isolation and quantitative PCR

Total RNA was extracted from cells using TRIzol reagent (Life Technologies, Bleiswijk, The Netherlands). For tissues, total RNA was isolated using the RNeasy Micro kit from Qiagen (Venlo, The Netherlands). Subsequently, 500 ng RNA was used to synthesize cDNA using iScript cDNA synthesis kit (Bio-Rad Laboratories, Veenendaal, The Netherlands). Messenger RNA levels of selected genes were determined by reverse transcription quantitative PCR using SensiMix (Bioline; GC Biotech, Alphen aan den Rijn, The Netherlands) on a CFX384 real-time PCR detection system (Bio-Rad Laboratories, Veenendaal, the Netherlands). The housekeeping gene *36b4* was used for normalization.

Histology/immunohistochemistry

Fresh WAT tissues were fixed in 4% paraformaldehyde, dehydrated and embedded in paraffin. Hematoxylin & Eosin staining was performed using standard protocols.

Plasma measurements

Plasma concentrations of glucose (Sopachem, Ochten, the Netherlands), triglycerides, cholesterol, ketone bodies (InstruChemie, Delfzijl, the Netherlands), glycerol (Sigma-Aldrich, Houten, the Netherlands) and non-esterified fatty acids (Wako Chemicals, Neuss, Germany; HR(2) Kit) were determined following the manufacturers' instructions.

Liver Triglycerides

Liver triglyceride levels were determined in 10% liver homogenates prepared in buffer containing Sucrose 250 mM, EDTA 1mM, Tris-HCl 10mM pH 7.5 using a commercially available kit from Instruchemie (Delfzijl, The Netherlands).

Microarray analysis

Microarray analysis was performed on inguinal adipose tissue samples from 5-6 mice of each group and liver samples from 5 mice per group. RNA was isolated as described above and subsequently purified using the RNeasy Micro kit from Qiagen (Venlo, The Netherlands). RNA integrity was verified with RNA 6000 Nano chips on an Agilent 2100 bioanalyzer (Agilent Technologies, Amsterdam, The Netherlands). Purified RNA (100 ng) was labelled with the Ambion WT expression kit (Carlsbad, CA) and hybridized to an Affymetrix Mouse Gene 1.1 ST array plate (Affymetrix, Santa Clara, CA). Hybridization, washing, and scanning were carried out on an Affymetrix GeneTitan platform according to the manufacturer's instructions. Normalized expression estimates were obtained from the raw intensity values applying the robust multi-array analysis preprocessing algorithm available in the Bioconductor library AffyPLM with default settings [32, 33]. Probe sets were defined according to Dai et al. [34]. In this method probes are assigned to Entrez IDs as a unique gene identifier. In this study, probes were reorganized based on the Entrez Gene database, build 37, version 1 (remapped CDF v22). The microarray dataset was filtered by only including probe sets with expression values higher than 20 on at least 4 arrays. In addition, an Inter Quartile Range (IQR) cut-off of 0.25 was used to filter out genes that showed no variation between the conditions, leaving a total of 8174 genes for further statistical analysis. The P values were calculated using an Intensity-Based Moderated T-statistic (IBMT) [35]. Genes were defined as significantly changed when $P < 0.001$.

Gene set enrichment analysis (GSEA) was used to identify gene sets that were enriched among the upregulated or downregulated genes [36]. Genes were ranked based on the IBMT-statistic and subsequently analyzed for over- or underrepresentation in predefined gene sets derived from Gene Ontology, KEGG, National Cancer Institute, PFAM, Biocarta, Reactome and WikiPathways pathway databases. Only gene sets consisting of more than 15 and fewer than 500 genes were taken into account. Statistical significance of GSEA results was determined using 1,000 permutations.

As an alternative strategy to identify pathways up- or down-regulated by cold or fasting, Ingenuity Pathway Analysis (Ingenuity Systems, Redwood City, CA) was performed. Input criteria were a relative fold change equal to or above 1.5 and an IBMT P-value < 0.001 . Array data have been submitted to the Gene Expression Omnibus (accession number pending).

The microarray analysis on livers of fed and fasted wildtype and PPAR α ^{-/-} mice was previously published (GSE17863)[37], as was the microarray analysis on WAT of PPAR agonist treated mice (GSE11295)[38].

Isolation and differentiation of primary adipocytes

WAT was dissected from wild-type and PPAR α ^{-/-} mice and put in DMEM supplemented with 1% Pen/Strep and 1% BSA. Tissues of 3 mice were pooled, minced with scissors and digested for 1 hr at 37°C in collagenase-containing medium (DMEM with 3.2 mM CaCl₂, 1.5 mg/mL collagenase type II (Sigma-Aldrich), 10% FBS, 0.5% BSA (Sigma-Aldrich) and 15 mM HEPES). After digestion, the cell mixture was passed over a 100 μ m cell strainer and centrifuged at 1600 rpm for 10 min. Supernatant was removed and the pellet containing the stromal vascular fraction was re-suspended in erythrocyte lysis buffer (155 mM NH₄Cl, 12 mM NaHCO₃, 0.1 mM EDTA) and incubated for 2–3 min at room temperature. Following neutralization, cells were centrifuged at 1200 rpm for 5 min. Cells were re-suspended in DMEM containing 10% FBS and 1% Pen/Strep and plated. Upon confluence, cells were differentiated following standard protocol of 3T3-L1 cells, as described previously [39].

Isolation and differentiation of human primary adipocytes derived from WAT

The isolation and differentiation of adipocytes derived from human WAT has been described before [40]. In short, the stromal vascular fraction was obtained from subcutaneous WAT during thyroid surgery using a collagenase digestion.

Differentiation was initiated for 7 days with differentiation medium containing biotin (33 μ M), pantothenate (17 μ M), insulin (100 nM), dexamethasone (100 nM), IBMX (250 μ M), rosiglitazone (5 μ M), T3 (2 nM), and transferrin (10 μ g/ml). Cells were transferred to maintenance medium consisting of biotin (33 μ M), pantothenate (17 μ M), insulin (100 nM), dexamethasone (10 nM), T3 (2 nM), and transferrin (10 μ g/ml) for another 5 days in the presence of absence of 300 nM GW7647.

The study was reviewed and approved by the ethics committee of Maastricht University Medical Center (METC 10-3-012, NL31367.068.10). Informed consent was obtained before surgery, and participants did not receive a stipend.

Oxygen consumption in differentiated adipocytes derived from human BAT

Differentiated adipocytes were incubated for 1 hr at 37°C in unbuffered XF assay medium supplemented with 2 mM GlutaMAX, 1 mM sodium pyruvate and 25 mM glucose. To determine NE-stimulated mitochondrial uncoupling, oxygen

consumption was measured using bioanalyzer from Seahorse Bioscience after addition of 2 μM oligomycin, which inhibited ATPase, followed by 1 μM NE. Maximal respiration was determined following 0.3 μM FCCP-induced determined. 1 μM antimycin A and rotenone was added to correct for non-mitochondrial respiration.

Statistical analysis

Data are presented as mean \pm SEM. Comparisons between two groups were made using two-tailed Student's t-test. $P < 0.05$ was considered as statistically significant. Excel software (version 2016) was used for statistical analysis.

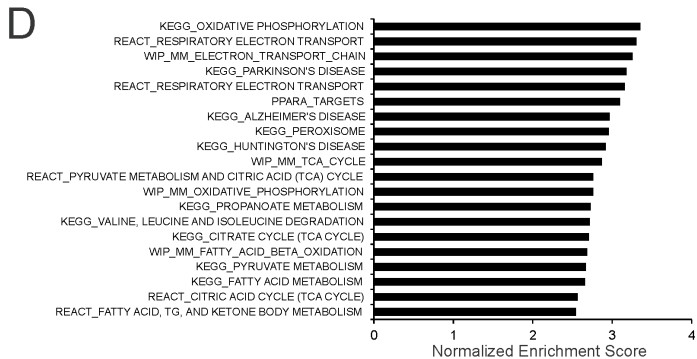
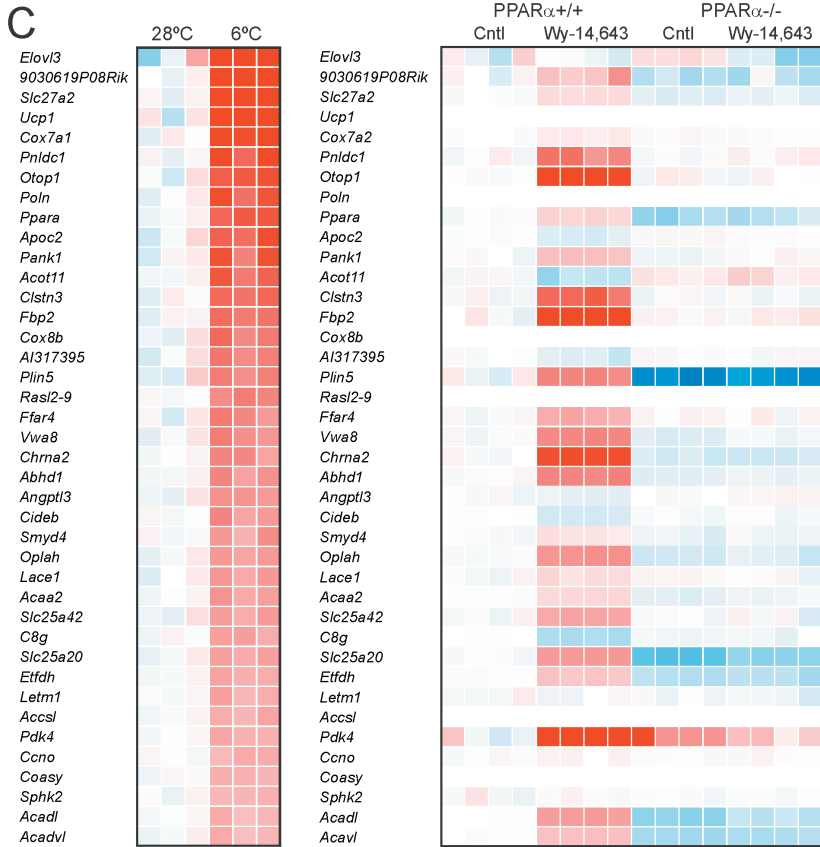
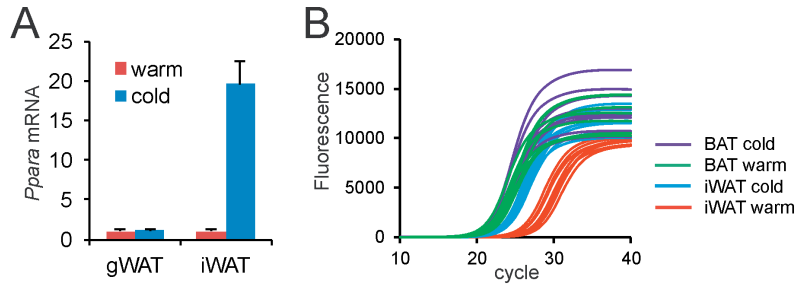
RESULTS

PPAR α and PPAR α target genes are upregulated during cold-induced browning

Quantitative PCR indicated that *Ppara* mRNA levels were markedly increased in inguinal WAT but not gonadal WAT after 10 days of cold exposure as compared to thermoneutrality (Figure 1A), suggesting a role of PPAR α in cold-induced browning in mice. The mRNA expression level of *Ppara* in inguinal WAT after cold approaches the robust expression level of *Ppara* in brown fat (Figure 1B). Analysis of an existing microarray dataset (GSE51080) indicated that *Ppara* is among the most highly induced genes in murine inguinal adipose tissue in response to cold (Figure 1C) [41]. Along with *Ppara* and genes associated with browning such as *Ucp1*, *Cidea* and *Elovl3*, many target genes of PPAR α were highly induced by cold in inguinal WAT, including *Pank1*, *Slc25a20*, *Pdk4*, *Fbp2*, *Plin5*, *Acadl* and *Acaa2* (Figure 1C). A large similarity was observed between the inductions in gene expression elicited by cold in inguinal adipose tissue and the gene expression changes caused by PPAR α activation in the liver using a synthetic PPAR α agonist (Figure 1C), again suggesting activation of PPAR α in inguinal WAT during cold. Similar results were obtained using another microarray dataset on the effect of cold in murine inguinal WAT (GSE13432, Supplemental figure 1) [42]. According to gene set enrichment analysis, PPAR α target genes were also highly enriched among the cold-induced genes (Figure 1D). Together, these data suggest a possible role for PPAR α in cold-induced browning.

Figure 1 (opposite). PPAR α is highly upregulated during cold-induced browning.

(A) Relative gene expression of PPAR α in gonadal WAT and inguinal WAT of wildtype mice after 10 days at 28°C (warm, n=6-8) or 5°C (cold, n=10)[51]. Data are presented as mean \pm SEM. (B) Quantitative PCR amplification curves of *Ppara* in inguinal WAT and BAT of wildtype mice exposed to cold (5°C) or thermoneutrality (28°C, warm) for 10 days. (C) Heatmap of the top 40 most highly induced genes in subcutaneous adipose tissue of mice after 10 days at 6°C as compared to 10 days at 28°C (GSE51080). In parallel, the expression profiles are shown of the same genes in livers of wild type and PPAR α ^{-/-} mice treated with Wy-14.643 for 5 days (GSE8295). (D) Top 20 gene sets induced by cold-exposure in subcutaneous adipose tissue of mice after 7 days at 4°C as compared to 7 days at 30°C (GSE13432), determined by gene set enrichment analysis. Gene sets were ranked according to normalized enrichment score.



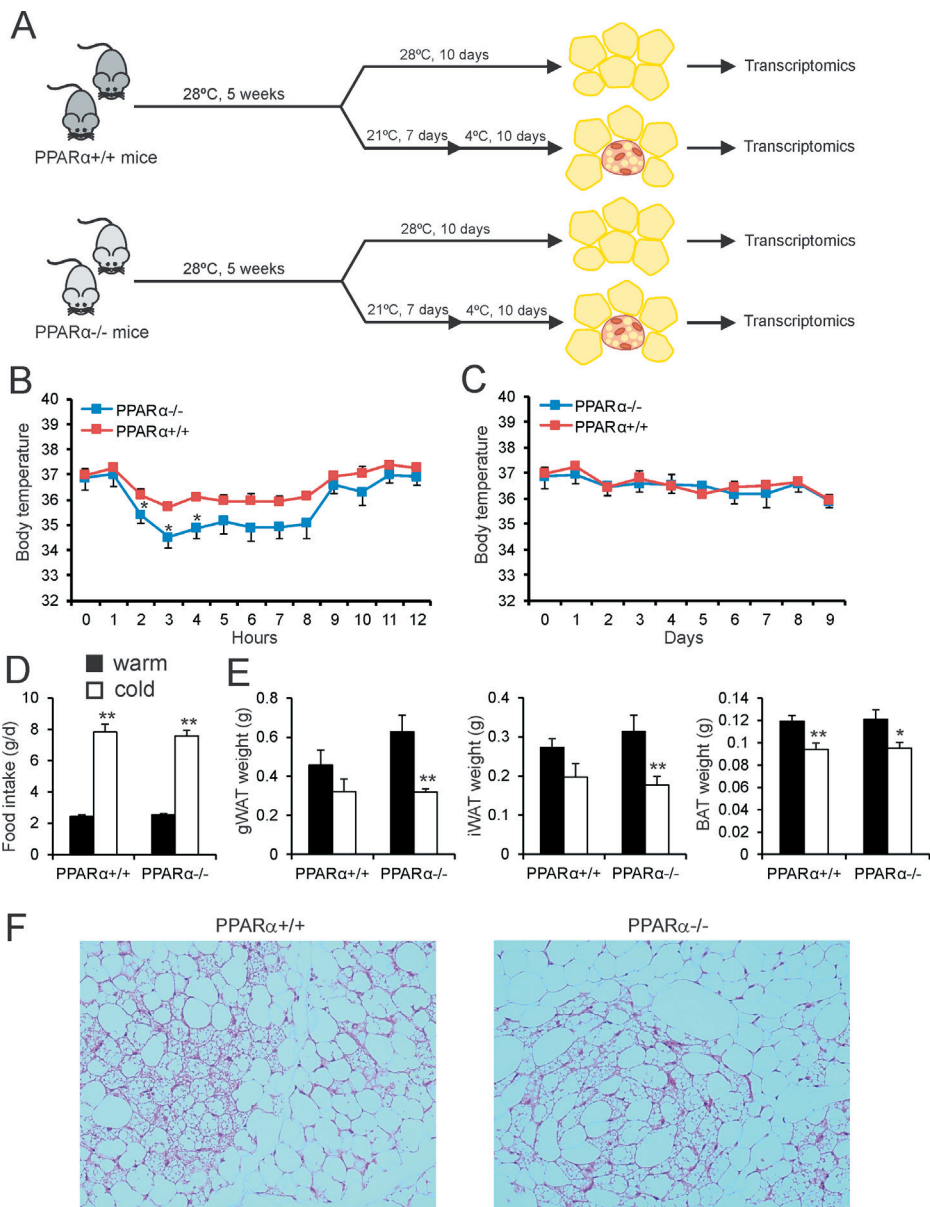


Figure 2. Transient hypothermia in *PPARα*^{-/-} mice exposed to cold.

(A) Schematic representation of the cold intervention in wildtype and *PPARα*^{-/-} mice. (B-C) Body temperature during the first 12 hours of cold exposure and assessed daily during the full 10 days of cold exposure. Asterisk indicates significantly different from wildtype mice according to Student's t-test ($P < 0.05$). (D) Feed intake after 9 days of exposure to cold (5°C, cold) or thermoneutrality (28°C, warm). (E) Adipose tissue weights of gonadal WAT, inguinal WAT and BAT of wild type and *PPARα*^{-/-} mice exposed to cold (5°C) or thermoneutrality (28°C) for 10 days. $N = 10$ per group. Asterisk indicates significantly different from thermoneutral mice according to Student's t-test (* $P < 0.05$, ** $P < 0.01$). (F) Representative Hematoxylin and eosin staining of inguinal WAT of cold-exposed wildtype and *PPARα*^{-/-} mice. Inguinal WAT shows large variability in the degree of browning. Sections of inguinal WAT that show very significant browning were selected. Images are at 100x magnification.

Cold-induced changes in WAT morphology are unaltered in PPAR α ^{-/-} mice

To investigate the role of PPAR α in cold-induced browning, male wildtype and PPAR α ^{-/-} mice were studied after 10 days of cold exposure (5°C) (Figure 2A). For comparison, another group of wildtype and PPAR α ^{-/-} were studied after a prolonged stay at thermoneutrality (28°C). Cold exposure caused a transient decrease in body temperature, which was significantly more pronounced in the PPAR α ^{-/-} mice than in the wildtype mice (Figure 2B). The difference in body temperature disappeared after prolonged cold exposure (Figure 2C). As expected, cold exposure markedly increased food intake (Figure 2D). However, no differences in food intake were observed between wildtype and PPAR α ^{-/-} mice (Figure 2D). Also, no differences in the weight of the inguinal WAT, gonadal WAT and interscapular BAT depots were observed between wildtype and PPAR α ^{-/-} mice, neither in the thermoneutral nor in the cold-exposed mice (Figure 2E). To examine any potential morphological differences in the inguinal WAT of wildtype and PPAR α ^{-/-} mice, we performed H&E staining (Figure 2F). The inguinal WAT of both sets of mice showed the characteristic features of browning, as revealed by the presence of numerous multilocular brown fat-like cells. However, no obvious differences could be observed in the degree of browning between the wildtype and PPAR α ^{-/-} mice (Figure 2F).

Next, we measured the levels of various metabolites in the blood plasma. In the cold-exposed mice, levels of non-esterified fatty acids and cholesterol were significantly higher in plasma of PPAR α ^{-/-} mice compared to wildtype mice, which was not observed under thermoneutral conditions (Figure 3). By contrast, plasma levels of triglycerides, glycerol, ketones, and glucose were not significantly different between cold-exposed PPAR α ^{-/-} and wildtype mice. These data indicate that the absence of PPAR α leads to a modest metabolic phenotype in cold-exposed mice.

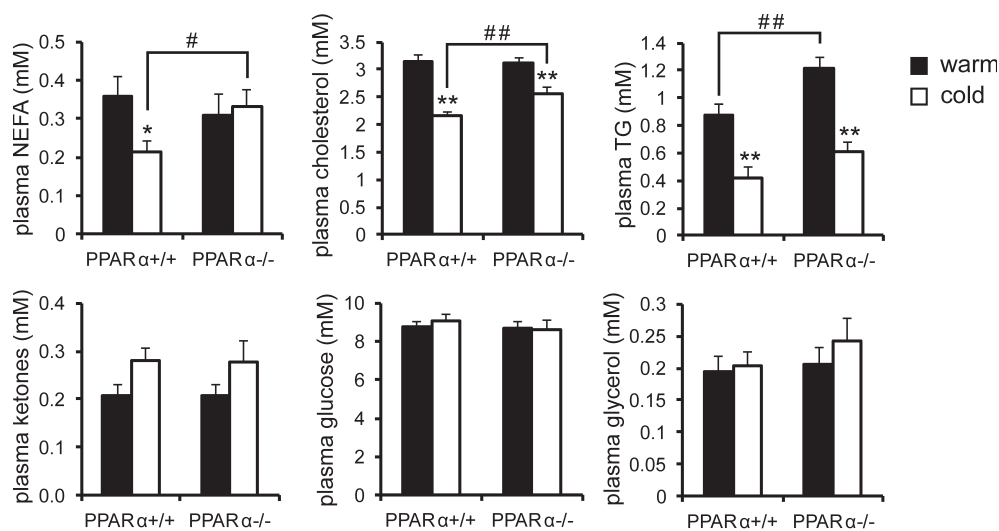


Figure 3. Cold does not amplify differences in plasma metabolites between wildtype and PPAR α ^{-/-} mice. Plasma metabolite concentrations in wildtype and PPAR α ^{-/-} mice exposed to cold (5°C) or thermoneutrality (28°C) for 10 days. Asterisk indicates significantly different from thermoneutral mice according to Student's t-test (*P<0.05, **P<0.01). Pound sign indicates significant difference between wildtype and PPAR α ^{-/-} mice according to Student's t-test (#P<0.05, ##P<0.01). N=10 per group.

Cold induces similar changes in gene expression in wildtype and PPAR α ^{-/-} mice at the whole genome level

To gain insight into the role of PPAR α in cold-induced browning, we performed whole genome expression profiling on the inguinal WAT depot of wildtype and PPAR α ^{-/-} mice exposed to thermoneutrality or cold. As a strong positive reference for PPAR α -dependent gene regulation, a parallel whole genome expression analysis was performed on the livers of wildtype and PPAR α ^{-/-} mice subjected to fasting for 24 hours or fed ad libitum.

Volcano plot analysis indicated that the differences in gene expression in inguinal WAT between cold-exposed wildtype and PPAR α ^{-/-} mice are very modest (Figure 4A), certainly when compared with the differences in liver gene expression between wildtype and PPAR α ^{-/-} mice after fasting (Figure 4B). Indeed, after cold, expression of only 50 genes was significantly lower and expression of 20 genes was significantly higher in inguinal WAT of PPAR α ^{-/-} as compared to wildtype mice (P<0.001, fold-change>1.2)(Figure 4C). By comparison, after fasting, expression of 1224 genes was significantly lower and expression of 1328 genes was significantly higher in the liver of PPAR α ^{-/-} as compared to wildtype mice (P<0.001, fold-change>1.2)(Figure 4C).

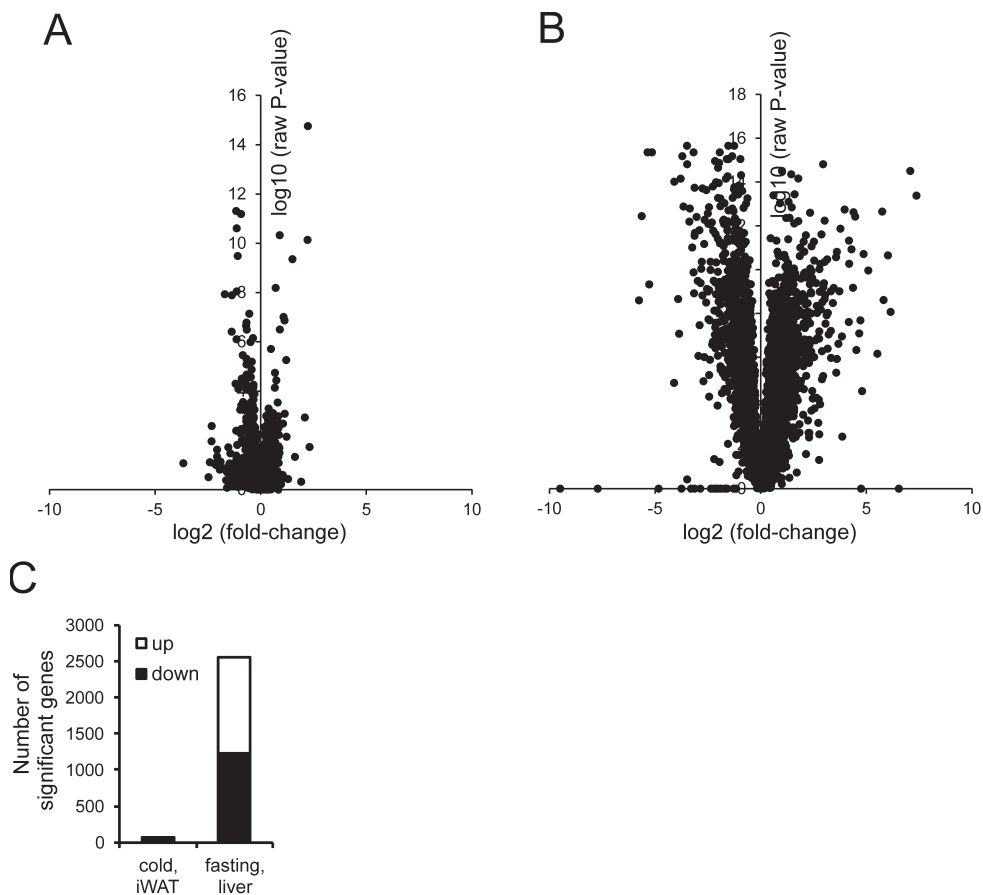


Figure 4. Comparative analysis of the effect of cold and fasting in wildtype and $PPAR\alpha^{-/-}$ mice.

A) Volcano plot in which $^2\log(\text{fold-change})$ is plotted against $^{-10}\log(\text{P-value})$ for comparison between inguinal WAT of wildtype and $PPAR\alpha^{-/-}$ mice after 10 day cold exposure (B) Volcano plot in which $^2\log(\text{fold-change})$ is plotted against $^{-10}\log(\text{P-value})$ for comparison between liver of wildtype and $PPAR\alpha^{-/-}$ mice after 24 hour fasting. (C) Number of genes in inguinal WAT that are significantly different between wildtype and $PPAR\alpha^{-/-}$ mice after 10 day cold exposure, and the number of genes in liver that are significantly different between wildtype and $PPAR\alpha^{-/-}$ mice after 24 hour fasting. The number of differentially expressed genes was calculated based on a statistical significance cut-off of $P < 0.001$ (IBMT regularised paired t-test) and fold-change > 1.20 . Genes were separated according to up- or down-regulation.

Principle component analysis and hierarchical clustering clearly separated the inguinal WAT samples of the cold-exposed mice and the thermoneutral mice, illustrating the pronounced impact of cold on overall gene expression in inguinal WAT (Figure 5A). However, within the cold and thermoneutral groups, wildtype and $PPAR\alpha^{-/-}$ mice did not separate into distinct clusters, suggesting a minimal effect of $PPAR\alpha$ deletion on overall gene regulation in cold-exposed inguinal WAT. By contrast, principle component analysis and hierarchical clustering markedly separated the livers of fasted wildtype and $PPAR\alpha^{-/-}$ mice (Figure 5B).

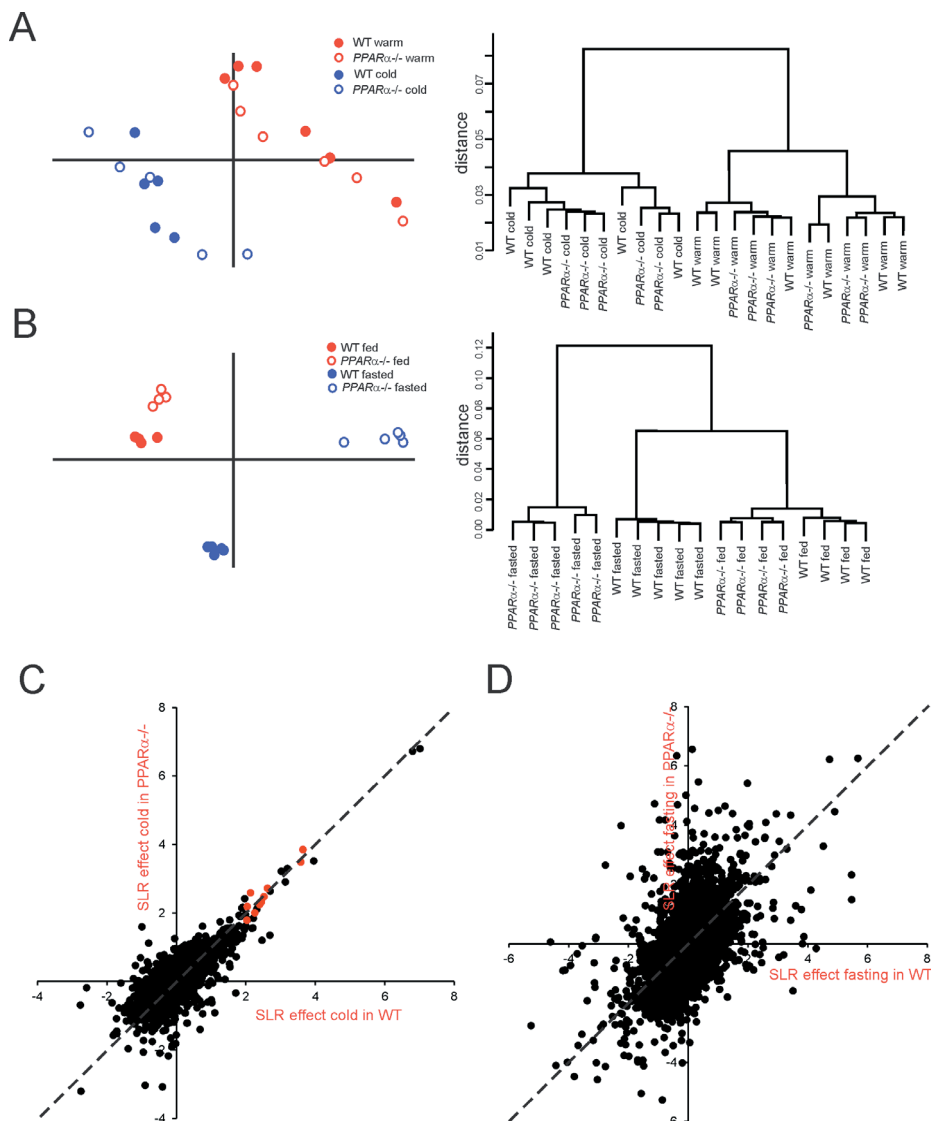


Figure 5. Distinct clustering of inguinal WAT of thermoneutral and cold-exposed wildtype and $PPAR\alpha^{-/-}$ mice.

(A) Left panel: Principle component analysis of transcriptomics data from inguinal WAT of the thermoneutral and cold-exposed wildtype and $PPAR\alpha^{-/-}$ mice. The graph shows the clear separation of mice according to treatment, while the two genotypes are mixed. Right panel: Hierarchical clustering of transcriptomics data from the thermoneutral and cold-exposed wildtype and $PPAR\alpha^{-/-}$ mice. The dendrogram reveals the distinct clustering and separation based on treatment, but not based on genotype. (B) Left panel: Principle component analysis of transcriptomics data from livers of fed and fasted wildtype and $PPAR\alpha^{-/-}$ mice. The graph shows the clear separation between the genotypes in both fed and fasted state. Right panel: Hierarchical clustering of transcriptomics data from the fed and fasted wildtype and $PPAR\alpha^{-/-}$ mice. The dendrogram reveals the distinct clustering and separation according to treatment and genotypes. (C) Correlation plot showing gene expression changes in response to cold in wildtype (x-axis) versus $PPAR\alpha^{-/-}$ mice (y-axis) (expressed as signal log ratio). Well established $PPAR\alpha$ target genes are highlighted in red (*Cox7a1*, *Slc27a2*, *Cidea*, *Gys2*, *Pank1*, *Gyk*, *Plin5*, *Pdk4*, *Slc25a20*, *Hadhb*). (D) Correlation plot showing gene expression changes in response to fasting in wildtype (x-axis) versus $PPAR\alpha^{-/-}$ mice (y-axis) (expressed as signal log ratio).

Scatter plot analysis confirmed that the effect of cold on overall gene expression in inguinal WAT is nearly identical in wildtype and PPAR α ^{-/-} mice (Figure 5C). Also, the cold-induced changes in gene expression of several classical PPAR α target genes was virtually identical in inguinal WAT of wildtype and PPAR α ^{-/-} mice (Figure 5C, red dots). By contrast, the effect of fasting on overall gene expression in liver was very distinct between wildtype and PPAR α ^{-/-} mice, illustrating the importance of PPAR α in hepatic gene regulation during fasting (Figure 5D). These data indicate that at the whole genome level, inguinal WAT of PPAR α ^{-/-} mice cannot be distinguished from inguinal WAT of wildtype mice, both at thermoneutral and cold conditions. In contrast, livers of PPAR α ^{-/-} mice can easily be distinguished from wildtype mice, in particular after fasting.

Cold-sensitive pathways are similarly induced in inguinal WAT in wildtype and PPAR α ^{-/-} mice

To further evaluate the browning effect in wildtype and PPAR α ^{-/-} mice, we compared the effect of cold on biological pathways in the two sets of mice using Ingenuity Pathway Analysis and Gene Set Enrichment Analysis. The most significant cold-induced pathways in the wildtype mice were mainly related to the electron transport chain and oxidative phosphorylation (Figure 6A). Consistent with the data presented above—showing a lack of difference in cold-induced expression changes between wildtype and PPAR α ^{-/-} mice—the enrichments scores for the cold-induced pathways were nearly identical in the wildtype mice and PPAR α ^{-/-} mice (Figure 6A). Similarly, according to Ingenuity Pathway Analysis, the most significant cold-induced pathways in inguinal WAT were related to oxidative phosphorylation, the tricarboxylic acid cycle, fatty acid oxidation, and other catabolic pathways, and had very similar significance scores in wildtype and PPAR α ^{-/-} (Figure 6B). Remarkably, the pathway named PPARA targets was equally induced by cold in wildtype and PPAR α ^{-/-} mice, indicating that PPAR α is dispensable for regulation of PPAR α targets by cold in inguinal WAT. By contrast, the results of Gene Set Enrichment Analysis and Ingenuity Pathway Analysis for the fasting-induced changes in hepatic gene expression were very distinct in the wildtype mice and PPAR α ^{-/-} mice. Specifically, enrichment scores and significance scores for many pathways related to PPAR signaling and fatty acid catabolism were very high in the wildtype mice yet were much lower or even opposite in the PPAR α ^{-/-} mice (Figure 6C and 6D). Taken together, these data show that at the pathway level, the absence of PPAR α does not have a noticeable influence on the induction of metabolic pathways by cold in inguinal WAT.

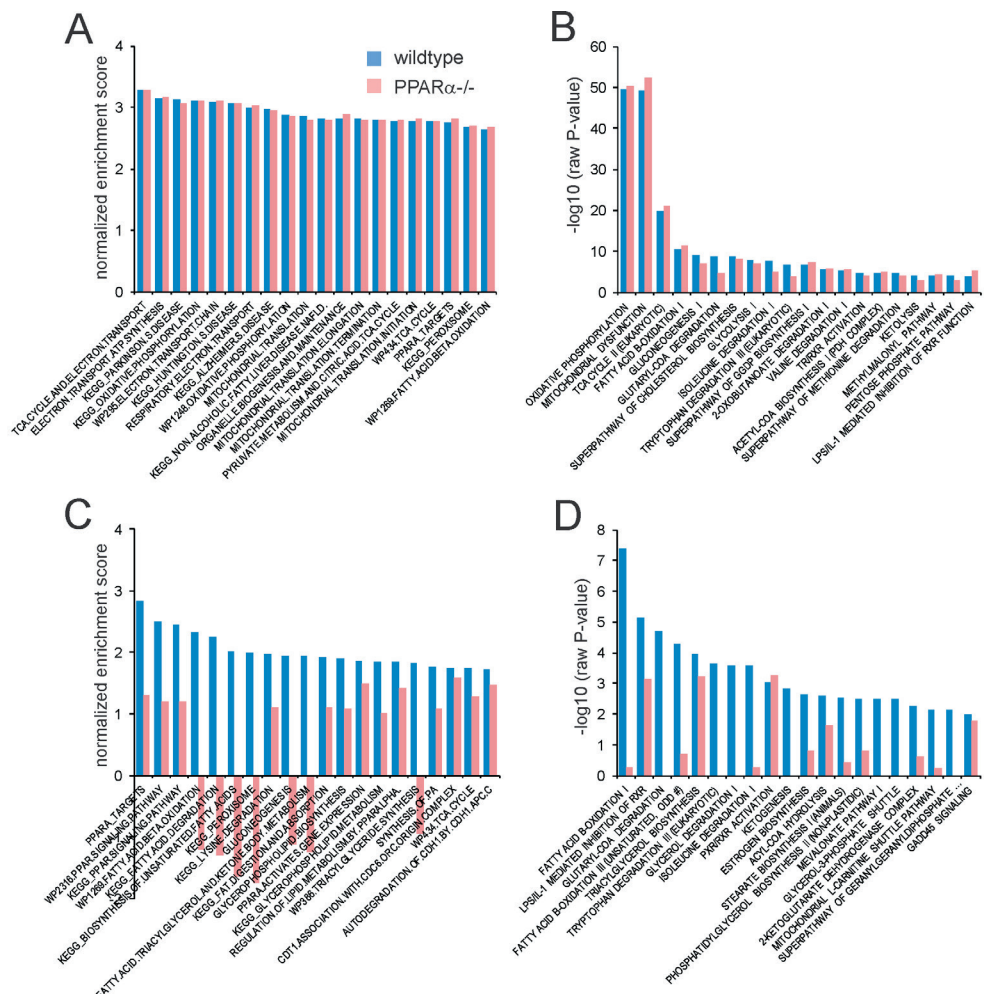


Figure 6. Minimal effect of $PPAR\alpha$ deletion in inguinal WAT at the pathway level.

A) Gene set enrichment analysis of the effect of 10 day cold exposure in inguinal WAT of wildtype (blue bars) and PPAR α ^{-/-} mice (red bars). The top 20 gene sets with the highest normalized enrichment scores in wildtype mice are shown. B) Ingenuity pathway analysis (Biological Pathways) of the effect of 10 day cold exposure in inguinal WAT of wildtype (blue bars) and PPAR α ^{-/-} mice (red bars). The top 20 most significant pathways in the wildtype mice are shown. C) Gene set enrichment analysis of the effect of 24h fasting in liver of wildtype (blue bars) and PPAR α ^{-/-} mice (red bars). The top 20 gene sets with the highest normalized enrichment scores in wildtype mice are shown. D) Ingenuity pathway analysis (Biological Pathways) of the effect of fasting in liver of wildtype (blue bars) and PPAR α ^{-/-} mice (red bars). The top 20 most significant pathways in the wildtype mice are shown.

Cold-sensitive genes are similarly induced in inguinal WAT in wildtype and PPAR α ^{-/-} mice

To further zoom in at the level of individual genes, we selected the top 50 of most highly induced genes by cold exposure in inguinal WAT in the wildtype mice, ranked according to fold-change (Figure 7A). As expected, the most highly induced gene by cold was *Ucp1*, followed by other well-known cold-induced genes such as *Elovl3*, *Cox7a1*, and *Cidea*. This top 50 list also includes many well-established PPAR α target genes in the liver, including *Gyk*, *Gys2*, *Plin5*, *Pdk4*, *Hadhb*, *Slc25a20*, *Gpd2*, and *Acadvl*, as well as *Ppara* itself (Figure 7A). Consistent with the data presented above, the cold-induced changes in gene expression were generally similar in the PPAR α ^{-/-} mice. Out of the 641 genes that were induced by cold (fold-change>1.5, P<0.001), only 5 genes had a significantly lower expression in the cold-exposed PPAR α ^{-/-} mice than in the cold-exposed wildtype mice (fold-change<-1.5, P<0.001). These genes include *2310069B03Rik*, *Adprhl1*, and the established PPAR α targets *Slc27a2*, *Fbp2*, and *Ehhad* [18]. A similar picture was observed for genes that were downregulated by cold (Figure 7B). Indeed, downregulation of gene expression by cold was generally unaffected in the PPAR α ^{-/-} mice. Out of the 420 genes that were downregulated by cold (fold-change<-1.5, P<0.001), only 2 genes had a significantly higher expression in the cold-exposed PPAR α ^{-/-} mice than in the exposed wildtype mice (fold-change>1.5, P<0.001), which were *Vnn1* and *Sema5a*. These data suggest that except for a very limited number of genes, mostly representing direct PPAR α target genes, the changes in gene expression in inguinal WAT induced by cold were nearly identical in wildtype and PPAR α ^{-/-} mice.

Role of PPAR α in *in vitro* browning

Next, to examine the potential role of PPAR α in *in vitro* browning, we first studied the differentiation of wildtype and PPAR α ^{-/-} stromal vascular cells from inguinal WAT. Adipocyte differentiation was accompanied by the marked induction of classical adipogenic markers, including *Pparg*, *Fabp4*, *Slc2a4*, and *Gpd1*, as well as induction of brown adipocyte markers, such as *Ppargc1a*, *Cidea*, *Elovl3* and *Ucp1* (Figure 8A). Intriguingly, whereas induction of classical adipogenic markers was not different between wildtype and PPAR α ^{-/-} adipocytes, expression of brown adipocyte markers was elevated in PPAR α ^{-/-} compared to wildtype adipocytes (Figure 8A). These data do not support the notion that PPAR α is required for the activation of the genes underlying browning.

A



B

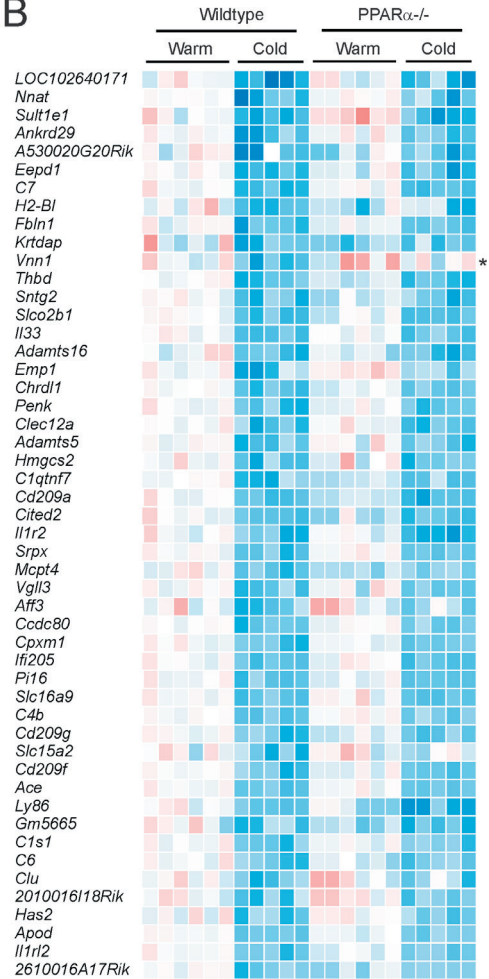


Figure 7. Cold induces parallel changes in gene expression in wildtype and $PPAR\alpha^{-/-}$ mice.

A) Comparative gene expression analysis in inguinal WAT of thermoneutral and cold-exposed wildtype and $PPAR\alpha^{-/-}$ mice, showing the top 50 most highly induced genes by cold in wildtype mice ($P < 0.001$, ranked according to fold-change). B) Comparative gene expression analysis in inguinal WAT of thermoneutral and cold-exposed wildtype and $PPAR\alpha^{-/-}$ mice, showing the top 50 most highly repressed genes by cold in wildtype mice ($P < 0.001$, ranked according to fold-change). Genes marked with asterisk were significantly different between and cold-exposed wildtype and $PPAR\alpha^{-/-}$ mice ($P < 0.001$).

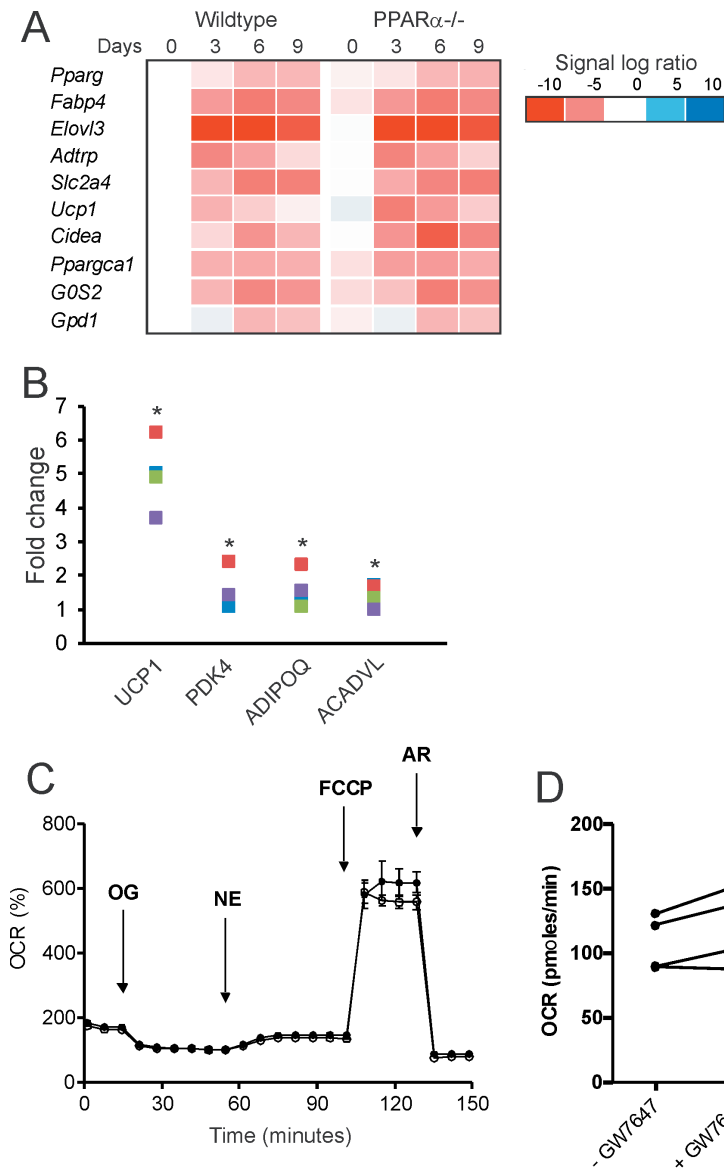


Figure 8. Role of PPAR α in *in vitro* browning.

(A) Stromal vascular cells of wildtype and PPAR $\alpha^{-/-}$ mice were differentiated towards brown-like adipocytes. Relative gene expression of adipogenic markers and brown adipocyte markers as determined by qPCR and expressed in a heatmap. (B) Differentiating human pre-adipocytes derived from subcutaneous WAT were treated with GW7647 (300 nM) for 5 days. Relative gene expression of *UCP1*, *PDK4*, *ADIPOQ* and *ACADVL* in differentiated adipocytes is shown. The different colors represent the primary adipocytes from 4 different individuals. For each individual, the expression level of the untreated adipocytes was set at 1. (C) Cellular respiration trace measured in adipocytes derived from human WAT on bioanalyzer from Seahorse with GW7647 (open circles) or without GW7647 (closed circles). (D) Basal cellular respiration in adipocytes derived from human WAT with or without GW7647 treatment during differentiation.

To investigate the ability of PPAR α to activate *in vitro* browning in human adipocytes, we treated human primary adipocytes obtained from subcutaneous adipose tissue with the synthetic PPAR α agonist GW7647. Consistent with previous data, GW7647 increased *UCP1* mRNA levels (Figure 8B)[27]. In addition, GW7647 modestly upregulated the expression of *PK4*, *ADIPOQ* and *ACADVL* (Figure 8B). Despite the approximately 5-fold increase in *UCP1* mRNA, no effect of GW7647 on norepinephrine-stimulated mitochondrial uncoupling or maximal respiration was detected in the cultured human adipocytes (Figure 8C,D). Hence, although pharmacological activation of PPAR α in primary human adipocytes had a modest stimulatory effect on genes related to browning, these changes did not translate into metabolic changes in uncoupled respiration.

PPAR γ activation but not PPAR α activation is able to markedly upregulate cold-induced genes in murine WAT

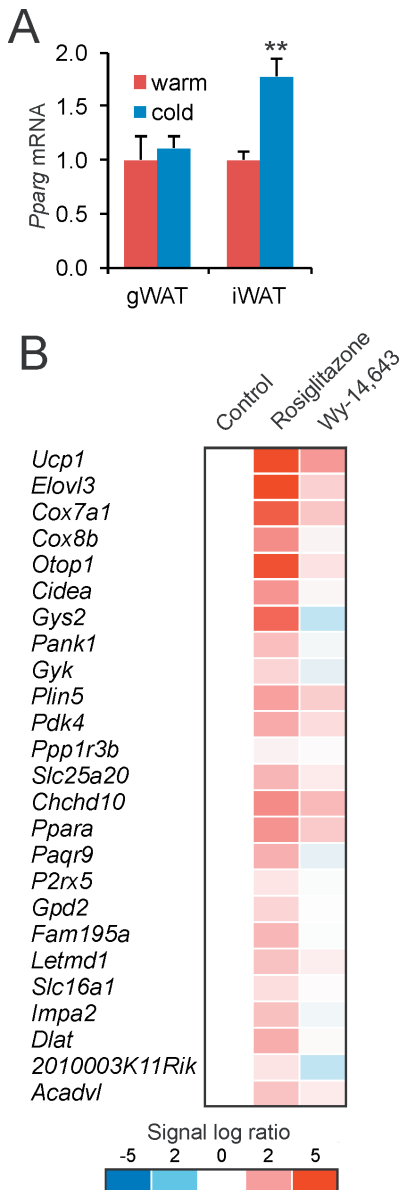
The *in vivo* and *in vitro* data presented above indicate that PPAR α is not required for (cold-induced) adipose tissue browning. This conclusion suggests that a transcription factor other than PPAR α may be responsible for the induction of PPAR target genes in inguinal WAT during cold. An obvious candidate is PPAR γ , as its expression in inguinal WAT is increased during cold (Figure 9A)[5]. In contrast, expression of PPAR δ was very stable in iWAT during cold-induced browning in all available microarray datasets (GSE13432, GSE01080, present study). To explore the possible role of PPAR γ , we compared the effect of PPAR γ and PPAR α activation in mice on the expression of cold-induced genes in adipose tissue using transcriptomics (Figure 9B). In this experiment, wildtype mice were given rosiglitazone or Wy-14,643 in the food for 1 week. Whereas PPAR γ activation by rosiglitazone markedly induced the expression of cold-induced genes in WAT, PPAR α activation by Wy-14,643 had a minimal effect (Figure 9B). The most highly induced genes by PPAR α in WAT were the PPAR α targets *Vnn1* (2.2-fold) and *Fabp1* (3.2-fold), neither of whom are induced by cold. These data indicate that PPAR γ activation but not PPAR α activation is able to markedly upregulate cold-induced genes in murine WAT.

Chronic cold does not lead to activation of PPAR α in the liver

Recently, it was demonstrated that short term cold exposure increases plasma long chain acyl-carnitine levels [43], concomitant with induction of the hepatic expression of several enzymes involved in acylcarnitine metabolism. Since many of these enzymes are under transcriptional control of PPAR α , we explored the possibility that PPAR α may be important for regulating lipid metabolism in the liver during cold. To that end, we measured the hepatic expression of several genes involved in acylcarnitine metabolism, as well as other target genes of PPAR α , in thermoneutral and cold-exposed wildtype and PPAR α ^{-/-} mice (Figure 10A). While the expression of most genes studied was reduced in the liver of PPAR α ^{-/-} mice, no interaction was

observed between cold and loss of PPAR α , meaning that the effect of loss of PPAR α was comparable in cold and thermoneutral conditions (Figure 10A).

An exception was *Fabp1*, expression of which was lower in PPAR $\alpha^{-/-}$ mice compared to wildtype mice at 5°C but not at 28°C. Importantly, the expression of genes involved in acylcarnitine metabolism and of other PPAR α targets was refractory to cold. In line with the gene expression data, liver triglyceride levels were higher in the PPAR $\alpha^{-/-}$ mice compared to wildtype mice, yet levels were similar in the cold and thermoneutral conditions (Figure 10B).



To assess the potential activation of PPAR α in liver during acute cold, we measured the hepatic expression of the same set of genes in wildtype and PPAR $\alpha^{-/-}$ mice exposed to cold for 24 hours. Although acute cold caused the marked upregulation of *Cpt1a* and *Slc22a5*, both of which are involved in acylcarnitine metabolism, the induction was similar in wildtype and PPAR $\alpha^{-/-}$ mice (Supplemental figure 2). Other PPAR α targets were not or only weakly activated by acute cold. Together, these data indicate that the role of PPAR α in liver does not become more important during acute or chronic cold, suggesting that cold does not lead to activation of PPAR α in the liver, unlike during fasting.

Figure 9. PPAR γ activation but not PPAR α activation is able to markedly upregulate cold-induced genes in murine WAT. A) Relative gene expression of *Pparg* in gonadal WAT and inguinal WAT of wildtype mice after 10 days at 28°C (warm, n=6-8) or 5°C (cold, n=10)[51]. Data are presented as mean \pm SEM. Asterisk indicates significantly different from thermoneutral mice according to Student's t-test (**P<0.01). B) Comparative analysis was performed between whole genome expression changes in WAT in response to 10 day cold exposure and in response to 7 day treatment with rosiglitazone (0.01 % wt/wt of feed) or Wy-14,643 (0.1 % wt/wt of feed). The top 25 most highly induced genes by 10 day cold exposure in WAT of wildtype mice were selected. The effect of 1 week treatment with rosiglitazone or Wy-14,643 on the expression of these genes in WAT of wildtype mice is shown (GSE11295). The top 25 list differs from figure 7 because certain genes were either not present on the microarray used for the rosiglitazone/Wy-14,643 study or did not meet the filtering criteria.

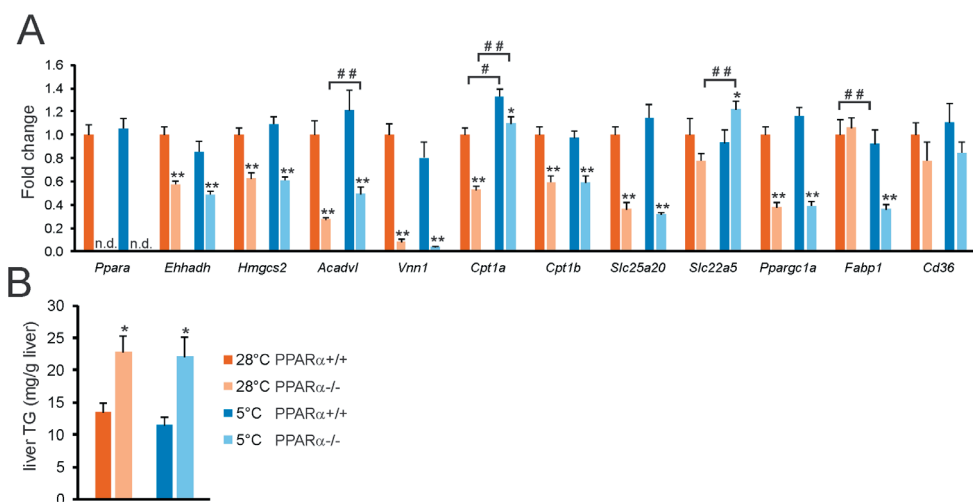


Figure 10. No interaction between cold and PPAR α ablation in hepatic gene regulation.

(A) Hepatic expression of selected genes in wildtype and PPAR α ^{-/-} mice exposed to cold (5°C) or thermoneutrality (28°C) for 10 days. (B) Liver triglycerides. N=10 per group. Error bars represent SEM. Asterisk indicates significantly different from wildtype mice under the same conditions according to Student's t-test (*P<0.05, **P<0.001). Pound sign indicates significant difference between cold and thermoneutral mice according to Student's t-test (#P<0.05, ##P<0.001).

DISCUSSION

Little is known about the regulatory mechanisms driving the metabolic adaptations during cold-induced browning. Whereas previous studies have found that loss of PPAR α leads to attenuation of CL316,243-induced adipose tissue browning [27, 29], here we find that PPAR α , despite its marked upregulation in inguinal WAT by cold, is completely dispensable for cold-induced browning in mice. Histological analysis of inguinal WAT showed clear browning upon cold but did not reveal any morphological differences between wildtype and PPAR α ^{-/-} mice. Transcriptomics analysis showed that the cold-induced changes in gene expression in inguinal WAT were fully maintained in the absence of PPAR α at the whole genome level, the pathway level, and the level of individual genes. Indeed, cold-sensitive thermogenic genes such as *Ucp1* and *Elov13* and numerous others were similarly induced by cold in wildtype and PPAR α ^{-/-} mice. Overall, our data indicate that PPAR α is not required for cold-induced browning in inguinal WAT. The lack of effect of PPAR α ablation on gene expression in inguinal WAT during cold contrasts starkly with the dramatic effect of PPAR α ablation on gene expression in liver during fasting, a well-known PPAR α -driven phenomena.

Several studies have examined the role of PPAR α in *in vivo* adipose tissue browning, either by treating mice with synthetic PPAR α agonists or by using PPAR α ^{-/-} mice, yielding somewhat conflicting results. For example, whereas in one study, chronic

treatment of mice with the PPAR α agonist fenofibrate led to the induction of thermogenic genes and the appearance of multilocular adipocytes in WAT [44], in another study, chronic treatment with fenofibrate failed to cause an increase in multilocular adipocytes in WAT [24]. Treatment of wildtype mice with CL316,243 upregulated PPAR α mRNA in white adipose tissue by 10-fold, suggesting a potential role of PPAR α in CL316,243-induced browning. Importantly, CL316,243 triggered morphological changes characteristic of browning in WAT of wildtype but not PPAR α ^{-/-} mice [29]. Transcriptomics analysis showed that the time-dependent expression changes in WAT following CL316,243 treatment were attenuated in PPAR α ^{-/-} mice [29]. In agreement with the known role of PPAR α in regulating fatty acid catabolism, many of the affected genes were involved in the transport/activation and oxidation of fatty acids. In another study, induction of thermogenic genes such as *Ucp1*, *Elovl3*, and *Cpt1b* by CL316,243 was shown to be attenuated in the absence of PPAR α ^{-/-}, both at room temperature and at thermoneutrality [27]. These data suggest that PPAR α has a stimulatory role in CL316,243-induced adipose tissue browning.

By contrast, our data indicate that PPAR α is not required for cold-induced browning. It thus appears that the role of PPAR α may be different between CL316,243-induced browning and cold-induced browning. The reason for this difference is not clear but may be related to the more diverse effects of cold versus the more targeted mechanism of action of CL316,243. Alternatively, the possible compensatory role of PPAR γ (see below) may be more readily recruitable during cold-induced browning than during CL316,243-induced browning.

Previously, it was shown that PPAR α and PPAR γ can regulate partially overlapping gene sets [45]. Based on our data, it is not possible to distinguish between the possibility that in wildtype mice: 1) PPAR α is not at all involved in gene regulation in inguinal WAT during cold, or 2) PPAR α drives the expression of several cold-induced genes in inguinal WAT, yet PPAR γ takes over the role of PPAR α in PPAR α ^{-/-} mice. The second scenario is reminiscent of the ability of PPAR γ to compensate for the absence of PPAR α in livers of PPAR α ^{-/-} mice chronically fed a high fat diet [46]. In that situation, the expression of PPAR γ goes up dramatically [46]. In favour of the first possibility, transcriptomics did not reveal a compensatory increase in PPAR γ expression in inguinal WAT of PPAR α ^{-/-} mice. Moreover, in contrast to PPAR γ activation, PPAR α activation had only minimal effects on thermogenic gene expression in WAT of wildtype mice. Accordingly, activation of PPAR γ but not PPAR α likely is a major driver of cold-induced changes in gene expression in inguinal white adipocytes. Even though several cold-induced genes involved in fatty acid catabolism are primarily known as targets of PPAR α , it has been shown that under certain conditions, PPAR γ is capable of upregulating classical PPAR α targets [46, 47]. Why PPAR α is dramatically upregulated in inguinal WAT during cold if it is not involved in regulating gene expression, remains unclear. The dispensable role of

PPAR α in cold-induced browning is consistent with the recent finding that PPAR α is not required for *in vivo* brown fat function [48].

In contrast to *Ppara* and *Ppar γ* , the expression of *Ppar δ* in inguinal WAT is completely refractory to cold. Although the lack of change in *Ppar δ* expression does not rule out a role of PPAR δ in cold-induced browning, it does make it unlikely. Arguing against a role of PPAR δ in adipose tissue browning, PPAR δ was recently shown to be dispensable for brown fat function [48].

Our experiments and studies of others in primary human adipocytes showed that PPAR α activation leads to increased expression of brown fat markers such as *UCP1*, *CIDEA*, *ELOVL3*, *CPT1B* [27]. Furthermore, when analysed by transcriptomics, PPAR α and PPAR γ activation in primary human adipocytes caused the induction of largely overlapping gene sets, reflecting a browning of human white adipocytes [27]. To what extent these changes upon pharmacological PPAR α activation reflect a physiological role of PPAR α in *in vitro* browning remains unclear. Unfortunately, technical limitations preclude investigation of the influence of inactivation of PPAR α on *in vitro* features of browning in primary human adipocytes.

In our study, 10 days of cold exposure caused a large increase in food intake, while it did not change the bodyweight of the mice, underlining the profound increase in energy demand during cold exposure in mice. The huge increase in energy expenditure and thermogenesis allowed the mice to maintain a stable body temperature during the entire 10 day intervention. Importantly, no differences in body temperature were observed between the two genotypes, except for the first 12 hours of cold acclimation, during which the PPAR α ^{-/-} mice had a slightly lower body temperature. The more significant drop in body temperature in the PPAR α ^{-/-} mice during the first hours of cold exposure is likely caused by the semi-fasting of the mice in the light cycle, when the mice are sleeping. Indeed, fasting by itself has been shown to provoke hypothermia in whole body and liver-specific PPAR α ^{-/-} mice [15, 49]. Based on these considerations, the previously observed decline in body temperature in PPAR α ^{-/-} mice upon 3 hours of cold exposure is probably due to the fact that the mice were fasted at the same time, and might not reflect a role of PPAR α in cold-induced thermogenesis per se [50].

Recently, it was shown that short term cold exposure leads to elevation of plasma long chain acyl-carnitine levels, concomitant with induction of the expression of enzymes involved in acylcarnitine metabolism in the liver, including *Cpt1b*, *Slc22a5*, *Slc25a20*, and *Crat* [43]. A mechanism was proposed in which NEFA derived from adipose tissue lipolysis activate the nuclear receptor HNF4 α in the liver, leading to induction of genes involved in acyl-carnitine production. Since the above genes are all direct targets of PPAR α , which is activated by fatty acids, it can be hypothesized that apart from HNF4 α , PPAR α may also be involved in the stimulation of acyl-

carnitine synthesis during short term cold. In our study, however, we could not find any evidence for upregulation of genes involved in carnitine synthesis after chronic cold. In addition, other target genes of PPAR α were also not induced in the liver after chronic cold. Interestingly, hepatic expression of *Cpt1a* and *Slc22a5*, both of which are involved in acylcarnitine metabolism, was elevated by acute cold. However, this induction was independent of PPAR α . Overall, these data suggest that hepatic PPAR α is not activated by acute or chronic cold. Interestingly, hepatic expression of *Fabp1* was lower in PPAR $\alpha^{-/-}$ mice specifically at 5°C, which may account for the elevated NEFA levels in PPAR $\alpha^{-/-}$ mice during cold.

In conclusion, we find that cold-induced changes in gene expression in inguinal WAT are unaltered in mice lacking PPAR α , indicating that PPAR α is dispensable for cold-induced browning.

Acknowledgements

This research was supported by CVON ENERGISE grant CVON2014-02.

References

- [1] Pescechera, A., Eckel, J., 2013. "Browning" of adipose tissue--regulation and therapeutic perspectives. *Archives of physiology and biochemistry* 119: 151-160.
- [2] Cousin, B., Cinti, S., Morroni, M., Raimbault, S., Ricquier, D., Penicaud, L., et al., 1992. Occurrence of brown adipocytes in rat white adipose tissue: molecular and morphological characterization. *Journal of cell science* 103 (Pt 4): 931-942.
- [3] Christian, M., 2015. Transcriptional fingerprinting of "browning" white fat identifies NRG4 as a novel adipokine. *Adipocyte* 4: 50-54.
- [4] Sidossis, L.S., Porter, C., Saraf, M.K., Borsheim, E., Radhakrishnan, R.S., Chao, T., et al., 2015. Browning of Subcutaneous White Adipose Tissue in Humans after Severe Adrenergic Stress. *Cell Metab* 22: 219-227.
- [5] Seale, P., 2015. Transcriptional Regulatory Circuits Controlling Brown Fat Development and Activation. *Diabetes* 64: 2369-2375.
- [6] Gross, B., Pawlak, M., Lefebvre, P., Staels, B., 2016. PPARs in obesity-induced T2DM, dyslipidaemia and NAFLD. *Nat Rev Endocrinol*.
- [7] Tateno, C., Yamamoto, T., Utoh, R., Yamasaki, C., Ishida, Y., Myoken, Y., et al., 2015. Chimeric mice with hepatocyte-humanized liver as an appropriate model to study human peroxisome proliferator-activated receptor-alpha. *Toxicologic pathology* 43: 233-248.
- [8] Varga, T., Czimmerer, Z., Nagy, L., 2011. PPARs are a unique set of fatty acid regulated transcription factors controlling both lipid metabolism and inflammation. *Biochim Biophys Acta* 1812: 1007-1022.
- [9] Gearing, K.L., Gottlicher, M., Teboul, M., Widmark, E., Gustafsson, J.A., 1993. Interaction of the peroxisome-proliferator-activated receptor and retinoid X receptor. *Proc Natl Acad Sci U S A* 90: 1440-1444.
- [10] Issemann, I., Prince, R.A., Tugwood, J.D., Green, S., 1993. The retinoid X receptor enhances the function of the peroxisome proliferator activated receptor. *Biochimie* 75: 251-256.
- [11] Keller, H., Dreyer, C., Medin, J., Mahfoudi, A., Ozato, K., Wahli, W., 1993. Fatty acids and retinoids control lipid metabolism through activation of peroxisome proliferator-activated receptor-retinoid X receptor heterodimers. *Proc Natl Acad Sci U S A* 90: 2160-2164.
- [12] Georgiadi, A., Kersten, S., 2012. Mechanisms of gene regulation by Fatty acids. *Advances in nutrition* 3: 127-134.
- [13] Bookout, A.L., Jeong, Y., Downes, M., Yu, R.T., Evans, R.M., Mangelsdorf, D.J., 2006. Anatomical profiling of nuclear receptor expression reveals a hierarchical transcriptional network. *Cell* 126: 789-799.
- [14] Escher, P., Braissant, O., Basu-Modak, S., Michalik, L., Wahli, W., Desvergne, B., 2001. Rat PPARs: quantitative analysis in adult rat tissues and regulation in fasting and refeeding. *Endocrinology* 142: 4195-4202.
- [15] Kersten, S., Seydoux, J., Peters, J.M., Gonzalez, F.J., Desvergne, B., Wahli, W., 1999. Peroxisome proliferator-activated receptor alpha mediates the adaptive response to fasting. *J Clin Invest* 103: 1489-1498.

- [16] Leone, T.C., Weinheimer, C.J., Kelly, D.P., 1999. A critical role for the peroxisome proliferator-activated receptor alpha (PPARalpha) in the cellular fasting response: the PPARalpha-null mouse as a model of fatty acid oxidation disorders. *Proc Natl Acad Sci U S A* 96: 7473-7478.
- [17] Regnier, M., Polizzi, A., Lippi, Y., Fouche, E., Michel, G., Lukowicz, C., et al., 2017. Insights into the role of hepatocyte PPARalpha activity in response to fasting. *Mol Cell Endocrinol*.
- [18] Kersten, S., 2014. Integrated physiology and systems biology of PPARalpha. *Molecular metabolism* 3: 354-371.
- [19] Lehmann, J.M., Moore, L.B., Smith-Oliver, T.A., Wilkison, W.O., Willson, T.M., Kliewer, S.A., 1995. An antidiabetic thiazolidinedione is a high affinity ligand for peroxisome proliferator-activated receptor gamma (PPAR gamma). *J Biol Chem* 270: 12953-12956.
- [20] Tontonoz, P., Hu, E., Spiegelman, B.M., 1994. Stimulation of adipogenesis in fibroblasts by PPAR gamma 2, a lipid-activated transcription factor. *Cell* 79: 1147-1156.
- [21] Barak, Y., Nelson, M.C., Ong, E.S., Jones, Y.Z., Ruiz-Lozano, P., Chien, K.R., et al., 1999. PPAR gamma is required for placental, cardiac, and adipose tissue development. *Mol Cell* 4: 585-595.
- [22] Majithia, A.R., Tsuda, B., Agostini, M., Gnanapradeepan, K., Rice, R., Peloso, G., et al., 2016. Prospective functional classification of all possible missense variants in PPARG. *Nat Genet* 48: 1570-1575.
- [23] Fukui, Y., Masui, S., Osada, S., Umesono, K., Motojima, K., 2000. A new thiazolidinedione, NC-2100, which is a weak PPAR-gamma activator, exhibits potent antidiabetic effects and induces uncoupling protein 1 in white adipose tissue of KKAY obese mice. *Diabetes* 49: 759-767.
- [24] Koh, Y.J., Park, B.H., Park, J.H., Han, J., Lee, I.K., Park, J.W., et al., 2009. Activation of PPAR gamma induces profound multilocularization of adipocytes in adult mouse white adipose tissues. *Experimental & molecular medicine* 41: 880-895.
- [25] Petrovic, N., Walden, T.B., Shabalina, I.G., Timmons, J.A., Cannon, B., Nedergaard, J., 2010. Chronic peroxisome proliferator-activated receptor gamma (PPARgamma) activation of epididymally derived white adipocyte cultures reveals a population of thermogenically competent, UCP1-containing adipocytes molecularly distinct from classic brown adipocytes. *J Biol Chem* 285: 7153-7164.
- [26] Gray, S.L., Dalla Nora, E., Backlund, E.C., Manieri, M., Virtue, S., Noland, R.C., et al., 2006. Decreased brown adipocyte recruitment and thermogenic capacity in mice with impaired peroxisome proliferator-activated receptor (P465L PPARgamma) function. *Endocrinology* 147: 5708-5714.
- [27] Barquissau, V., Beuzelin, D., Pisani, D.F., Beranger, G.E., Mairal, A., Montagner, A., et al., 2016. White-to-brite conversion in human adipocytes promotes metabolic reprogramming towards fatty acid anabolic and catabolic pathways. *Molecular metabolism* 5: 352-365.
- [28] Digby, J.E., Montague, C.T., Sewter, C.P., Sanders, L., Wilkison, W.O., O'Rahilly, S., et al., 1998. Thiazolidinedione exposure increases the expression of uncoupling protein 1 in cultured human preadipocytes. *Diabetes* 47: 138-141.
- [29] Li, P., Zhu, Z., Lu, Y., Granneman, J.G., 2005. Metabolic and cellular plasticity in white adipose tissue II: role of peroxisome proliferator-activated receptor-alpha. *Am J Physiol Endocrinol Metab* 289: E617-626.

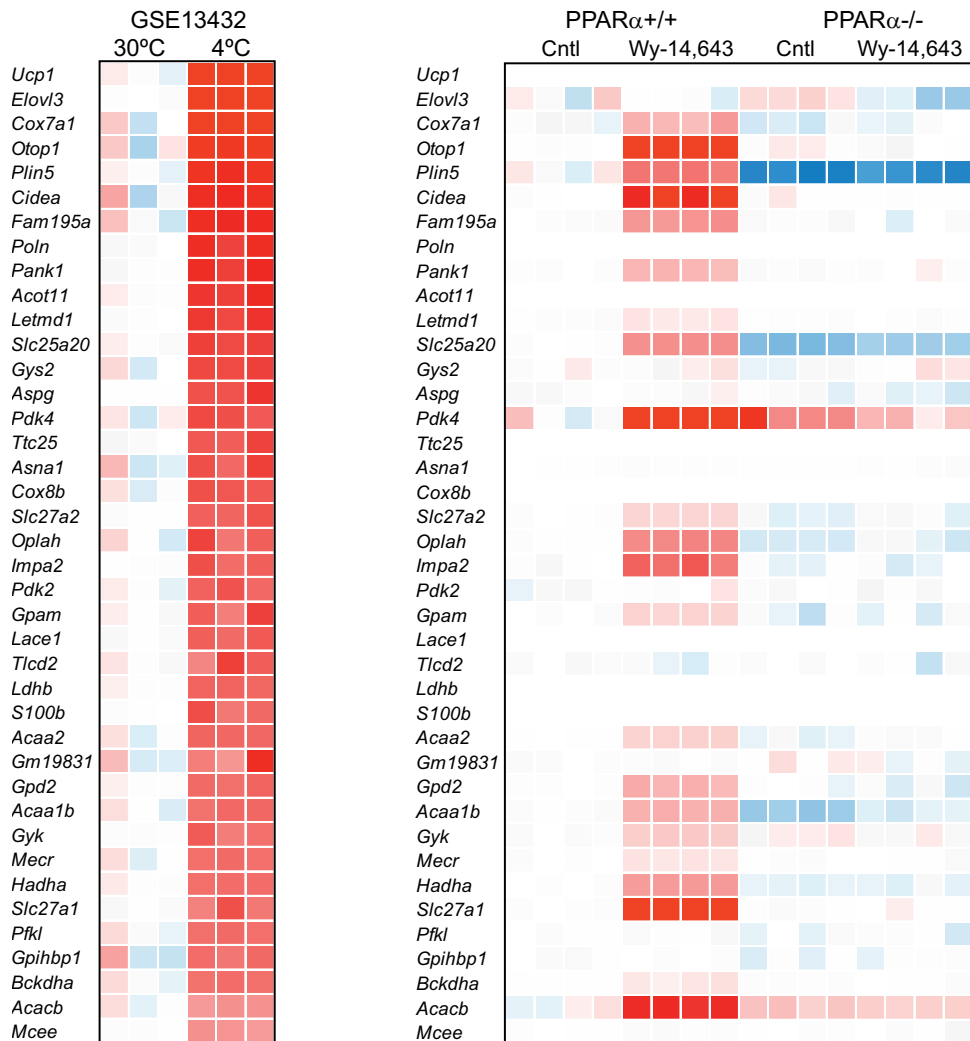
- [30] Xue, B., Coulter, A., Rim, J.S., Koza, R.A., Kozak, L.P., 2005. Transcriptional synergy and the regulation of *Ucp1* during brown adipocyte induction in white fat depots. *Mol Cell Biol* 25: 8311-8322.
- [31] Jankovic, A., Golic, I., Markelic, M., Stancic, A., Otasevic, V., Buzadzic, B., et al., 2015. Two key temporally distinguishable molecular and cellular components of white adipose tissue browning during cold acclimation. *J Physiol* 593: 3267-3280.
- [32] Bolstad, B.M., Irizarry, R.A., Astrand, M., Speed, T.P., 2003. A comparison of normalization methods for high density oligonucleotide array data based on variance and bias. *Bioinformatics* 19: 185-193.
- [33] Irizarry, R.A., Bolstad, B.M., Collin, F., Cope, L.M., Hobbs, B., Speed, T.P., 2003. Summaries of Affymetrix GeneChip probe level data. *Nucleic Acids Res* 31: e15.
- [34] Dai, M., Wang, P., Boyd, A.D., Kostov, G., Athey, B., Jones, E.G., et al., 2005. Evolving gene/transcript definitions significantly alter the interpretation of GeneChip data. *Nucleic Acids Res* 33: e175.
- [35] Sartor, M.A., Tomlinson, C.R., Wesselkamper, S.C., Sivaganesan, S., Leikauf, G.D., Medvedovic, M., 2006. Intensity-based hierarchical Bayes method improves testing for differentially expressed genes in microarray experiments. *BMC Bioinformatics* 7: 538.
- [36] Subramanian, A., Tamayo, P., Mootha, V.K., Mukherjee, S., Ebert, B.L., Gillette, M.A., et al., 2005. Gene set enrichment analysis: a knowledge-based approach for interpreting genome-wide expression profiles. *Proc Natl Acad Sci U S A* 102: 15545-15550.
- [37] Sanderson, L.M., Degenhardt, T., Koppen, A., Kalkhoven, E., Desvergne, B., Muller, M., et al., 2009. Peroxisome Proliferator-Activated Receptor β/δ (PPAR β/δ) but Not PPAR α Serves as a Plasma Free Fatty Acid Sensor in Liver. *Molecular and Cellular Biology* 29: 6257.
- [38] Stienstra, R., Duval, C., Keshtkar, S., van der Laak, J., Kersten, S., Muller, M., 2008. Peroxisome proliferator-activated receptor γ activation promotes infiltration of alternatively activated macrophages into adipose tissue. *J Biol Chem* 283: 22620-22627.
- [39] Alex, S., Lange, K., Amolo, T., Grinstead, J.S., Haakonsson, A.K., Szalowska, E., et al., 2013. Short-chain fatty acids stimulate angiopoietin-like 4 synthesis in human colon adenocarcinoma cells by activating peroxisome proliferator-activated receptor γ . *Mol Cell Biol* 33: 1303-1316.
- [40] Broeders, E.P., Nascimento, E.B., Havekes, B., Brans, B., Roumans, K.H., Tailleux, A., et al., 2015. The Bile Acid Chenodeoxycholic Acid Increases Human Brown Adipose Tissue Activity. *Cell Metab* 22: 418-426.
- [41] Rosell, M., Kaforou, M., Frontini, A., Okolo, A., Chan, Y.W., Nikolopoulou, E., et al., 2014. Brown and white adipose tissues: intrinsic differences in gene expression and response to cold exposure in mice. *Am J Physiol Endocrinol Metab* 306: E945-964.
- [42] Xue, Y., Petrovic, N., Cao, R., Larsson, O., Lim, S., Chen, S., et al., 2009. Hypoxia-independent angiogenesis in adipose tissues during cold acclimation. *Cell Metab* 9: 99-109.
- [43] Simcox, J., Geoghegan, G., Maschek, J.A., Bensard, C.L., Pasquali, M., Miao, R., et al., 2017. Global Analysis of Plasma Lipids Identifies Liver-Derived Acylcarnitines as a Fuel Source for Brown Fat Thermogenesis. *Cell Metab* 26: 509-522 e506.

- [44] Rachid, T.L., Penna-de-Carvalho, A., Bringham, I., Aguila, M.B., Mandarim-de-Lacerda, C.A., Souza-Mello, V., 2015. Fenofibrate (PPARalpha agonist) induces beige cell formation in subcutaneous white adipose tissue from diet-induced male obese mice. *Mol Cell Endocrinol* 402: 86-94.
- [45] Hummasti, S., Tontonoz, P., 2006. The peroxisome proliferator-activated receptor N-terminal domain controls isotype-selective gene expression and adipogenesis. *Mol Endocrinol* 20: 1261-1275.
- [46] Patsouris, D., Reddy, J.K., Muller, M., Kersten, S., 2006. Peroxisome proliferator-activated receptor alpha mediates the effects of high-fat diet on hepatic gene expression. *Endocrinology* 147: 1508-1516.
- [47] Yu, S., Matsusue, K., Kashireddy, P., Cao, W.Q., Yeldandi, V., Yeldandi, A.V., et al., 2003. Adipocyte-specific gene expression and adipogenic steatosis in the mouse liver due to peroxisome proliferator-activated receptor gamma1 (PPARgamma1) overexpression. *J Biol Chem* 278: 498-505.
- [48] Lasar, D., Rosenwald, M., Kiehlmann, E., Balaz, M., Tall, B., Opitz, L., et al., 2018. Peroxisome Proliferator Activated Receptor Gamma Controls Mature Brown Adipocyte Inducibility through Glycerol Kinase. *Cell Rep* 16:760-773.
- [49] Montagner, A., Polizzi, A., Fouche, E., Ducheix, S., Lippi, Y., Lasserre, F., et al., 2016. Liver PPARalpha is crucial for whole-body fatty acid homeostasis and is protective against NAFLD. *Gut* 65: 1202-1214.
- [50] Ahmadian, M., Abbott, M.J., Tang, T., Hudak, C.S., Kim, Y., Bruss, M., et al., 2011. Desnutrin/ATGL is regulated by AMPK and is required for a brown adipose phenotype. *Cell Metab* 13: 739-748.
- [51] Dijk, W., Heine, M., Vergnes, L., Boon, M.R., Schaart, G., Hesselink, M.K., et al., 2015. ANGPTL4 mediates shuttling of lipid fuel to brown adipose tissue during sustained cold exposure. *eLife* 4.

Supplemental materials

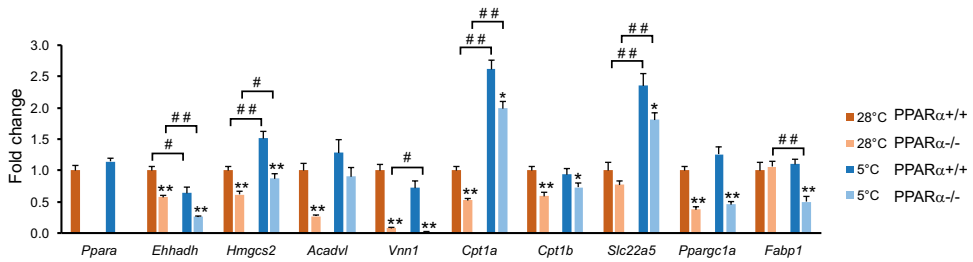
Supplemental table 1. List of primers used.

<i>Pparg</i>	CACAATGCCATCAGGTTTGG	GCTGGTCGATATCACTGGAGATC
<i>Fabp4</i>	AAGAAGTGGGAGTGGGCTTT	AATCCCCATTTACGCTGATG
<i>36B4</i>	ATGGGTACAAGCGCCTCCTG	GCCTTGACCTTTTCAGTAAG
<i>Elovl3</i>	TTCTCACGCGGGTAAAAATGG	GAGCAACAGATAGACGACCAC
<i>Adtrp</i>	TGTGGCGCTACGTTTCAGAC	CCGGCGACTAGGATGTAAGC
<i>Slc2a4</i>	GGAAGGAAAAGGGCTATGCTG	TGAGGAACCGTCCAAGAATGA
<i>Ucp1</i>	CCTGCTCTCTCGGAAACAA	TGTAGGCTGCCAATGAACA
<i>Cidea</i>	TGACATTCATGGGATTGCAGAC	GGCCAGTTGTGATGACTAAGAC
<i>Ppargca1</i>	AGACGGATTGCCCTCATTGTA	TGTAGCTGAGCTGAGTGTGG
<i>G0s2</i>	AGTGCTGCCTCTCTCCAC	TTTCATCTGAGCTCTGGGC
<i>Gpd1</i>	CTCGCCATCGCCCTCACTG	ACCGCTCACTCGCTCTTTC
<i>Ppara</i>	TATTCGGCTGAAGCTGGTGTAC	CTGGCATTGTTCGGTCT
<i>Ehhadh</i>	AAAGCTAGTTGGACCATACGG	ATGTAAGGCCAGTGGGAGATT
<i>Hmgcs2</i>	TTCTTGCGGTAGGCTGCATAG	TGGTGGATGGGAAGCTGTCTA
<i>Acadvl</i>	CACTCAGGCAGTTCTGGACA	TCCAGGGTAACGCTAACAC
<i>Vnn1</i>	CTTTCCTCGGGCTGTTTAC	CCTCCAGGTATGGGTAGATCGT
<i>Cpt1a</i>	CTCAGTGGGAGCGACTCTTCA	GGCCTCTGTGGTACACGACAA
<i>Cpt1b</i>	GAGCCAGATTCTGCACCATTG	CCCTGTGGGTCCTTCCAAG
<i>Slc25a20</i>	CCGAAACCCATCAGTCCGTTTAA	ACATAGGTGGCTGTCCAGACAA
<i>Slc22a5</i>	TTGGAGACGAAGGACGGACG	GCTCAGAGAAGTTGGCGATGG
<i>Fabp1</i>	ATGAACTTCTCCGGCAAGTACC	CTGACACCCCTTGATGTCC
<i>Cd36</i>	AGATGACGTGGCAAAGAACAG	CCTTGGCTAGATAACGAAGTCTG
<i>PDK4</i>	TGGAGCATTTCTCGCGTAC	ACAGGCAATTCTTGTGCAAA
<i>ACADVL</i>	GTCTGGTGGTCTTACCGC	CACGGGTCCAAGAAGTATGAT
<i>ADIPOQ</i>	TATCCCCAACATGCCATTCTG	TGGTAGGCAAAGTAGTACAGCC
<i>UCP1</i>	AGGATCGGCCTCTACGACAC	GCCAATGAATACTGCCACTC



Supplemental figure 1. PPAR α is highly upregulated during cold-induced browning.

(A) Heatmap of the top 40 most highly induced genes in subcutaneous adipose tissue of mice after 7 days at 4°C as compared to 7 days at 30°C (GSE13432). In parallel, the expression profiles are shown of the same genes in livers of wild type and PPAR α ^{-/-} mice treated with Wy-14.643 for 5 days (GSE8295).



Supplemental figure 2. Effect of PPARα ablation on hepatic gene expression during acute cold.

Hepatic expression of selected genes in wildtype and PPARα^{-/-} mice exposed to cold (5°C) or thermoneutrality (28°C) for 24h. Both groups of mice were housed at thermoneutrality (28°C) for 5 weeks prior to the intervention. Error bars represent SEM. Asterisk indicates significantly different from wildtype mice under the same conditions according to Student's t-test (*P<0.05, **P<0.001). Pound sign indicates significant difference between cold and thermoneutral mice according to Student's t-test (#P<0.05, ##P<0.001).

CHAPTER 5



Transcriptomic signature of fasting in human adipose tissue

Merel Defour, Charlotte C.J.R. Michielsen, Shauna D. O'Donovan,
Lydia A. Afman, Sander Kersten

ABSTRACT

Little is known about gene regulation by fasting in human adipose tissue. Accordingly, the objective of this study was to investigate the effects of fasting on adipose tissue gene expression in humans. To that end, subcutaneous adipose tissue biopsies were collected from eleven volunteers 2h and 26h after consumption of a standardized meal. For comparison, epididymal adipose tissue was collected from C57Bl/6J mice in the ab-libitum fed state and after a 16h fast. The timing of sampling adipose tissue roughly corresponds with the near depletion of liver glycogen. Transcriptome analysis was carried out using Affymetrix microarrays. We found that, 1) fasting downregulated numerous metabolic pathways in human adipose tissue, including triglyceride and fatty acid synthesis, glycolysis and glycogen synthesis, TCA cycle, oxidative phosphorylation, mitochondrial translation, and insulin signaling; 2) fasting downregulated genes involved in proteasomal degradation in human adipose tissue; 3) fasting had much less pronounced effects on the adipose tissue transcriptome in humans than mice; 4) although major overlap in fasting-induced gene regulation was observed between human and mouse adipose tissue, many genes were differentially regulated in the two species, including genes involved in insulin signaling (*PRKAG2*, *PFKFB3*), PPAR signaling (*PPARG*, *ACSL1*, *HMGCS2*, *SLC22A5*, *ACOT1*), glycogen metabolism (*PCK1*, *PYGB*), and lipid droplets (*PLIN1*, *PNPLA2*, *CIDEA*, *CIDEA*). In conclusion, although numerous genes and pathways are regulated similarly by fasting in human and mouse adipose tissue, many genes show very distinct responses to fasting in humans and mice. Our data provide a useful resource to study adipose tissue function during fasting.

INTRODUCTION

Throughout human history, one of the greatest threats to the survival of our ancestors were long periods with little to no food. As a consequence, starvation has been a key evolutionary pressure shaping human energy metabolism. In the modern world of caloric excess, the intricate architecture of human energy metabolism that once helped humans to survive starvation now contributes to the unprecedented growth in obesity and related metabolic diseases [1].

Following the cessation of food intake, the body goes through different phases of metabolic adaptation aimed at maximally prolonging survival [2]. In the first phase, consumed nutrients are digested, absorbed and stored. In the second phase, glycogen stores in the liver are utilized to maintain blood glucose levels. At this stage, the adipose tissue switches from a net lipid storage organ to a lipid release organ, raising non-esterified fatty acid levels in the blood. In the third phase, the liver glycogen stores are almost completely emptied and gluconeogenesis becomes the primary glucose production pathway, which is accompanied by rapid degradation of muscle protein in order to provide gluconeogenic amino acids. In the fourth phase, which lasts for weeks, the production of ketone bodies in the liver is strongly activated, partly replacing glucose as fuel for the brain and allowing gluconeogenesis and muscle proteolysis to be sustained at a low level. In the fifth phase, ketone bodies become the dominant fuel for the brain and other tissues almost entirely rely on fatty acids as fuel [3].

In addition to the five phases of fasting outlined above, another model exists that separates prolonged fasting into 3 stages. According to this model, stage 1 is characterized by blood glucose levels being maintained by glycogenolysis and by gluconeogenesis from amino acids. In stage 2, which might last for several weeks, liver glycogen is depleted, fatty acids are the overall main energy source, and ketone bodies gradually become the major fuel for the brain. Finally, stage 3 starts when the fat stores are exhausted and protein becomes the primary energy source for the body, reflecting the last resort to produce energy and delay imminent death [4,5].

As the principal energy depot, the adipose tissue plays a critical role in the adaptive response to fasting. Fasting activates intracellular lipolysis in adipocytes, thereby releasing free fatty acids and glycerol. At the same time, fasting represses extracellular lipolysis, leading to reduced uptake and storage of circulating triglyceride-derived fatty acids [4]. Many of the changes in adipose tissue metabolism are mediated by changes in the activity of key metabolic enzymes, which in turn are partly driven by changes in mRNA levels of the corresponding genes, as well as other relevant genes [6,7].

Besides storing excess lipids, adipose tissue also has an important endocrine function [8]. Indeed, adipose tissue produces a variety of cytokines and adipokines, many of which are involved in immune and metabolic regulation, including leptin, adiponectin, and ANGPTL4 [9–12]. The plasma level of a number of adipokines is dependent on feeding status. For example, while leptin levels are highest in the fed state, plasma ANGPTL4 levels peak during fasting [13,14]. The changes in plasma levels of adipokines partly stem from regulation at the level of gene transcription.

Despite the importance of gene regulation in the adaptive response to fasting, few efforts have been undertaken to obtain a comprehensive view of the impact of fasting on gene expression in adipose tissue. So far, studies have investigated the effect of fasting on the adipose tissue transcriptome in rats, chickens, pigs, and mice, showing marked changes in gene expression [4,7,15–17]. By contrast, surprisingly little is known about the effect of fasting on gene expression in human adipose tissue. Accordingly, in this study we aimed to study the effect of fasting on the adipose tissue transcriptome in humans. In addition, a comparison was made between the fasting-induced changes in gene expression in adipose tissue of humans and mice.

METHODS

FASTING study

Twenty-four healthy volunteers aged 40–70 years with a BMI of 22–30 kg/m² were included in the FASTING study. Details of the study are described elsewhere [18]. In this study, the primary outcome measure used for the statistical power calculation was the plasma ANGPTL4 concentration. Based upon a calculated standard deviation of the response variable of 14 ng/mL, and a power of 90 percent that the study will detect a treatment difference at a two-sided 0.05 significance level, the number of research subjects needed to show an effect was calculated at 21. To obviate a possible drop-out of 10%, 24 subjects were included in the study. One volunteer failed to complete the study. At the start of the study the volunteers consumed a standardized meal until full (*ad libitum*), consisting of 22 energy% protein, 24 energy% fat, 51 energy% carbohydrate and 476 kJ per 100 gram. After consumption of the standardized meal at 18.00h, subjects were not allowed to eat but could drink water for the next 26 hours. Two hours after consumption of the meal at 20.00, blood samples were taken and a subcutaneous adipose tissue biopsy was collected from the periumbilical area, representing the fed state. Twenty-four hours later at 20.00 and thus 26 hours after consumption of the meal, a second blood sample and subcutaneous adipose tissue biopsy was collected from the opposite side of the umbilicus, representing the fasting state. The two blood samples and adipose tissue biopsies were thus taken at the same time of the day, thereby avoiding the potential influence of circadian rhythmicity.

The subcutaneous adipose tissue samples were obtained by needle biopsy from the periumbilical area under local anesthesia. The samples were rinsed to get rid of remaining blood, separated into 3-4 aliquots, and snap frozen in liquid nitrogen. All samples were stored in aliquots at -80°C. The first two aliquots were used for immunoblotting and measurement of lipoprotein lipase activity [18]. The third aliquot was used for transcriptome analysis. The FASTING study was approved by the Medical Ethics Committee of Wageningen University and registered at ClinicalTrials.gov, identifier: NCT03757767.

Animal study

The 24 mice included in this study were male 3- to 4-month-old wildtype mice on a C57Bl/6J background. The mice were individually housed at 21-22°C under specific pathogen-free conditions and followed a 6:00-18:00 day-night cycle with ad libitum access to food and water. Twelve mice were fasted for 16 hours from 17:00 until 9:00 the next day, while having full access to water. The other 12 mice had ad libitum access to food and water. Both sets of mice were euthanized at 9:00, thereby avoiding the potential influence of circadian rhythmicity. For both the mice and the human subjects, the timing of adipose tissue and blood collection represents the beginning of the inactive phase. Anesthesia was performed using a mixture of isoflurane (1.5%), nitrous oxide (70%), and oxygen (30%). Blood was collected by orbital puncture into EDTA tubes. The mice were euthanized by cervical dislocation, after which the adipose tissues were excised and snap frozen liquid nitrogen. For RNA isolation and microarray analysis, the upper part of the epididymal adipose tissue was used. All samples were stored in aliquots at -80°C. Eight mice per group were randomly selected for analysis of the adipose tissue transcriptome. The study was performed at the Centre for Small Animals, which is part of the Centralized Facilities for Animal Research at Wageningen University and Research (CARUS), and were approved by the Local Animal Ethics Committee of Wageningen University.

Quantification of plasma parameters

Human and mouse blood samples were collected in EDTA-coated tubes and centrifuged at 4°C for 15 min at 10000 g. Plasma was collected and stored at -80°C. For the human plasma samples, non-esterified fatty acids (NEFA) and β -hydroxybutyrate were measured using kits from WAKO Diagnostics (Cat: 3055 and 417-73501/413-73601, WAKO Diagnostics, Germany) according to the manufacturer's protocol. Glucose and triglycerides were determined in lithium heparin plasma samples by the hexokinase and lipase assay, respectively. Analyses were performed by hospital Gelderse Vallei (Ede, the Netherlands), using the Siemens Dimension Vista® System (Siemens Healthcare, The Hague, the Netherlands). For the mouse samples, plasma concentrations of glucose (Sopachem, Ochten, the Netherlands), triglycerides and cholesterol (InstruChemie, Delfzijl, the Netherlands), glycerol (Sigma-Aldrich, Houten,

the Netherlands), β -hydroxybutyrate (Sigma-Aldrich, Houten, the Netherlands) and non-esterified fatty acids (Wako Chemicals, Neuss, Germany; HR(2) Kit) were determined according to manufacturers' instructions. Plasma metabolite levels are only reported for the 11 individuals for which complete transcriptome data were collected.

RNA isolation and transcriptome analysis

After assessing the primary outcome measures, a complete set of adipose tissue samples was only available for 16 subjects. From these 16 subjects, 12 subjects were randomly selected for inclusion in the microarray. This number is based on the capacity of the Affymetrix array plate. The adipose tissue biopsies were processed to isolate RNA and perform transcriptomics. Total RNA was isolated from human subcutaneous and mouse epididymal adipose tissue using TRIzol reagent (Thermo Fisher Scientific, the Netherlands) and purified using the Qiagen RNeasy Mini kit (Qiagen, the Netherlands). RNA integrity was verified with RNA 6000 Nano chips on an Agilent 2100 bioanalyzer (Agilent Technologies, Amsterdam, The Netherlands). RIN scores for all samples were 7 or higher. Purified RNA (100 ng) was labeled with the Ambion WT expression kit (Carlsbad, CA) and hybridized to an Affymetrix Mouse Gene 2.1 ST array plate (Affymetrix, Santa Clara, CA) or Human Gene 2.1 ST 24 Array Plate (Affymetrix, Santa Clara, CA). Hybridization, washing, and scanning were carried out on an Affymetrix GeneTitan platform according to the manufacturer's instructions. One subject was removed from the analysis because a sample failed quality control, resulting in a complete transcriptome dataset for 11 subjects (8 women and 3 men). Probes were assigned to Entrez IDs as a unique gene identifier according to Dai et al. [19]. Normalized expression estimates were obtained from the raw intensity values applying the robust multi-array analysis preprocessing algorithm available in the Bioconductor library AffyPLM with default settings [20,21]. The P values for the comparison between fed and fasted samples were calculated using an Intensity-Based Moderated T-statistic (IBMT) [22]. Genes were defined as significantly changed when $P < 0.001$. Paired analysis was carried out for the human samples. Unpaired analysis was carried out for the mouse samples.

For validation, messenger RNA levels of selected genes were measured by reverse transcription quantitative PCR using SensiMix (Bioline; GC Biotech, Alphen aan den Rijn, The Netherlands) on a CFX384 real-time PCR detection system (Bio-Rad Laboratories, Veenendaal, the Netherlands). The *HSP90* gene was used for normalization.

Gene set enrichment analysis (GSEA) was used to identify gene sets that were enriched among the upregulated or downregulated genes [23]. Genes were ranked based on the IBMT-statistic and subsequently analyzed for over- or underrepresentation in predefined gene sets derived from Gene Ontology, KEGG,

National Cancer Institute, PFAM, Biocarta, Reactome and WikiPathways pathway databases. Only gene sets consisting of more than 15 and fewer than 500 genes were taken into account. Statistical significance of GSEA results was determined using 1,000 permutations. EnrichR analysis was carried out on lists of genes that met specific criteria as indicated in the results section [24,25].

Cibersort was used to determine the heterogeneity in the adipose tissue transcriptomes, as human fat biopsies taken by needle biopsy can be contaminated by other tissues and blood cells. Cibersort is a transcriptome-based in silico deconvolution method that uses gene expression data to provide an estimate of the abundances of cell types in a mixed cell population [26]. The specific adipose tissue gene expression signature used was derived from Lenz et al. [27].

Array data have been submitted to the Gene Expression Omnibus (accession number GSE154612).

Statistical analysis

Statistical analysis of the plasma metabolites and qPCR was carried out by Student's t-test. Paired analysis was done for the human samples and unpaired analysis for the mouse samples. Statistical significance was assigned at $P < 0.05$.

RESULTS

The main objective of the FASTING study was to determine the effect of a prolonged fast on ANGPTL4 gene and protein expression in human subcutaneous adipose tissue, and to link these effects with changes in LPL expression and activity. The results of these analyses have been published [18], showing that ANGPTL4 levels in human adipose tissue are increased by fasting, likely via increased plasma cortisol and free fatty acids and decreased plasma insulin, resulting in decreased LPL activity. A secondary objective was to study the effect of fasting on whole genome expression in adipose tissue. Participants received a standardized meal at 18.00h, followed by blood sampling and collection of an adipose tissue biopsy at 20.00h, representing the fed state. At 20.00h the next day, a second blood sample and adipose tissue biopsy were collected. Accordingly, the two blood samples and adipose tissue biopsies were taken at the same time, thereby avoiding the potential influence of circadian rhythmicity. The participant characteristics are listed in Supplemental table 1.

Plasma levels of several metabolites are presented in Table 1. In the human volunteers and in mice, the changes in plasma metabolites during fasting were as expected, with glucose and triglycerides significantly going down, and non-esterified fatty acids and β -hydroxybutyrate significantly going up (Table 1). Plasma

cholesterol concentrations increased significantly by fasting in humans but not in mice. Despite the shorter duration of fasting, the absolute changes in plasma triglycerides, non-esterified fatty acids, β -hydroxybutyrate, and glucose were more pronounced in mice than in humans (Table 1).

Table 1. Effect of fasting on plasma concentrations of selected metabolites in humans (n=11) and mice (n=12 per group). Concentrations are in millimolar \pm SD.

mean	Human			Mouse		
	fed	fasted	p value	fed	fasted	p value
glucose	4.97 \pm 0.44	4.58 \pm 0.20	2.28E-02	9.92 \pm 3.15	5.94 \pm 1.09	7.75E-07
NEFA	0.41 \pm 0.10	0.76 \pm 0.17	1.47E-05	0.28 \pm 0.06	0.90 \pm 0.20	1.36E-18
TAG	1.96 \pm 1.33	0.91 \pm 0.28	1.13E-02	1.84 \pm 0.57	0.71 \pm 0.21	2.61E-11
cholesterol	5.87 \pm 0.89	6.24 \pm 0.90	2.66E-03	2.59 \pm 0.33	2.35 \pm 0.64	9.96E-02
β -hydroxybutyrate	0.07 \pm 0.04	0.98 \pm 0.37	8.73E-06	0.25 \pm 0.25	1.74 \pm 0.38	2.09E-09

Dissimilarity in basal gene expression in human and mouse adipose tissue

To determine the transcriptional response to fasting in humans, we performed whole genome expression profiling on the subcutaneous adipose tissue biopsies of 11 subjects using microarrays. To determine the transcriptional response to fasting in mice, we applied the same analysis pipeline on epididymal adipose tissue collected from 8 ad libitum fed mice and 8 mice that had fasted for 16 hours. The duration of fasting in mice and humans roughly coincides with the end of phase 3 of the five phases model of fasting, when hepatic glycogen levels are nearly depleted [2,28]. Using NCBI homologene, human genes were coupled to the mouse homologs and vice versa, generating 16502 pairs. Ultimately, expression data were available for 12502 human-mouse homologs.

First, for the 25 most highly expressed genes, we visualized the variation in adipose gene expression among the various subjects. Overall, the variation in gene expression was relatively small, indicating uniformity in the composition of the adipose tissue samples (Figure 1). Interestingly, *SAA1* (serum amyloid A1), *ECH1*, and *ANXA1* mRNA were significantly lower in males than females, whereas the opposite pattern was observed for *RPS11*.

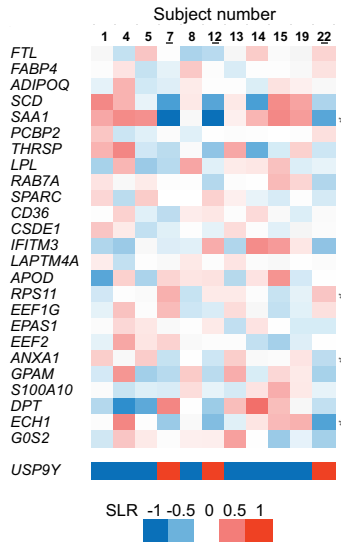


Figure 1. Inter-individual variation in human adipose tissue gene expression.

Inter-individual variation in expression of the 25 most abundant genes in human adipose tissue. The heatmap shows the difference in expression value of each subject compared to mean expression value of all subjects, expressed as signal log ratio (SLR). *USP9Y* is a gene located on the Y chromosome. Male subjects are underlined. Genes significantly different between men and women are marked with asterisk ($P < 0.01$).

Fasting more profoundly impacts adipose tissue gene expression in mice than in humans

5

To determine the magnitude of the effect of fasting on gene expression in human and mouse adipose tissue, we generated Volcano plots. The plots revealed that the overall fold changes in gene expression and the statistical significance were much higher in mouse adipose tissue than in human adipose tissue (Figure 2A). Using a P value cut-off of 0.001, 260 genes were upregulated by fasting and 557 genes were downregulated by fasting in human adipose tissue (Figure 2B, Supplemental table 2). Conversely, using the same criteria, 1035 genes were upregulated by fasting in mouse adipose tissue and 1378 genes were downregulated (Figure 2B, Supplemental table 2). The number of significantly regulated genes was higher when using FDR Benjamini-Hochberg < 0.05 . For the remainder of the paper we used the more conservative $P < 0.001$ as statistical cut-off for differentially expressed genes.

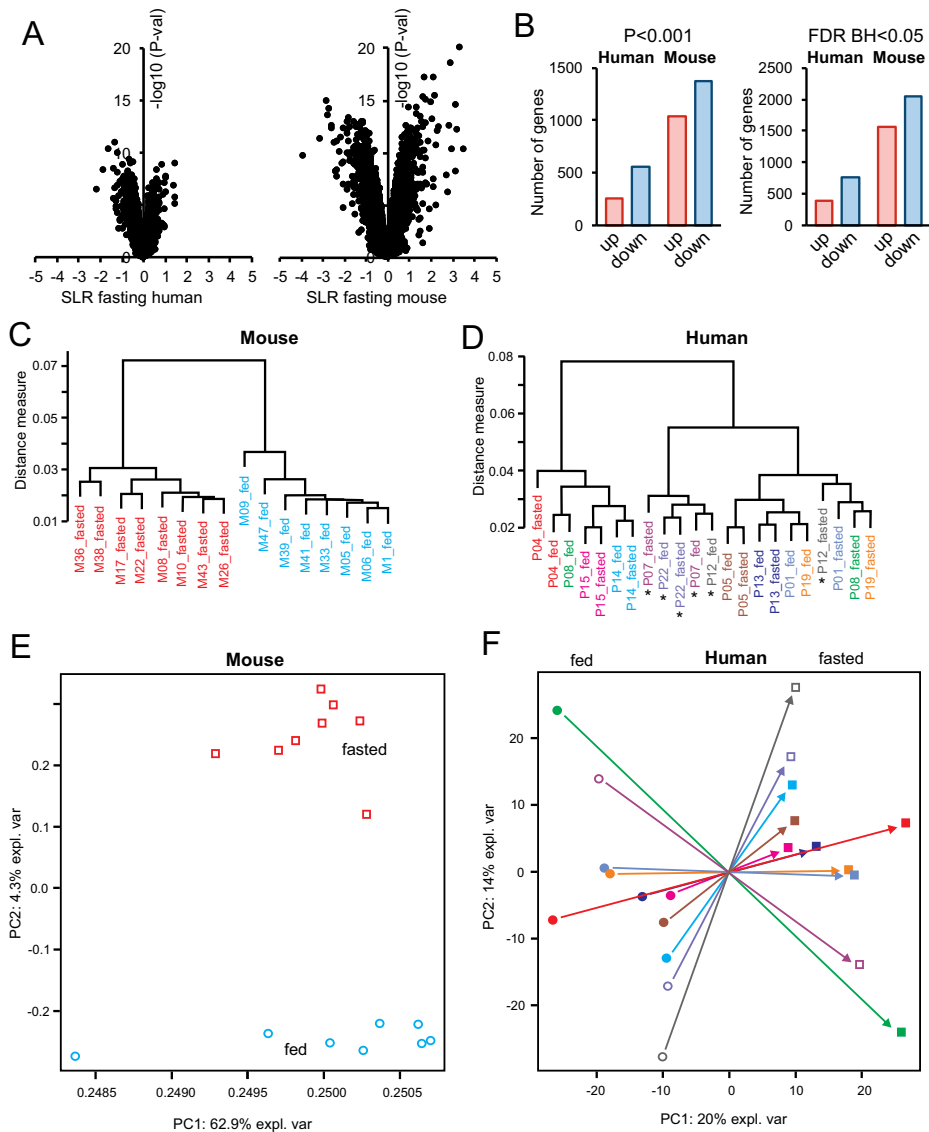


Figure 2. Comparative analysis of fasting-induced whole genome expression changes in mouse and human adipose tissue.

A) Volcano plot showing the relation between mean signal log ratio ($2\log[\text{fold-change}]$, x-axis) and the $-\log_{10}$ of the P-value (y-axis) for the effect of fasting in humans (left) and mice (right). B) Number of significantly up- and downregulated genes by fasting in human and mouse adipose tissue (left, $P < 0.001$; right, FDR BH < 0.05). C) Hierarchical clustering of transcriptomics data of adipose tissue from mice, showing clear separation by feeding status. Distance criteria are based on Pearson correlation with average linkage. D) Hierarchical clustering of transcriptomics data of adipose tissue from human subjects in the fed or fasted state. Individual subjects are indicated by different colors. Male subjects are indicated by asterisk. Clustering was mostly by donor and not by feeding status. Principle component analysis of transcriptomics data of adipose tissue from fed and fasted mice (E) and human subjects (F). Fed samples are indicated by circles, fasted samples by squares. Individual subjects are indicated by different colors. Males are indicated by open symbol, females are indicated by closed symbols.

Hierarchical clustering clearly separated the mouse adipose tissue samples according to feeding status (Figure 2C). By contrast, the human adipose tissue samples mostly clustered by donor (Figure 2D). The male subjects formed a separate cluster, which was partly disrupted by fasting. Similar to the clustering analysis, Principle Component Analysis also clearly separated the mice according to feeding status (Figure 2E). Even though the scatter in the human adipose tissue samples was much larger than in the mouse adipose tissue samples, a clear and consistent shift could be observed upon fasting (Figure 2F). It is obvious, though, that the magnitude of the impact of fasting on adipose tissue gene expression is quite divergent between different participants. Taken together, these data indicate that fasting has a major effect on gene expression in human adipose tissue, although less pronounced than in mouse adipose tissue.

Effect of fasting on gene expression in human adipose tissue

Subsequently, we concentrated on the effect of fasting on gene expression in human adipose tissue. To estimate the cellular heterogeneity of the biopsies and to study the possible effect of fasting on the cellular composition, we performed Cibersort analysis (Figure 3A). Cibersort is a transcriptome-based *in silico* deconvolution method that uses gene expression data to provide an estimate of the abundances of cell types in a mixed cell population [26]. Adipocytes and adipose stem cells were the dominant cells types in the fat biopsies (Figure 3A, Supplemental figure 1A-D). A number of fat biopsies showed deviating cellular composition. For example, one sample showed a relatively high content of myeloid dendritic cells. Overall, this analysis indicates limited heterogeneity in the composition of the adipose tissue biopsies and furthermore suggests a lack of an effect of fasting on the cellular composition of human adipose tissue.

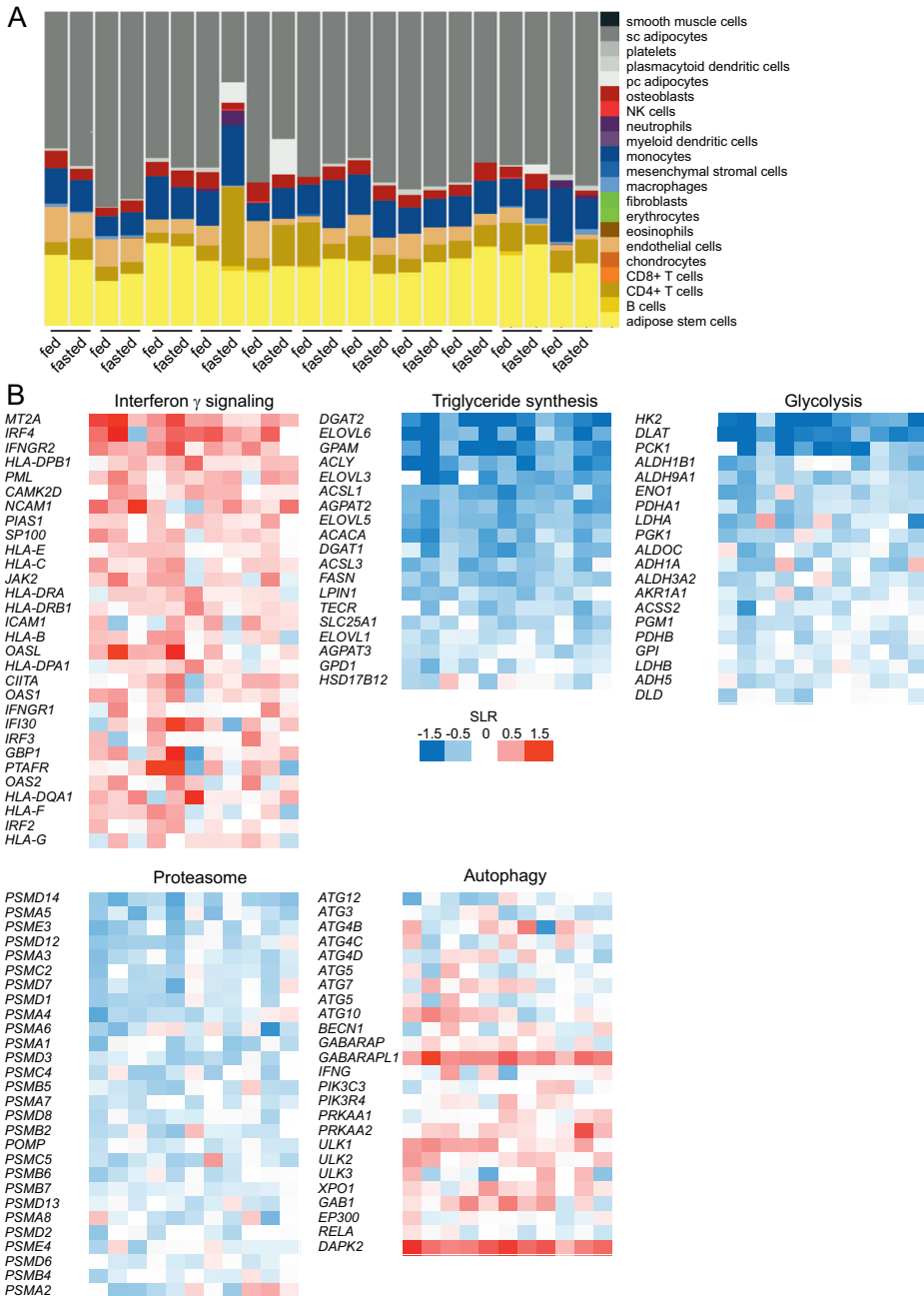


Figure 3. Fasting modulates specific pathways in human adipose tissue.

A) Cibersort analysis on transcriptomics data of adipose tissue from human subjects in the fed or fasted state, showing limited cellular heterogeneity of the biopsies. Fasting did not significantly alter the relative abundance of any of the different cell types in the adipose tissue biopsies. B) Gene Set Enrichment Analysis on transcriptomics data of adipose tissue from human subjects in the fasted versus fed state. The gene sets shown are either positively enriched (interferon γ signalling) or negatively enriched (triglyceride synthesis, glycolysis, proteasome) by fasting. The autophagy gene set was self-assembled and did not emerge from the GSEA. The heatmap shows the fasting-induced gene expression changes in the 11 individual subjects for the positively or negatively enriched genes in a gene set, expressed as signal log ratio. Red indicates upregulated, blue indicates downregulated.

To analyze the effect of fasting on biological pathways, we performed Gene Set Enrichment Analysis. Using a cut-off value of $q < 0.10$, only 3 gene sets were significantly upregulated by fasting in human volunteers and >200 gene sets were significantly downregulated (Supplemental table 3). The gene sets upregulated by fasting in human adipose tissue were related to immunity and included staphylococcus aureus infection and interferon γ signaling (Figure 3B). By contrast, the gene sets downregulated by fasting covered a wide range of metabolic processes, many of which are expected to be repressed by fasting, including triglyceride synthesis, TCA cycle, glycolysis, oxidative phosphorylation, insulin signaling, SREBP signaling, and mitochondrial translation (Figure 3B, Supplemental table 3, Supplemental figure 2). Intriguingly, the gene set proteasome was also significantly downregulated by fasting (Figure 3B), as were many other gene sets that are largely composed of proteasomal genes (Supplemental table 3), indicating that fasting downregulates expression of proteasomal genes in human adipose tissue. By comparison, genes related to autophagy were not altered by fasting, except for *GABARAPL1* and *DAPK2*, which were markedly induced by fasting ($P < 0.001$, Figure 3B).

To further zoom in on the metabolic pathways, the fasting-induced changes in expression of metabolic genes ($P < 0.001$) were visualized in a manually constructed biochemical map (Figure 4A). The map shows that many genes involved in uptake, synthesis, elongation/desaturation, and storage of fatty acids as triglycerides are downregulated by fasting. Also, fasting leads to suppression of many genes involved in uptake, storage, and degradation of glucose, as well as genes involved in cholesterol synthesis and uptake. In addition, the TCA is clearly repressed by fasting (Figure 4A). The map illustrates the pronounced fasting-induced repression of anabolic genes and pathways in human adipose tissue. Intriguingly, the expression of fatty acid transporters *SLC27A1* and *SLC27A2* was upregulated by fasting, whereas *SLC27A4* was downregulated by fasting. Another interesting observation was that insulin-receptor substrate 1 (*IRS1*, involved in insulin signaling) was downregulated by fasting, whereas *IRS2* was upregulated by fasting. Quantitative PCR data confirming clear regulation by fasting of a number of metabolic genes is shown in Figure 4B.

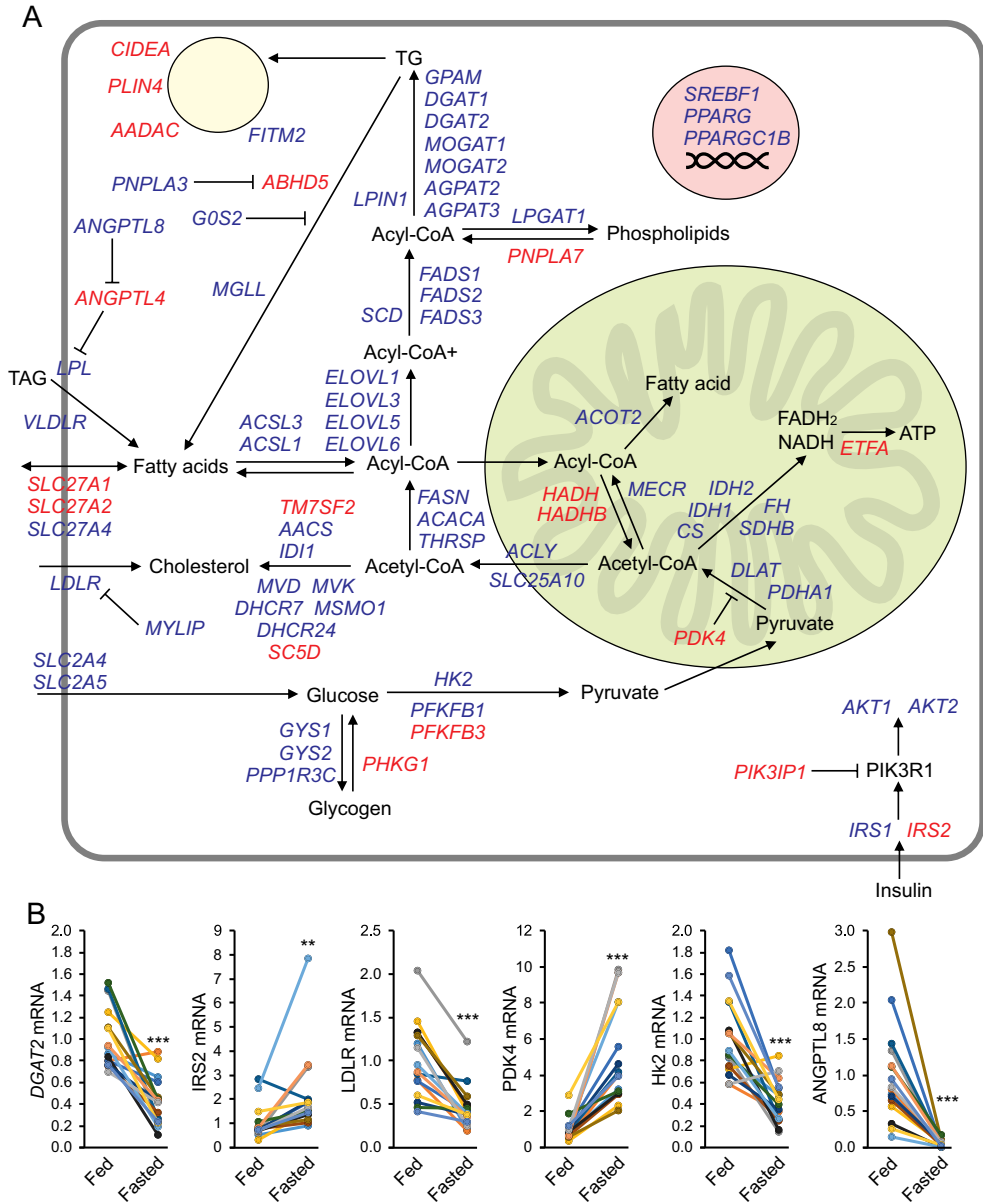


Figure 4. Manually constructed biochemical map of fasting-induced changes in expression of metabolic genes in human adipose tissue.

A) Genes involved in metabolism and significantly altered by fasting in human adipose tissue ($P < 0.001$) were included in this biochemical map. The downregulated genes are depicted in blue and the upregulated genes in red. A pronounced fasting-induced repression of anabolic genes and pathways is observed. B) Quantitative PCR of selected genes in human adipose tissue. ** $P \leq 0.01$, *** $P \leq 0.001$.

Similarities in fasting-induced gene regulation between human and mouse adipose tissue

Next, we addressed to what extent the fasting-induced changes in gene expression are similar in human and mouse adipose tissue. 77 genes were consistently upregulated by fasting in human and mouse adipose tissue ($P < 0.001$; Figure 5A,B; Supplemental table 4). Pathway analysis of these genes via EnrichR did not yield anything significant, suggesting that the commonly induced genes are involved in many different biological processes and thus functionally very diverse. Examples of genes induced by fasting in adipose tissue of both species include *PDK4* (pyruvate dehydrogenase kinase 4, inhibits glycolysis), *IRS2* (insulin receptor substrate 2, involved in insulin signaling), *ANGPTL4* (a.k.a. fasting-induced adipose factor, inhibits lipoprotein lipase), *ADRB2* (beta2 adrenergic receptor, essential for adrenergic signaling), and *THBS1* and *THBS2* (Thrombospondin 1 and 2, adipokines associated with insulin resistance) (Figure 5B) [29]

Interestingly, more than twice as many genes (173) were consistently downregulated by fasting in human and mouse adipose tissue (Figure 6A,B; Supplemental table 5). Pathway analysis of these genes using EnrichR showed enrichment for genes involved in triglyceride and fatty acid synthesis, cholesterol synthesis, glycolysis, and the TCA cycle, indicating that the suppression of these pathways by fasting is well conserved in humans and mice (Figure 6C). Interestingly, fasting also consistently downregulated numerous collagen encoding genes (*COL11A1*, *COL15A1*, *COL5A1*, *COL5A3*, *COL3A1*) (Figure 6B).

Differences in fasting-induced gene regulation between human and mouse adipose tissue

In the subsequent analyses, we focused on the differences in fasting-induced gene regulation between human and mouse adipose tissue. To that end, for all genes the signal log ratios (SLR) for the fasting effect in human and mouse adipose tissue were visualized in a correlation plot (Figure 7A). The response to fasting of the two most highly induced (*PDK4*) and repressed (*PNPLA3*) genes was highly consistent between human and mouse adipose tissue. Although many genes were consistently up- or downregulated by fasting in the two species, the plot shows a large degree of scatter, indicating substantial divergence in the effect of fasting in human and mouse adipose tissue (Figure 7A). Genes showing opposite regulation by fasting in human and mouse adipose tissue include *STC1* (up in mouse, down in human, encoding secreted glycoprotein stanniocalcin 1) and *CIDEA* (slightly down in mouse, up in human, encoding lipid droplet-associated protein). As control, we compared the fasting-induced gene expression changes in our study with those of an independent study, in which mice of the same strain were fasted for 24 hours [16] (Figure 7B). There was a striking resemblance in gene regulation by fasting between these two

studies, as shown by the limited scatter, indicating that the effects of fasting on mouse adipose tissue gene expression are highly reproducible.

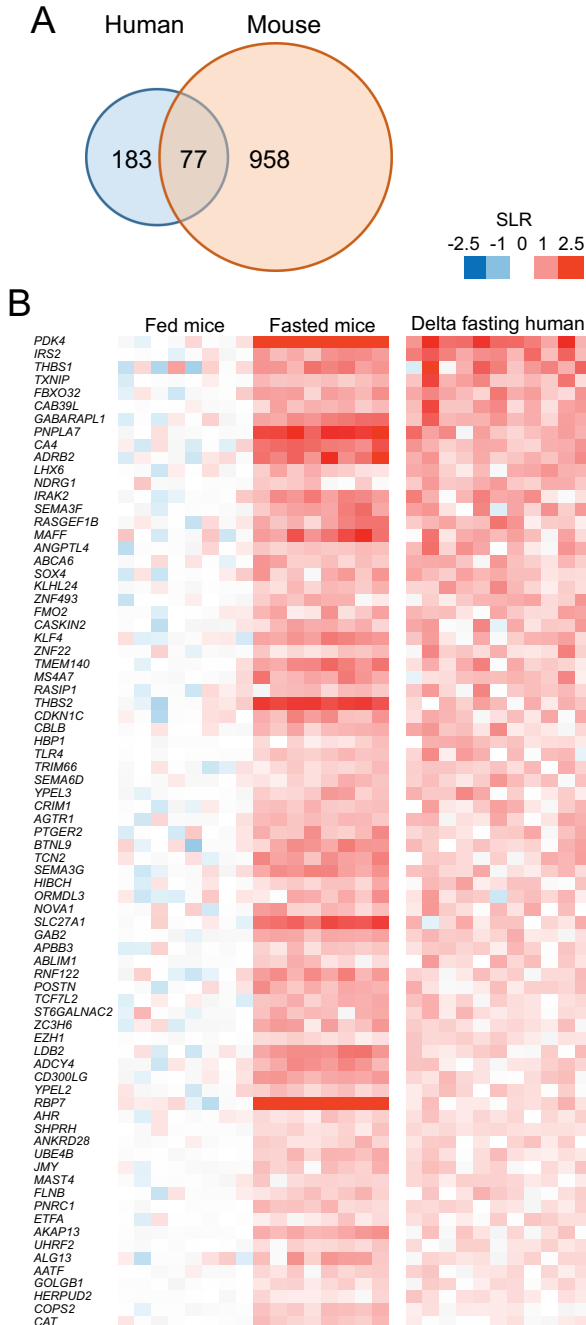


Figure 5. Overlap in upregulation of gene expression by fasting in human and mouse adipose tissue.

A) Venn diagram showing overlap in upregulation of gene expression by fasting in human and mouse adipose tissue ($P < 0.001$). B). Heatmap of the 77 genes commonly induced by fasting in human and mouse adipose tissue. The average signal log ratio of the fed mice was set at 0. The values for human adipose tissue represent the signal log ratio of the change in expression by fasting in each subject.

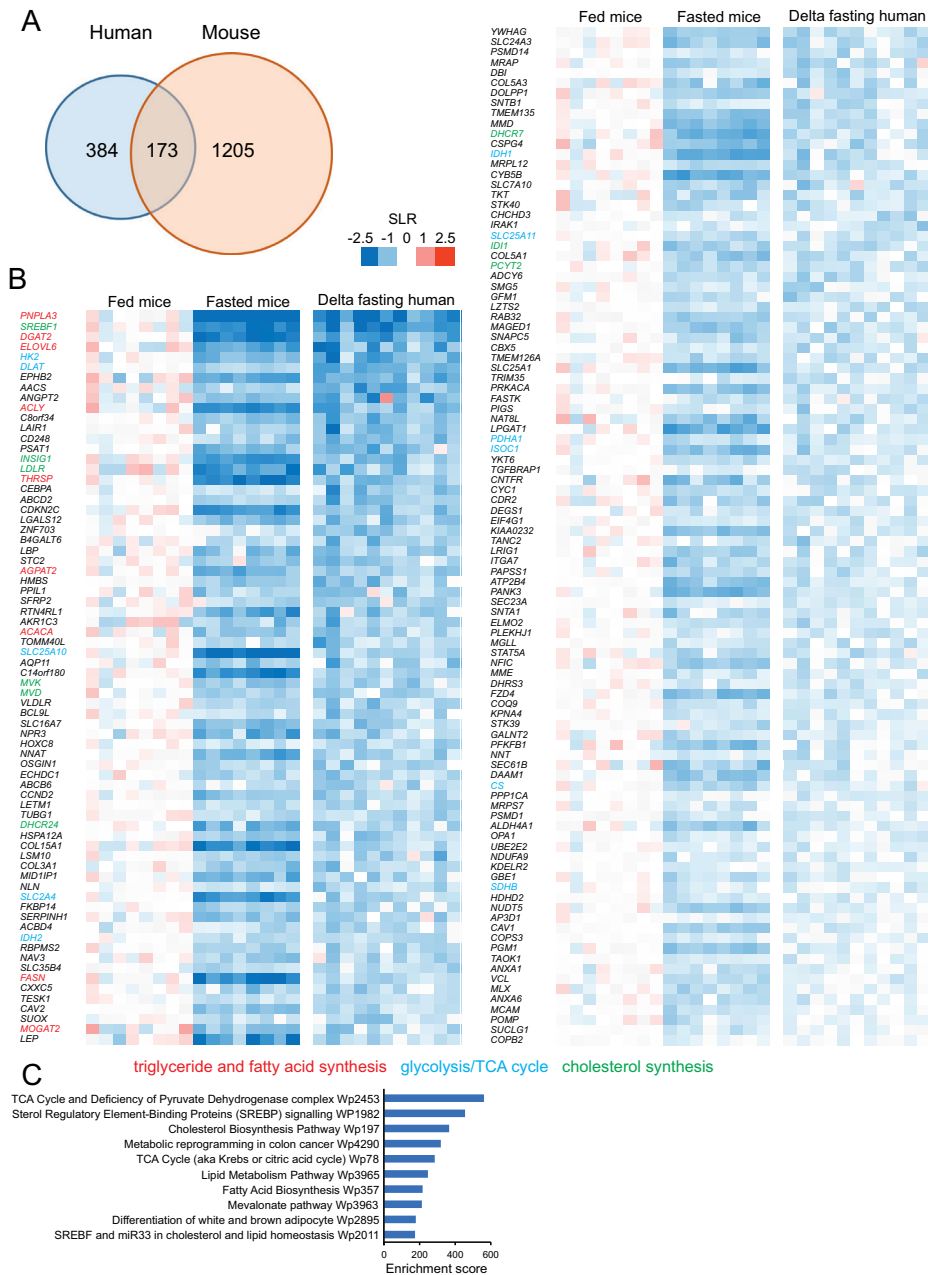


Figure 6. Overlap in downregulation of gene expression by fasting in human and mouse adipose tissue.
 A) Venn diagram showing overlap in downregulation of gene expression by fasting in human and mouse adipose tissue ($P < 0.001$). B) Heatmap of the 173 genes commonly repressed by fasting in human and mouse adipose tissue. The average signal log ratio of the fed mice was set at 0. The values for human adipose tissue represent the signal log ratio of the change in expression by fasting in each subject. Genes involved in triglyceride and fatty acid synthesis are shown in red, genes involved in glycolysis/TCA cycle in blue, and genes involved in cholesterol synthesis in green. C) The top 10 pathways based on EnrichR pathway analysis of the 173 genes commonly repressed by fasting in human and mouse adipose tissue. Pathway are ranked by enrichment score.

To probe the most differentially regulated genes, for each gene we calculated the difference in SLR of the fasting effect in human and mouse ($\Delta\text{SLR} = \text{SLR}_{\text{fast}}^{\text{human}} - \text{SLR}_{\text{fast}}^{\text{mouse}}$). Out of 12502 genes, 135 genes had a $\Delta\text{SLR} > 1$ and 173 genes had a $\Delta\text{SLR} < -1$ (Figure 7C). For comparison, these numbers were 18 and 35 for the ΔSLR of the fasting effect between the two mouse studies (not shown). Pathway analysis by EnrichR for the 135 genes with $\Delta\text{SLR} > 1$ showed strong enrichment for the AMPK, insulin, and FOXO signaling pathways, suggesting that these pathways are more strongly induced by fasting in human adipose tissue and/or more strongly repressed by fasting in mouse adipose tissue (Figure 7D). Visualization of expression changes of individual genes clearly indicated that genes in the insulin signaling pathway were markedly repressed by fasting in mouse adipose tissue but not or much more weakly in human adipose tissue. (Figure 7E). Pathway analysis by EnrichR for the 173 genes with $\Delta\text{SLR} < -1$ showed strong enrichment for the PPAR signaling pathway and fatty acid biosynthesis, suggesting that these pathways are more strongly induced by fasting in mouse adipose tissue and/or more strongly repressed by fasting in human adipose tissue (Figure 7F). Indeed, numerous genes among the 173 genes with $\Delta\text{SLR} < -1$ were PPAR target genes, which, with the exception of *FASD1* and *FADS2*, were induced by fasting in mouse adipose tissue but not or much more weakly in human adipose tissue (Figure 7G). The differential regulation of PPAR target genes by fasting in human and mouse adipose tissue could not be attributed to differential expression of the three PPARs, which was similar in human and mouse adipose tissue (Figure 7H). Interestingly, *PPARG* mRNA was downregulated by fasting in human but not mouse adipose tissue (Figure 7G).

The top 50 genes with the highest and lowest ΔSLR for the fasting effect between human and mouse adipose tissue are shown in Figure 8A. Even though *PNPLA3* was consistently repressed by fasting in human and mouse adipose tissue, it still made the list, as the fold-repression was much more pronounced in mouse than in human adipose tissue. The same applied to other lipogenic genes such as *FASN* and *THRSP*. Among the genes that stood out were several genes involved in glucose metabolism. Expression of *GPD1* (glycerol 3 phosphate dehydrogenase 1) and *PYGB* (glycogen phosphorylase) were markedly downregulated by fasting in mouse adipose tissue but not or minimally altered in human adipose tissue (Figure 8B). By contrast, *PCK1* (phosphoenolpyruvate carboxykinase) was upregulated by fasting in mouse adipose tissue but downregulated in human adipose tissue. Other genes of interest were *KLB* (beta Klotho, encoding a co-receptor for the FGF receptors), which was downregulated by fasting in humans but upregulated by fasting in mice, whereas the exact reverse was observed for *FGF2*.

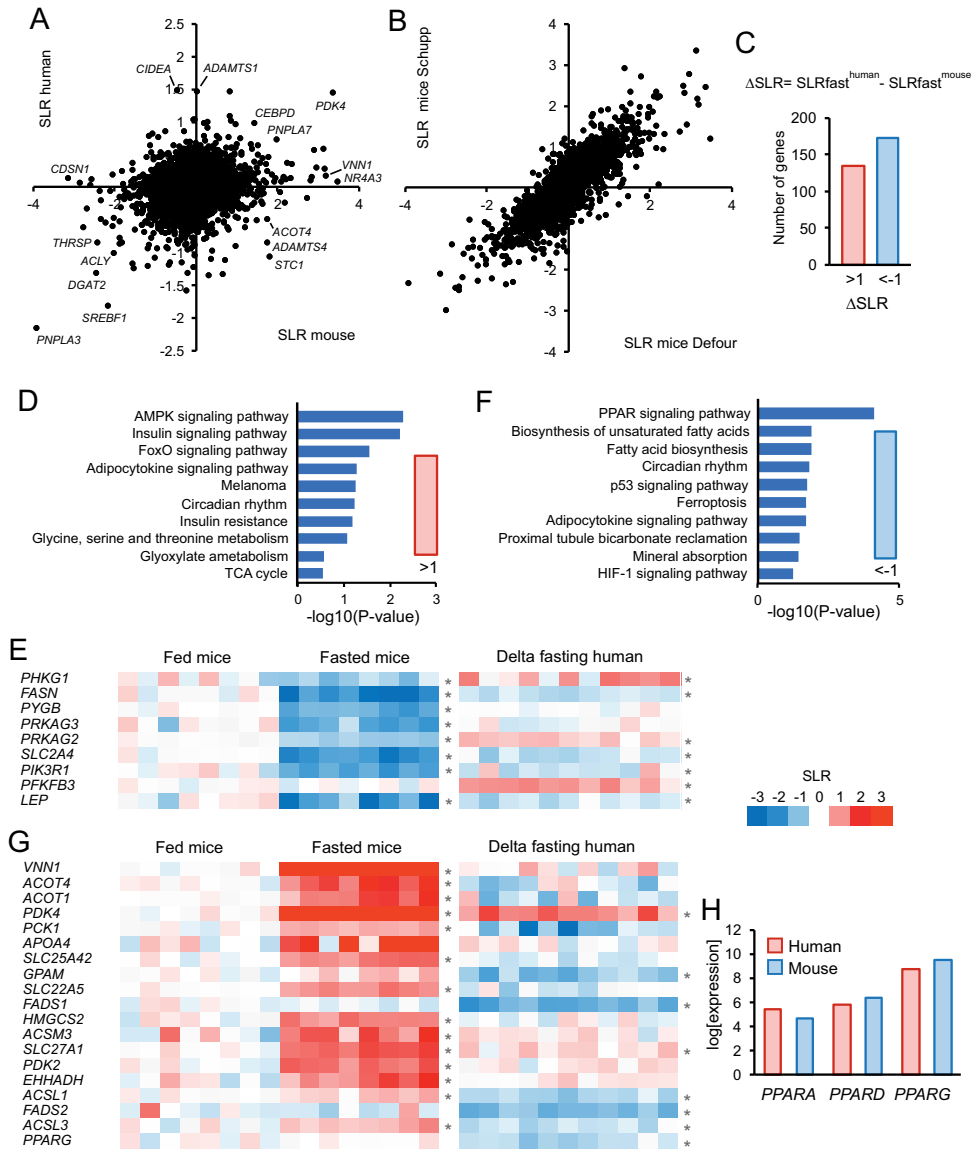
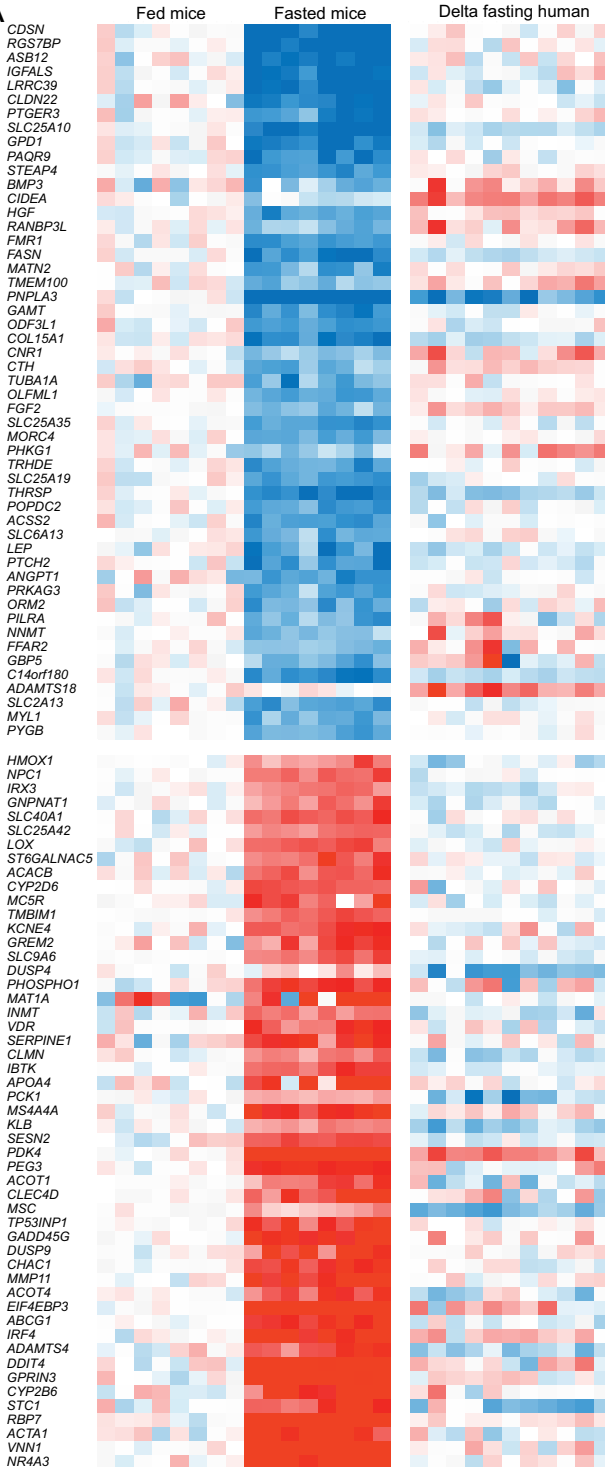


Figure 7. Differential gene regulation by fasting between human and mouse adipose tissue.

A) Plot showing the correlation of the fasting effect expressed as signal log ratio between human adipose tissue (y-axis) and mouse adipose tissue (x-axis). Plot includes all 12502 genes. B) Plot showing the correlation of the fasting effect in adipose tissue expressed as signal log ratio between our mouse study and the study by Schupp et al. [16]. C) Bar chart showing the number of genes for which the difference in signal log ratio for the fasting effect between human and mouse adipose tissue was higher than 1 or lower than -1. D) The top 10 pathways based on EnrichR pathway analysis of the 135 genes with $\Delta\text{SLR} > 1$. E) Heatmap of enriched genes in the insulin signaling pathway. Significantly changed genes are indicated with asterisk ($P < 0.001$). F) The top 10 pathways based on EnrichR pathway analysis of the 173 genes with $\Delta\text{SLR} < -1$. G) Heatmap of enriched genes in the PPAR signaling pathway. Significantly changed genes are indicated with asterisk ($P < 0.001$). H) Mean expression levels of *PPARA*, *PPARD* and *PPARG* in human and mouse adipose tissue.

A



B

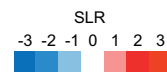
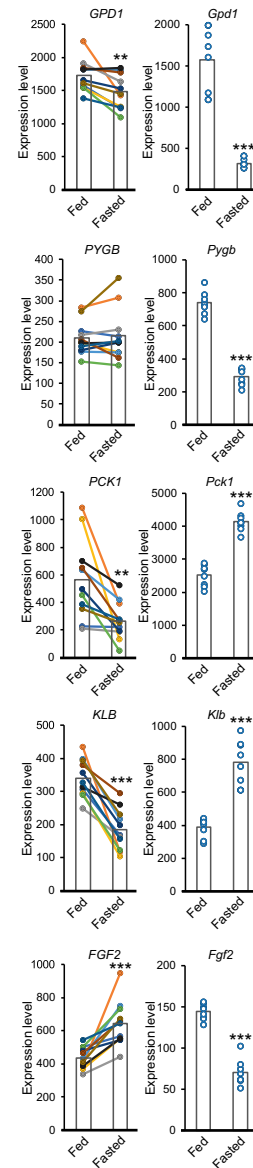


Figure 8 (opposite). Differences in gene regulation by fasting between human and mouse adipose tissue.

A) Genes were ranked according to absolute difference in Δ SLR, representing the difference in signal log ratio for the fasting effect between human and mouse adipose tissue. The top 50 genes with the highest Δ SLR (top half) and lowest Δ SLR (bottom half) are depicted in a heatmap. B) Gene expression profiles of individual genes in response to fasting in human and mouse adipose tissue: *GPD1* (glycerol-3-phosphate dehydrogenase 1), *PYGB* (glycogen phosphorylase), *PCK1* (phosphoenolpyruvate carboxykinase), *KLB* (beta Klotho, encoding a co-receptor for the FGF receptors) and *FGF2* (fibroblast growth factor 2). * $P < 0.05$, ** $P \leq 0.01$, *** $P \leq 0.001$.

Comparison of fasting effect on lipolytic gene expression in human and mouse adipose tissue.

To further compare the fasting-induced transcriptional responses, we zoomed in on two metabolic processes known to be modulated by fasting in adipose tissue, which are lipid droplet formation/degradation (Figure 9A) and extracellular lipolysis (Figure 9B). Lipid droplet degradation is thought to be mainly regulated via covalent modification of the key enzymes adipose triglyceride lipase (PNPLA2) and hormone sensitive lipase (LIPE). Nevertheless, important changes occur at the mRNA level as well. Here, marked differences were observed between human and mouse adipose tissue. Whereas *PNPLA2* mRNA was not affected by fasting in human adipose tissue, it was significantly induced in mouse adipose tissue (Figure 9A). *LIPE* mRNA showed a minor but statistically significant increase upon fasting in human but not mouse adipose tissue. The lipolytic activator *ABHD5* was induced by fasting in human and mouse adipose tissue, as were the β 2-adrenergic receptor *ADRB2* and the transcription factor *IRF4*, whereas the lipolytic inhibitor *GOS2* was consistently repressed by fasting (Figure 9A). The biggest contrast was observed for *CIDEA* mRNA, levels of which declined upon fasting in humans but increased in mice, and *CIDEA* mRNA, in which this pattern was reversed. Finally, *PLIN1* mRNA levels did not change in human adipose tissue but decreased upon fasting in mouse adipose tissue. Overall, the fasting-induced changes in mRNA levels of key lipolytic enzymes, regulators and receptors are not always consistent between human and mouse adipose tissue.

Compared to lipid droplet-associated genes, more consistency in the response to fasting was observed for genes involved in extracellular lipolysis (Figure 8B). Extracellular lipolysis is catalyzed by lipoprotein lipase (LPL) and is required for uptake of circulating triglycerides into adipose tissue. *LPL* mRNA declined slightly upon fasting in human adipose tissue but did not change in mouse adipose tissue. Intriguingly, expression of the LPL anchor and transporter *GPIHBP1* was induced by fasting in both human and mouse adipose tissue. Also, mRNA levels of the LPL inhibitor *ANGPTL4* were consistently upregulated by fasting in human and mouse adipose tissue, whereas *ANGPTL8*, which antagonizes *ANGPTL4*, and the VLDL receptor *VLDLR* were consistently downregulated by fasting. Finally, *CD36* mRNA was very modestly increased by fasting in mouse adipose tissue but remained unchanged in human adipose tissue. Collectively, these data indicate that transcriptional regulation of extracellular lipolysis by fasting is very similar in human and mouse adipose tissue, especially for the key LPL regulators *GPIHBP1*, *ANGPTL4* and *ANGPTL8*.

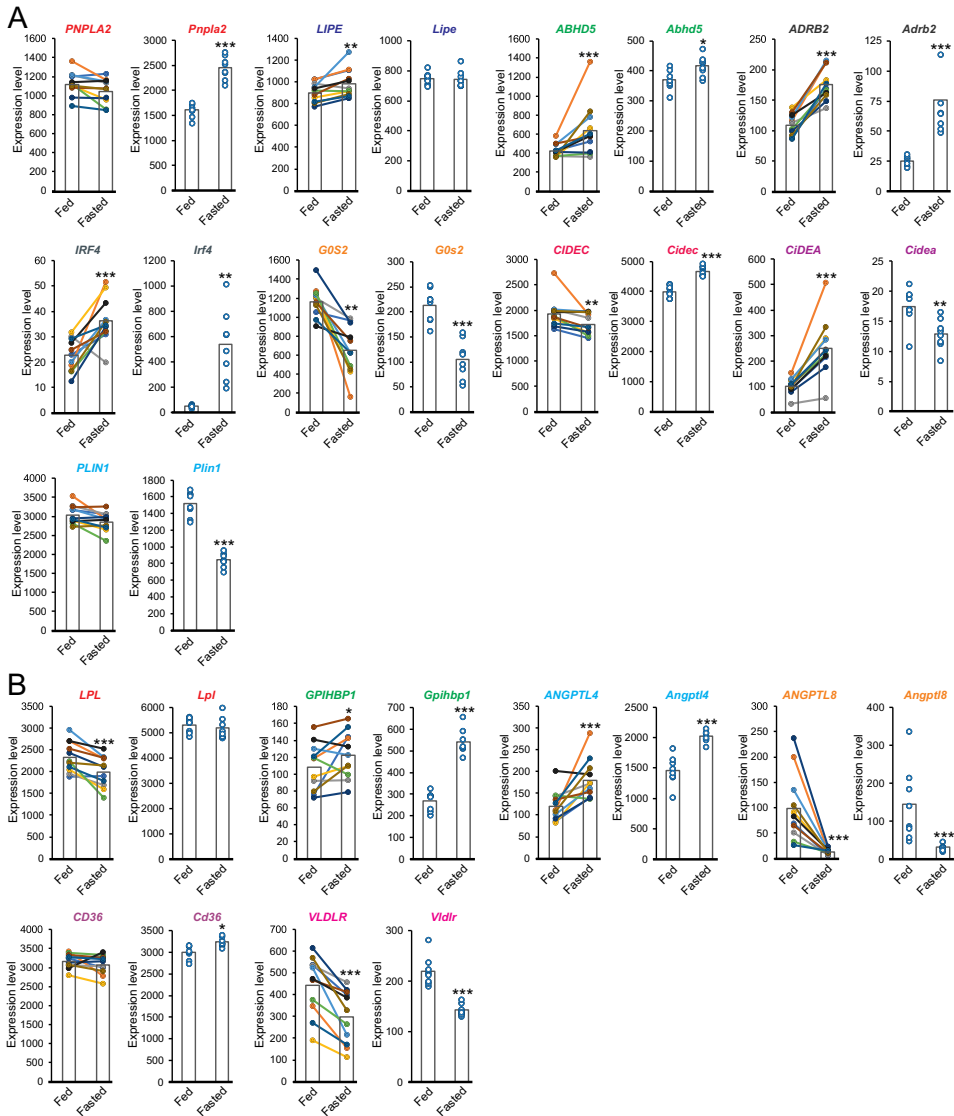


Figure 9. Comparison of fasting effect on lipolytic gene expression in human and mouse adipose tissue.

A) Gene expression profiles of individual genes involved in lipid droplet formation and degradation in response to fasting in human and mouse adipose tissue. B) Gene expression profiles of individual genes involved in extracellular lipolysis in response to fasting in human and mouse adipose tissue. Human genes are indicated in upper case, mouse genes are indicated in lower case. * $P < 0.05$, ** $P \leq 0.01$, *** $P \leq 0.001$.

DISCUSSION

In this paper we for the first time have characterized the effect of fasting on the human adipose tissue transcriptome, showing that: 1) genes upregulated by fasting were functionally very diverse, and were not part of a clear pattern of regulation of specific metabolic pathways; 2) fasting downregulated numerous metabolic pathways, including triglyceride and fatty acid synthesis, glycolysis and glycogen synthesis, TCA cycle, oxidative phosphorylation, mitochondrial translation, and insulin signaling; 3) fasting downregulated numerous genes involved in proteasomal degradation; 4) fasting had less pronounced effects on the adipose tissue transcriptome in humans than in mice; 5) although major overlap in fasting-induced gene regulation was observed between human and mouse adipose tissue, many genes were differentially regulated by fasting in humans and mice, including genes involved in insulin signaling, PPAR signaling, glycogen metabolism, and lipid droplets. Collectively, our data provide a useful resource for the study of the response to fasting in human adipose tissue.

Numerous studies have given insight into the regulation of key metabolic genes by fasting in mice, showing that fasting downregulates adipose expression of *Lep* [30], *Pnpla3* [31], *Angptl8* [32], *Slc2a4* [33], *Grb14* [34], *Srebf1* [35], *Fasn* [33,35] and *GOs2* [36,37]. Other genes were previously shown to be upregulated by fasting in adipose tissue of mice, including *Pnpla2* [38], *Angptl4* [13] and *Irf4* [39]. Here, we show that the above genes were all significantly regulated by fasting in the same direction in human and mouse adipose tissue, except for *Pnpla2*.

Fasting caused a dramatic decrease in plasma insulin levels in human subjects [18]. Accordingly, it is not surprising that the insulin signaling pathway was markedly repressed by fasting. The decrease in insulin signaling may explain the repression of genes involved in uptake, synthesis, elongation, desaturation, and storage of fatty acids, genes involved in synthesis and uptake of cholesterol, and genes involved in uptake and storage of glucose [40]. In addition, fasting led to repression of genes involved in the TCA cycle, oxidative phosphorylation, and amino acid metabolism. The downregulation of these pathways may reflect a reduced need for ATP and NAD(P)H required for fatty acid and triglyceride synthesis. The downregulation of the above pathways by fasting in adipose tissue of humans is in agreement with previous transcriptomics studies done on adipose tissue of rats and pigs [7,17].

The fasting-induced changes in gene expression are likely mediated via a number of insulin-sensitive transcription factors, including SREBP1 [35], FOXO1 [41], PPARG [42] and IRF4 [39]. Expression of *SREBF1*, encoding SREBP1, was highly suppressed by fasting in human and mouse adipose tissue, while expression of *FOXO1* was modestly but significantly suppressed by fasting in human adipose tissue and remained unchanged in mouse adipose tissue. The modest regulation

of *FOXO1* mRNA is in line with the notion that FOXO1 activity is mainly regulated via phosphorylation [43]. Interestingly, *PPARG* mRNA levels were markedly reduced by fasting in human but not mouse adipose tissue. Previously, *IRF4* was shown to be induced by fasting in an insulin- and FOXO1-dependent manner, to stimulate adipose tissue lipolysis, and to mediate the induction of *Pnpla2* and *Adrb3* by fasting in mouse adipose tissue [39]. In our study, *IRF4* mRNA was strongly induced by fasting in mouse adipose tissue and more modestly in human adipose tissue, which may be due to stronger repression of insulin signaling by fasting in mice. It can be hypothesized that the much lower expression and the more modest induction of *IRF4* in humans versus mouse adipose tissue may explain the lack of induction *PNPLA2* by fasting in human adipose tissue.

One of the surprising findings was that the expression of numerous proteasomal genes was significantly downregulated by fasting in human adipose tissue. Downregulation of proteasomal gene expression during fasting may serve to reduce the degradation of metabolic enzymes and other valuable adipocyte proteins that are needed to support lipolysis and other essential processes in adipose tissue during fasting. Our data do not indicate that fasting leads to a general activation of genes involved in autophagy, with the exception of *GABARAPL1* and *DAPK2*, which were strongly induced by fasting. Currently, the importance of autophagy in triglyceride hydrolysis in adipose tissue during fasting remains unsubstantiated.

Interestingly, fasting downregulated numerous collagen encoding genes in human and mouse adipose tissue. Downregulation of collagen-encoding and ECM-associated genes upon fasting was observed even more prominently in seals [44], and may reflect the structural changes needed to accommodate the shrinkage of adipocytes during fasting, as stored triglycerides are degraded and fatty acids are released into the circulation. Indeed, fat loss is associated with marked changes in collagen abundance and composition in adipose tissue, as seen in patients who underwent bariatric surgery [45]. Our data do not support an upregulation by fasting of adipose genes involved in cytoskeleton reorganization, such as actin polymerization and cell-to-cell adhesion machinery, which was previously observed in pigs [7].

A number of fasting-induced gene expression changes were of particular interest. Intriguingly, the expression of fatty acid transporters *SLC27A1* and *SLC27A2*, also known as long chain fatty acid transport proteins 1 and 2, was upregulated by fasting in human adipose tissue, whereas *SLC27A4* was downregulated. The upregulation of *SLC27A1* by fasting is seemingly at odds with its purported role in insulin-induced fatty acid transport [46]. The role of *SLC27A4* in adipose tissue is unclear. Studies with *Slc27a4* deficient mice have indicated that *SLC27A4* is not crucial for fatty acid uptake into adipocytes [47]. Based on the direction of the regulation of these genes by fasting, one could speculate about a role of *SLC27A4* in insulin-induced transport

of plasma TG-derived fatty acids for subsequent storage, whereas SLC27A1 and SLC27A2 might participate in the fasting-induced export of fatty acids released by intracellular lipolysis. Another intriguing observation was that *IRS1* mRNA was downregulated by fasting in human adipose tissue, whereas *IRS2* mRNA was upregulated. Both *IRS1* and *IRS2* play a role in the signaling cascade of insulin. The downregulation of *IRS1* mRNA by fasting is in agreement with its stimulatory effect on insulin-stimulated glucose transport in adipocytes [48,49]. In contrast, *IRS2* does not seem to impact on glucose transport in adipocytes [50], but instead may mediate the anti-lipolytic action of insulin in adipose tissue [50]. Accordingly, the observed upregulation of *IRS2* during fasting might reflect a negative feedback loop on the inhibition of lipolysis. Conversely, in the fed state, the downregulation of *IRS2* might limit the inhibitory effect of insulin on lipolysis.

Our analysis highlighted numerous genes involved in lipid or glucose metabolism that were differentially regulated by fasting in mouse and human adipose tissue. For example, several target genes of PPAR were significantly upregulated by fasting in mice but significantly downregulated in humans, including *PCK1*, *CIDEA*, *ACSL1*, and *ACSL3*. Other genes were significantly downregulated by fasting in mice but significantly upregulated in humans, including *CIDEA* and *PRKAG2*. Hence, caution should be exercised in extrapolating results from fasting in mouse adipose tissue to humans. It should be mentioned, though, that many genes and metabolic pathways were consistently up- or down-regulated by fasting in human and mouse adipose tissue.

One of the genes that was oppositely regulated by fasting in human and mouse adipose tissue was *PCK1*. Mouse data have shown that during fasting, when glucose uptake into adipose tissue is low, *PCK1* is upregulated to enable glyceroneogenesis, producing glycerol 3-phosphate from gluconeogenic substrates [33,51]. The glycerol 3-phosphate formed is used to support the re-esterification of fatty acids released by lipolysis. Intriguingly, *PCK1* mRNA was downregulated by fasting in human adipose tissue, suggesting that glyceroneogenesis does not need to be activated during fasting in humans. This observation may imply that synthesis of glycerol 3-phosphate from glucose, which is mediated by *GPD1*, is sufficiently maintained in fasted human adipose tissue to accommodate re-esterification of fatty acids. In this context, it is interesting to mention that expression of *GPD1* was unchanged by fasting in human adipose tissue but markedly downregulated in mouse adipose tissue.

A number of studies have previously examined the effect of fasting on the adipose tissue transcriptome in other animal species, including rats, pigs, mice and chicken [4,7,15–17]. Differences in transcriptome platforms and duration of fasting preclude a systematic quantitative analysis of the effect of fasting in the different species. Instead, a qualitative overall comparison of the outcomes of the various studies

was conducted. Due to limited duration of fasting (5 hours), the study in chickens was excluded from this analysis [15]. The comparative analysis showed that genes involved in fatty acid and triglyceride synthesis such as *FASN*, *ACLY* and *DGAT2* were consistently downregulated by fasting across all species, as were genes involved in cholesterol synthesis, such as *MVK* and *DHCR7*. By contrast, genes involved in fatty acid elongation and desaturation, such as *SCD* and the *FADS* genes, were downregulated by fasting in humans and rats but not in mice. Genes encoding the enzymes of the TCA cycle were downregulated by fasting in humans, mice and pigs. With respect to induction of gene expression, a gene that was commonly upregulated by fasting in all species was *ANGPTL4*. Other metabolically relevant genes such as *ADRB2*, *IRS2*, and *PNPLA7*, were consistently upregulated by fasting in rats, mice and humans. Overall, based on differences in study designs and limitations in the analysis and presentation of the available data, it is not possible to assess which animal model most closely mimics the transcriptional response to fasting in human adipose tissue. The most suitable model will likely depend on the pathway and gene being studied, as well as other considerations, including the possibility to perform gene targeting.

Our study also has limitations. First of all, it is difficult to match the duration of fasting in mice to the duration of fasting in humans. The moment of sampling of adipose tissue in the mice and human subjects roughly corresponds with the end of phase 3 of the five phases model of fasting [2,28]. Although the human volunteers fasted 10 hours longer than the mice, the impact of fasting on gene expression was more pronounced in the mice. Nevertheless, we suspect that the conclusions of the human-mouse comparison would not have changed much if we would have extended the human fast to 48 hours. Second, we compared abdominal subcutaneous human adipose tissue with epididymal mouse adipose tissue. Unfortunately, there is no good mouse equivalent for abdominal subcutaneous human adipose tissue. In many mouse studies, subcutaneous adipose tissue often refers to the inguinal adipose tissue depot, which unlike epididymal adipose tissue and human subcutaneous adipose tissue is highly sensitive to cold-induced browning [52,53]. Recently, it was shown that the response of certain genes to fasting, including *Pnpla2*, *Lipe*, *Srebf1*, and *Ppara*, may differ between different mouse fat depots [38]. In the current set-up, we cannot fully exclude that the differences in fasting-induced gene regulation between human and mouse adipose tissue are related to the sampling of the epididymal mouse adipose tissue. Third, baseline and fasting-induced gene expression was much more variable in humans than in mice, thereby reducing the statistical power and limiting the number of significant genes in humans. Fourth, the majority of the human subjects were female, whereas the mouse study was performed in males. The number of subjects was insufficient to perform a thorough analysis of the differences in response to fasting between men and women. Finally, we investigated the response to fasting in human and mouse adipose tissue at the

level of mRNA. Ideally, it would have been better to study the effect of fasting at the protein level.

In conclusion, although numerous genes and pathways were regulated similarly by fasting in human and mouse adipose tissue, many genes showed very distinct responses to fasting between the two species, suggesting the need for caution when extrapolating findings from mice to humans. Our data provide a useful resource to study adipose tissue function during fasting.

Acknowledgements

This research was supported by CVON ENERGISE grant CVON2014-02.

References

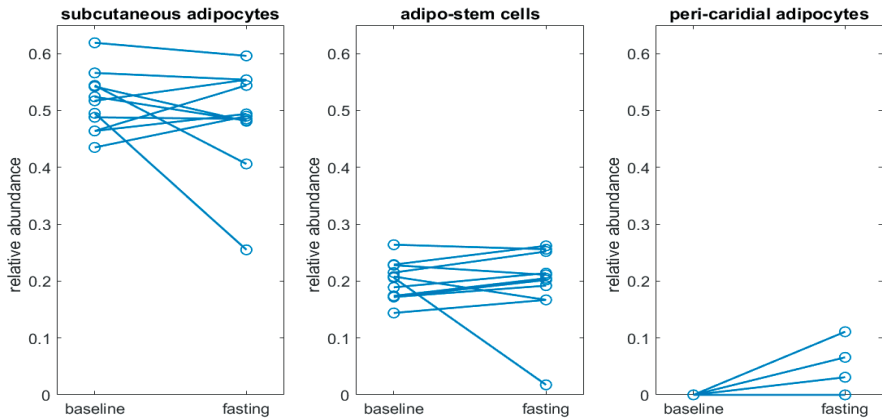
- [1] Flier, J.S., 1995. The adipocyte: storage depot or node on the energy information superhighway? *Cell* 80(1): 15–8, Doi: 10.1016/0092-8674(95)90445-x.
- [2] Cahill, G.F., 2006. Fuel Metabolism in Starvation. *Annual Review of Nutrition* 26(1): 1–22, Doi: 10.1146/annurev.nutr.26.061505.111258.
- [3] Owen, O.E., Morgan, A.P., Kemp, H.G., Sullivan, J.M., Herrera, M.G., Cahill, G.F., 1967. Brain metabolism during fasting. *The Journal of Clinical Investigation* 46(10): 1589–95, Doi: 10.1172/JCI105650.
- [4] Ibrahim, M., Ayoub, D., Wasselin, T., Van Dorselaer, A., Le Maho, Y., Raclot, T., et al., 2020. Alterations in rat adipose tissue transcriptome and proteome in response to prolonged fasting. *Biological Chemistry* 401(3): 389–405, Doi: 10.1515/hsz-2019-0184.
- [5] Bertile, F., Schaeffer, C., Le Maho, Y., Raclot, T., Van Dorselaer, A., 2009. A proteomic approach to identify differentially expressed plasma proteins between the fed and prolonged fasted states. *Proteomics* 9(1): 148–58, Doi: 10.1002/pmic.200701001.
- [6] Bertile, F., Raclot, T., 2004. Differences in mRNA expression of adipocyte-derived factors in response to fasting, refeeding and leptin. *Biochimica et Biophysica Acta - Molecular and Cell Biology of Lipids* 1683(1–3): 101–9, Doi: 10.1016/j.bbali.2004.05.001.
- [7] Lkhagvadorj, S., Qu, L., Cai, W., Couture, O.P., Barb, C.R., Hausman, G.J., et al., 2009. Microarray gene expression profiles of fasting induced changes in liver and adipose tissues of pigs expressing the melanocortin-4 receptor D298N variant. *Physiological Genomics* 38(1): 98–111, Doi: 10.1152/physiolgenomics.90372.2008.
- [8] Trayhurn, P., Beattie, J.H., 2001. Physiological role of adipose tissue: white adipose tissue as an endocrine and secretory organ. *Proceedings of the Nutrition Society* 60(3): 329–39, Doi: 10.1079/pns200194.
- [9] Ahima, R.S., Flier, J.S., 2000. Leptin. *Annu. Rev. Physiol.* 62: 413–37.
- [10] Zhang, Y., Proenca, R., Maffei, M., Barone, M., Leopold, L., Friedman, J.M., 1994. Positional cloning of the mouse obese gene and its human homologue. *Nature* 372(6505): 425–32, Doi: 10.1038/372425a0.
- [11] Hu, E., Liang, P., Spiegelman, B.M., 1996. AdipoQ is a novel adipose-specific gene dysregulated in obesity. *The Journal of Biological Chemistry* 271(18): 10697–703, Doi: 10.1074/jbc.271.18.10697.
- [12] Yoon, J.C., Chickering, T.W., Rosen, E.D., Dussault, B., Qin, Y., Soukas, A., et al., 2000. Peroxisome proliferator-activated receptor gamma target gene encoding a novel angiopoietin-related protein associated with adipose differentiation. *Molecular and Cellular Biology* 20(14): 5343–9, Doi: 10.1128/mcb.20.14.5343-5349.2000.
- [13] Kersten, S., Mandard, S., Tan, N.S., Escher, P., Metzger, D., Chambon, P., et al., 2000. Characterization of the fasting-induced adipose factor FIAF, a novel peroxisome proliferator-activated receptor target gene. *The Journal of Biological Chemistry* 275(37): 28488–93, Doi: 10.1074/jbc.M004029200.
- [14] Kolaczynski, J.W., Considine, R. V., Ohannesian, J., Marco, C., Opentanova, I., Nyce, M.R., et al., 1996. Responses of leptin to short-term fasting and refeeding in humans: a link with ketogenesis but not ketones themselves. *Diabetes* 45(11): 1511–5, Doi: 10.2337/diab.45.11.1511.

- [15] Ji, B., Ernest, B., Gooding, J.R., Das, S., Saxton, A.M., Simon, J., et al., 2012. Transcriptomic and metabolomic profiling of chicken adipose tissue in response to insulin neutralization and fasting. *BMC Genomics* 13(1), Doi: 10.1186/1471-2164-13-441.
- [16] Schupp, M., Chen, F., Briggs, E.R., Rao, S., Pelzmann, H.J., Pessentheiner, A.R., et al., 2013. Metabolite and transcriptome analysis during fasting suggest a role for the p53-Ddit4 axis in major metabolic tissues. *BMC Genomics* 14(1): 1–20, Doi: 10.1186/1471-2164-14-758.
- [17] Li, R.Y., Zhang, Q.H., Liu, Z., Qiao, J., Zhao, S.X., Shao, L., et al., 2006. Effect of short-term and long-term fasting on transcriptional regulation of metabolic genes in rat tissues. *Biochemical and Biophysical Research Communications* 344(2): 562–70, Doi: 10.1016/j.bbrc.2006.03.155.
- [18] Ruppert, P.M.M., Michielsen, C.C.J.R., Hazebroek, E.J., Pirayesh, A., Olivecrona, G., Afman, L.A., et al., 2020. Fasting induces ANGPTL4 and reduces LPL activity in human adipose tissue. *Molecular Metabolism*: 101033, Doi: 10.1016/j.molmet.2020.101033.
- [19] Dai, M., Wang, P., Boyd, A.D., Kostov, G., Athey, B., Jones, E.G., et al., 2005. Evolving gene/transcript definitions significantly alter the interpretation of GeneChip data. *Nucleic Acids Research* 33(20): 1–9, Doi: 10.1093/nar/gni179.
- [20] Irizarry, R.A., Bolstad, B.M., Collin, F., Cope, L.M., Hobbs, B., Speed, T.P., 2003. Summaries of Affymetrix GeneChip probe level data. *Nucleic Acids Research* 31(4): e15, Doi: 10.1093/nar/gng015.
- [21] Bolstad, B.M., Irizarry, R.A., Astrand, M., Speed, T.P., 2003. A comparison of normalization methods for high density oligonucleotide array data based on variance and bias. *Bioinformatics (Oxford, England)* 19(2): 185–93, Doi: 10.1093/bioinformatics/19.2.185.
- [22] Sartor, M.A., Tomlinson, C.R., Wesselkamper, S.C., Sivaganesan, S., Leikauf, G.D., Medvedovic, M., 2006. Intensity-based hierarchical Bayes method improves testing for differentially expressed genes in microarray experiments. *BMC Bioinformatics* 7: 538, Doi: 10.1186/1471-2105-7-538.
- [23] Subramanian, A., Tamayo, P., Mootha, V.K., Mukherjee, S., Ebert, B.L., Gillette, M.A., et al., 2005. Gene set enrichment analysis: a knowledge-based approach for interpreting genome-wide expression profiles. *Proceedings of the National Academy of Sciences of the United States of America* 102(43): 15545–50, Doi: 10.1073/pnas.0506580102.
- [24] Chen, E.Y., Tan, C.M., Kou, Y., Duan, Q., Wang, Z., Meirelles, G.V., et al., 2013. Enrichr: interactive and collaborative HTML5 gene list enrichment analysis tool. *BMC Bioinformatics* 14: 128, Doi: 10.1186/1471-2105-14-128.
- [25] Kuleshov, M. V., Jones, M.R., Rouillard, A.D., Fernandez, N.F., Duan, Q., Wang, Z., et al., 2016. Enrichr: a comprehensive gene set enrichment analysis web server 2016 update. *Nucleic Acids Research* 44(W1): W90-7, Doi: 10.1093/nar/gkw377.
- [26] Newman, A.M., Steen, C.B., Liu, C.L., Gentles, A.J., Chaudhuri, A.A., Scherer, F., et al., 2019. Determining cell type abundance and expression from bulk tissues with digital cytometry. *Nature Biotechnology* 37(7): 773–82, Doi: 10.1038/s41587-019-0114-2.
- [27] Lenz, M., Arts, I.C.W., Peeters, R.L.M., de Kok, T.M., Ertaylan, G., 2020. Adipose tissue in health and disease through the lens of its building blocks. *Scientific Reports* 10(1): 10433, Doi: 10.1038/s41598-020-67177-1.

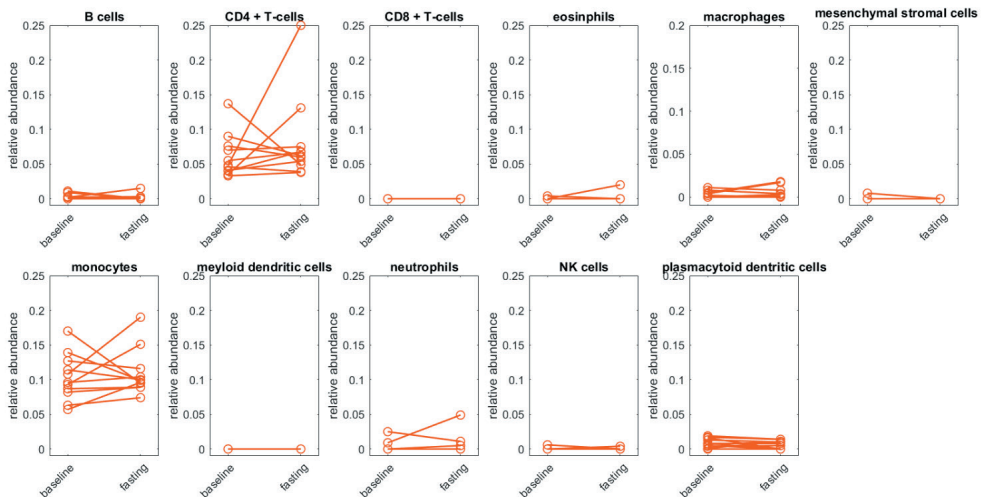
- [28] Geisler, C.E., Hepler, C., Higgins, M.R., Renquist, B.J., 2016. Hepatic adaptations to maintain metabolic homeostasis in response to fasting and refeeding in mice. *Nutrition & Metabolism* 13: 62, Doi: 10.1186/s12986-016-0122-x.
- [29] Varma, V., Yao-Borengasser, A., Bodles, A.M., Rasouli, N., Phanavanh, B., Nolen, G.T., et al., 2008. Thrombospondin-1 is an adipokine associated with obesity, adipose inflammation, and insulin resistance. *Diabetes* 57(2): 432–9, Doi: 10.2337/db07-0840.
- [30] Saladin, R., De Vos, P., Guerre-Millo, M., Leturque, A., Girard, J., Staels, B., et al., 1995. Transient increase in obese gene expression after food intake or insulin administration. *Nature* 377(6549): 527–9, Doi: 10.1038/377527a0.
- [31] Baulande, S., Lasnier, F., Lucas, M., Pairault, J., 2001. Adiponutrin, a transmembrane protein corresponding to a novel dietary- and obesity-linked mRNA specifically expressed in the adipose lineage. *The Journal of Biological Chemistry* 276(36): 33336–44, Doi: 10.1074/jbc.M105193200.
- [32] Zhang, R., 2012. Lipasin, a novel nutritionally-regulated liver-enriched factor that regulates serum triglyceride levels. *Biochemical and Biophysical Research Communications* 424(4): 786–92, Doi: 10.1016/j.bbrc.2012.07.038.
- [33] Becker, D.J., Ongemba, L.N., Brichard, V., Henquin, J.C., Brichard, S.M., 1995. Diet- and diabetes-induced changes of ob gene expression in rat adipose tissue. *FEBS Letters* 371(3): 324–8, Doi: 10.1016/0014-5793(95)00943-4.
- [34] Cariou, B., Capitaine, N., Le Marcis, V., Vega, N., Béréziat, V., Kergoat, M., et al., 2004. Increased adipose tissue expression of Grb14 in several models of insulin resistance. *FASEB Journal : Official Publication of the Federation of American Societies for Experimental Biology* 18(9): 965–7, Doi: 10.1096/fj.03-0824fje.
- [35] Kim, J.B., Sarraf, P., Wright, M., Yao, K.M., Mueller, E., Solanes, G., et al., 1998. Nutritional and insulin regulation of fatty acid synthetase and leptin gene expression through ADD1/SREBP1. *The Journal of Clinical Investigation* 101(1): 1–9, Doi: 10.1172/JCI14111.
- [36] Nielsen, T.S., Vendelbo, M.H., Jessen, N., Pedersen, S.B., Jørgensen, J.O., Lund, S., et al., 2011. Fasting, but not exercise, increases adipose triglyceride lipase (ATGL) protein and reduces G(0)/G(1) switch gene 2 (G0S2) protein and mRNA content in human adipose tissue. *The Journal of Clinical Endocrinology and Metabolism* 96(8): E1293-7, Doi: 10.1210/jc.2011-0149.
- [37] Oh, S.-A., Suh, Y., Pang, M.-G., Lee, K., 2011. Cloning of avian G(0)/G(1) switch gene 2 genes and developmental and nutritional regulation of G(0)/G(1) switch gene 2 in chicken adipose tissue. *Journal of Animal Science* 89(2): 367–75, Doi: 10.2527/jas.2010-3339.
- [38] Tang, H.-N., Tang, C.-Y., Man, X.-F., Tan, S.-W., Guo, Y., Tang, J., et al., 2017. Plasticity of adipose tissue in response to fasting and refeeding in male mice. *Nutrition & Metabolism* 14: 3, Doi: 10.1186/s12986-016-0159-x.
- [39] Eguchi, J., Wang, X., Yu, S., Kershaw, E.E., Chiu, P.C., Dushay, J., et al., 2011. Transcriptional control of adipose lipid handling by IRF4. *Cell Metabolism* 13(3): 249–59, Doi: 10.1016/j.cmet.2011.02.005.
- [40] Czech, M.P., Tencerova, M., Pedersen, D.J., Aouadi, M., 2013. Insulin signalling mechanisms for triacylglycerol storage. *Diabetologia* 56(5): 949–64, Doi: 10.1007/s00125-013-2869-1.

- [41] Wu, Y., Pan, Q., Yan, H., Zhang, K., Guo, X., Xu, Z., et al., 2018. Novel mechanism of FOXO1 phosphorylation in glucagon signaling in control of glucose homeostasis. *Diabetes* 67(11): 2167–82, Doi: 10.2337/db18-0674.
- [42] Vidal-Puig, A., Jimenez-Liñan, M., Lowell, B.B., Hamann, A., Hu, E., Spiegelman, B., et al., 1996. Regulation of PPAR γ gene expression by nutrition and obesity in rodents. *Journal of Clinical Investigation* 97(11): 2553–61, Doi: 10.1172/JCI118703.
- [43] Xing, Y.-Q., Li, A., Yang, Y., Li, X.-X., Zhang, L.-N., Guo, H.-C., 2018. The regulation of FOXO1 and its role in disease progression. *Life Sciences* 193: 124–31, Doi: 10.1016/j.lfs.2017.11.030.
- [44] Martinez, B., Khudyakov, J., Rutherford, K., Crocker, D.E., Gemmell, N., Ortiz, R.M., 2018. Adipose transcriptome analysis provides novel insights into molecular regulation of prolonged fasting in northern elephant seal pups. *Physiological Genomics* 50(7): 495–503, Doi: 10.1152/physiolgenomics.00002.2018.
- [45] Liu, Y., Aron-Wisniewsky, J., Marcelin, G., Genser, L., Le Naour, G., Torcivia, A., et al., 2016. Accumulation and Changes in Composition of Collagens in Subcutaneous Adipose Tissue After Bariatric Surgery. *The Journal of Clinical Endocrinology and Metabolism* 101(1): 293–304, Doi: 10.1210/jc.2015-3348.
- [46] Wu, Q., Ortegon, A.M., Tsang, B., Doege, H., Feingold, K.R., Stahl, A., 2006. FATP1 is an insulin-sensitive fatty acid transporter involved in diet-induced obesity. *Molecular and Cellular Biology* 26(9): 3455–67, Doi: 10.1128/MCB.26.9.3455-3467.2006.
- [47] Lenz, L.-S., Marx, J., Chamulitrat, W., Kaiser, I., Gröne, H.-J., Liebisch, G., et al., 2011. Adipocyte-specific inactivation of Acyl-CoA synthetase fatty acid transport protein 4 (Fatp4) in mice causes adipose hypertrophy and alterations in metabolism of complex lipids under high fat diet. *The Journal of Biological Chemistry* 286(41): 35578–87, Doi: 10.1074/jbc.M111.226530.
- [48] Tamemoto, H., Kadowaki, T., Tobe, K., Yagi, T., Sakura, H., Hayakawa, T., et al., 1994. Insulin resistance and growth retardation in mice lacking insulin receptor substrate-1. *Nature* 372(6502): 182–6, Doi: 10.1038/372182a0.
- [49] Araki, E., Lipes, M.A., Patti, M.E., Brüning, J.C., Haag, B. 3rd., Johnson, R.S., et al., 1994. Alternative pathway of insulin signalling in mice with targeted disruption of the IRS-1 gene. *Nature* 372(6502): 186–90, Doi: 10.1038/372186a0.
- [50] Previs, S.F., Withers, D.J., Ren, J.M., White, M.F., Shulman, G.I., 2000. Contrasting effects of IRS-1 versus IRS-2 gene disruption on carbohydrate and lipid metabolism in vivo. *Journal of Biological Chemistry* 275(50): 38990–4, Doi: 10.1074/jbc.M006490200.
- [51] Cadoudal, T., Leroyer, S., Reis, A.F., Tordjman, J., Durant, S., Fouque, F., et al., 2005. Proposed involvement of adipocyte glyceroneogenesis and phosphoenolpyruvate carboxykinase in the metabolic syndrome. *Biochimie* 87(1): 27–32, Doi: 10.1016/j.biochi.2004.12.005.
- [52] Seale, P., Conroe, H.M., Estall, J., Kajimura, S., Frontini, A., Ishibashi, J., et al., 2011. Prdm16 determines the thermogenic program of subcutaneous white adipose tissue in mice. *Journal of Clinical Investigation* 121(1): 96–105, Doi: 10.1172/JCI44271.
- [53] van der Lans, A.A.J.J., Hoeks, J., Brans, B., Vijgen, G.H.E.J., Visser, M.G.W., Vosselman, M.J., et al., 2013. Cold acclimation recruits human brown fat and increases nonshivering thermogenesis. *The Journal of Clinical Investigation* 123(8): 3395–403, Doi: 10.1172/JCI68993.

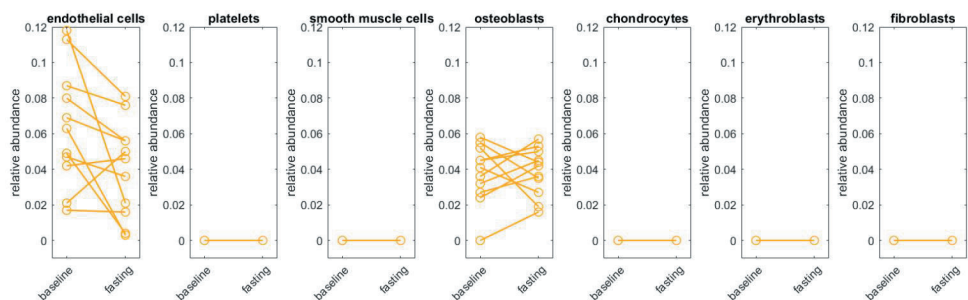
Supplemental materials



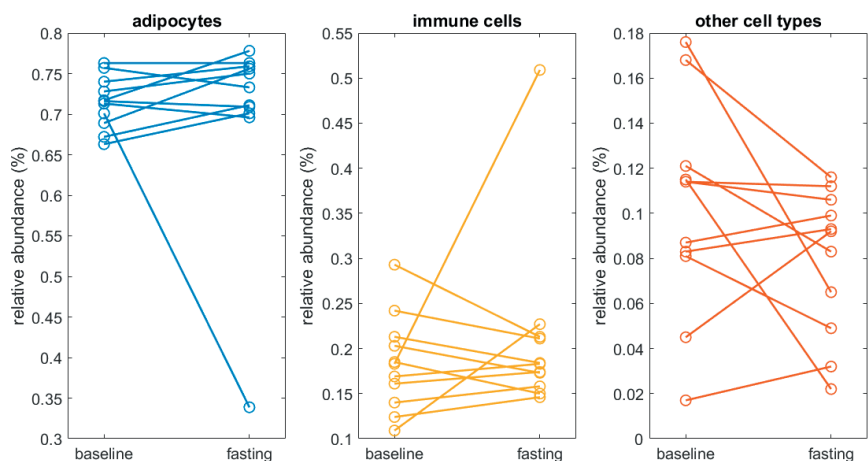
Supplemental Figure 1A. Relative abundances of adipocyte cell types in adipose biopsies collected from 11 individuals at baseline and after fasting. No consistent and significant trend is observed in relative abundance of any adipocyte cell type following a period of fasting. For pericardial adipocytes the predicted relative abundance is low both at baseline and following fasting in 8 of 11 individuals. This may be a legacy of the tissue decoder algorithm. Statistical testing was performed by two-tailed t-test adjusted for multiple testing correction using the Benjamini-Hochberg correction.



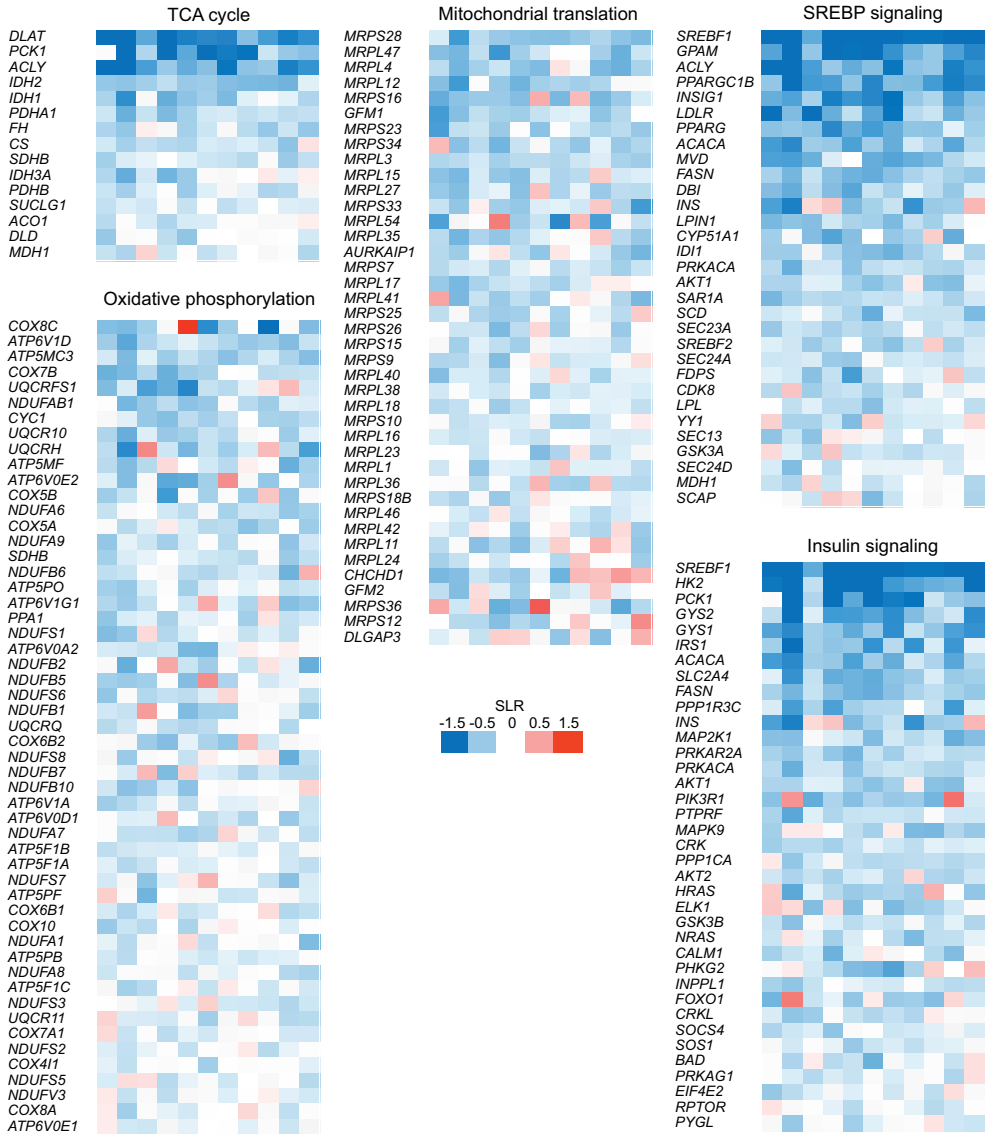
Supplemental Figure 1B. Relative abundances of immune cell types in adipose tissue biopsied collected in 11 individuals at baseline and after fasting. No consistent and significant trend is observed in relative abundance of any immune cell type following a period of fasting.



Supplemental Figure 1C. Relative abundances of other cell types in adipose tissue biopsies collected across 11 individuals at baseline and after fasting. No consistent and significant trend is observed in relative abundance of any cell type following a period of fasting.



Supplemental Figure 1D. Relative abundances of different cell types classes across 11 individuals at baseline and after fasting. No obvious and consistent trend is observed in relative abundance of the aggregated cell types following a period of fasting. One sample has a very different composition with the tissue decoder predicting just 34% of the cells falling into this generic adipocyte cell category with 51% immune cells.



Supplemental figure 2. Gene Set Enrichment Analysis on transcriptomics data of adipose tissue from human subjects in the fed or fasted state. The genesets shown are negatively enriched by fasting. The heatmap shows the fasting-induced gene expression changes in the individual subjects. Red indicates upregulated, blue indicates downregulated.

Supplemental table 1

Participants, n	11
Gender, n males (%)	3 (27%)
Age, years	56 ± 9 (OF 42 – 69)
Weight, kg	73.9 ± 11.7
BMI, kg/m ²	26.1 ± 2.8
Plasma cholesterol, mM	6.23 ± 0.90
HDL cholesterol, mM	1.69 ± 0.30
LDL cholesterol, mM	3.47 ± 0.71

Supplemental table 2

SYMBOL	SLR	P value
<i>PNPLA3</i>	-2.16	3.48E-07
<i>SREBF1</i>	-1.83	4.37E-09
<i>FADS1</i>	-1.60	4.58E-11
<i>DUSP4</i>	-1.37	2.47E-06
<i>MSC</i>	-1.35	3.74E-09
<i>FADS2</i>	-1.32	1.02E-11
<i>DGAT2</i>	-1.32	2.46E-07
<i>ELOVL6</i>	-1.26	2.62E-05
<i>KLHL31</i>	-1.24	1.40E-05
<i>HK2</i>	-1.23	5.42E-06
<i>DLAT</i>	-1.21	1.14E-10
<i>EPHB2</i>	-1.18	7.88E-09
<i>IRF8</i>	-1.17	6.16E-05
<i>AACS</i>	-1.16	1.57E-07
<i>GPAM</i>	-1.12	1.35E-06
<i>ANGPT2</i>	-1.09	2.71E-04
<i>STC1</i>	-1.08	3.39E-04
<i>DUSP14</i>	-1.06	7.12E-08
<i>ACLY</i>	-1.02	6.95E-07
<i>ARHGAP20</i>	-0.99	1.49E-05
<i>PPARGC1B</i>	-0.98	8.93E-08
<i>C8orf34</i>	-0.95	3.32E-08
<i>LRRN3</i>	-0.95	1.09E-04
<i>LAIR1</i>	-0.95	1.57E-05
<i>CD248</i>	-0.94	1.73E-09
<i>NR2F6</i>	-0.92	4.60E-08
<i>KLB</i>	-0.91	5.67E-06

SYMBOL	SLR	P value
<i>PPIF</i>	-0.90	1.92E-08
<i>PSAT1</i>	-0.89	4.39E-06
<i>COL11A1</i>	-0.89	1.87E-04
<i>HSPB8</i>	-0.89	1.11E-05
<i>SLC2A5</i>	-0.87	3.38E-05
<i>INSIG1</i>	-0.87	3.49E-07
<i>CITED4</i>	-0.87	1.80E-05
<i>LDLR</i>	-0.87	3.21E-05
<i>THRSP</i>	-0.86	1.34E-07
<i>ADAMTS4</i>	-0.85	9.91E-07
<i>CEBPA</i>	-0.85	1.81E-05
<i>MOGAT1</i>	-0.84	9.40E-04
<i>TFPI2</i>	-0.83	1.86E-04
<i>ABCD2</i>	-0.82	8.16E-07
<i>ELOVL3</i>	-0.82	2.70E-05
<i>TUBB2A</i>	-0.81	1.24E-05
<i>CDKN2C</i>	-0.80	4.31E-08
<i>LOXL1</i>	-0.80	2.84E-07
<i>PDXK</i>	-0.80	3.12E-08
<i>KLHL25</i>	-0.79	1.47E-05
<i>MN1</i>	-0.79	3.91E-06
<i>FSTL3</i>	-0.78	5.79E-08
<i>LGALS12</i>	-0.78	2.36E-06
<i>GYS2</i>	-0.77	3.23E-05
<i>GYS1</i>	-0.76	1.89E-07
<i>ZNF703</i>	-0.75	2.31E-07
<i>ADORA1</i>	-0.74	2.23E-04
<i>B4GALT6</i>	-0.74	1.22E-06

SYMBOL	SLR	P value	SYMBOL	SLR	P value
<i>ACSL1</i>	-0.73	9.37E-09	<i>ZNRF3</i>	-0.62	4.25E-05
<i>KLHDC8B</i>	-0.72	2.84E-08	<i>C14orf180</i>	-0.62	2.61E-07
<i>SLC25A33</i>	-0.72	2.06E-04	<i>MVK</i>	-0.61	2.01E-05
<i>LBP</i>	-0.71	4.15E-06	<i>MVD</i>	-0.61	2.36E-05
<i>ISOC2</i>	-0.71	8.38E-08	<i>PAK1IP1</i>	-0.60	5.25E-07
<i>STC2</i>	-0.71	1.06E-05	<i>VLDLR</i>	-0.60	6.17E-06
<i>AGPAT2</i>	-0.71	6.09E-09	<i>SLC7A4</i>	-0.60	3.64E-05
<i>OLFM2</i>	-0.70	1.86E-06	<i>TUFT1</i>	-0.60	5.33E-04
<i>HMBS</i>	-0.70	7.47E-05	<i>EHBP1</i>	-0.60	1.79E-06
<i>PPIL1</i>	-0.70	2.61E-05	<i>BCL9L</i>	-0.60	1.39E-05
<i>PDXP</i>	-0.70	4.73E-06	<i>SLC16A7</i>	-0.60	1.39E-06
<i>NME1</i>	-0.69	6.77E-06	<i>NPR3</i>	-0.60	1.56E-05
<i>CEBPB</i>	-0.69	3.22E-06	<i>HOXC8</i>	-0.59	1.16E-06
<i>MAL2</i>	-0.68	1.12E-05	<i>ANKRD9</i>	-0.59	1.95E-05
<i>ELOVL5</i>	-0.67	4.50E-10	<i>LRRC59</i>	-0.59	1.57E-07
<i>HECW2</i>	-0.67	3.01E-06	<i>NNAT</i>	-0.59	1.75E-06
<i>SFRP2</i>	-0.66	3.96E-07	<i>DGAT1</i>	-0.59	2.00E-06
<i>SPON2</i>	-0.66	4.35E-04	<i>POR</i>	-0.59	3.53E-07
<i>TMEM104</i>	-0.66	1.52E-05	<i>SPRY4</i>	-0.59	6.45E-05
<i>RTN4RL1</i>	-0.66	1.65E-04	<i>OSGIN1</i>	-0.58	1.77E-04
<i>AKR1C3</i>	-0.66	3.43E-06	<i>PIM3</i>	-0.58	6.46E-07
<i>IRS1</i>	-0.66	4.36E-05	<i>FAT1</i>	-0.58	1.32E-07
<i>TRIM6</i>	-0.65	1.53E-04	<i>FGFR2</i>	-0.58	1.54E-04
<i>ADRA2A</i>	-0.65	5.27E-04	<i>ECHDC1</i>	-0.58	3.01E-07
<i>PPARG</i>	-0.64	2.78E-07	<i>CCND1</i>	-0.57	6.21E-07
<i>ACACA</i>	-0.64	7.51E-07	<i>ABCB6</i>	-0.57	2.36E-05
<i>FAT2</i>	-0.64	6.35E-04	<i>PREB</i>	-0.57	4.88E-07
<i>FAT3</i>	-0.64	1.78E-04	<i>HEXIM1</i>	-0.57	3.10E-06
<i>HSPB7</i>	-0.64	1.75E-07	<i>CCND2</i>	-0.57	4.00E-07
<i>DCUN1D3</i>	-0.64	8.15E-06	<i>HSPA8</i>	-0.57	4.16E-08
<i>FADS3</i>	-0.64	1.00E-07	<i>SLC9A3R1</i>	-0.57	7.10E-04
<i>CKB</i>	-0.63	8.51E-07	<i>TXNDC9</i>	-0.57	2.96E-04
<i>TOMM40L</i>	-0.63	1.57E-04	<i>C11orf24</i>	-0.57	1.56E-06
<i>SLC25A10</i>	-0.63	2.22E-07	<i>PHF23</i>	-0.57	3.99E-05
<i>AQP11</i>	-0.62	2.39E-04	<i>COQ10A</i>	-0.57	3.81E-05
<i>CLMN</i>	-0.62	1.79E-05	<i>LETM1</i>	-0.57	1.55E-06
<i>PNO1</i>	-0.62	4.71E-04	<i>ADIPOR2</i>	-0.56	1.02E-09
<i>GLRX2</i>	-0.62	5.11E-06	<i>TUBG1</i>	-0.56	3.58E-07

SYMBOL	SLR	P value	SYMBOL	SLR	P value
<i>DHCR24</i>	-0.56	3.58E-06	<i>GPR180</i>	-0.50	1.08E-06
<i>PLA2G4A</i>	-0.56	2.27E-04	<i>DSEL</i>	-0.50	3.96E-04
<i>HSPA12A</i>	-0.56	2.60E-05	<i>PSMD9</i>	-0.50	1.60E-04
<i>B4GALT5</i>	-0.55	5.10E-08	<i>DPH2</i>	-0.50	9.68E-04
<i>COL15A1</i>	-0.55	5.85E-07	<i>CDO1</i>	-0.50	5.80E-05
<i>LSM10</i>	-0.55	7.93E-04	<i>PSEN2</i>	-0.50	8.40E-05
<i>SRP19</i>	-0.55	6.61E-06	<i>TMEM138</i>	-0.49	1.49E-06
<i>COL3A1</i>	-0.55	1.10E-05	<i>PDE4DIP</i>	-0.49	1.85E-04
<i>MID1IP1</i>	-0.54	3.14E-05	<i>ARPC5L</i>	-0.49	7.65E-04
<i>NLN</i>	-0.54	1.33E-05	<i>TNFAIP8L1</i>	-0.49	8.41E-05
<i>RAI1</i>	-0.54	9.08E-05	<i>TESK1</i>	-0.49	8.89E-10
<i>SLC2A4</i>	-0.53	7.01E-06	<i>KLC2</i>	-0.49	2.61E-04
<i>UBTD1</i>	-0.53	8.66E-04	<i>GDPD5</i>	-0.48	1.52E-04
<i>USP33</i>	-0.53	3.20E-08	<i>CAV2</i>	-0.48	1.11E-07
<i>RRP1B</i>	-0.53	1.32E-05	<i>SUOX</i>	-0.48	1.28E-04
<i>MRPS28</i>	-0.53	1.46E-06	<i>NDST1</i>	-0.48	1.66E-07
<i>FKBP14</i>	-0.53	4.38E-05	<i>MOGAT2</i>	-0.48	8.75E-04
<i>MPV17L</i>	-0.53	3.22E-04	<i>DYNLL2</i>	-0.48	1.48E-07
<i>SERPINH1</i>	-0.53	1.31E-04	<i>SLC5A6</i>	-0.48	7.76E-05
<i>HEATR3</i>	-0.52	1.28E-05	<i>LEP</i>	-0.48	2.43E-06
<i>ACBD4</i>	-0.52	3.39E-05	<i>OSBPL11</i>	-0.48	9.72E-07
<i>FHOD1</i>	-0.52	1.95E-04	<i>DACH1</i>	-0.48	4.81E-04
<i>PALLD</i>	-0.52	1.77E-05	<i>SLC16A1</i>	-0.47	6.55E-04
<i>IDH2</i>	-0.52	1.39E-07	<i>THOP1</i>	-0.47	9.91E-04
<i>RBPMS2</i>	-0.52	3.12E-05	<i>PNMA1</i>	-0.47	9.92E-06
<i>NAV3</i>	-0.52	4.08E-05	<i>FZD5</i>	-0.47	4.36E-04
<i>CBR1</i>	-0.52	1.92E-04	<i>SUB1</i>	-0.47	6.39E-05
<i>ACSL3</i>	-0.52	1.11E-06	<i>TSGA10</i>	-0.47	2.30E-04
<i>SURF4</i>	-0.51	1.17E-07	<i>CPEB4</i>	-0.47	3.51E-07
<i>EEF1B2</i>	-0.51	1.04E-04	<i>HEPACAM</i>	-0.47	3.89E-06
<i>SLC35B4</i>	-0.51	2.70E-06	<i>MARK1</i>	-0.47	1.31E-05
<i>LAMB3</i>	-0.51	4.44E-06	<i>VGLL3</i>	-0.47	7.16E-05
<i>PUS7</i>	-0.51	7.79E-06	<i>TMEM164</i>	-0.47	1.13E-04
<i>CCT5</i>	-0.51	9.58E-06	<i>CAP2</i>	-0.47	1.78E-05
<i>LTV1</i>	-0.51	1.08E-05	<i>CKMT2</i>	-0.46	2.29E-04
<i>FASN</i>	-0.51	1.34E-08	<i>PPP1R3C</i>	-0.46	3.56E-04
<i>CXXC5</i>	-0.50	4.27E-05	<i>MRAS</i>	-0.46	2.40E-05
<i>SLC22A3</i>	-0.50	6.53E-05	<i>YWHAG</i>	-0.46	2.32E-06

SYMBOL	SLR	P value	SYMBOL	SLR	P value
<i>SLC24A3</i>	-0.46	2.07E-05	<i>MRPL4</i>	-0.42	3.20E-04
<i>AIFM2</i>	-0.45	5.71E-05	<i>LPIN1</i>	-0.41	2.81E-05
<i>DNAJB1</i>	-0.45	5.18E-05	<i>TBC1D24</i>	-0.41	7.38E-04
<i>PSMD14</i>	-0.45	3.23E-06	<i>DHCR7</i>	-0.41	7.30E-05
<i>KCTD10</i>	-0.45	9.60E-05	<i>POLR3B</i>	-0.41	4.63E-04
<i>OAF</i>	-0.45	4.73E-04	<i>B4GALT7</i>	-0.41	2.70E-04
<i>RRP15</i>	-0.45	9.56E-05	<i>MTCH2</i>	-0.41	2.72E-04
<i>SLC27A4</i>	-0.45	6.18E-04	<i>CSPG4</i>	-0.41	7.21E-05
<i>CDR2L</i>	-0.45	5.86E-04	<i>IDH1</i>	-0.41	3.74E-04
<i>MAT2A</i>	-0.45	5.52E-07	<i>STARD7</i>	-0.41	7.29E-07
<i>TMEM64</i>	-0.45	1.23E-05	<i>ITGA11</i>	-0.41	3.75E-04
<i>GPC6</i>	-0.44	9.61E-06	<i>FAH</i>	-0.41	9.63E-05
<i>MRAP</i>	-0.44	4.61E-04	<i>CEBPG</i>	-0.41	1.01E-05
<i>DBI</i>	-0.44	5.01E-05	<i>TRIM8</i>	-0.41	4.59E-06
<i>SLC1A3</i>	-0.44	1.41E-05	<i>SEMA3C</i>	-0.41	2.01E-05
<i>NIP7</i>	-0.44	3.21E-04	<i>MRPL12</i>	-0.40	2.33E-04
<i>COL5A3</i>	-0.44	3.37E-04	<i>S100A16</i>	-0.40	5.59E-04
<i>SGCG</i>	-0.44	2.44E-05	<i>CY5B</i>	-0.40	5.46E-06
<i>MED8</i>	-0.44	2.58E-06	<i>QDPR</i>	-0.40	8.36E-05
<i>MMP28</i>	-0.44	5.19E-04	<i>WSB2</i>	-0.40	1.27E-07
<i>NEIL2</i>	-0.43	5.35E-04	<i>RRP9</i>	-0.40	2.77E-04
<i>KIF5B</i>	-0.43	3.82E-08	<i>DYNLL1</i>	-0.40	1.96E-04
<i>PRR5</i>	-0.43	7.57E-04	<i>HSPA5</i>	-0.40	3.25E-06
<i>ATP2A2</i>	-0.43	6.41E-07	<i>MAP2K1</i>	-0.40	3.83E-05
<i>DOLPP1</i>	-0.43	2.46E-04	<i>ST6GAL1</i>	-0.40	4.17E-04
<i>PLEKHG6</i>	-0.43	5.74E-04	<i>HIVEP3</i>	-0.40	2.14E-04
<i>EYA2</i>	-0.43	3.85E-04	<i>RNF6</i>	-0.40	1.17E-05
<i>SNTB1</i>	-0.43	1.24E-04	<i>ALDH9A1</i>	-0.40	3.56E-06
<i>LOXL2</i>	-0.43	3.14E-05	<i>GTPBP4</i>	-0.40	2.03E-04
<i>TMEM135</i>	-0.43	9.20E-06	<i>OSR1</i>	-0.40	9.07E-04
<i>CUEDC1</i>	-0.42	1.07E-04	<i>SLC7A10</i>	-0.39	6.13E-04
<i>MMD</i>	-0.42	4.97E-07	<i>NIPA2</i>	-0.39	1.56E-04
<i>ALDH1B1</i>	-0.42	4.58E-04	<i>TKT</i>	-0.39	1.51E-05
<i>MRPL47</i>	-0.42	2.81E-04	<i>STK40</i>	-0.39	4.59E-06
<i>DDX21</i>	-0.42	1.35E-05	<i>PPTC7</i>	-0.39	1.51E-04
<i>BCR</i>	-0.42	4.82E-05	<i>LACTB</i>	-0.39	1.90E-04
<i>GPR158</i>	-0.42	2.66E-04	<i>LMO4</i>	-0.39	3.00E-04
<i>ATP6V1D</i>	-0.42	8.45E-06	<i>CHCHD3</i>	-0.39	6.64E-04

SYMBOL	SLR	P value	SYMBOL	SLR	P value
<i>SPRY1</i>	-0.39	1.95E-05	<i>SLC39A7</i>	-0.36	1.12E-04
<i>YTHDF2</i>	-0.39	4.05E-04	<i>MAGED1</i>	-0.36	6.57E-05
<i>IRAK1</i>	-0.39	6.08E-04	<i>PISD</i>	-0.36	5.86E-04
<i>SLC25A11</i>	-0.39	5.13E-06	<i>HOOK2</i>	-0.36	4.08E-04
<i>UTP15</i>	-0.39	5.74E-04	<i>SNAPC5</i>	-0.36	6.73E-04
<i>IDI1</i>	-0.38	4.49E-04	<i>TMEM11</i>	-0.36	4.26E-04
<i>COL5A1</i>	-0.38	1.83E-04	<i>GNG11</i>	-0.36	1.18E-04
<i>GRWD1</i>	-0.38	9.90E-04	<i>PGM3</i>	-0.36	6.33E-04
<i>SLC25A30</i>	-0.38	7.04E-05	<i>PSMA5</i>	-0.36	5.09E-04
<i>ACTN1</i>	-0.38	1.10E-05	<i>MRPS23</i>	-0.36	7.51E-04
<i>FOXP4</i>	-0.38	4.68E-05	<i>SEC61A1</i>	-0.35	2.36E-07
<i>PCYT2</i>	-0.38	2.71E-04	<i>SLC31A1</i>	-0.35	1.44E-04
<i>MPDU1</i>	-0.38	3.62E-04	<i>HLTF</i>	-0.35	8.31E-06
<i>ZDHHC8</i>	-0.38	9.11E-04	<i>CBX5</i>	-0.35	1.25E-04
<i>TUBB6</i>	-0.38	3.47E-05	<i>TMEM126A</i>	-0.35	6.12E-04
<i>RNF41</i>	-0.38	1.15E-06	<i>KPNA1</i>	-0.35	1.15E-04
<i>ADCY6</i>	-0.37	9.10E-05	<i>GNG2</i>	-0.35	2.14E-04
<i>APBB1IP</i>	-0.37	1.44E-04	<i>LARP1</i>	-0.35	1.10E-06
<i>SLC39A11</i>	-0.37	2.39E-04	<i>CDC42EP1</i>	-0.35	8.67E-04
<i>GIPC1</i>	-0.37	5.36E-05	<i>SLC25A1</i>	-0.35	5.99E-05
<i>CCDC92</i>	-0.37	9.70E-05	<i>UBP1</i>	-0.35	6.56E-05
<i>IMPAD1</i>	-0.37	7.50E-05	<i>TRIM35</i>	-0.35	6.33E-04
<i>SMG5</i>	-0.37	3.67E-04	<i>UBE2J1</i>	-0.34	1.31E-05
<i>TPST2</i>	-0.37	2.18E-04	<i>STIP1</i>	-0.34	2.12E-04
<i>COX7B</i>	-0.37	2.20E-04	<i>PRKACA</i>	-0.34	2.56E-06
<i>GFM1</i>	-0.37	1.41E-04	<i>LASP1</i>	-0.34	1.91E-06
<i>LZTS2</i>	-0.37	2.15E-04	<i>RAN</i>	-0.34	2.06E-05
<i>C4orf19</i>	-0.37	7.94E-04	<i>FASTK</i>	-0.34	4.74E-04
<i>FXN</i>	-0.37	8.17E-05	<i>PIGS</i>	-0.34	3.02E-04
<i>RAB32</i>	-0.37	5.61E-04	<i>AKT1</i>	-0.34	1.46E-04
<i>PRKAR2A</i>	-0.37	5.11E-06	<i>REST</i>	-0.34	1.11E-05
<i>VKORC1L1</i>	-0.37	1.60E-05	<i>NAT8L</i>	-0.34	5.17E-05
<i>TP53I13</i>	-0.37	5.47E-04	<i>CLEC14A</i>	-0.34	7.91E-04
<i>TIMM13</i>	-0.37	7.84E-05	<i>LPGAT1</i>	-0.34	5.82E-05
<i>PSKH1</i>	-0.37	1.41E-04	<i>GIMAP8</i>	-0.34	2.43E-04
<i>TSKU</i>	-0.37	7.56E-04	<i>PDHA1</i>	-0.34	3.61E-05
<i>DCUN1D5</i>	-0.37	5.79E-04	<i>PPM1B</i>	-0.34	1.43E-04
<i>CACYBP</i>	-0.36	5.77E-04	<i>MYLIP</i>	-0.34	5.04E-04

SYMBOL	SLR	P value	SYMBOL	SLR	P value
<i>FRMD6</i>	-0.34	4.23E-04	<i>MTA2</i>	-0.31	1.59E-05
<i>SAR1A</i>	-0.33	1.86E-06	<i>PAPSS1</i>	-0.31	7.13E-04
<i>TAF1B</i>	-0.33	7.33E-04	<i>SCD</i>	-0.30	9.61E-05
<i>NDUFAB1</i>	-0.33	1.30E-04	<i>TXNDC11</i>	-0.30	1.56E-05
<i>ISOC1</i>	-0.33	1.45E-04	<i>HSPA9</i>	-0.30	1.31E-05
<i>YKT6</i>	-0.33	2.38E-06	<i>ATP2B4</i>	-0.30	1.13E-05
<i>WDR43</i>	-0.33	9.44E-05	<i>C1QBP</i>	-0.30	2.36E-04
<i>SLC17A5</i>	-0.33	2.43E-04	<i>PGK1</i>	-0.30	1.01E-04
<i>TGFBRAP1</i>	-0.33	5.69E-05	<i>PANK3</i>	-0.30	2.99E-05
<i>HCRT</i>	-0.33	7.33E-04	<i>SEC23A</i>	-0.30	3.26E-06
<i>USP31</i>	-0.33	1.44E-04	<i>SNTA1</i>	-0.30	2.24E-04
<i>CNTFR</i>	-0.33	2.19E-04	<i>POMGNT1</i>	-0.30	2.41E-04
<i>MRPS34</i>	-0.33	9.56E-04	<i>ELMO2</i>	-0.30	2.57E-04
<i>POLR3H</i>	-0.33	1.91E-04	<i>PLEKHJ1</i>	-0.30	7.12E-04
<i>CYC1</i>	-0.33	6.59E-05	<i>MGLL</i>	-0.30	3.58E-04
<i>CDR2</i>	-0.32	9.79E-04	<i>ALKBH5</i>	-0.30	1.64E-04
<i>DEGS1</i>	-0.32	6.51E-05	<i>CNN3</i>	-0.30	3.70E-06
<i>OGFOD1</i>	-0.32	1.68E-05	<i>STAT5A</i>	-0.30	7.03E-04
<i>MRPL3</i>	-0.32	1.65E-06	<i>MYLK</i>	-0.30	3.11E-05
<i>EIF4G1</i>	-0.32	2.30E-05	<i>E2F4</i>	-0.30	4.65E-04
<i>KIAA0232</i>	-0.32	6.31E-05	<i>SKP2</i>	-0.29	9.34E-04
<i>TANC2</i>	-0.32	8.14E-04	<i>NFIC</i>	-0.29	5.11E-05
<i>YIF1A</i>	-0.32	6.26E-05	<i>SLC6A8</i>	-0.29	2.84E-04
<i>CLPTM1L</i>	-0.32	8.49E-06	<i>TXNRD1</i>	-0.29	1.18E-04
<i>PSME3</i>	-0.32	1.41E-04	<i>ARL8A</i>	-0.29	9.90E-05
<i>NCLN</i>	-0.32	2.58E-04	<i>MME</i>	-0.29	1.93E-04
<i>CHMP7</i>	-0.32	6.20E-04	<i>ENY2</i>	-0.29	7.59E-04
<i>ARF4</i>	-0.32	6.33E-06	<i>MYBBP1A</i>	-0.29	7.50E-04
<i>GNA11</i>	-0.31	5.72E-04	<i>SNTB2</i>	-0.29	1.13E-04
<i>NQO1</i>	-0.31	2.55E-05	<i>SYNCRIP</i>	-0.29	5.34E-04
<i>ACOT2</i>	-0.31	7.79E-04	<i>UHMK1</i>	-0.29	1.87E-04
<i>LRIG1</i>	-0.31	5.87E-04	<i>NUFIP2</i>	-0.29	3.31E-04
<i>NEO1</i>	-0.31	4.71E-04	<i>PFDN2</i>	-0.29	6.36E-05
<i>ADRM1</i>	-0.31	6.77E-05	<i>RNF34</i>	-0.29	9.33E-04
<i>ARFGAP3</i>	-0.31	3.29E-04	<i>ILF2</i>	-0.29	2.95E-04
<i>WDR12</i>	-0.31	6.81E-04	<i>PSMD10</i>	-0.29	4.18E-04
<i>ITGA7</i>	-0.31	1.79E-05	<i>PTPRF</i>	-0.29	1.07E-04
<i>FBXW7</i>	-0.31	6.23E-04	<i>FH</i>	-0.29	6.82E-04

SYMBOL	SLR	P value	SYMBOL	SLR	P value
<i>DHRS3</i>	-0.29	5.30E-05	<i>TOR1A</i>	-0.26	9.91E-04
<i>FZD4</i>	-0.28	1.14E-04	<i>TNIP1</i>	-0.26	1.24E-04
<i>PTBP1</i>	-0.28	1.30E-05	<i>DDX5</i>	-0.25	1.35E-05
<i>SH3GLB1</i>	-0.28	1.04E-05	<i>CLCN7</i>	-0.25	5.72E-04
<i>STK38L</i>	-0.28	2.82E-04	<i>MRPS7</i>	-0.25	5.74E-05
<i>COQ9</i>	-0.28	1.17E-04	<i>TST</i>	-0.25	3.86E-04
<i>KPNA4</i>	-0.28	3.90E-05	<i>PSMC2</i>	-0.25	3.45E-04
<i>SEH1L</i>	-0.28	7.78E-05	<i>PLOD1</i>	-0.25	2.38E-04
<i>RRBP1</i>	-0.27	1.26E-04	<i>PSMD1</i>	-0.25	3.88E-04
<i>HSPA4</i>	-0.27	1.01E-04	<i>GORASP2</i>	-0.25	4.73E-05
<i>PCMT1</i>	-0.27	3.25E-04	<i>SEC24A</i>	-0.25	7.26E-05
<i>STK39</i>	-0.27	3.98E-05	<i>ARHGDI4</i>	-0.25	6.76E-04
<i>SLC25A32</i>	-0.27	3.24E-04	<i>ALDH4A1</i>	-0.25	5.52E-04
<i>CCT3</i>	-0.27	9.77E-05	<i>SLC9A6</i>	-0.25	8.82E-04
<i>CRTC3</i>	-0.27	2.10E-04	<i>USP16</i>	-0.25	9.06E-04
<i>SCO1</i>	-0.27	8.85E-05	<i>EMP1</i>	-0.25	6.42E-04
<i>TMEM60</i>	-0.27	7.08E-04	<i>CCT2</i>	-0.25	4.34E-05
<i>GALNT2</i>	-0.27	2.37E-04	<i>GSK3B</i>	-0.25	6.27E-05
<i>PSMD12</i>	-0.27	8.07E-04	<i>OPA1</i>	-0.24	1.64E-04
<i>PFKFB1</i>	-0.27	7.96E-04	<i>UBE2E2</i>	-0.24	1.32E-04
<i>ALAS1</i>	-0.27	3.40E-04	<i>NDUFA9</i>	-0.24	9.77E-04
<i>NNT</i>	-0.27	9.51E-04	<i>KDELR2</i>	-0.24	7.63E-06
<i>ABCF1</i>	-0.27	3.34E-05	<i>RXRA</i>	-0.24	4.18E-04
<i>SEC61B</i>	-0.27	5.93E-04	<i>GBE1</i>	-0.24	1.80E-04
<i>GLYAT</i>	-0.27	5.79E-04	<i>NPLOC4</i>	-0.24	1.62E-04
<i>LSG1</i>	-0.26	2.48E-04	<i>IBTK</i>	-0.24	2.67E-04
<i>SKI</i>	-0.26	1.06E-04	<i>SDHB</i>	-0.24	6.06E-04
<i>TMEM165</i>	-0.26	3.57E-05	<i>VPS4A</i>	-0.24	1.73E-04
<i>PSMA3</i>	-0.26	2.65E-04	<i>SBDS</i>	-0.24	1.90E-05
<i>CRK</i>	-0.26	2.21E-05	<i>WASF3</i>	-0.24	9.85E-04
<i>DAAM1</i>	-0.26	4.55E-04	<i>ECHS1</i>	-0.24	9.05E-05
<i>CS</i>	-0.26	1.13E-04	<i>RAB35</i>	-0.24	5.47E-04
<i>RRAGA</i>	-0.26	8.62E-04	<i>ELOVL1</i>	-0.23	3.82E-04
<i>SMARCD1</i>	-0.26	5.23E-04	<i>SPEN</i>	-0.23	3.88E-04
<i>ARL1</i>	-0.26	6.70E-04	<i>INPPL1</i>	-0.23	8.08E-04
<i>PPP1CA</i>	-0.26	3.60E-04	<i>HDHD2</i>	-0.23	8.56E-04
<i>NDUFA6</i>	-0.26	1.30E-04	<i>NUDT5</i>	-0.23	1.62E-04
<i>AKT2</i>	-0.26	3.52E-04	<i>RASA3</i>	-0.23	6.25E-04

SYMBOL	SLR	P value
<i>CHD4</i>	-0.23	3.03E-04
<i>ZBTB7A</i>	-0.23	7.35E-04
<i>HSPB1</i>	-0.23	2.37E-04
<i>SFPQ</i>	-0.23	3.99E-04
<i>TIMM50</i>	-0.23	6.61E-04
<i>SHOC2</i>	-0.22	5.75E-05
<i>LPL</i>	-0.22	9.38E-05
<i>DDX24</i>	-0.22	5.56E-04
<i>UBQLN1</i>	-0.22	8.83E-05
<i>PWP1</i>	-0.22	8.61E-04
<i>AP3D1</i>	-0.22	4.25E-05
<i>CALB2</i>	-0.22	1.06E-04
<i>EEA1</i>	-0.22	8.20E-04
<i>YAP1</i>	-0.22	5.38E-04
<i>BCL7B</i>	-0.22	2.51E-04
<i>CAV1</i>	-0.22	7.39E-05
<i>GTF3A</i>	-0.22	1.67E-04
<i>COPS3</i>	-0.21	8.64E-04
<i>AP2M1</i>	-0.21	8.73E-04
<i>IDE</i>	-0.21	2.93E-04
<i>CHD9</i>	-0.21	6.87E-05
<i>DNAJC11</i>	-0.21	9.75E-04
<i>PGM1</i>	-0.21	4.68E-04
<i>ARCN1</i>	-0.21	1.61E-04
<i>STRN3</i>	-0.20	8.81E-05
<i>TAOK1</i>	-0.20	4.24E-04
<i>ANXA1</i>	-0.20	3.69E-05
<i>FMNL2</i>	-0.20	9.18E-04
<i>GFPT1</i>	-0.20	7.65E-04
<i>VCL</i>	-0.20	2.97E-04
<i>WWP1</i>	-0.20	6.36E-04
<i>MLX</i>	-0.19	3.69E-04
<i>FMOD</i>	-0.19	8.39E-04
<i>COPB1</i>	-0.19	7.16E-04
<i>PSMA7</i>	-0.18	7.46E-04
<i>ANXA6</i>	-0.18	8.79E-04
<i>SOS1</i>	-0.18	2.83E-04
<i>TULP4</i>	-0.18	8.67E-04

SYMBOL	SLR	P value
<i>EIF4G2</i>	-0.17	6.63E-04
<i>MCAM</i>	-0.17	3.45E-04
<i>GPI</i>	-0.17	8.31E-04
<i>POMP</i>	-0.17	4.89E-04
<i>SUCLG1</i>	-0.17	9.00E-04
<i>CLTC</i>	-0.15	7.62E-04
<i>PPIB</i>	-0.15	6.65E-04
<i>COPB2</i>	-0.15	8.54E-04
<i>CAT</i>	0.13	4.52E-04
<i>DPT</i>	0.13	4.58E-04
<i>COPS2</i>	0.14	6.75E-04
<i>NID1</i>	0.16	6.56E-04
<i>SERINC3</i>	0.16	3.31E-04
<i>EPS15</i>	0.17	6.18E-04
<i>CCNI</i>	0.17	7.41E-04
<i>KIAA1109</i>	0.17	1.22E-04
<i>NUP214</i>	0.18	7.81E-04
<i>SMARCC2</i>	0.18	7.34E-05
<i>RERE</i>	0.19	6.31E-04
<i>EFEMP1</i>	0.19	2.78E-04
<i>TRA2A</i>	0.20	5.94E-04
<i>PXDN</i>	0.20	5.35E-04
<i>NFE2L1</i>	0.21	1.64E-04
<i>SYNE2</i>	0.21	1.63E-04
<i>MAT2B</i>	0.21	1.55E-04
<i>HADH</i>	0.21	4.45E-04
<i>PTPN14</i>	0.21	8.31E-04
<i>PCM1</i>	0.21	9.24E-05
<i>HEBP2</i>	0.21	2.34E-04
<i>ACVR1C</i>	0.21	9.11E-04
<i>PODN</i>	0.22	4.99E-04
<i>CLK1</i>	0.22	7.47E-05
<i>HERPUD2</i>	0.22	3.08E-04
<i>LETMD1</i>	0.22	6.96E-04
<i>TOX4</i>	0.22	1.90E-04
<i>BCAS3</i>	0.23	3.65E-04
<i>OGT</i>	0.23	1.66E-06
<i>GOLGB1</i>	0.23	3.36E-04

SYMBOL	SLR	P value	SYMBOL	SLR	P value
<i>STEAP4</i>	0.23	4.64E-04	<i>CPNE1</i>	0.28	1.32E-04
<i>GATAD1</i>	0.23	2.69E-04	<i>WDR48</i>	0.28	4.51E-04
<i>MBNL2</i>	0.23	7.53E-04	<i>YPEL2</i>	0.28	1.64E-04
<i>AATF</i>	0.23	5.20E-04	<i>BAZ2B</i>	0.28	3.71E-05
<i>ALG13</i>	0.23	5.09E-04	<i>PBX3</i>	0.28	7.24E-04
<i>MYO18A</i>	0.24	8.88E-04	<i>CD300LG</i>	0.28	6.10E-04
<i>HELZ</i>	0.24	2.00E-05	<i>MAST2</i>	0.29	7.88E-04
<i>R3HDM2</i>	0.24	9.10E-05	<i>ADCY4</i>	0.29	1.52E-04
<i>HLA-DMA</i>	0.24	5.56E-05	<i>AZIN1</i>	0.29	3.14E-04
<i>UHRF2</i>	0.24	8.78E-04	<i>CLSTN2</i>	0.29	2.47E-04
<i>DMTF1</i>	0.24	2.05E-05	<i>TPCN1</i>	0.29	3.25E-04
<i>CYBRD1</i>	0.24	6.66E-06	<i>EMP2</i>	0.29	2.62E-04
<i>FCHSD2</i>	0.25	5.36E-04	<i>LDB2</i>	0.29	6.74E-05
<i>ZKSCAN1</i>	0.25	1.53E-04	<i>EZH1</i>	0.29	2.03E-06
<i>NISCH</i>	0.25	5.06E-04	<i>TBC1D2B</i>	0.29	2.34E-04
<i>AKAP13</i>	0.25	4.89E-04	<i>ZC3H6</i>	0.30	8.86E-06
<i>ETFA</i>	0.25	1.25E-04	<i>RFX3</i>	0.30	3.50E-04
<i>PNRC1</i>	0.25	6.40E-06	<i>WDR19</i>	0.30	5.45E-04
<i>CEPT1</i>	0.25	3.81E-04	<i>ST6GALNAC2</i>	0.30	2.00E-04
<i>FLNB</i>	0.26	7.26E-04	<i>MAP2K5</i>	0.30	7.41E-04
<i>MAST4</i>	0.26	1.39E-04	<i>TTN</i>	0.30	7.01E-04
<i>CRBN</i>	0.26	7.00E-05	<i>SLC43A1</i>	0.30	5.27E-04
<i>DSG2</i>	0.26	8.37E-04	<i>TCF7L2</i>	0.30	2.48E-05
<i>GHR</i>	0.26	6.10E-05	<i>CTSK</i>	0.30	4.11E-04
<i>JMY</i>	0.26	8.45E-04	<i>PML</i>	0.30	5.71E-04
<i>TBC1D17</i>	0.26	4.56E-04	<i>ECHDC3</i>	0.31	5.63E-04
<i>UBE4B</i>	0.26	3.13E-05	<i>ARHGEF15</i>	0.31	7.06E-04
<i>ANKRD28</i>	0.26	7.45E-04	<i>CHL1</i>	0.31	9.83E-04
<i>MAP4K3</i>	0.27	4.95E-06	<i>POSTN</i>	0.31	1.46E-04
<i>PHF3</i>	0.27	3.97E-05	<i>EDNRA</i>	0.31	2.60E-04
<i>SHPRH</i>	0.27	2.72E-06	<i>CRY2</i>	0.31	2.23E-04
<i>EIF4EBP2</i>	0.27	2.95E-07	<i>EFHC1</i>	0.31	4.05E-04
<i>AHR</i>	0.27	1.28E-05	<i>ANTXR2</i>	0.31	1.80E-04
<i>XRCC1</i>	0.27	4.75E-04	<i>RNF122</i>	0.32	6.10E-04
<i>RBP7</i>	0.27	1.81E-04	<i>GNAZ</i>	0.32	4.04E-04
<i>SERPING1</i>	0.28	3.41E-04	<i>PDCD1LG2</i>	0.32	6.08E-04
<i>FCHO2</i>	0.28	5.07E-05	<i>IMMP2L</i>	0.33	5.31E-04
<i>FBXL20</i>	0.28	4.93E-05	<i>INPP5B</i>	0.33	6.93E-04

SYMBOL	SLR	P value	SYMBOL	SLR	P value
<i>GPR146</i>	0.33	4.33E-04	<i>TWIST2</i>	0.40	3.99E-04
<i>SIPA1L1</i>	0.33	5.67E-04	<i>AGTR1</i>	0.40	8.50E-05
<i>ABCA8</i>	0.33	6.17E-05	<i>CAPN3</i>	0.41	2.46E-05
<i>NUMA1</i>	0.33	3.68E-06	<i>SESTD1</i>	0.41	2.51E-06
<i>ABLIM1</i>	0.34	3.24E-04	<i>CRIM1</i>	0.41	7.94E-05
<i>SATB1</i>	0.34	6.42E-05	<i>YPEL3</i>	0.41	2.27E-04
<i>PLA2G6</i>	0.34	3.02E-05	<i>CCDC28A</i>	0.41	3.95E-04
<i>KSR1</i>	0.34	1.43E-04	<i>PLCE1</i>	0.41	8.09E-05
<i>BST2</i>	0.34	1.19E-04	<i>SLC25A27</i>	0.41	5.00E-06
<i>SNRK</i>	0.35	3.75E-05	<i>SEMA6D</i>	0.42	8.02E-05
<i>PHLDB2</i>	0.35	3.16E-05	<i>TRIM66</i>	0.42	2.14E-05
<i>ATP6V0A1</i>	0.35	1.37E-06	<i>NOS3</i>	0.42	6.65E-04
<i>ANK3</i>	0.35	5.41E-04	<i>TLR4</i>	0.42	6.55E-04
<i>LEPR</i>	0.35	1.35E-04	<i>MYO16</i>	0.43	5.86E-04
<i>APBB3</i>	0.35	1.44E-04	<i>SEMA3A</i>	0.43	8.93E-08
<i>FGD4</i>	0.35	4.32E-06	<i>FMO4</i>	0.43	6.44E-05
<i>ZNF275</i>	0.35	5.11E-05	<i>HBP1</i>	0.43	3.40E-05
<i>ELF2</i>	0.36	1.72E-04	<i>C3orf67</i>	0.43	1.37E-04
<i>GAB2</i>	0.36	2.04E-05	<i>ADH1C</i>	0.44	1.23E-04
<i>SLC27A1</i>	0.36	6.80E-04	<i>AKAP9</i>	0.44	6.32E-07
<i>NOVA1</i>	0.36	4.48E-04	<i>CBLB</i>	0.44	9.36E-05
<i>CLIP4</i>	0.37	3.68E-04	<i>CDKN1C</i>	0.45	3.58E-05
<i>ORMDL3</i>	0.37	4.80E-04	<i>RNASE4</i>	0.45	2.79E-05
<i>KLF7</i>	0.37	6.49E-04	<i>PERP</i>	0.45	3.05E-05
<i>HIBCH</i>	0.37	7.52E-05	<i>SLC24A1</i>	0.45	7.11E-04
<i>GNAI1</i>	0.38	5.72E-05	<i>IFNGR2</i>	0.45	3.11E-05
<i>TULP3</i>	0.38	3.63E-06	<i>PLSCR4</i>	0.45	1.84E-07
<i>TTLL3</i>	0.38	6.95E-04	<i>NPFF</i>	0.45	5.05E-05
<i>PLSCR1</i>	0.38	1.78E-04	<i>APOL6</i>	0.45	1.97E-05
<i>SPATA6</i>	0.39	8.63E-04	<i>CTH</i>	0.45	3.94E-04
<i>HTRA3</i>	0.39	1.63E-05	<i>THBS2</i>	0.45	2.45E-05
<i>TESK2</i>	0.39	5.97E-04	<i>SESN3</i>	0.45	1.21E-06
<i>SEMA3G</i>	0.39	7.89E-06	<i>RASIP1</i>	0.46	1.78E-04
<i>TCN2</i>	0.39	1.34E-04	<i>OR11H6</i>	0.46	4.17E-04
<i>BTNL9</i>	0.39	2.12E-05	<i>ABCA9</i>	0.46	5.27E-06
<i>ZFP36L1</i>	0.40	2.36E-05	<i>DSE</i>	0.46	1.42E-04
<i>PTGER2</i>	0.40	3.91E-04	<i>FOXP2</i>	0.46	1.42E-04
<i>SH3D19</i>	0.40	1.07E-06	<i>MS4A7</i>	0.47	6.99E-05

SYMBOL	SLR	P value
<i>TMEM140</i>	0.48	3.35E-05
<i>TSC22D1</i>	0.48	6.40E-05
<i>ABHD5</i>	0.48	6.40E-04
<i>DYNC2L1</i>	0.48	1.31E-05
<i>MET</i>	0.48	1.62E-04
<i>PRKAG2</i>	0.49	1.47E-05
<i>BBS10</i>	0.49	5.65E-06
<i>ZNF182</i>	0.49	3.19E-05
<i>TTC8</i>	0.49	2.78E-04
<i>ZNF22</i>	0.49	2.06E-04
<i>KLF4</i>	0.49	7.03E-05
<i>ATP6V1B1</i>	0.49	6.99E-04
<i>CASKIN2</i>	0.50	3.22E-04
<i>BAIAP2L1</i>	0.50	3.77E-05
<i>FMO2</i>	0.51	1.47E-06
<i>NEDD4L</i>	0.51	1.01E-06
<i>TM7SF2</i>	0.51	4.11E-05
<i>PLD1</i>	0.51	1.15E-06
<i>ECHDC2</i>	0.51	1.71E-06
<i>ZNF493</i>	0.51	1.06E-05
<i>KLHL24</i>	0.52	5.97E-06
<i>FGF2</i>	0.52	3.90E-06
<i>FHL1</i>	0.52	3.91E-05
<i>SOX4</i>	0.52	5.38E-07
<i>ICK</i>	0.52	2.11E-06
<i>AVPI1</i>	0.52	3.53E-07
<i>IL10RA</i>	0.52	8.73E-04
<i>SYTL3</i>	0.53	5.45E-05
<i>IL16</i>	0.53	4.49E-07
<i>PTPRQ</i>	0.53	8.09E-05
<i>RTN1</i>	0.53	7.71E-06
<i>HOXA6</i>	0.54	3.09E-06
<i>ABCA6</i>	0.54	1.87E-07
<i>ENPP1</i>	0.55	5.56E-05
<i>CITED2</i>	0.56	2.01E-07
<i>C5</i>	0.56	4.43E-05
<i>HOXA3</i>	0.56	5.77E-05
<i>ANGPTL4</i>	0.57	2.03E-04
<i>CCNG2</i>	0.57	2.15E-06

SYMBOL	SLR	P value
<i>ALDH1A1</i>	0.58	3.45E-07
<i>AADAC</i>	0.58	3.67E-04
<i>MAFF</i>	0.58	8.86E-05
<i>RASGEF1B</i>	0.58	1.23E-05
<i>SEMA3F</i>	0.59	1.40E-04
<i>IRAK2</i>	0.59	2.63E-04
<i>FFAR3</i>	0.59	4.95E-04
<i>PLEKHH2</i>	0.59	1.05E-05
<i>NDRG1</i>	0.60	4.98E-09
<i>DCT</i>	0.60	1.84E-05
<i>LHX6</i>	0.61	4.14E-06
<i>NMNAT2</i>	0.61	6.83E-05
<i>TMEM100</i>	0.63	2.43E-04
<i>ABCB11</i>	0.63	5.75E-04
<i>ADRB2</i>	0.63	1.24E-07
<i>CA4</i>	0.64	3.86E-08
<i>ANKRD53</i>	0.66	7.53E-06
<i>SULF1</i>	0.67	1.82E-05
<i>LYPLA2</i>	0.68	2.71E-04
<i>PNPLA7</i>	0.72	1.79E-06
<i>GABARAPL1</i>	0.73	9.73E-08
<i>CAB39L</i>	0.73	6.77E-06
<i>FBXO32</i>	0.74	3.24E-07
<i>BMP3</i>	0.76	5.90E-04
<i>TXNIP</i>	0.76	3.85E-05
<i>PLXNB3</i>	0.77	8.44E-06
<i>PHKG1</i>	0.84	6.68E-04
<i>DAPK2</i>	0.84	1.58E-09
<i>PIK3IP1</i>	0.90	1.16E-06
<i>THBS1</i>	0.94	8.84E-04
<i>C6</i>	0.96	2.82E-05
<i>HMGB2</i>	0.98	7.93E-08
<i>MOCS1</i>	1.02	6.33E-07
<i>PFKFB3</i>	1.03	3.05E-08
<i>IRS2</i>	1.06	2.16E-08
<i>PDK4</i>	1.43	1.31E-07
<i>ADAMTS18</i>	1.44	2.17E-06
<i>SLC27A2</i>	1.45	8.99E-06
<i>CIDEA</i>	1.46	1.20E-09

Supplemental table 3

GSEA upregulated human			
NAME	NES	P val	Q val
WP1836.INTERFERON.GAMMA.SIGNALING	2.22	0.00	0.00
KEGG_STAPHYLOCOCCUS.AUREUS.INFECTION	2.04	0.00	0.02
INTERFERON.GAMMA.SIGNALING	1.96	0.00	0.05
GSEA downregulated human			
NAME	NES	P val	Q val
TRIGLYCERIDE.BIOSYNTHESIS	2.57	0.00	0.00
CROSS.PRESENTATION.OF.SOLUBLE.EXOGENOUS.ANTIGENS.ENDOSOMES.	-2.55	0.00	0.00
UBIQUITIN.DEPENDENT.DEGRADATION.OF.CYCLIN.D	-2.51	0.00	0.00
WP2773.DEGRADATION.OF.BETA.CATENIN.BY.THE.DESTRUCTION.COMPLEX	-2.51	0.00	0.00
WP1982.SREBP.SIGNALING	-2.50	0.00	0.00
AUF1.HNRNP.D0.DESTABILIZES.MRNA	-2.50	0.00	0.00
DEGRADATION.OF.GLI2.BY.THE.PROTEASOME	-2.48	0.00	0.00
ASYMMETRIC.LOCALIZATION.OF.PCP.PROTEINS	-2.48	0.00	0.00
DEGRADATION.OF.DVL	-2.47	0.00	0.00
HH.LIGAND.BIOGENESIS.DISEASE	-2.47	0.00	0.00
UBIQUITIN.DEPENDENT.DEGRADATION.OF.CYCLIN.D1	-2.47	0.00	0.00
WP1896.REGULATION.OF.APOPTOSIS	-2.47	0.00	0.00
SCF.BETA.TRCP.MEDIATED.DEGRADATION.OF.EMI1	-2.46	0.00	0.00
HEDGEHOG.LIGAND.BIOGENESIS	-2.46	0.00	0.00
DEGRADATION.OF.GLI1.BY.THE.PROTEASOME	-2.45	0.00	0.00
MITOCHONDRIAL.TRANSLATION.ELONGATION	-2.45	0.00	0.00
KEGG_PROTEASOME	-2.44	0.00	0.00
DEGRADATION.OF.AXIN	-2.44	0.00	0.00
REGULATION.OF.ORNITHINE.DECARBOXYLASE.ODC.	-2.44	0.00	0.00
REGULATION.OF.ACTIVATED.PAK.2P34.BY.PROTEASOME.MEDIATED.DEGRADATION	-2.43	0.00	0.00
WP2359.PARKIN.UBIQUITIN.PROTEASOMAL.SYSTEM.PATHWAY	-2.41	0.00	0.00
MITOCHONDRIAL.TRANSLATION	-2.41	0.00	0.00
CDK.MEDIATED.PHOSPHORYLATION.AND.REMOVAL.OF.CDC6	-2.41	0.00	0.00
VPU.MEDIATED.DEGRADATION.OF.CD4	-2.41	0.00	0.00
PROCESSING.DEFECTIVE.HH.VARIANTS.ABROGATE.LIGAND.SECRETION	-2.40	0.00	0.00
UBIQUITIN.MEDIATED.DEGRADATION.OF.PHOSPHORYLATED.CDC25A	-2.40	0.00	0.00
MITOCHONDRIAL.TRANSLATION.INITIATION	-2.40	0.00	0.00
FATTY.ACYL.COA.BIOSYNTHESIS	-2.39	0.00	0.00
MITOCHONDRIAL.TRANSLATION.TERMINATION	-2.39	0.00	0.00
VIF.MEDIATED.DEGRADATION.OF.APOBEC3G	-2.37	0.00	0.00
GLI3.IS.PROCESSED.TO.GLI3R.BY.THE.PROTEASOME	-2.36	0.00	0.00
AUTODEGRADATION.OF.THE.E3.UBIQUITIN.LIGASE.COP1	-2.35	0.00	0.00
DELETIONS.IN.THE.AMER1.GENE.DESTABILIZE.THE.DESTRUCTION.COMPLEX	-2.35	0.00	0.00
PCP.CE.PATHWAY	-2.35	0.00	0.00
KEGG_BIOSYNTHESIS.OF.UNSATURATED.FATTY.ACIDS	-2.35	0.00	0.00
APC.C.CDC20.MEDIATED.DEGRADATION.OF.MITOTIC.PROTEINS	-2.35	0.00	0.00
REGULATION.OF.MRNA.STABILITY.BY.PROTEINS.THAT.BIND.AU.RICH.ELEMENTS	-2.35	0.00	0.00
P53.INDEPENDENT.G1.S.DNA.DAMAGE.CHECKPOINT	-2.35	0.00	0.00

GSEA downregulated human				
NAME	NES	P val	Q val	
WP2733.REGULATION.OF.MRNA.STABILITY.BY.PROTEINS.THAT.BIND.AU.RICH.ELEMENTS	-2.35	0.00	0.00	
ACTIVATION.OF.APC.C.AND.APC.C.CDC20.MEDIATED.DEGRADATION.OF.MITOTIC.PROTEINS	-2.34	0.00	0.00	
SCF.SKP2.MEDIATED.DEGRADATION.OF.P27.P21	-2.34	0.00	0.00	
MISSPLICED.GSK3BETA.MUTANTS.STABILIZE.BETA.CATENIN	-2.33	0.00	0.00	
APC.TRUNCATION.MUTANTS.ARE.NOT.K63.POLYUBIQUITINATED	-2.32	0.00	0.00	
APC.C.CDC20.MEDIATED.DEGRADATION.OF.SECURIN	-2.32	0.00	0.00	
APC.TRUNCATION.MUTANTS.HAVE.IMPAIRED.AXIN.BINDING	-2.32	0.00	0.00	
STABILIZATION.OF.P53	-2.32	0.00	0.00	
AXIN.MISSENSE.MUTANTS.DESTABILIZE.THE.DESTRUCTION.COMPLEX	-2.32	0.00	0.00	
P53.INDEPENDENT.DNA.DAMAGE.RESPONSE	-2.31	0.00	0.00	
DEGRADATION.OF.BETA.CATENIN.BY.THE.DESTRUCTION.COMPLEX	-2.30	0.00	0.00	
CDC20.PHOSPHO.APC.C.MEDIATED.DEGRADATION.OF.CYCLIN.A	-2.30	0.00	0.00	
S37.MUTANTS.OF.BETA.CATENIN.AREN.T.PHOSPHORYLATED	-2.29	0.00	0.00	
T41.MUTANTS.OF.BETA.CATENIN.AREN.T.PHOSPHORYLATED	-2.29	0.00	0.00	
WP1782.APC.C.MEDIATED.DEGRADATION.OF.CELL.CYCLE.PROTEINS	-2.29	0.00	0.00	
TRUNCATIONS.OF.AMER1.DESTABILIZE.THE.DESTRUCTION.COMPLEX	-2.29	0.00	0.00	
S45.MUTANTS.OF.BETA.CATENIN.AREN.T.PHOSPHORYLATED	-2.29	0.00	0.00	
AMER1.MUTANTS.DESTABILIZE.THE.DESTRUCTION.COMPLEX	-2.29	0.00	0.00	
KEGG_PARKINSON.S.DISEASE	-2.29	0.00	0.00	
MITOCHONDRIAL.PROTEIN.IMPORT	-2.29	0.00	0.00	
AXIN.MUTANTS.DESTABILIZE.THE.DESTRUCTION.COMPLEX.ACTIVATING.WNT.SIGNALING	-2.29	0.00	0.00	
WP1902.RESPIRATORY.ELECTRON.TRANSPORT.ATP.SYNTHESIS.BY.CHEMIOSMOTIC.COUPLING.AND.HEAT.PRODUCTION.BY.UNCOUPLING.PROTEINS.	-2.29	0.00	0.00	
RESPIRATORY.ELECTRON.TRANSPORT.ATP.SYNTHESIS.BY.CHEMIOSMOTIC.COUPLING.AND.HEAT.PRODUCTION.BY.UNCOUPLING.PROTEINS.	-2.28	0.00	0.00	
S33.MUTANTS.OF.BETA.CATENIN.AREN.T.PHOSPHORYLATED	-2.28	0.00	0.00	
CYTOSOLIC.TRNA.AMINOACYLATION	-2.28	0.00	0.00	
AUTODEGRADATION.OF.CDH1.BY.CDH1.APC.C	-2.28	0.00	0.00	
APC.C.CDH1.MEDIATED.DEGRADATION.OF.CDC20.AND.OTHER.APC.C.CDH1.TARGETED.PROTEINS.IN.LATE.MITOSIS.EARLY.G1	-2.28	0.00	0.00	
BIOC_PROTEASOMEPATHWAY	-2.28	0.00	0.00	
WP111.ELECTRON.TRANSPORT.CHAIN	-2.28	0.00	0.00	
REGULATION.OF.APC.C.ACTIVATORS.BETWEEN.G1.S.AND.EARLY.ANAPHASE	-2.27	0.00	0.00	
PHOSPHORYLATION.SITE.MUTANTS.OF.CTNNB1.ARE.NOT.TARGETED.TO.THE.PROTEASOME.BY.THE.DESTRUCTION.COMPLEX	-2.27	0.00	0.00	
P53.DEPENDENT.G1.S.DNA.DAMAGE.CHECKPOINT	-2.26	0.00	0.00	
TCF7L2.MUTANTS.DON.T.BIND.CTBP	-2.26	0.00	0.00	
KEGG_PROTEIN.PROCESSING.IN.ENDOPLASMIC.RETICULUM	-2.26	0.00	0.00	
CYCLIN.A.CDK2.ASSOCIATED.EVENTS.AT.S.PHASE.ENTRY	-2.26	0.00	0.00	
TRUNCATED.APC.MUTANTS.DESTABILIZE.THE.DESTRUCTION.COMPLEX	-2.26	0.00	0.00	
DELETIONS.IN.THE.AXIN.GENES.IN.HEPATOCELLULAR.CARCINOMA.RESULT.IN.ELEVATED.WNT.SIGNALING	-2.26	0.00	0.00	
REGULATION.OF.MITOTIC.CELL.CYCLE	-2.25	0.00	0.00	
P53.DEPENDENT.G1.DNA.DAMAGE.RESPONSE	-2.24	0.00	0.00	

GSEA downregulated human

NAME	NES	P val	Q val
ORGANELLE.BIOGENESIS.AND.MAINTENANCE	-2.24	0.00	0.00
APC.C.MEDIATED.DEGRADATION.OF.CELL.CYCLE.PROTEINS	-2.24	0.00	0.00
ER.PHAGOSOME.PATHWAY	-2.23	0.00	0.00
WP534.GLYCOLYSIS.AND.GLUONEOGENESIS	-2.23	0.00	0.00
THE.CITRIC.ACID.TCA.CYCLE.AND.RESPIRATORY.ELECTRON.TRANSPORT	-2.23	0.00	0.00
G1.S.DNA.DAMAGE.CHECKPOINTS	-2.22	0.00	0.00
PREFOLDIN.MEDIATED.TRANSFER.OF.SUBSTRATE.TO.CCT.TRIC	-2.21	0.00	0.00
CHAPERONIN.MEDIATED.PROTEIN.FOLDING	-2.21	0.00	0.00
ACTIVATION.OF.NF.KAPPAB.IN.B.CELLS	-2.20	0.00	0.00
WP1785.ASPARAGINE.N.LINKED.GLYCOSYLATION	-2.20	0.00	0.00
WP2717.MITOCHONDRIAL.PROTEIN.IMPORT	-2.20	0.00	0.00
PPARA_TARGETS	-2.20	0.00	0.00
PROTEIN.FOLDING	-2.20	0.00	0.00
WP623.OXIDATIVE.PHOSPHORYLATION	-2.19	0.00	0.00
WP2796.CLASS.I.MHC.MEDIATED.ANTIGEN.PROCESSING.AMP.PRESENTATION	-2.19	0.00	0.00
CYCLIN.E.ASSOCIATED.EVENTS.DURING.G1.S.TRANSITION	-2.19	0.00	0.00
CDT1.ASSOCIATION.WITH.THE.CDC6.ORC.ORIGIN.COMPLEX	-2.19	0.00	0.00
KEGG_CITRATE.CYCLE.TCA.CYCLE.	-2.19	0.00	0.00
KEGG_ALZHEIMER.S.DISEASE	-2.18	0.00	0.00
WP2766.THE.CITRIC.ACID.TCA.CYCLE.AND.RESPIRATORY.ELECTRON. TRANSPORT.	-2.18	0.00	0.00
SYNTHESIS.OF.VERY.LONG.CHAIN.FATTY.ACYL.COAS	-2.17	0.00	0.00
BETA.CATENIN.INDEPENDENT.WNT.SIGNALING	-2.17	0.00	0.00
RESPIRATORY.ELECTRON.TRANSPORT	-2.16	0.00	0.00
WP2746.SIGNALING.BY.THE.B.CELL.RECEPTOR.BCR.	-2.16	0.00	0.00
RNF.MUTANTS.SHOW.ENHANCED.WNT.SIGNALING.AND.PROLIFERATION	-2.15	0.00	0.00
WP1817.FATTY.ACID.TRIACYLGLYCEROL.AND.KETONE.BODY.METABOLISM	-2.15	0.00	0.00
DISASSEMBLY.OF.DESTRUCTION.COMPLEX.AND.RECRUITMENT.OF.AXIN. TO.MEMBRANE	-2.14	0.00	0.00
WP1892.PROTEIN.FOLDING	-2.13	0.00	0.00
ANTIGEN.PROCESSING.CROSS.PRESENTATION	-2.13	0.00	0.00
MISSPLICED.LRP5.MUTANTS.HAVE.ENHANCED.BETA.CATENIN.DEPENDENT. SIGNALING	-2.13	0.00	0.00
WP183.PROTEASOME.DEGRADATION	-2.13	0.00	0.00
COOPERATION.OF.PREFOLDIN.AND.TRIC.CCT.IN.ACTIN.AND.TUBULIN.FOLDING	-2.12	0.00	0.00
KEGG_RIBOSOME.BIOGENESIS.IN.EUKARYOTES	-2.12	0.00	0.00
TCF.DEPENDENT.SIGNALING.IN.RESPONSE.TO.WNT	-2.12	0.00	0.00
WP2684.HOST.INTERACTIONS.OF.HIV.FACTORS	-2.11	0.00	0.00
RNA.POLYMERASE.I.PROMOTER.ESCAPE	-2.11	0.00	0.00
REGULATION.OF.APOPTOSIS	-2.11	0.00	0.00
WP1938.TRNA.AMINOACYLATION	-2.11	0.00	0.00
WP2003.MIR.TARGETED.GENES.IN.LEUKOCYTES.TARBASE	-2.11	0.00	0.00
XAV939.INHIBITS.TANKYRASE.STABILIZING.AXIN	-2.11	0.00	0.00
RNA.POLYMERASE.I.TRANSCRIPTION.TERMINATION	-2.10	0.00	0.00
TRNA.AMINOACYLATION	-2.09	0.00	0.00
HOST.INTERACTIONS.OF.HIV.FACTORS	-2.09	0.00	0.00
METABOLISM.OF.PORPHYRINS	-2.09	0.00	0.00

GSEA downregulated human

NAME	NES	P val	Q val
REGULATION.OF.CHOLESTEROL.BIOSYNTHESIS.BY.SREBP.SREBF.	-2.08	0.00	0.00
IRE1ALPHA.ACTIVATES.CHAPERONES	-2.08	0.00	0.00
WP2693.METABOLISM.OF.AMINO.ACIDS.AND.DERIVATIVES	-2.08	0.00	0.00
SIGNALING.BY.WNT.IN.CANCER	-2.07	0.00	0.00
KEGG_TERPENOID.BACKBONE.BIOSYNTHESIS	-2.06	0.00	0.00
FATTY.ACID.TRIACYLGLYCEROL.AND.KETONE.BODY.METABOLISM	-2.05	0.00	0.00
KEGG_FATTY.ACID.ELONGATION	-2.04	0.00	0.00
KEGG_PYRIMIDINE.METABOLISM	-2.04	0.00	0.00
XBP1.S.ACTIVATES.CHAPERONE.GENES	-2.03	0.00	0.00
WP2002.MIR.TARGETED.GENES.IN.EPITHELIUM.TARBASE	-2.03	0.00	0.00
KEGG_GLYCEROLIPID.METABOLISM	-2.03	0.00	0.00
HIV.INFECTION	-2.03	0.00	0.00
WP1831.INTEGRATION.OF.ENERGY.METABOLISM	-2.03	0.00	0.00
KEGG_OXIDATIVE.PHOSPHORYLATION	-2.03	0.00	0.00
WP3.TRANSCRIPTIONAL.ACTIVATION.BY.NRF2	-2.03	0.00	0.00
METABOLISM.OF.AMINO.ACIDS.AND.DERIVATIVES	-2.02	0.00	0.00
WP2004.MIR.TARGETED.GENES.IN.LYMPHOCYTES.TARBASE	-2.02	0.00	0.00
KEGG_PYRUVATE.METABOLISM	-2.02	0.00	0.00
KEGG_RNA.POLYMERASE	-2.02	0.00	0.00
SIGNALING.BY.WNT	-2.01	0.00	0.00
WP405.EUKARYOTIC.TRANSCRIPTION.INITIATION	-2.01	0.00	0.00
GLUCONEOGENESIS	-2.01	0.00	0.00
METABOLISM.OF.RNA	-2.01	0.00	0.00
FORMATION.OF.TUBULIN.FOLDING.INTERMEDIATES.BY.CCT.TRIC	-2.00	0.00	0.00
WP2006.MIR.TARGETED.GENES.IN.SQUAMOUS.CELL.TARBASE	-2.00	0.00	0.00
WP325.TRIACYLGLYCERIDE.SYNTHESIS	-2.00	0.00	0.00
MRNA.SPLICING.MINOR.PATHWAY	-2.00	0.00	0.00
M.G1.TRANSITION	-1.99	0.00	0.00
KEGG_NON.ALCOHOLIC.FATTY.LIVER.DISEASE.NAFLD.	-1.99	0.00	0.00
KEGG_HUNTINGTON.S.DISEASE	-1.99	0.00	0.00
ACTIVATION.OF.GENE.EXPRESSION.BY.SREBF.SREBP.	-1.99	0.00	0.00
MRNA.SPLICING	-1.99	0.00	0.00
DNA.REPLICATION.PRE.INITIATION	-1.98	0.00	0.00
UNFOLDED.PROTEIN.RESPONSE.UPR.	-1.98	0.00	0.00
WP2667.ACTIVATION.OF.CHAPERONE.GENES.BY.XBP1.S.	-1.98	0.00	0.00
REGULATION.OF.HSF1.MEDIATED.HEAT.SHOCK.RESPONSE	-1.98	0.00	0.00
MRNA.SPLICING.MAJOR.PATHWAY	-1.98	0.00	0.00
PROCESSING.OF.CAPPED.INTRON.CONTAINING.PRE.MRNA	-1.97	0.00	0.00
TRANSPORT.TO.THE.GOLGI.AND.SUBSEQUENT.MODIFICATION	-1.97	0.00	0.00
ASSOCIATION.OF.TRIC.CCT.WITH.TARGET.PROTEINS.DURING.BIOSYNTHESIS	-1.97	0.00	0.00
MITOTIC.G1.G1.S.PHASES	-1.96	0.00	0.00
WP2785.M.G1.TRANSITION	-1.96	0.00	0.00
PYRUVATE.METABOLISM.AND.CITRIC.ACID.TCA.CYCLE	-1.95	0.00	0.00
ASSEMBLY.OF.THE.PRE.REPLICATIVE.COMPLEX	-1.95	0.00	0.00
RNA.POLYMERASE.III.TRANSCRIPTION.TERMINATION	-1.94	0.00	0.00
WP1946.CORI.CYCLE	-1.94	0.00	0.00

GSEA downregulated human				
NAME	NES	P val	Q val	
METABOLISM.OF.MRNA	-1.94	0.00	0.00	
G1.S.TRANSITION	-1.92	0.00	0.00	
CITRIC.ACID.CYCLE.TCA.CYCLE.	-1.91	0.00	0.00	
WP78.TCA.CYCLE	-1.90	0.00	0.00	
RNA.POLYMERASE.I.TRANSCRIPTION.INITIATION	-1.90	0.00	0.00	
ORC1.REMOVAL.FROM.CHROMATIN	-1.90	0.00	0.00	
SWITCHING.OF.ORIGINS.TO.A.POST.REPLICATIVE.STATE	-1.89	0.00	0.00	
MRNA.CAPPING	-1.89	0.00	0.00	
WP2706.ACTIVATION.OF.GENE.EXPRESSION.BY.SREBP.SREBF.	-1.89	0.00	0.00	
CLASS.I.MHC.MEDIATED.ANTIGEN.PROCESSING.PRESENTATION	-1.89	0.00	0.00	
WP357.FATTY.ACID.BIOSYNTHESIS	-1.88	0.00	0.00	
KEGG_AMINOACYL.TRNA.BIOSYNTHESIS	-1.88	0.00	0.00	
ANTIGEN.PROCESSING.UBIQUITINATION.PROTEASOME.DEGRADATION	-1.88	0.00	0.00	
S.PHASE	-1.88	0.00	0.00	
WP197.CHOLESTEROL.BIOSYNTHESIS	-1.88	0.00	0.00	
WP1861.MRNA.CAPPING	-1.87	0.00	0.00	
REGULATION.OF.INSULIN.SECRETION	-1.86	0.00	0.00	
RNA.POLYMERASE.III.CHAIN.ELONGATION	-1.86	0.00	0.00	
REMOVAL.OF.LICENSING.FACTORS.FROM.ORIGINS	-1.86	0.00	0.00	
WP1898.REGULATION.OF.DNA.REPLICATION	-1.86	0.00	0.00	
WP2005.MIR.TARGETED.GENES.IN.MUSCLE.CELL.TARBASE	-1.86	0.00	0.00	
MITOTIC.METAPHASE.AND.ANAPHASE	-1.85	0.00	0.01	
WP1848.METABOLISM.OF.CARBOHYDRATES	-1.85	0.00	0.01	
APOPTOSIS	-1.84	0.00	0.01	
WP1858.MITOTIC.G1.G1.S.PHASES	-1.84	0.00	0.01	
WP1889.PROCESSING.OF.CAPPED.INTRON.CONTAINING.PRE.MRNA	-1.84	0.00	0.01	
INTEGRATION.OF.ENERGY.METABOLISM	-1.84	0.00	0.01	
WP2757.MITOTIC.METAPHASE.AND.ANAPHASE	-1.84	0.00	0.01	
ASPARAGINE.N.LINKED.GLYCOSYLATION	-1.83	0.00	0.01	
KEGG_GLYCOLYSIS.GLUONEOGENESIS	-1.83	0.00	0.01	
SIGNALING.BY.HEDGEHOG	-1.83	0.00	0.01	
GLUCOSE.METABOLISM	-1.82	0.00	0.01	
REGULATION.OF.DNA.REPLICATION	-1.82	0.00	0.01	
WP1795.CHOLESTEROL.BIOSYNTHESIS	-1.81	0.00	0.01	
RNA.POL.II.CTD.PHOSPHORYLATION.AND.INTERACTION.WITH.CE	-1.81	0.00	0.01	
TRANSCRIPTION	-1.81	0.00	0.01	
DEPOLYMERISATION.OF.THE.NUCLEAR.LAMINA	-1.81	0.01	0.01	
SYNTHESIS.OF.DNA	-1.81	0.00	0.01	
RNA.POLYMERASE.I.RNA.POLYMERASE.III.AND.MITOCHONDRIAL.	-1.80	0.00	0.01	
TRANSCRIPTION	-1.80	0.00	0.01	
MITOTIC.ANAPHASE	-1.80	0.00	0.01	
CELLULAR.RESPONSE.TO.HEAT.STRESS	-1.80	0.00	0.01	
FORMATION.OF.THE.HIV.1.EARLY.ELONGATION.COMPLEX	-1.80	0.00	0.01	
HEDGEHOG.OFF.STATE	-1.78	0.00	0.01	
RNA.POLYMERASE.II.TRANSCRIPTION.ELONGATION	-1.78	0.00	0.01	
GLYCOGEN.STORAGE.DISEASES	-1.78	0.00	0.01	

GSEA downregulated human			
NAME	NES	P val	Q val
POST.ELONGATION.PROCESSING.OF.INTRONLESS.PRE.MRNA	-1.78	0.00	0.01
GLUCAGON.LIKE.PEPTIDE.1.GLP1.REGULATES.INSULIN.SECRETION	-1.78	0.00	0.01
PROCESSING.OF.CAPPED.INTRONLESS.PRE.MRNA	-1.77	0.00	0.01
WP2011.SREBF.AND.MIR33.IN.CHOLESTEROL.AND.LIPID.HOMEOSTASIS	-1.77	0.00	0.01
ASSEMBLY.OF.COLLAGEN.FIBRILS.AND.OTHER.MULTIMERIC.STRUCTURES	-1.77	0.00	0.01
MYOCLONIC.EPILEPSY.OF.LAFORA	-1.77	0.00	0.01
POST.CHAPERONIN.TUBULIN.FOLDING.PATHWAY	-1.77	0.00	0.01
FORMATION.OF.THE.EARLY.ELONGATION.COMPLEX	-1.77	0.00	0.01
WP2772.S.PHASE	-1.77	0.00	0.01
RNA.POLYMERASE.II.TRANSCRIPTION.INITIATION.AND.PROMOTER.CLEARANCE	-1.77	0.00	0.01
WP1846.MEMBRANE.TRAFFICKING	-1.77	0.00	0.01
DOWNSTREAM.SIGNALING.EVENTS.OF.B.CELL.RECEPTOR.BCR	-1.77	0.00	0.01
DNA.REPLICATION	-1.76	0.00	0.01
CELL.CYCLE.CHECKPOINTS	-1.76	0.00	0.01
SEPARATION.OF.SISTER.CHROMATIDS	-1.76	0.00	0.01
SIGNALING.BY.HIPPO	-1.76	0.01	0.01
TAT.MEDIATED.ELONGATION.OF.THE.HIV.1.TRANSCRIPT	-1.76	0.00	0.01
M.PHASE	-1.76	0.00	0.01
RNA.POLYMERASE.III.ABORTIVE.AND.RETRACTIVE.INITIATION	-1.75	0.00	0.01
METABOLISM.OF.CARBOHYDRATES	-1.75	0.00	0.01
FORMATION.OF.HIV.1.ELONGATION.COMPLEX.CONTAINING.HIV.1.TAT	-1.75	0.00	0.01
RNA.POLYMERASE.II.PROMOTER.ESCAPE	-1.75	0.00	0.01
WP1403.AMPK.SIGNALING	-1.75	0.00	0.01
CHOLESTEROL.BIOSYNTHESIS	-1.75	0.00	0.01
ACTIVATION.OF.BH3.ONLY.PROTEINS	-1.75	0.00	0.02
KEGG_INSULIN.SIGNALING.PATHWAY	-1.74	0.00	0.02
WP1905.RNA.POLYMERASE.I.RNA.POLYMERASE.III.AND.MITOCHONDRIAL. TRANSCRIPTION	-1.74	0.00	0.02
WP428.WNT.SIGNALING.PATHWAY	-1.74	0.00	0.02
FORMATION.OF.HIV.ELONGATION.COMPLEX.IN.THE.ABSENCE.OF.HIV.TAT	-1.74	0.00	0.02
FORMATION.OF.RNA.POL.II.ELONGATION.COMPLEX	-1.74	0.00	0.02
KEGG_PEROXISOME	-1.74	0.00	0.02
WP500.GLYCOGEN.METABOLISM	-1.74	0.01	0.02
HIV.TRANSCRIPTION.INITIATION	-1.74	0.01	0.02
ADP.SIGNALLING.THROUGH.P2Y.PURINOCEPTOR.1	-1.74	0.00	0.02
FORMATION.OF.ATP.BY.CHEMIOSMOTIC.COUPLING	-1.73	0.01	0.02
RNA.POLYMERASE.II.TRANSCRIPTION.INITIATION	-1.73	0.00	0.02
HIV.TRANSCRIPTION.ELONGATION	-1.73	0.01	0.02
MICRORNA.MIRNA.BIOGENESIS	-1.73	0.01	0.02
ZINC.TRANSPORTERS	-1.73	0.01	0.02
SIGNALING.BY.THE.B.CELL.RECEPTOR.BCR.	-1.73	0.00	0.02
RNA.POLYMERASE.III.TRANSCRIPTION	-1.73	0.00	0.02
SYNTHESIS.AND.INTERCONVERSION.OF.NUCLEOTIDE.DI.AND.TRIPHOSPHATES	-1.72	0.01	0.02
WP2714.SIGNALING.BY.HIPPO	-1.72	0.01	0.02
WP236.ADIPOGENESIS	-1.72	0.00	0.02
WP1775.CELL.CYCLE.CHECKPOINTS	-1.72	0.00	0.02

GSEA downregulated human			
NAME	NES	P val	Q val
RNA.POLYMERASE.III.TRANSCRIPTION.INITIATION.FROM.TYPE.3.PROMOTER	-1.72	0.01	0.02
WP2038.REGULATION.OF.MICROTUBULE.CYTOSKELETON	-1.72	0.01	0.02
RNA.POLYMERASE.II.TRANSCRIPTION.PRE.INITIATION.AND.PROMOTER.OPENING	-1.71	0.00	0.02
RNA.POLYMERASE.II.HIV.PROMOTER.ESCAPE	-1.71	0.00	0.02
N.GLYCAN.ANTENNAE.ELONGATION	-1.71	0.01	0.02
WP1541.ENERGY.METABOLISM	-1.71	0.01	0.02
METABOLISM.OF.NUCLEOTIDES	-1.71	0.00	0.02
RNA.POLYMERASE.II.PRE.TRANSCRIPTION.EVENTS	-1.70	0.00	0.02
KEGG_CYSTEINE.AND.METHIONINE.METABOLISM	-1.70	0.00	0.02
KEGG_PROTEIN.EXPORT	-1.70	0.00	0.02
NRF2_TARGETS	-1.69	0.00	0.02
HIV.LIFE.CYCLE	-1.69	0.00	0.02
RNA.POLYMERASE.II.TRANSCRIPTION	-1.69	0.00	0.02
KEGG_RNA.TRANSPORT	-1.69	0.00	0.02
G1.PHASE	-1.69	0.00	0.02
TRANSCRIPTION.OF.THE.HIV.GENOME	-1.69	0.00	0.02
ATTENUATION.PHASE	-1.69	0.01	0.02
WP391.MITOCHONDRIAL.GENE.EXPRESSION	-1.68	0.01	0.02
WP1851.METABOLISM.OF.NUCLEOTIDES	-1.68	0.01	0.02
WP1890.PROCESSING.OF.CAPPED.INTRONLESS.PRE.MRNA	-1.68	0.02	0.02
WP2798.ASSEMBLY.OF.COLLAGEN.FIBRILS.AND.OTHER.MULTIMERIC.STRUCTURES	-1.68	0.01	0.03
INTRINSIC.PATHWAY.FOR.APOPTOSIS	-1.68	0.01	0.03
RNA.POLYMERASE.III.TRANSCRIPTION.INITIATION	-1.67	0.01	0.03
NUCLEAR.ENVELOPE.BREAKDOWN	-1.67	0.00	0.03
FORMATION.OF.TRANSCRIPTION.COUPLED.NER.TC.NER.REPAIR.COMPLEX	-1.67	0.01	0.03
BIOC_GSK3PATHWAY	-1.67	0.02	0.03
WP1925.SYNTHESIS.OF.DNA	-1.67	0.00	0.03
KEGG_AMPK.SIGNALING.PATHWAY	-1.66	0.00	0.03
CYCLIN.D.ASSOCIATED.EVENTS.IN.G1	-1.66	0.01	0.03
BIOC_IGF1RPATHWAY	-1.66	0.02	0.03
INTERACTIONS.OF.VPR.WITH.HOST.CELLULAR.PROTEINS	-1.66	0.01	0.03
BIOC_CELLCYCLEPATHWAY	-1.66	0.02	0.03
HSF1.ACTIVATION	-1.66	0.01	0.03
DUAL.INCISION.REACTION.IN.TC.NER	-1.65	0.01	0.03
TRANSCRIPTIONAL.ACTIVATION.OF.MITOCHONDRIAL.BIOGENESIS	-1.65	0.00	0.03
KEGG_HIPPO.SIGNALING.PATHWAY	-1.65	0.00	0.03
WP1906.RNA.POLYMERASE.II.TRANSCRIPTION	-1.65	0.00	0.03
PPARA.ACTIVATES.GENE.EXPRESSION	-1.65	0.00	0.03
KEGG_WNT.SIGNALING.PATHWAY	-1.64	0.00	0.04
COLLAGEN.FORMATION	-1.64	0.00	0.04
KEGG_MRNA.SURVEILLANCE.PATHWAY	-1.64	0.00	0.04
WP2525.TRANS.SULFURATION.AND.ONE.CARBON.METABOLISM	-1.63	0.02	0.04
RNA.POLYMERASE.III.TRANSCRIPTION.INITIATION.FROM.TYPE.1.PROMOTER	-1.63	0.01	0.04
KEGG_PORPHYRIN.AND.CHLOROPHYLL.METABOLISM	-1.63	0.01	0.04

GSEA downregulated human			
NAME	NES	P val	Q val
WP2533.GLYCEROPHOSPHOLIPID.BIOSYNTHETIC.PATHWAY	-1.63	0.03	0.04
CELL.CYCLE.MITOTIC	-1.63	0.00	0.04
BETA.CATENIN.PHOSPHORYLATION.CASCADE	-1.62	0.02	0.04
MEMBRANE.TRAFFICKING	-1.62	0.00	0.04
BIOC_CK1PATHWAY	-1.62	0.03	0.04
KEGG_PPAR.SIGNALING.PATHWAY	-1.62	0.01	0.04
MITOTIC.M.M.G1.PHASES	-1.61	0.00	0.04
TRISTETRAPROLIN.TTP.DESTABILIZES.MRNA	-1.61	0.03	0.04
RNA.POLYMERASE.I.CHAIN.ELONGATION	-1.61	0.01	0.04
DOWNREGULATION.OF.TGF.BETA.RECEPTOR.SIGNALING	-1.60	0.02	0.05
VIRAL.MESSENGER.RNA.SYNTHESIS	-1.60	0.01	0.05
GLYCEROPHOSPHOLIPID.BIOSYNTHESIS	-1.60	0.01	0.05
REGULATION.OF.LIPID.METABOLISM.BY.PEROXISOME.PROLIFERATOR. ACTIVATED.RECEPTOR.ALPHA.PPARALPHA.	-1.60	0.00	0.05
ACTIVATION.OF.BAD.AND.TRANSLOCATION.TO.MITOCHONDRIA	-1.60	0.02	0.05
WP2683.INFLUENZA.LIFE.CYCLE	-1.60	0.00	0.05
WP2715.METABOLISM.OF.NON.CODING.RNA	-1.60	0.01	0.05

Supplemental table 4. List of genes in fig 5b

Gene	SLR mouse	P val mouse	SLR human	P val human
<i>PDK4</i>	3.38	1.03E-20	1.44	1.31E-07
<i>IRS2</i>	0.86	4.36E-09	1.07	2.16E-08
<i>THBS1</i>	1.04	3.58E-04	0.98	8.84E-04
<i>TXNIP</i>	0.53	9.58E-09	0.78	3.85E-05
<i>FBXO32</i>	0.79	2.31E-07	0.76	3.24E-07
<i>CAB39L</i>	0.59	1.00E-08	0.77	6.77E-06
<i>GABARAPL1</i>	1.13	3.68E-09	0.75	9.73E-08
<i>PNPLA7</i>	1.97	1.90E-15	0.72	1.79E-06
<i>CA4</i>	1.39	2.63E-11	0.66	3.86E-08
<i>ADRB2</i>	1.51	1.36E-07	0.64	1.24E-07
<i>LHX6</i>	0.47	2.12E-04	0.60	4.14E-06
<i>NDRG1</i>	0.32	9.20E-04	0.61	4.98E-09
<i>IRAK2</i>	0.99	3.19E-09	0.62	2.63E-04
<i>SEMA3F</i>	0.89	2.00E-08	0.59	1.40E-04
<i>RASGEF1B</i>	0.87	5.52E-06	0.58	1.23E-05
<i>MAFF</i>	1.38	1.65E-07	0.59	8.86E-05
<i>ANGPTL4</i>	0.48	3.73E-05	0.59	2.03E-04
<i>ABCA6</i>	0.56	4.18E-06	0.55	1.87E-07
<i>SOX4</i>	0.59	5.71E-04	0.54	5.38E-07
<i>KLHL24</i>	0.48	8.76E-08	0.51	5.97E-06
<i>ZNF493</i>	0.50	1.31E-04	0.51	1.06E-05
<i>FMO2</i>	0.55	2.45E-04	0.50	1.47E-06
<i>CASKIN2</i>	0.61	3.49E-06	0.51	3.22E-04
<i>KLF4</i>	0.98	1.62E-09	0.49	7.03E-05
<i>ZNF22</i>	0.39	7.10E-05	0.50	2.06E-04
<i>TMEM140</i>	1.10	6.47E-11	0.48	3.35E-05
<i>MS4A7</i>	0.88	8.97E-08	0.45	6.99E-05
<i>RASIP1</i>	0.49	1.41E-04	0.47	1.78E-04
<i>THBS2</i>	1.87	1.57E-13	0.45	2.45E-05
<i>CDKN1C</i>	0.81	2.85E-06	0.44	3.58E-05
<i>CBLB</i>	0.60	3.40E-08	0.47	9.36E-05
<i>HBP1</i>	0.28	9.57E-05	0.43	3.40E-05
<i>TLR4</i>	0.48	5.01E-09	0.43	6.55E-04
<i>TRIM66</i>	0.36	7.31E-04	0.42	2.14E-05
<i>SEMA6D</i>	0.41	4.35E-05	0.43	8.02E-05
<i>YPEL3</i>	0.53	4.38E-06	0.43	2.27E-04
<i>CRIM1</i>	0.51	4.71E-07	0.42	7.94E-05
<i>AGTR1</i>	0.56	5.82E-07	0.42	8.50E-05
<i>PTGER2</i>	0.66	6.82E-05	0.39	3.91E-04
<i>BTNL9</i>	0.89	2.17E-05	0.40	2.12E-05
<i>TCN2</i>	0.91	2.63E-09	0.38	1.34E-04
<i>SEMA3G</i>	0.97	3.97E-09	0.39	7.89E-06
<i>HIBCH</i>	0.44	8.95E-06	0.38	7.52E-05
<i>ORMDL3</i>	0.55	6.48E-04	0.37	4.80E-04
<i>NOVA1</i>	0.58	3.11E-05	0.37	4.48E-04
<i>SLC27A1</i>	1.58	1.39E-13	0.36	6.80E-04

Gene	SLR mouse	P val mouse	SLR human	P val human
<i>GAB2</i>	0.74	1.76E-10	0.36	2.04E-05
<i>APBB3</i>	0.42	7.20E-05	0.35	1.44E-04
<i>ABLIM1</i>	0.38	4.94E-05	0.34	3.24E-04
<i>RNF122</i>	0.91	4.94E-08	0.32	6.10E-04
<i>POSTN</i>	0.70	5.36E-07	0.31	1.46E-04
<i>TCF7L2</i>	0.60	1.19E-07	0.31	2.48E-05
<i>ST6GALNAC2</i>	0.57	1.12E-05	0.31	2.00E-04
<i>ZC3H6</i>	0.68	4.34E-06	0.29	8.86E-06
<i>EZH1</i>	0.30	4.04E-06	0.30	2.03E-06
<i>LDB2</i>	1.08	2.49E-10	0.31	6.74E-05
<i>ADCY4</i>	0.89	1.51E-08	0.29	1.52E-04
<i>CD300LG</i>	0.82	1.16E-10	0.28	6.10E-04
<i>YPEL2</i>	0.45	7.45E-05	0.28	1.64E-04
<i>RBP7</i>	3.16	2.81E-15	0.27	1.81E-04
<i>AHR</i>	0.33	2.77E-04	0.28	1.28E-05
<i>SHPRH</i>	0.32	6.33E-05	0.27	2.72E-06
<i>ANKRD28</i>	0.37	1.65E-05	0.25	7.45E-04
<i>UBE4B</i>	0.53	1.65E-08	0.27	3.13E-05
<i>JMY</i>	0.44	1.03E-05	0.27	8.45E-04
<i>MAST4</i>	0.34	4.97E-05	0.27	1.39E-04
<i>FLNB</i>	0.41	7.14E-05	0.27	7.26E-04
<i>PNRC1</i>	0.46	1.12E-07	0.25	6.40E-06
<i>ETFA</i>	0.25	8.24E-04	0.25	1.25E-04
<i>AKAP13</i>	0.76	5.64E-11	0.25	4.89E-04
<i>UHRF2</i>	0.32	8.64E-06	0.24	8.78E-04
<i>ALG13</i>	0.65	1.75E-04	0.23	5.09E-04
<i>AATF</i>	0.34	2.34E-05	0.24	5.20E-04
<i>GOLGB1</i>	0.30	2.18E-05	0.22	3.36E-04
<i>HERPUD2</i>	0.21	6.25E-04	0.23	3.08E-04
<i>COPS2</i>	0.49	3.81E-08	0.15	6.75E-04
<i>CAT</i>	0.46	4.74E-08	0.13	4.52E-04

Supplemental table 5. List of genes in fig 6b

Gene	SLR mouse	P val mouse	SLR human	P val human
<i>PNPLA3</i>	-3.82	2.04E-10	-2.22	3.48E-07
<i>SREBF1</i>	-2.07	4.36E-12	-1.87	4.37E-09
<i>DGAT2</i>	-2.39	1.33E-11	-1.36	2.46E-07
<i>ELOVL6</i>	-1.50	6.40E-08	-1.30	2.62E-05
<i>HK2</i>	-1.11	2.88E-10	-1.29	5.42E-06
<i>DLAT</i>	-0.62	1.32E-08	-1.23	1.14E-10
<i>EPHB2</i>	-1.46	2.23E-07	-1.18	7.88E-09
<i>AACS</i>	-0.63	1.41E-04	-1.19	1.57E-07
<i>ANGPT2</i>	-0.92	4.58E-07	-1.10	2.71E-04
<i>ACLY</i>	-1.94	9.17E-10	-1.03	6.95E-07
<i>C8orf34</i>	-0.93	5.95E-09	-0.98	3.32E-08
<i>LAIR1</i>	-0.63	6.68E-06	-0.99	1.57E-05
<i>CD248</i>	-0.65	1.85E-06	-0.95	1.73E-09
<i>PSAT1</i>	-1.12	3.64E-11	-0.91	4.39E-06
<i>INSIG1</i>	-1.78	1.96E-12	-0.88	3.49E-07
<i>LDLR</i>	-1.73	1.48E-07	-0.86	3.21E-05
<i>THRSP</i>	-2.39	7.22E-09	-0.88	1.34E-07
<i>CEBPA</i>	-0.39	2.47E-06	-0.87	1.81E-05
<i>ABCD2</i>	-0.63	1.13E-10	-0.85	8.16E-07
<i>CDKN2C</i>	-1.83	8.40E-13	-0.81	4.31E-08
<i>LGALS12</i>	-1.06	1.97E-09	-0.79	2.36E-06
<i>ZNF703</i>	-0.33	4.33E-04	-0.77	2.31E-07
<i>B4GALT6</i>	-0.46	1.85E-04	-0.76	1.22E-06
<i>LBP</i>	-0.96	2.36E-05	-0.73	4.15E-06
<i>STC2</i>	-0.67	7.65E-05	-0.75	1.06E-05
<i>AGPAT2</i>	-1.22	9.76E-10	-0.72	6.09E-09
<i>HMBS</i>	-0.80	1.57E-09	-0.72	7.47E-05
<i>PPIL1</i>	-0.64	8.86E-05	-0.69	2.61E-05
<i>SFRP2</i>	-0.47	5.42E-04	-0.66	3.96E-07
<i>RTN4RL1</i>	-1.40	1.96E-09	-0.69	1.65E-04
<i>AKR1C3</i>	-0.72	5.28E-04	-0.68	3.43E-06
<i>ACACA</i>	-0.88	3.15E-06	-0.66	7.51E-07
<i>TOMM40L</i>	-0.50	7.20E-05	-0.65	1.57E-04
<i>SLC25A10</i>	-2.66	3.44E-14	-0.64	2.22E-07
<i>AQP11</i>	-0.78	2.77E-06	-0.63	2.39E-04
<i>C14orf180</i>	-1.99	4.87E-13	-0.62	2.61E-07
<i>MVK</i>	-0.85	1.00E-08	-0.62	2.01E-05
<i>MVD</i>	-0.69	2.26E-06	-0.60	2.36E-05
<i>VLDLR</i>	-0.61	2.64E-08	-0.63	6.17E-06
<i>BCL9L</i>	-0.41	2.11E-04	-0.62	1.39E-05
<i>SLC16A7</i>	-1.04	7.92E-12	-0.62	1.39E-06
<i>NPR3</i>	-1.23	5.72E-06	-0.63	1.56E-05
<i>HOXC8</i>	-0.39	4.18E-05	-0.59	1.16E-06
<i>NNAT</i>	-1.28	6.66E-11	-0.60	1.75E-06
<i>OSGIN1</i>	-0.58	5.86E-06	-0.56	1.77E-04
<i>ECHDC1</i>	-0.65	2.32E-06	-0.60	3.01E-07

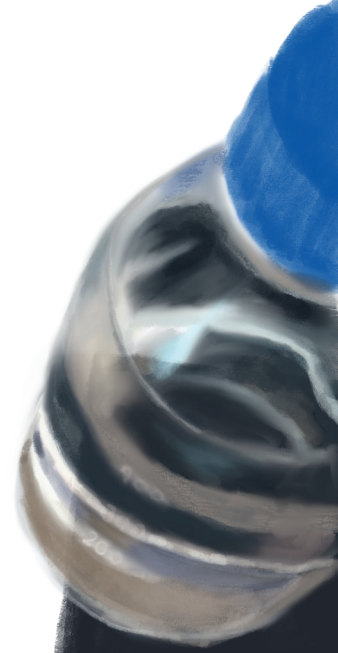
Gene	SLR mouse	P val mouse	SLR human	P val human
<i>ABCB6</i>	-0.40	9.43E-05	-0.57	2.36E-05
<i>CCND2</i>	-0.89	2.37E-09	-0.58	4.00E-07
<i>LETM1</i>	-0.50	1.81E-07	-0.57	1.55E-06
<i>TUBG1</i>	-0.48	4.21E-05	-0.55	3.58E-07
<i>DHCR24</i>	-1.17	1.68E-07	-0.58	3.58E-06
<i>HSPA12A</i>	-0.78	1.36E-09	-0.59	2.60E-05
<i>COL15A1</i>	-2.12	1.12E-10	-0.57	5.85E-07
<i>LSM10</i>	-0.68	2.07E-08	-0.55	7.93E-04
<i>COL3A1</i>	-0.76	3.84E-07	-0.57	1.10E-05
<i>MID1IP1</i>	-1.19	9.27E-10	-0.53	3.14E-05
<i>NLN</i>	-0.39	4.13E-06	-0.55	1.33E-05
<i>SLC2A4</i>	-1.84	1.32E-13	-0.55	7.01E-06
<i>FKBP14</i>	-0.68	6.33E-08	-0.54	4.38E-05
<i>SERPINH1</i>	-0.95	2.01E-08	-0.52	1.31E-04
<i>ACBD4</i>	-0.41	2.45E-04	-0.53	3.39E-05
<i>IDH2</i>	-0.51	1.06E-07	-0.51	1.39E-07
<i>RBPMS2</i>	-0.67	5.13E-08	-0.51	3.12E-05
<i>NAV3</i>	-0.76	3.82E-07	-0.52	4.08E-05
<i>SLC35B4</i>	-0.53	4.99E-07	-0.53	2.70E-06
<i>FASN</i>	-2.25	5.68E-09	-0.52	1.34E-08
<i>CXXC5</i>	-0.64	1.73E-05	-0.52	4.27E-05
<i>TESK1</i>	-0.44	1.09E-05	-0.50	8.89E-10
<i>CAV2</i>	-0.94	1.61E-11	-0.50	1.11E-07
<i>SUOX</i>	-0.45	6.04E-05	-0.50	1.28E-04
<i>MOGAT2</i>	-0.95	5.55E-05	-0.48	8.75E-04
<i>LEP</i>	-1.88	2.34E-05	-0.50	2.43E-06
<i>FZD5</i>	-0.45	9.14E-04	-0.49	4.36E-04
<i>YWHAG</i>	-0.77	1.07E-11	-0.48	2.32E-06
<i>SLC24A3</i>	-0.82	2.16E-08	-0.48	2.07E-05
<i>PSMD14</i>	-0.31	3.48E-05	-0.46	3.23E-06
<i>MRAP</i>	-0.58	2.83E-07	-0.45	4.61E-04
<i>DBI</i>	-0.34	1.66E-06	-0.46	5.01E-05
<i>COL5A3</i>	-0.80	9.86E-06	-0.45	3.37E-04
<i>DOLPP1</i>	-0.74	6.57E-08	-0.44	2.46E-04
<i>SNTB1</i>	-0.30	2.23E-04	-0.45	1.24E-04
<i>TMEM135</i>	-0.91	1.40E-11	-0.44	9.20E-06
<i>MMD</i>	-1.08	1.68E-13	-0.44	4.97E-07
<i>DHCR7</i>	-1.27	4.23E-10	-0.41	7.30E-05
<i>CSPG4</i>	-0.97	4.32E-07	-0.42	7.21E-05
<i>IDH1</i>	-1.38	2.63E-13	-0.43	3.74E-04
<i>MRPL12</i>	-0.54	5.22E-07	-0.43	2.33E-04
<i>CY5B</i>	-1.36	6.69E-12	-0.41	5.46E-06
<i>SLC7A10</i>	-0.64	3.28E-08	-0.39	6.13E-04
<i>TKT</i>	-0.68	7.78E-05	-0.40	1.51E-05
<i>STK40</i>	-0.46	3.27E-04	-0.39	4.59E-06
<i>CHCHD3</i>	-0.33	1.55E-05	-0.37	6.64E-04
<i>IRAK1</i>	-0.26	5.04E-04	-0.38	6.08E-04

Gene	SLR mouse	P val mouse	SLR human	P val human
<i>SLC25A11</i>	-0.50	2.89E-08	-0.38	5.13E-06
<i>IDI1</i>	-0.71	2.78E-06	-0.40	4.49E-04
<i>COL5A1</i>	-0.80	3.92E-07	-0.39	1.83E-04
<i>PCYT2</i>	-0.56	7.69E-08	-0.39	2.71E-04
<i>ADCY6</i>	-0.50	4.99E-08	-0.40	9.10E-05
<i>SMG5</i>	-0.35	1.14E-04	-0.38	3.67E-04
<i>GFM1</i>	-0.48	1.61E-06	-0.39	1.41E-04
<i>LZTS2</i>	-0.42	5.85E-06	-0.37	2.15E-04
<i>RAB32</i>	-0.73	1.21E-09	-0.37	5.61E-04
<i>MAGED1</i>	-0.80	2.29E-10	-0.38	6.57E-05
<i>SNAPC5</i>	-0.58	8.15E-06	-0.36	6.73E-04
<i>CBX5</i>	-0.35	1.41E-05	-0.37	1.25E-04
<i>TMEM126A</i>	-0.51	3.52E-06	-0.35	6.12E-04
<i>SLC25A1</i>	-1.23	1.35E-09	-0.35	5.99E-05
<i>TRIM35</i>	-0.23	9.11E-04	-0.35	6.33E-04
<i>PRKACA</i>	-0.96	8.51E-11	-0.35	2.56E-06
<i>FASTK</i>	-0.43	1.21E-05	-0.34	4.74E-04
<i>PIGS</i>	-0.33	3.14E-04	-0.35	3.02E-04
<i>NAT8L</i>	-0.88	2.75E-05	-0.35	5.17E-05
<i>LPGAT1</i>	-1.41	7.73E-11	-0.35	5.82E-05
<i>PDHA1</i>	-0.47	6.05E-06	-0.35	3.61E-05
<i>ISOC1</i>	-1.03	8.70E-11	-0.34	1.45E-04
<i>YKT6</i>	-0.49	3.75E-07	-0.33	2.38E-06
<i>TGFBRAP1</i>	-0.21	7.38E-04	-0.34	5.69E-05
<i>CNTFR</i>	-0.89	4.50E-05	-0.33	2.19E-04
<i>CYC1</i>	-0.52	6.31E-07	-0.32	6.59E-05
<i>CDR2</i>	-0.67	4.90E-06	-0.32	9.79E-04
<i>DEGS1</i>	-0.38	1.42E-04	-0.33	6.51E-05
<i>EIF4G1</i>	-0.32	3.34E-06	-0.33	2.30E-05
<i>KIAA0232</i>	-0.96	1.90E-11	-0.32	6.31E-05
<i>TANC2</i>	-0.32	5.59E-04	-0.34	8.14E-04
<i>LRIG1</i>	-0.71	1.50E-07	-0.33	5.87E-04
<i>ITGA7</i>	-0.64	4.31E-06	-0.32	1.79E-05
<i>PAPSS1</i>	-0.56	1.54E-07	-0.33	7.13E-04
<i>ATP2B4</i>	-0.94	1.16E-10	-0.31	1.13E-05
<i>PANK3</i>	-1.21	5.60E-13	-0.31	2.99E-05
<i>SEC23A</i>	-0.27	2.53E-05	-0.31	3.26E-06
<i>SNTA1</i>	-0.55	3.48E-04	-0.30	2.24E-04
<i>ELMO2</i>	-0.45	8.92E-08	-0.31	2.57E-04
<i>PLEKHJ1</i>	-0.31	9.37E-04	-0.29	7.12E-04
<i>MGLL</i>	-0.36	4.38E-06	-0.31	3.58E-04
<i>STAT5A</i>	-0.55	3.61E-05	-0.31	7.03E-04
<i>NFIC</i>	-0.81	3.71E-08	-0.31	5.11E-05
<i>MME</i>	-0.39	2.61E-05	-0.31	1.93E-04
<i>DHRS3</i>	-0.29	5.63E-04	-0.30	5.30E-05
<i>FZD4</i>	-1.05	5.98E-11	-0.29	1.14E-04
<i>COQ9</i>	-0.43	8.41E-06	-0.28	1.17E-04

Gene	SLR mouse	P val mouse	SLR human	P val human
<i>KPNA4</i>	-0.35	1.64E-06	-0.28	3.90E-05
<i>STK39</i>	-0.34	5.01E-04	-0.29	3.98E-05
<i>GALNT2</i>	-0.42	7.16E-05	-0.28	2.37E-04
<i>PFKFB1</i>	-0.90	4.33E-07	-0.28	7.96E-04
<i>NNT</i>	-0.30	1.72E-04	-0.29	9.51E-04
<i>SEC61B</i>	-0.77	2.20E-04	-0.28	5.93E-04
<i>DAAM1</i>	-0.90	3.27E-10	-0.26	4.55E-04
<i>CS</i>	-0.62	1.60E-07	-0.26	1.13E-04
<i>PPP1CA</i>	-0.22	1.08E-04	-0.25	3.60E-04
<i>MRPS7</i>	-0.33	2.83E-04	-0.25	5.74E-05
<i>PSMD1</i>	-0.33	7.56E-05	-0.26	3.88E-04
<i>ALDH4A1</i>	-0.84	3.64E-07	-0.26	5.52E-04
<i>OPA1</i>	-0.30	6.76E-04	-0.24	1.64E-04
<i>UBE2E2</i>	-0.27	4.06E-04	-0.25	1.32E-04
<i>NDUFA9</i>	-0.33	7.21E-05	-0.24	9.77E-04
<i>KDELR2</i>	-0.23	9.75E-04	-0.24	7.63E-06
<i>GBE1</i>	-0.48	6.71E-06	-0.25	1.80E-04
<i>SDHB</i>	-0.29	9.18E-04	-0.23	6.06E-04
<i>HDHD2</i>	-0.37	9.25E-06	-0.24	8.56E-04
<i>NUDT5</i>	-0.76	1.19E-08	-0.24	1.62E-04
<i>AP3D1</i>	-0.21	8.18E-04	-0.22	4.25E-05
<i>CAV1</i>	-0.76	1.93E-12	-0.22	7.39E-05
<i>COPS3</i>	-0.28	4.31E-04	-0.22	8.64E-04
<i>PGM1</i>	-0.85	8.42E-11	-0.21	4.68E-04
<i>TAOK1</i>	-0.30	2.54E-06	-0.21	4.24E-04
<i>ANXA1</i>	-0.43	1.28E-05	-0.20	3.69E-05
<i>VCL</i>	-0.52	2.35E-08	-0.19	2.97E-04
<i>MLX</i>	-0.52	8.71E-06	-0.19	3.69E-04
<i>ANXA6</i>	-0.49	6.92E-06	-0.19	8.79E-04
<i>MCAM</i>	-0.44	9.61E-08	-0.18	3.45E-04
<i>POMP</i>	-0.38	4.09E-04	-0.16	4.89E-04
<i>SUCLG1</i>	-0.34	2.84E-05	-0.17	9.00E-04
<i>COPB2</i>	-0.18	5.67E-04	-0.15	8.54E-04
<i>CAT</i>	0.46	4.74E-08	0.13	4.52E-04
<i>COPS2</i>	0.49	3.81E-08	0.15	6.75E-04
<i>HERPUD2</i>	0.21	6.25E-04	0.23	3.08E-04
<i>GOLGB1</i>	0.30	2.18E-05	0.22	3.36E-04
<i>AATF</i>	0.34	2.34E-05	0.24	5.20E-04
<i>ALG13</i>	0.65	1.75E-04	0.23	5.09E-04
<i>UHRF2</i>	0.32	8.64E-06	0.24	8.78E-04
<i>AKAP13</i>	0.76	5.64E-11	0.25	4.89E-04
<i>ETFA</i>	0.25	8.24E-04	0.25	1.25E-04
<i>PNRC1</i>	0.46	1.12E-07	0.25	6.40E-06
<i>FLNB</i>	0.41	7.14E-05	0.27	7.26E-04
<i>MAST4</i>	0.34	4.97E-05	0.27	1.39E-04
<i>JMY</i>	0.44	1.03E-05	0.27	8.45E-04
<i>UBE4B</i>	0.53	1.65E-08	0.27	3.13E-05

Gene	SLR mouse	P val mouse	SLR human	P val human
<i>ANKRD28</i>	0.37	1.65E-05	0.25	7.45E-04
<i>SHPRH</i>	0.32	6.33E-05	0.27	2.72E-06
<i>AHR</i>	0.33	2.77E-04	0.28	1.28E-05
<i>RBP7</i>	3.16	2.81E-15	0.27	1.81E-04
<i>YPEL2</i>	0.45	7.45E-05	0.28	1.64E-04
<i>CD300LG</i>	0.82	1.16E-10	0.28	6.10E-04
<i>ADCY4</i>	0.89	1.51E-08	0.29	1.52E-04
<i>LDB2</i>	1.08	2.49E-10	0.31	6.74E-05
<i>EZH1</i>	0.30	4.04E-06	0.30	2.03E-06
<i>ZC3H6</i>	0.68	4.34E-06	0.29	8.86E-06
<i>ST6GALNAC2</i>	0.57	1.12E-05	0.31	2.00E-04
<i>TCF7L2</i>	0.60	1.19E-07	0.31	2.48E-05
<i>POSTN</i>	0.70	5.36E-07	0.31	1.46E-04
<i>RNF122</i>	0.91	4.94E-08	0.32	6.10E-04
<i>ABLIM1</i>	0.38	4.94E-05	0.34	3.24E-04
<i>APBB3</i>	0.42	7.20E-05	0.35	1.44E-04
<i>GAB2</i>	0.74	1.76E-10	0.36	2.04E-05
<i>SLC27A1</i>	1.58	1.39E-13	0.36	6.80E-04
<i>NOVA1</i>	0.58	3.11E-05	0.37	4.48E-04
<i>ORMDL3</i>	0.55	6.48E-04	0.37	4.80E-04
<i>HIBCH</i>	0.44	8.95E-06	0.38	7.52E-05
<i>SEMA3G</i>	0.97	3.97E-09	0.39	7.89E-06
<i>TCN2</i>	0.91	2.63E-09	0.38	1.34E-04
<i>BTNL9</i>	0.89	2.17E-05	0.40	2.12E-05
<i>PTGER2</i>	0.66	6.82E-05	0.39	3.91E-04
<i>AGTR1</i>	0.56	5.82E-07	0.42	8.50E-05
<i>CRIM1</i>	0.51	4.71E-07	0.42	7.94E-05
<i>YPEL3</i>	0.53	4.38E-06	0.43	2.27E-04
<i>SEMA6D</i>	0.41	4.35E-05	0.43	8.02E-05
<i>TRIM66</i>	0.36	7.31E-04	0.42	2.14E-05
<i>TLR4</i>	0.48	5.01E-09	0.43	6.55E-04
<i>HBP1</i>	0.28	9.57E-05	0.43	3.40E-05
<i>CBLB</i>	0.60	3.40E-08	0.47	9.36E-05
<i>CDKN1C</i>	0.81	2.85E-06	0.44	3.58E-05
<i>THBS2</i>	1.87	1.57E-13	0.45	2.45E-05
<i>RASIP1</i>	0.49	1.41E-04	0.47	1.78E-04
<i>MS4A7</i>	0.88	8.97E-08	0.45	6.99E-05
<i>TMEM140</i>	1.10	6.47E-11	0.48	3.35E-05
<i>ZNF22</i>	0.39	7.10E-05	0.50	2.06E-04
<i>KLF4</i>	0.98	1.62E-09	0.49	7.03E-05
<i>CASKIN2</i>	0.61	3.49E-06	0.51	3.22E-04
<i>FMO2</i>	0.55	2.45E-04	0.50	1.47E-06
<i>ZNF493</i>	0.50	1.31E-04	0.51	1.06E-05
<i>KLHL24</i>	0.48	8.76E-08	0.51	5.97E-06
<i>SOX4</i>	0.59	5.71E-04	0.54	5.38E-07
<i>ABCA6</i>	0.56	4.18E-06	0.55	1.87E-07
<i>ANGPTL4</i>	0.48	3.73E-05	0.59	2.03E-04

Gene	SLR mouse	P val mouse	SLR human	P val human
<i>MAFF</i>	1.38	1.65E-07	0.59	8.86E-05
<i>RASGEF1B</i>	0.87	5.52E-06	0.58	1.23E-05
<i>SEMA3F</i>	0.89	2.00E-08	0.59	1.40E-04
<i>IRAK2</i>	0.99	3.19E-09	0.62	2.63E-04
<i>NDRG1</i>	0.32	9.20E-04	0.61	4.98E-09
<i>LHX6</i>	0.47	2.12E-04	0.60	4.14E-06
<i>ADRB2</i>	1.51	1.36E-07	0.64	1.24E-07
<i>CA4</i>	1.39	2.63E-11	0.66	3.86E-08
<i>PNPLA7</i>	1.97	1.90E-15	0.72	1.79E-06
<i>GABARAPL1</i>	1.13	3.68E-09	0.75	9.73E-08
<i>CAB39L</i>	0.59	1.00E-08	0.77	6.77E-06
<i>FBXO32</i>	0.79	2.31E-07	0.76	3.24E-07
<i>TXNIP</i>	0.53	9.58E-09	0.78	3.85E-05
<i>THBS1</i>	1.04	3.58E-04	0.98	8.84E-04
<i>IRS2</i>	0.86	4.36E-09	1.07	2.16E-08
<i>PDK4</i>	3.38	1.03E-20	1.44	1.31E-07



CHAPTER 6

AT

Probing metabolic memory in the hepatic response to fasting

Merel Defour, Guido J.E.J. Hooiveld, Michel van Weeghel, Sander Kersten

ABSTRACT

Tissues may respond differently to a particular stimulus if they have been previously exposed to that same stimulus. Here we tested the hypothesis that a strong metabolic stimulus such as fasting may influence the hepatic response to a subsequent fast and thus elicit a memory effect. Overnight fasting in mice significantly increased plasma free fatty acids, glycerol, β -hydroxybutyrate and liver triglycerides, and decreased plasma glucose, plasma triglycerides, and liver glycogen levels. In addition, fasting dramatically changed the liver transcriptome, upregulating genes involved in gluconeogenesis and in uptake, oxidation, storage, and mobilization of fatty acids, and downregulating genes involved in fatty acid synthesis, fatty acid elongation/desaturation, and cholesterol synthesis. Fasting also markedly impacted the liver metabolome, causing a decrease in the levels of numerous amino acids, glycolytic intermediated, TCA cycle intermediates, and nucleotides. However, these fasting-induced changes were unaffected by two previous overnight fasts. Also, no significant effect was observed of prior fasting on glucose tolerance. Finally, analysis of the effect of fasting on the transcriptome in hepatocyte humanized mouse livers indicated modest similarity in gene regulation in mouse and human liver cells. In general, genes involved in metabolic pathways were up- or downregulated to a lesser extent in human liver cells than mouse liver cells. In conclusion, we found that previous exposure to fasting in mice did not influence the hepatic response to a subsequent fast, arguing against the concept of metabolic memory in the liver. Our data provide a useful resource for the study of liver metabolism during fasting.

INTRODUCTION

Throughout human history, probably the greatest threats to survival were long periods of food deprivation. Consequently, starvation has been an important evolutionary pressure shaping human energy metabolism. The key design features of human energy metabolism were highly beneficial to our ancestors, allowing them to survive long periods with insufficient caloric intake [1]. In a modern world of excess calories, however, the adaptive mechanisms for surviving prolonged fasting contribute to an unprecedented growth in obesity and its related co-morbidities. Better understanding of the underlying principles and mechanisms driving the adaptive response to fasting should be valuable in the design of new therapeutic strategies for metabolic diseases.

Two organs that play a central role in the metabolic response to fasting are adipose tissue and the liver [2]. The adipose tissue is the body's energy depot and releases fatty acids to be used as fuel by other tissues [2]. The liver serves as a true metabolic hub during fasting and is the recipient of a major share of the fatty acids released by the adipose tissue. The incoming fatty acids are oxidized, metabolized into ketone bodies, or converted back into triglycerides to be stored and secreted [3]. In addition, the liver carries out gluconeogenesis from amino acids and other substrates to maintain blood glucose levels when glucose absorption from the intestine is non-existent [4,5]. Via its exclusive ability to produce glucose and ketone bodies, the liver ensures that the energy needs of the metabolically active brain is met, which unlike other tissues and organs is unable to utilize fatty acids as fuel [6].

The adaptive response of the liver to fasting is driven by changes in blood levels of key metabolic hormones, such as insulin and glucagon, and is effectuated by changes in enzyme activity through regulation at the transcriptional, translational, and post-translational level. Perhaps the most important regulatory mechanism in the adaptive response to fasting is via changes in gene transcription. Indeed, fasting triggers profound changes in the hepatic expression of numerous genes involved in glucose and lipid metabolism [7,8]. Important transcription factors and transcriptional co-activators involved in the adaptive response to changes in fasting in liver are PPAR α , Foxo1, CREB3L3, GR, CREB, PGC1alpha and TFEB [3,9–11].

We posed the question whether the response of the liver to fasting may depend on previous exposure to fasting, reflecting a metabolic memory. Currently, there is no evidence to support this notion. However, this possibility isn't completely remote. Indeed, it has been shown that macrophages respond differently after a second stimulation with an inflammatory component such as LPS. These data indicate that macrophages show a memory to an inflammatory stimulus, a phenomenon referred to as innate memory [12]. Evidence has been presented that innate memory is at least partly mediated via changes in intracellular metabolism and metabolites

triggered by the inflammatory stimulus, which leave a lasting mark on the cells via epigenetic mechanisms such as histone acetylation [13,14]. Borrowing from this concept, we hypothesized that a strong metabolic stressor may also leave a lasting mark and elicit some form of metabolic memory in the liver.

Hence, the aim of this study was to explore the evidence for metabolic memory in response to a strong metabolic stressor such as fasting. As the liver coordinates the metabolic response to fasting, we focused our studies on the liver.

METHODS

Animals

The mice included in the fasting studies described below were male wildtype mice. The mice were bred and maintained in the same facility for more than 20 generations. During the intervention the mice were individually housed at 21-22°C under specific pathogen-free conditions and followed a 6:00-18:00 day-night cycle. Mice were fed a standard chow diet after weaning. At the end of the studies, mice were euthanized between 8.30 – 10.00 in the morning. The mice were first anesthetized with a mixture of isoflurane (1.5%), nitrous oxide (70%), and oxygen (30%), followed by collection of blood by eye extraction into EDTA tubes. Mice were euthanized by cervical dislocation, after which tissues were excised and snap frozen in liquid nitrogen.

The animal studies were all carried out at the Centre for Small Animals, which is part of the Centralized Facilities for Animal Research at Wageningen University and Research (CARUS), and were approved by the Local Animal Ethics Committee of Wageningen University (2016.W-0093.011).

Fasting intervention

Eleven 3-4 month-old mice on a Sv129 background were euthanized after fasting for 24 hours. Twelve mice were euthanized in the ab-libitum fed state. During fasting, the mice had free access to water.

Repeated fasting intervention.

Forty-eight C57BL/6 mice were included in the study, and randomly divided over 4 groups of 12 mice each. The mice in the group Fed-Fed-Fed were fed ab-libitum throughout the study. The mice in the group Fed-Fed-Fast underwent a single 16h fast immediately prior to euthanasia. The mice in the group Fast-Fast-Fed underwent two prior 16h fasts with an interval of 18 days and were euthanized in the ad-libitum fed state. The mice in the group Fast-Fast-Fast underwent two prior 16h fasts with an interval of 18 days and underwent an additional 16h fast immediately prior to euthanasia. The growth curves and food intake of the mice

were monitored closely, starting shortly after weaning. The second and third fasting intervention was performed when all mice were back at their regular growth curves for several days. In between the fasting episodes, the mice had ad-libitum access to food and water. During fasting, the mice had free access to water.

Intraperitoneal glucose tolerance test.

One week before euthanasia, the mice were fasted for 5 h followed by a glucose tolerance test. The mice were injected intraperitoneally with glucose (1 g/kg body weight) (Baxter, Deerfield, IL). Blood samples from tail vein bleeding were tested for glucose levels at different time points after glucose injection using a GLUCOFIX Tech glucometer and glucose sensor test strips (Menarini Diagnostics, Valkenswaard, The Netherlands).

Quantification of plasma parameters

Blood samples were collected into EDTA-coated tubes and centrifuged at 4°C for 15 min at 12,000 g. Plasma was collected and stored at -80°C.

Plasma concentrations of glucose (Sopachem, Ochten, the Netherlands), triglycerides (TG), cholesterol (Instruchemie, Delfzijl, the Netherlands), glycerol (Sigma-Aldrich, Houten, the Netherlands) and free fatty acids (Wako Chemicals, Neuss, Germany; HR(2) Kit) were determined according to manufacturers' instructions.

Liver glycogen and triglycerides

For measurement of liver glycogen, liver pieces were dissolved in 10 volumes of 1 M NaOH and incubated at 55 °C. After 1-2 hours an equal volume of 1 M HCl was added, followed by centrifugation for 5 min at 3000 rpm. Subsequently, 5 µL of supernatant was added to 50 µL of amyloglucosidase (1000 U/ml in 0.2 M sodium acetate buffer pH 4.8) and incubated for 2 hours with shaking (700 rpm) at 42 °C. After short centrifugation, glucose was measured using glucose assay (Sopachem, Ochten, the Netherlands).

Liver pieces of ~50 mg were homogenized to a 5% lysate (m/v) using 10 mM Tris, 2 mM EDTA, 0.25 M sucrose, pH 7.5. Homogenates were assayed for triglycerides using a kit for triglycerides (Instruchemie, Delfzijl, the Netherlands).

Histology

Liver tissues were snap frozen or fresh tissues were collected in 4% paraformaldehyde, dehydrated and embedded in paraffin. Thin sections of the samples were made at 5 µm using a microtome and placed onto glass slides followed by overnight incubation at 37°C. The tissues were stained in Mayer hematoxylin solution for 10 min and in

eosin for 10 s at room temperature with intermediate washings in ethanol. The tissues were allowed to dry at room temperature followed by imaging using a light microscope.

RNA isolation and microarray analysis

Microarray analysis was performed on liver samples from 4-5 mice per group for the fasting intervention and 7-8 mice per group for the repeated fasting intervention. Total RNA was extracted from liver tissues using TRIzol reagent (Life Technologies, Bleiswijk, The Netherlands). Next, total RNA was isolated using the RNeasy Micro kit from Qiagen (Venlo, The Netherlands).

RNA integrity was verified with RNA 6000 Nano chips on an Agilent 2100 bioanalyzer (Agilent Technologies, Amsterdam, The Netherlands). Purified RNA (100 ng) was labeled with the Ambion WT expression kit (Carlsbad, CA) and hybridized to Affymetrix mouse NuGO arrays (NuGO_Mm1a520177) or an Affymetrix Mouse Gene 2.1 ST array plate (Affymetrix, Santa Clara, CA). Hybridization, washing, and scanning were carried out on an Affymetrix GeneTitan platform according to the manufacturer's instructions. Probe sets were defined according to Dai et al. [15]. In this method, probes are assigned to Entrez IDs as a unique gene identifier. P values were calculated using an Intensity-Based Moderated T-statistic (IBMT). Genes were defined as significantly changed when $P < 0.001$. Alternatively, an FDR value was calculated as the measure of significance for the false discovery rate. An FDR value < 0.05 was considered statistically significant. To identify the pathways significantly altered by 16h fasting, Ingenuity Pathway Analysis (Ingenuity Systems, Redwood City, CA) was performed. Input criteria were a relative fold change equal to or above 1.5 and a P value equal to or below 0.001. In addition, we used gene set enrichment analysis (GSEA) to identify gene sets that were enriched among the genes upregulated or downregulated by 16h fasting. Array data have been submitted to the Gene Expression Omnibus under accession number (GSE156254, GSE17863).

For the fasting study in hepatocyte humanized mice, RNAseq data available via Gene Expression Omnibus were processed and mapped to the human and mouse genome (GSE126587). A common gene list of 9545 genes was generated.

Metabolomics

Metabolomics was performed as previously described, with minor adjustments [16]. A 75 μL mixture of the following internal standards in water was added to each sample: adenosine-15N5-monophosphate (100 μM), adenosine-15N5-triphosphate (1 mM), D4-alanine (100 μM), D7-arginine (100 μM), D3-aspartic acid (100 μM), D3-carnitine (100 μM), D4-citric acid (100 μM), 13C1-citrulline (100 μM), 13C6-fructose-

1,6-diphosphate (100 μ M), guanosine-15N5-monophosphate (100 μ M), guanosine-15N5-triphosphate (1 mM), 13C6-glucose (1 mM), 13C6-glucose-6-phosphate (100 μ M), D3-glutamic acid (100 μ M), D5-glutamine (100 μ M), 13C6-isoleucine (100 μ M), D3-leucine (100 μ M), D4-lysine (100 μ M), D3-methionine (100 μ M), D6-ornithine (100 μ M), D5-phenylalanine (100 μ M), D7-proline (100 μ M), 13C3-pyruvate (100 μ M), D3-serine (100 μ M), D5-tryptophan (100 μ M), D4-tyrosine (100 μ M), D8-valine (100 μ M). Subsequently, 425 μ L water, 500 μ L methanol and 1 mL chloroform were added to the same 2 mL tube before thorough mixing and centrifugation for 10 min at 14,000 rpm. The top layer, containing the polar phase, was transferred to a new 1.5 mL tube and dried using a vacuum concentrator at 60°C. Dried samples were reconstituted in 100 μ L methanol/water (6/4; v/v). Metabolites were analyzed using a Waters Acquity ultra-high-performance liquid chromatography system coupled to a Bruker Impact II™ Ultra-High Resolution Qq-Time-Of-Flight mass spectrometer. Samples were kept at 12°C during analysis and 5 μ L of each sample was injected. Chromatographic separation was achieved using a Merck Millipore SeQuant ZIC-CHILIC column (PEEK 100 x 2.1 mm, 3 μ m particle size). Column temperature was held at 30°C. Mobile phase consisted of (A) 1:9 acetonitrile:water and (B) 9:1 acetonitrile:water, both containing 5 mM ammonium acetate. Using a flow rate of 0.25 mL/min, the LC gradient consisted of: 100% B for 0-2 min, ramp to 0% B at 28 min, 0% B for 28-30 min, ramp to 100% B at 31 min, 100% B for 31-35 min. MS data were acquired using negative and positive ionization in full scan mode over the range of m/z 50-1200. Data were analyzed using Bruker TASQ software version 2.1.22.3. All reported metabolite intensities were normalized to internal standards with comparable retention times and response in the MS. Metabolite identification has been based on a combination of accurate mass, (relative) retention times and fragmentation spectra, compared to the analysis of a library of standards.

Statistical analysis

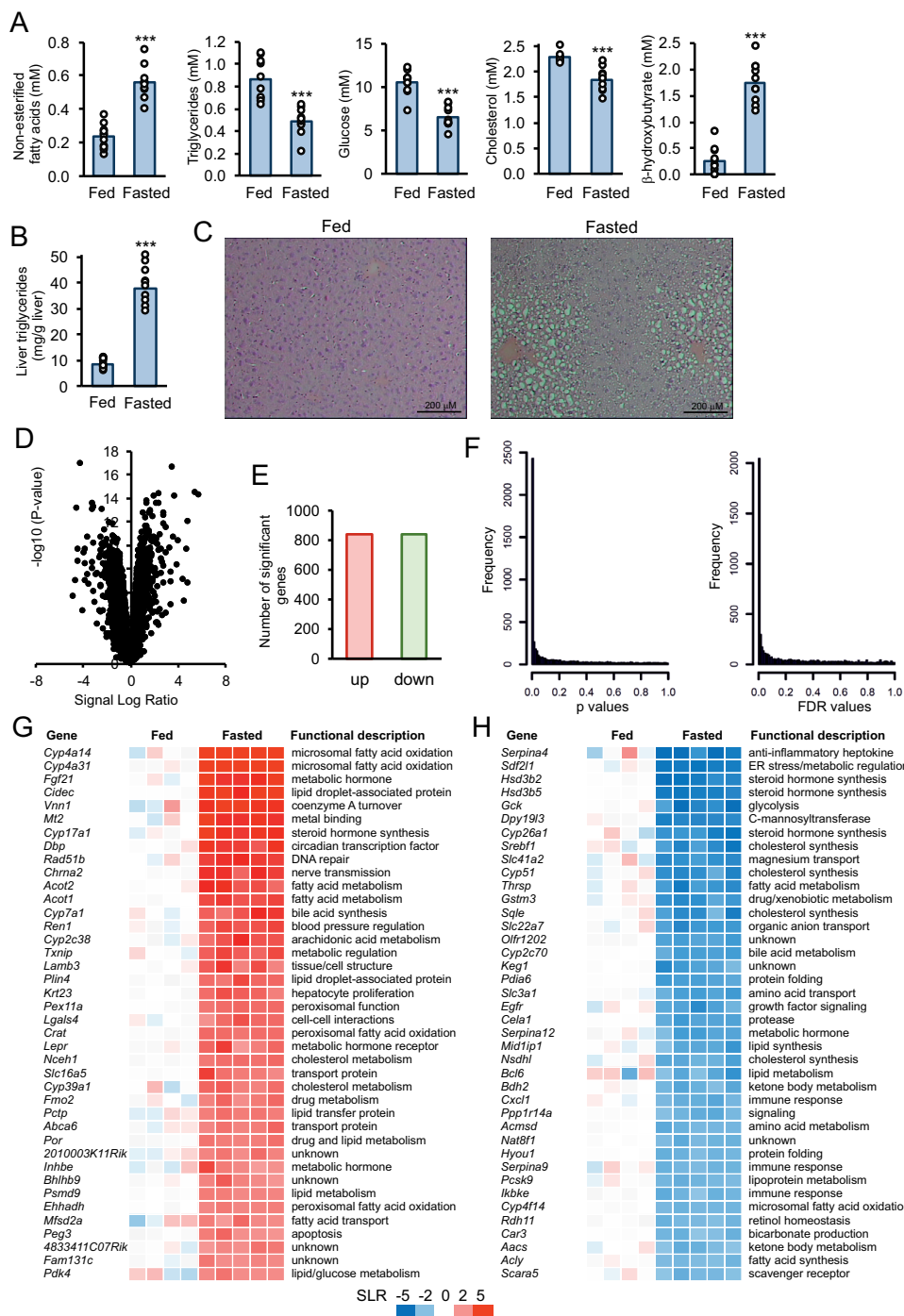
Data are presented as mean \pm SEM. Statistical analysis was performed by two-way ANOVA followed by Tukey's post hoc multiple comparison test. Comparisons between two groups were made using two-tailed Student's *t*-test. $P < 0.05$ was considered as statistically significant. SPSS software (version 21; SPSS Inc., Chicago, IL) was used for statistical analysis.

RESULTS

We first studied the effect of a single overnight fast on metabolic parameters and the liver transcriptome. Compared to ad libitum fed mice, fasting led to significant increases in plasma levels of non-esterified fatty acids and β -hydroxybutyrate, and significant decreases in plasma glucose, triglycerides, and cholesterol (Figure 1A). Fasting also caused a significant 4-fold increase in liver triglycerides (Figure 1B). The excess lipid storage lipid was mainly seen in the periportal area (Figure 1C). According to transcriptome analysis performed on 4-5 mice per group, fasting led to major changes in hepatic gene expression, as shown by Volcano plot (Figure 1D). Using a statistical significance threshold of $P < 0.001$, fasting increased the expression of 842 genes and decreased expression of 842 genes (Figure 1E, Supplemental table 1 and 2). The P-value and FDR-value distribution—showing a skewed distribution towards lower values—underscored the marked effect of fasting on hepatic gene expression in mice (Figure 1F). The top 40 most highly upregulated genes contains many genes involved in lipid metabolism, and many have been identified as target genes of PPAR α , including *Cyp4a14*, *Vnn1*, *Fgf21*, *Acot1*, *Cidec*, *Crat* and *Ehhadh* (Figure 1G). Gene set enrichment analysis confirmed that the upregulated genes were significantly enriched for pathways related to fatty acid oxidation, ketone body synthesis, and glycerophospholipid metabolism, all of which are known to be regulated by fasting (Supplemental figure 1A). In addition, the upregulated genes were highly enriched for targets of the transcription factor PPAR α . Heatmaps of WP1269.FATTY.ACID.BETA.OXIDATION and PEROXISOME illustrate a clear stimulatory effect of fasting on these pathways (Supplemental figure 1B). The top 40 most highly downregulated genes contains many genes involved in cholesterol and steroid hormone synthesis, complemented by genes involved in protein folding, amino acid metabolism, and the immune response (Figure 1H). Gene set enrichment analysis indicated that the downregulated genes were highly enriched for pathways describing cholesterol biosynthesis, drug metabolism, complement, and coagulation (Supplemental figure 1C). A heatmap of CHOLESTEROL.BIOSYNTHESIS illustrates a clear suppressive effect of fasting on this pathway (Supplemental figure 1D).

Figure 1. (opposite) Effect of a single fast on plasma metabolites and hepatic gene expression in mice.

Wildtype Sv129 mice were euthanized in the ad libitum fed state or after a single 24h fast. A) Plasma metabolite concentrations. B) Liver triglycerides concentrations. Asterisk indicates significantly different according to Student's t-test (* $P < 0.05$, ** $P \leq 0.01$, *** $P \leq 0.001$). $n = 11-12$ mice per group. C) H&E staining of representative liver sections. D) Volcano plot showing the relation between mean signal log ratio ($2\log[\text{fold-change}]$, x-axis) and the $-10\log$ of the P-value (y-axis) for the comparison between fed and fasted mice. E) Number of genes significantly different between fed and fasted mice ($P < 0.001$). F) P value and FDR value distribution for the comparison between fed and fasted mice, showing a skewed distribution towards lower values. G) Heatmap of the top 40 most highly upregulated genes by fasting ($P \leq 0.001$), ranked according to fold-change. H) Heatmap of the top 40 most highly downregulated genes by fasting ($P \leq 0.001$), ranked according to fold-change. SLR, signal log ratio.



To further zoom in at the level of individual genes, the fasting-induced changes in expression of metabolic genes ($P < 0.001$) were visualized in a manually constructed biochemical map (Figure 2). The map shows that many genes involved in uptake, oxidation, storage, and mobilization of fatty acids were upregulated by fasting. In addition, fasting induced the expression of several genes involved in gluconeogenesis. By contrast, fasting was associated with the downregulation of numerous genes involved in fatty acid synthesis, fatty acid elongation/desaturation, and cholesterol synthesis (Figure 2). The map illustrates the huge impact of fasting on the expression of metabolic genes in the liver of mice.

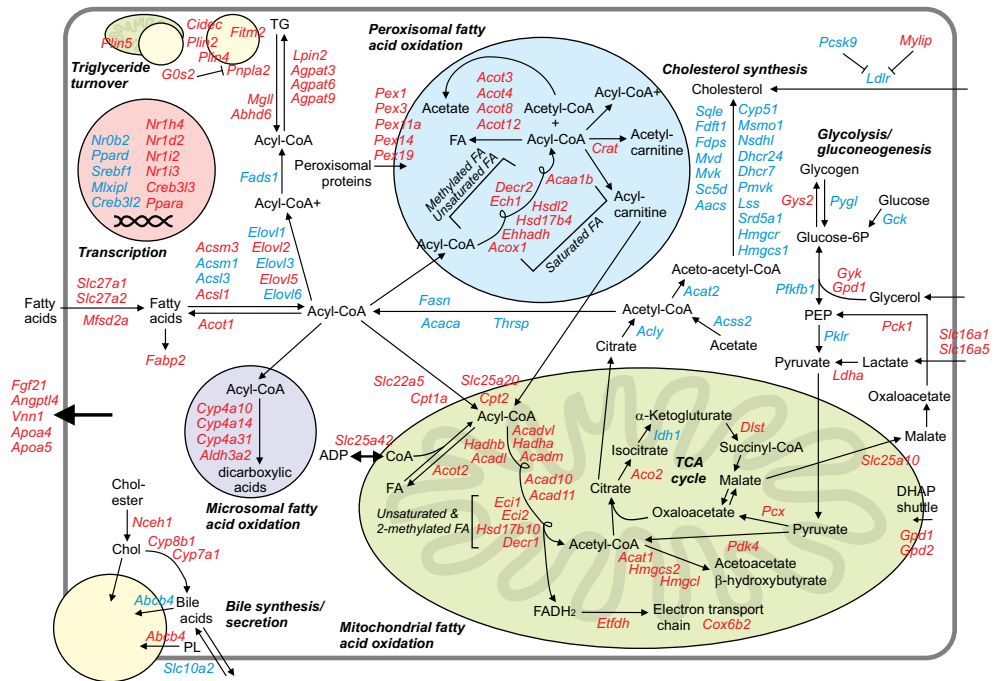


Figure 2. Effect of a single fast on expression of metabolic genes in mouse liver. Manually constructed biochemical map of fasting-induced changes in expression of metabolic genes in mouse liver. Genes involved in metabolism and significantly altered by 24h fasting ($P < 0.001$, fold change > 1.5) were included in the map. The downregulated genes are depicted in blue and the upregulated genes in red.

We next studied whether previous exposure to fasting might influence the metabolic response to a subsequent fast. To that end, a protocol was followed in which a group of 24 mice was subjected to two 16h fasting episodes, each time being allowed to return to their normal growth trajectory. In contrast, another group of 24 mice was fed ad libitum. Of the first set of 24 mice, 12 mice were euthanized after a 16h fast (Fast-Fast-Fast), and 12 mice were euthanized in the ad libitum fed state (Fast-Fast-Fed) (Figure 3A). Also, of the second set of 24 mice, 12 mice were euthanized after a 16h fast (Fed-Fed-Fast), and 12 mice were euthanized in the ad libitum fed state (Fed-Fed-Fed) (Figure 3A). The changes in bodyweight of the different groups of mice are shown in Figure 3B, showing a transient decrease in bodyweight in the mice that underwent the two 16h fasting episodes.

Various measurements were performed to study the possible effect of previous fasting on liver and whole body metabolism. Having previously fasted did not affect glucose tolerance (Figure 3C). Also, while plasma levels of non-esterified fatty acids, glycerol and β -hydroxybutyrate were significantly increased by the final 16-hour-fast, they were unaffected by previous fasting (Figure 3D,E). Similarly, plasma levels of triglycerides and glucose were significantly decreased by the final 16-hour-fast, but were unaltered by previous fasting (Figure 3E). Plasma cholesterol was not significantly affected by either the final 16-hour-fast or by previous fasting (Figure 3E).

Fasting is known to increase triglyceride levels and decrease glycogen levels in the liver. Indeed, the final 16-hour-fast markedly raised hepatic triglycerides (Figure 3F) and reduced hepatic glycogen level (Figure 3G). However, neither hepatic triglycerides nor glycogen were significantly affected by previous fasting. Also, examination of liver histology by H&E staining showed elevated lipid storage in fasted mice but did not reveal an effect of previous fasting on lipid storage and other histological features (Figure 3G).

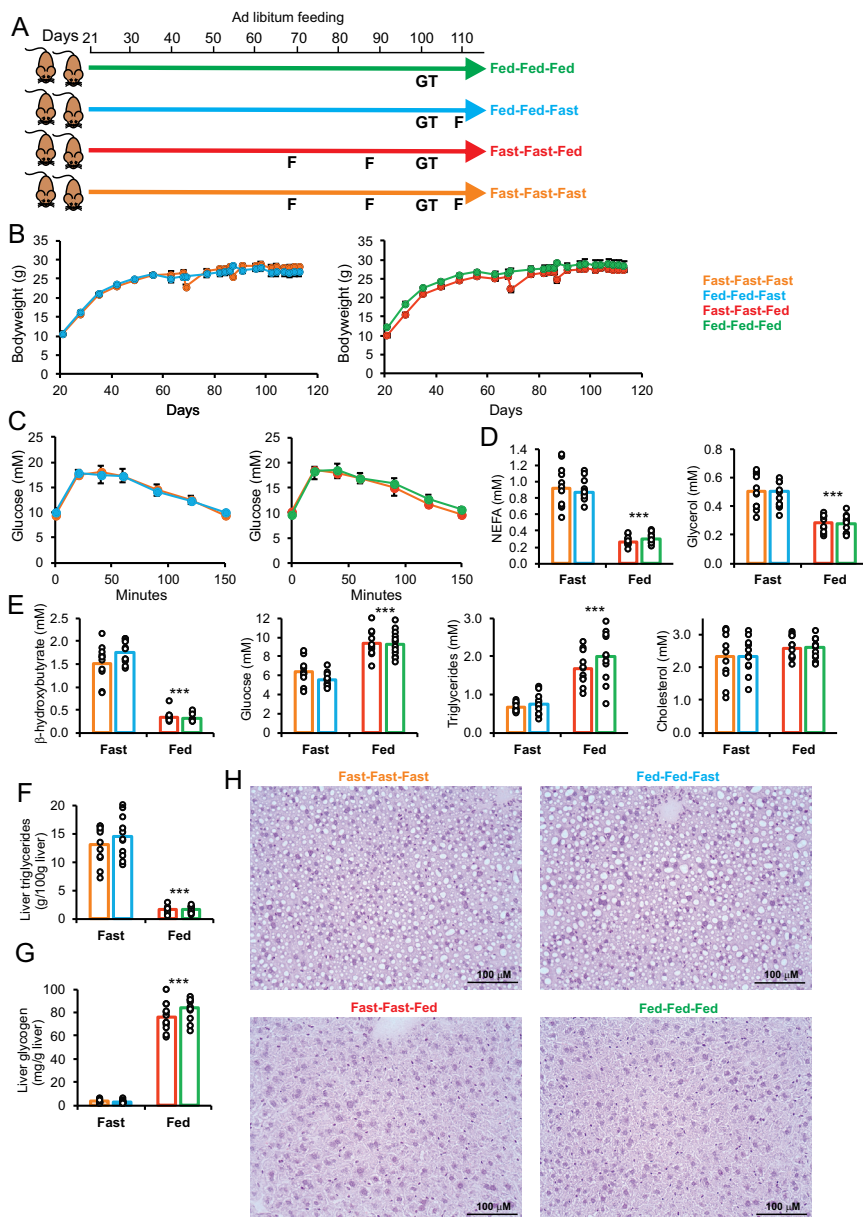


Figure 3. Previous exposure to fasting does not influence the levels of plasma metabolites in the fed or fasted state. A) Schematic representation of the design of the study and color coding of the four groups. F=16h fast, GT=glucose tolerance test. B) Bodyweight from the moment of weaning. C) Intraperitoneal glucose tolerance test. D) Plasma non-esterified fatty acids (NEFA) and glycerol concentrations. E) Plasma concentrations of β -hydroxybutyrate, glucose, triglycerides, and cholesterol. F) Liver triglyceride concentrations. G) Liver glycogen concentrations. H) H&E staining of representative liver sections. Asterisks indicates significant effect of feeding status at euthanasia (2-way ANOVA, $P \leq 0.001$). Error bars represent SEM. $N=12$ mice/group.

To examine if previous fasting might influence the acute effect of fasting on hepatic gene expression, we performed transcriptome analysis on all 4 groups, with 8 biological replicates per group. In order to thoroughly answer this question, we subsequently carried out a variety of different statistical and computational analyses. First, we analyzed the data using various clustering tools. Hierarchical clustering clearly separated the mice by the final 16-hour-fast. However, no separation according to previous fasting was observed (Figure 4A). Similarly, principle component analysis revealed two distinct clusters of mice based on the final 16-hour-fast but did not reveal any clustering according to previous fasting (Figure 4B). A similar result was obtained by multidimensional scaling (Figure 4C).

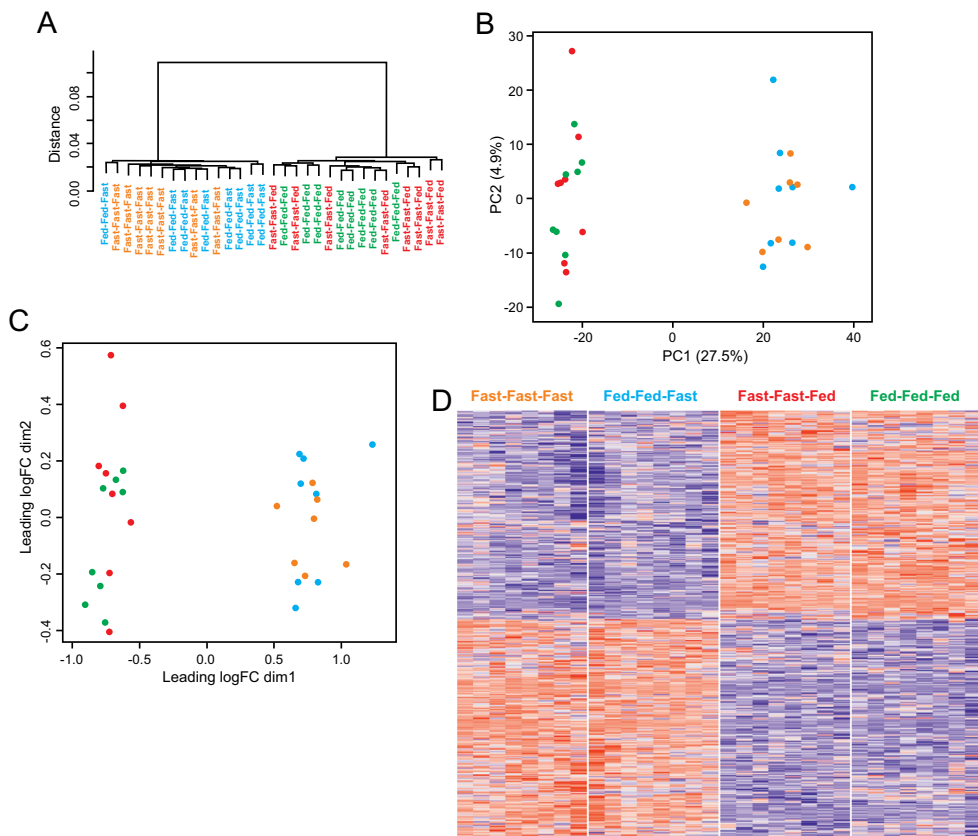


Figure 4. Previous fasting does not influences the overall transcriptomic response to fasting in mouse liver.

A) Hierarchical clustering of transcriptomics data of mouse liver, showing clear separation by feeding status but not by previous fasting. Distance criteria are based on Pearson correlation with average linkage. Principle component analysis (B) and Multidimensional scaling (C) of transcriptomics data of mouse liver, showing clear separation by feeding status but not by previous fasting. D) Heatmap of all genes with FDR q value <0.05 for at least one comparison, showing a clear effect of feeding status, but not of previous fasting.

Next we selected all genes with FDR value below 0.05 across all comparisons and performed clustering and visualization of expression levels by heatmap. The FDR value corrects for multiple testing. The data clearly illustrate the marked effect of the final 16-hour-fast on liver gene expression (Figure 4D). However, no effect of previous fasting was observed, as the group Fast-Fast-Fast was indistinguishable from the group Fed-Fed-Fast, and the group Fast-Fast-Fed was indistinguishable from the group Fed-Fed-Fed. These data indicate that previous fasting did not have any effect on the overall gene expression profile in liver, whereas an acute 16-hour-fast markedly influenced overall gene expression.

Although previous fasting did not noticeably alter the overall gene expression profile, this leaves open the possibility that previous fasting may influence the expression of individual genes. Accordingly, to identify differentially expressed genes, for all genes the log-mean expression value for the mice that underwent previous fasting was plotted against the log-mean expression value for the mice that did not undergo previous fasting. A separate analysis was done for the mice euthanized in the fed state and mice euthanized after an acute fast. Interestingly, nearly all genes were on or very close to the 45° line (Figure 5A), indicating that across all genes, previous fasting did not have a noticeable effect on hepatic gene expression, either in the fed state or after an acute fast. Only a very small number of genes deviated from the 45° line (Figure 5A). To uncover these aberrantly regulated genes, we plotted all genes in a Volcano plot, comparing hepatic expression levels in mice that underwent two previous episodes of fasting vs. the mice that did not. In the mice that were euthanized after an acute 16-hour-fast (Figure 5B, left), this comparison did not yield a single gene that was altered more than 2-fold ($SLR=1$) and met statistical significance ($P<0.001$). In the mice that were euthanized in the fed state (Figure 5B, right), the gene expression changes again were very minor. Only one gene was altered more than 2-fold and was statistically significant.

The very low number of genes altered significantly by previous fasting and the fact that these genes seemed to be functionally unrelated raised the suspicion that these genes were false positives. To follow up on that suspicion, we analyzed the unadjusted p value and FDR value distribution of the comparison Fast-Fast-Fast vs Fed-Fed-Fast and Fast-Fast-Fed vs Fed-Fed-Fed. For either comparison, the unadjusted p values were more or less uniformly distributed across the p value range, while the FDR values were either very close to or equal to one, or were skewed towards one (Figure 5C). Not a single gene met the FDR value threshold of 0.05 for either comparison. Overall, this analysis confirmed our suspicion that genes with a low P-value are probably false positives. Indeed, when we randomly distributed the 16 mice that were fasted at euthanasia across two groups and performed statistical analysis for the comparison between these two groups, we obtained a similar number of significant genes (3-5, $P<0.001$) as for the correct group assignment.

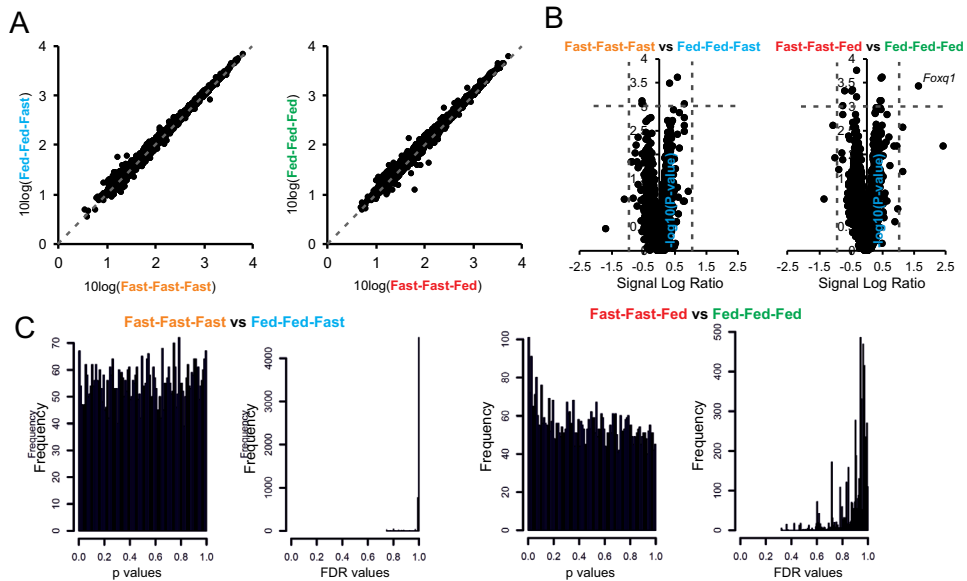


Figure 5. Individual gene expression is not influenced by previous fasting.

A) $^{10}\log$ -mean expression value of previously fasted mice was plotted against the $^{10}\log$ -mean expression value of mice that never fasted. Separate analysis was done for mice euthanized in the fasted state (left figure) or fed state (right figure). B) Volcano plot comparing hepatic expression levels in mice that underwent previous fasting and mice that did not. Separate plots were made for mice euthanized in the fasted state (left figure) or fed state (right figure). C) Analysis of the unadjusted p value and FDR value distribution of the comparison between mice that underwent previous episodes of fasting vs. the mice that did not. Separate analysis was done for mice euthanized in the fasted state (left figure) or fed state (right figure). The uniform distribution of the unadjusted p-values indicates a lack of an effect of previous fasting on hepatic gene expression.

Confirming the results in figure 1, in the mice that underwent previous fasting as well as in the mice that did not undergo previous fasting, the final 16-hour-fast profoundly changed hepatic gene expression (Figure 6A). We then zoomed in on the 50 genes most highly induced or repressed by the final 16-hour-fast (Figure 6B). Substantial overlap was observed with the genes shown in Figure 1G for both upregulation (for example *Cyp4a14*, *Acot1*, *Cidec*, *Slc16a5*, *Vnn1*, *Ehhadh*, *Cyp17a1*) and downregulation (for example *Hsd3b2*, *Srebf1*, *Sqle*, *Pcsk9*, *Gck*, *Serpina4*). However, it is clear from the direct comparison Fed-Fed-Fast vs Fast-Fast-Fast that previous fasting did not have any influence on the expression of fasting-induced genes (Figure 6B).

It is conceivable that the effects of previous fasting are extremely small and only become noticeable when studying pathways. Accordingly, we performed gene set enrichment analysis on the comparison Fast-Fast-Fast vs Fed-Fed-Fast and Fast-Fast-Fed vs Fed-Fed-Fed. Interestingly, no gene sets were significantly upregulated (FDR value < 0.05) in 16-hour-fasted mice exposed to previous fasting and 16-hour-fasted mice fed ad libitum, and only 2 genesets were significantly upregulated. Also, no

gene sets were significantly upregulated (FDR value<0.05) in ad libitum fed mice exposed to previous fasting and mice fed ad libitum throughout, and only 3 gene sets were significantly downregulated. Other pathway analysis tools such as EnrichR or Ingenuity could not be used because there were no significant genes to feed into the analysis.

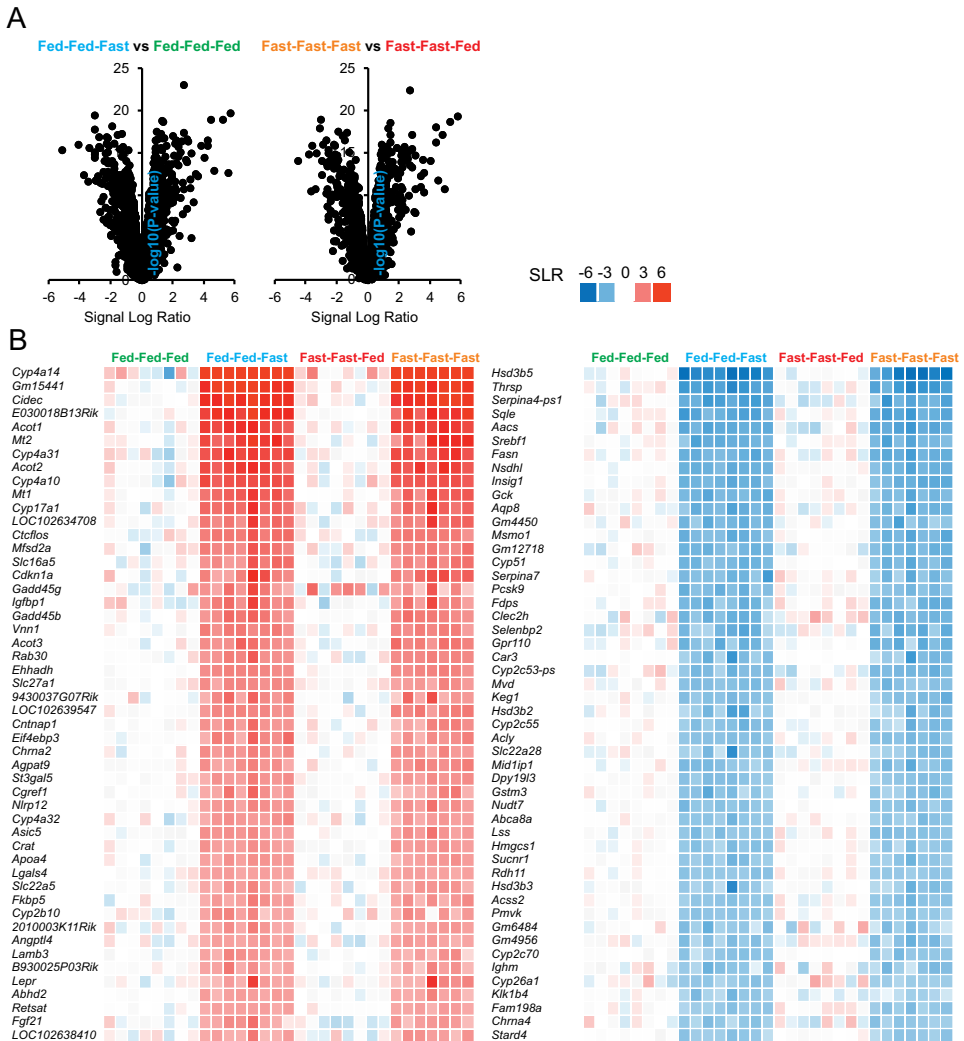


Figure 6. Effect of fasting on hepatic gene expression is not influenced by previous fasting. A) Volcano plot showing the relation between mean signal log ratio ($^2\log[\text{fold-change}]$, x-axis) and the $^{-10}\log$ of the P-value (y-axis) for the comparison between fed and fasted mice. Separate analysis was done for mice that never fasted (left figure) and mice that underwent previous fasting (right figure). B) Heatmaps of the top 50 most highly upregulated (left) or downregulated (right) genes by the final 16h fast, ($P \leq 0.001$), ranked according to fold-change. SLR, signal log ratio.

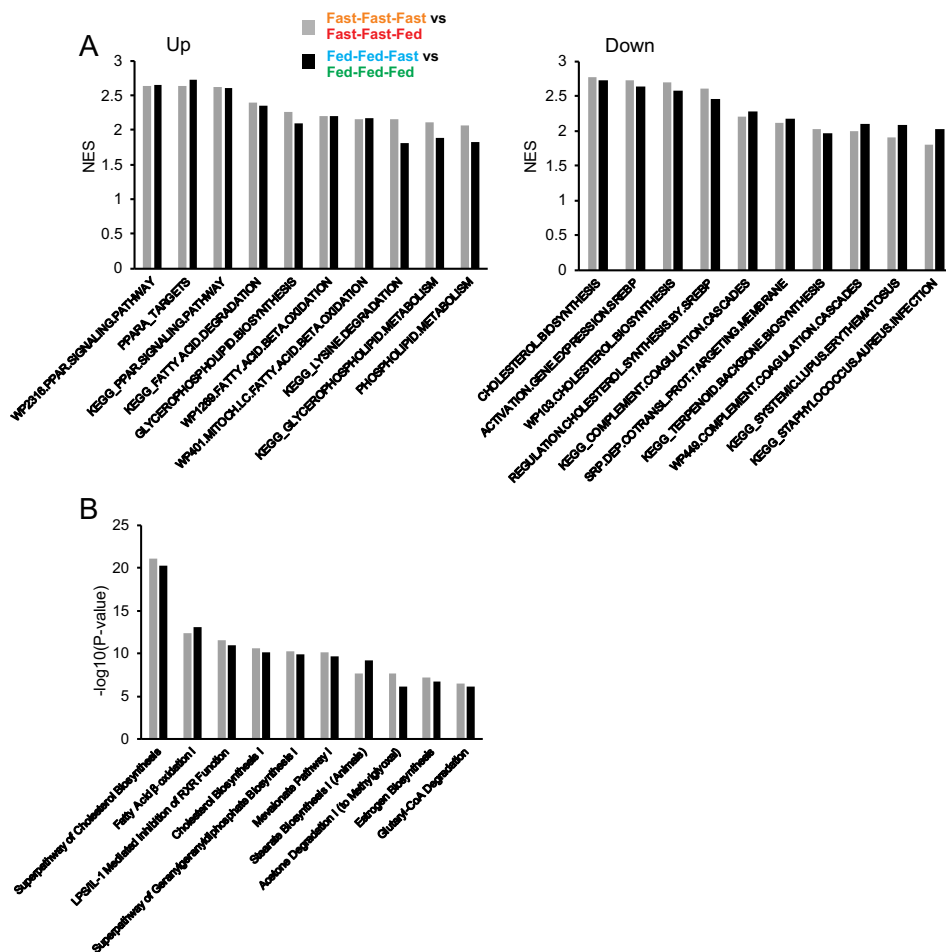


Figure 7. Previous fasting does not influence the effect of fasting on metabolism-related pathways. A) Gene Set Enrichment Analysis showing the 10 pathways with the highest normalized enrichment score for upregulation (left) and downregulation (right) of gene expression by 16h fasting. Parallel analysis was performed for mice that never fasted (black bars) and mice that underwent previous fasting (grey bars). B) Ingenuity pathway analysis showing the top 10 most significantly changes pathways by 16h fasting. Parallel analysis was performed for mice that never fasted (black bars) and mice that underwent previous fasting (grey bars).

We also determined whether the effect of the final 16-hour-fast on specific pathways was different between mice subjected to previous fasting and mice fed ad libitum throughout. According to GSEA and Ingenuity pathway analysis (Figure 7A,B), the final 16-hour-fast significantly changed numerous metabolism-related pathways, including PPAR signaling (up), fatty acid oxidation (up), cholesterol biosynthesis (down), and complement and coagulation (down). However, these effect were indistinguishable between mice that underwent previous fasting and mice that did not. Collectively, these data convincingly demonstrate that previous fasting did not significantly influence hepatic gene expression, either in the ad libitum fed state or after a 16- hour-fast.

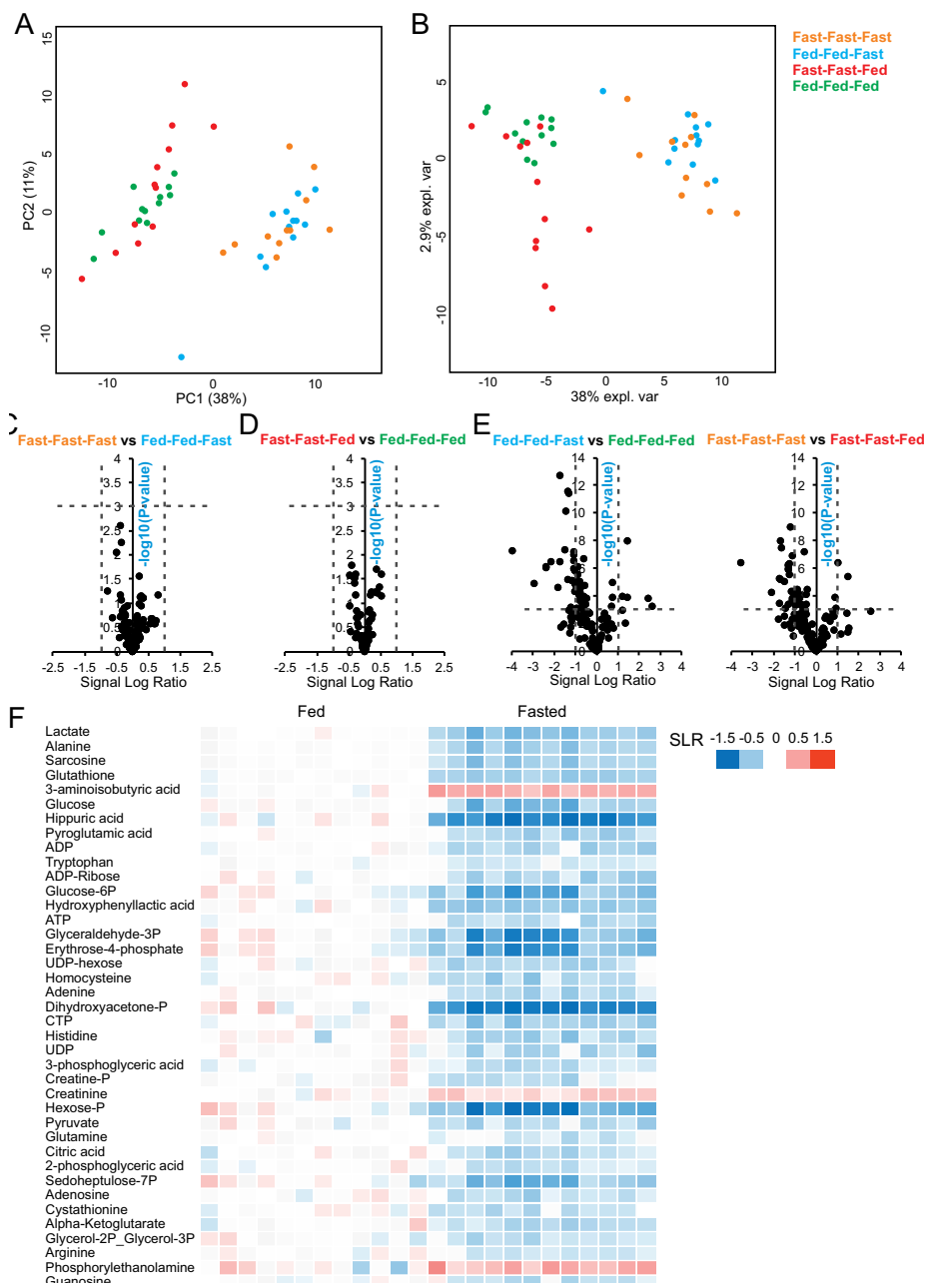


Figure 8. Previous fasting does not influence the metabolic response to fasting in mouse liver.

Principle component analysis (A) and Multidimensional scaling (B) of metabolomics data of mouse liver, showing clear separation by feeding status but not by previous fasting. C) Volcano plot comparing hepatic metabolite levels in fasted mice that underwent previous fasting and mice that did not. D) Volcano plot comparing hepatic metabolite levels in fed mice that underwent previous fasting and mice that did not. E) Volcano plot comparing hepatic metabolite levels in fed and 16h fasted mice. Separate analysis was done for mice that never fasted (left figure) and mice that underwent previous fasting (right figure). F) Heatmap of the 40 metabolites most significantly changed by 16h fasting ($P \leq 0.001$), ranked according to P-value.

To investigate if previous fasting had any influence on various intracellular metabolites in the liver, we performed metabolomics using a platform aimed at polar metabolites, which include amino acids, other organic acids, and nucleotides. Similar to the gene expression data, principle component analysis revealed two distinct clusters of mice based on the final 16-hour-fast, but did not show any clustering according to previous fasting (Figure 8A). A similar result was obtained by PLS-DA (Figure 8B). These data indicate that previous fasting did not have any effect on the overall metabolite profile in liver, whereas an acute 16-hour-fast markedly influenced liver metabolite levels.

To assess if levels of individual metabolites in the liver were affected by previous fasting, we plotted all 135 metabolites in a Volcano plot, comparing hepatic metabolite levels in mice that underwent two prior episodes of fasting vs mice that did not. Consistent with the clustering, not a single metabolite was altered by previous fasting by more than 2-fold (SLR=1) or met the statistical significance threshold ($P < 0.001$), both in the mice that were euthanized after an acute 16-hour-fast (Figure 8C), and in the mice that were euthanized in the ab libitum fed state (Figure 8D). By contrast, a large number of metabolites was significantly changed by a single 16-hour-fast (Figure 8E). A heatmap of the 40 most significantly changed metabolites by a single 16-hour-fast is shown in Figure 8F. Remarkably, levels of nearly all metabolites decreased upon fasting, including many amino acids, glycolytic intermediates, TCA cycle intermediates, and nucleotides. The changes in liver metabolite levels upon fasting are illustrated in Figure 9.

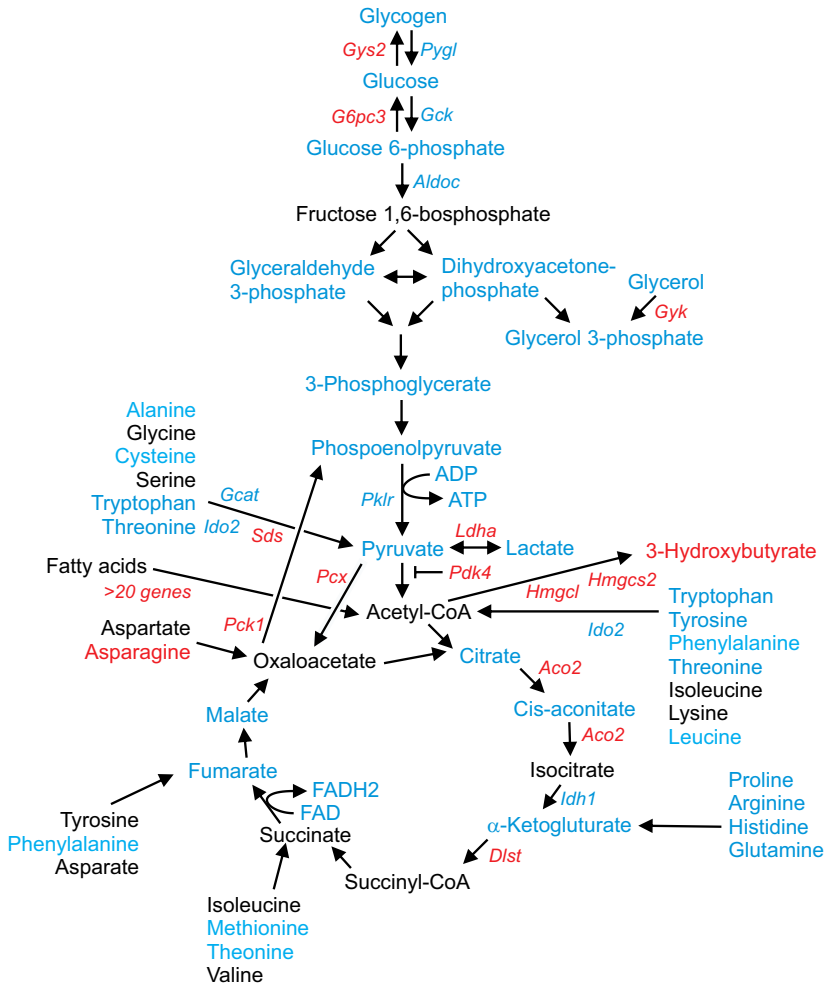


Figure 9. Changes in liver metabolite and gene expression levels after fasting.

Manually constructed map showing changes in liver metabolites after 16h fasting in mice. Metabolites that were significantly decreased by fasting ($P < 0.05$) are depicted in blue. Metabolites that were significantly increased by fasting ($P < 0.05$) are depicted in red. Genes, depicted in italic, that were significantly decreased by fasting ($P < 0.001$, $FC < -1.5$) are depicted in blue. Genes, depicted in italic, that were significantly increased by fasting ($P < 0.001$, $FC > 1.5$) are depicted in red.

Our study failed to show any effect of previous fasting on hepatic gene expression in mice. However, a single 16-hour-fast markedly influenced hepatic gene expression. To what extent the observed fasting-induced changes in liver gene expression are applicable to humans is unclear. To answer that question, we analyzed a RNAseq dataset obtained from livers of hepatocyte humanized mice collected in the fed and fasted state. In these chimeric mice, the liver mainly consist of human hepatocytes, yet substantial numbers of mouse hepatocytes are still present. By using RNAseq, it is possible to perform a separate analysis of the gene expression changes in the human and mouse liver cells. For both the human and mouse expression data, the most highly expressed genes encoded albumin, apoB, and apoA1, confirming that hepatocytes represent the major cell type (data not shown). Using a statistical threshold of $P < 0.001$, 46 genes were significantly upregulated by fasting in human cells, compared to 328 in mouse cells (Figure 10A, Supplementary table 3 and 4). The number of downregulated genes was similar in the human and mouse cells at 162 and 145, respectively (Figure 10A, Supplementary table 5 and 6). These data indicate that fasting had a stronger stimulatory effect on gene expression in the mouse cells than in the human cells. Similar results were obtained when using FDR Benjamini-Hochberg statistical threshold of 0.05 (Figure 10A). Visualization of the signal log ratios in a correlation plot indicated modest similarity in the fasting-induced gene expression changes in the human and mouse cells (Figure 10B). Whereas several genes were consistently induced or repressed by fasting in the human and mouse liver cells, other genes showed very distinct responses. For example, *Cyp8b1* was highly induced by fasting in the mouse cells but not in the human cells. Conversely, *Igf1* was highly suppressed by fasting in the human cells but not in the mouse cells. All genes for which the difference in signal log ratio for the effect of fasting in human and mouse cells exceeded the value of 2 are shown in Supplemental table 7.

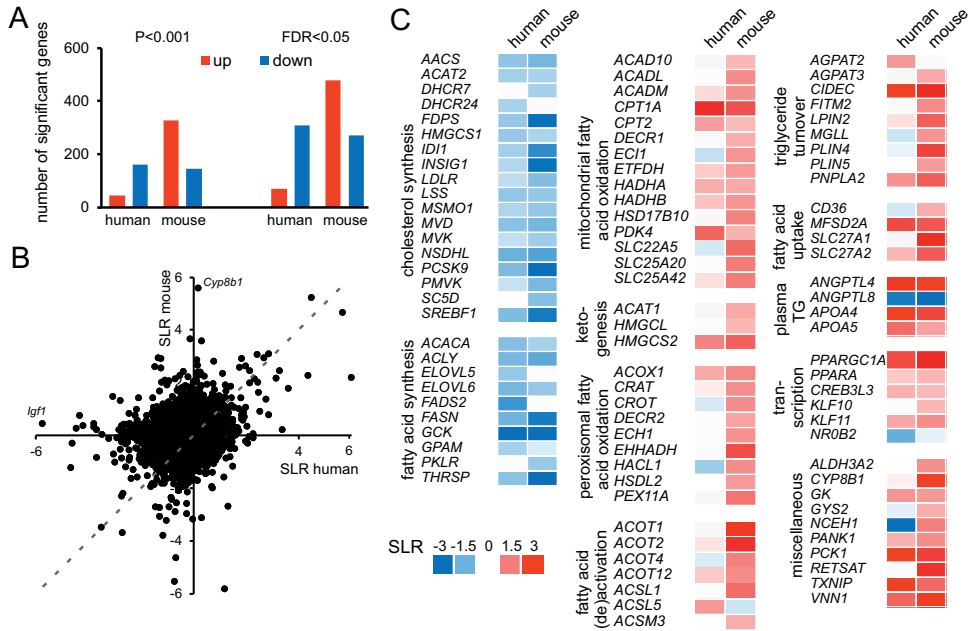


Figure 10. Effect of fasting on liver gene expression in hepatocyte humanized mice.

A) Number of human and mouse genes significantly up- or down-regulated by fasting in hepatocyte humanized mice (P < 0.001 or FDR Benjamini Hochberg < 0.05). B) Plot showing the correlation of the fasting effect expressed as signal log ratio for mouse genes (y-axis) and human genes (x-axis). Plot includes all 9545 common genes. C) Heatmap of all genes involved in lipid and glucose metabolism that were significantly altered by fasting (P < 0.005) in mouse cells or human cells. Genes were organized into specific functional categories.

To examine the possible differential metabolic effects of fasting in human and mouse liver cells, we focused our attention on key metabolic pathways activated or repressed by fasting, such as cholesterol synthesis, fatty acid oxidation, and triglyceride turnover (Figure 2). In general, fasting more strongly affected gene expression in the mouse cells than the human cells (Figure 10C). This was particularly evident for peroxisomal fatty acid oxidation. With the exception of *ACOX1*, all genes in this pathway were induced by fasting in mouse but not in human cells. Also, with the exception of *CPT1A* and *PDK4*, genes involved in mitochondrial fatty acid oxidation were more strongly induced by fasting in mouse than humans cells. Genes that were similarly induced by fasting in human and mouse cells included *PCK1*, *ANGPTL4*, *PPARGC1A*, *CIDECD* and *MFSD2A*. With respect to downregulation, genes in the cholesterol synthesis pathway were more strongly repressed by fasting in the mouse cells than the human cells. Overall, these data indicate that fasting-induced changes in gene expression in mouse hepatocytes cannot automatically be extrapolated to human hepatocytes.

DISCUSSION

Currently, it is unknown whether the liver is able to remember a strong metabolic stimulus. In this study, we find that previous exposure to fasting does not influence the hepatic response to a subsequent fast, thus arguing against a memory effect of fasting in the liver. Specifically, the fasting-induced changes in plasma NEFA, ketones, glucose, glycerol, and triglycerides, as well as the increase in liver triglyceride and decrease in glycogen levels upon fasting were not significantly affected by previous episodes of fasting. Furthermore, previous fasting had no effect on the liver transcriptome and metabolome, measured either in the fed or fasted state. Specifically, the fasting-induced upregulation of numerous genes and pathways connected with PPAR α and fatty acid oxidation, as well as the fasting-induced downregulation of numerous genes and pathways related to cholesterol synthesis, fatty acid synthesis and glycolysis, were all unaffected by previous fasting. Finally, no significant effect was observed of previous fasting on glucose tolerance. Collectively, our data do not support the hypothesis that a strong metabolic stressor such as fasting leaves a lasting mark in the liver and confers some form of metabolic memory.

Our study is largely based on the concept of innate memory, which argues that innate immune cells such as macrophages hold the ability to ‘remember’ earlier challenges [17]. The concept was operationalized in primary human monocytes as a more distinct immunological response after a second immunological challenge as opposed to the first immunological challenge [18,19]. Currently, the exact mechanisms underlying innate memory of immune cells remain unclear. Nevertheless, evidence has been presented that this memory may be coupled to changes in intracellular metabolism, which in turn may influence genome function via epigenetic mechanisms [20–22]. As innate memory is based on *ex vivo* studies in primary human monocytes, a more fitting comparison for liver cells would be to expose primary human hepatocytes to a fasting mimic such as serum starvation or low glucose concentration in the medium. Due to the inevitable and relatively rapid deterioration of hepatocytes in culture, and because of the difficulty mimicking the hepatic fasting response, we opted for an *in vivo* study.

A negative result as observed in the present study inevitably raises questions about the study design and to what extent it was appropriate to answer the primary research question. First, it could be argued that the number and duration of prior fasting episodes was insufficient to trigger a memory effect in the liver. The limited number and duration of fasting episodes was partly driven by ethical considerations, as an overnight fast is a severe stressor for mice. In addition, we modelled the study according to the innate immune memory concept, which is based on a one-time exposure to an inflammatory stimulus. Finally, we wanted to make sure that the mice had fully recovered from each overnight fast and had returned to their

normal growth trajectory, to avoid any confounding due to weight loss, as loss of bodyweight and fat mass are known to impact metabolic parameters and liver gene expression [23]. In the future, it would be of interest to study the potential training effect of more frequent and possibly longer fasting episodes, while still each time allowing the mice to return to their normal growth curve. Second, the argument could be raised that the time between the second prior fasting episode and euthanasia was too long, which may have caused the memory effect to fade out. However, we hypothesized that the memory effect would be long lasting, thus allowing for a considerable time lapse between previous fasting and the final fast [24]. We also wanted to make sure that the mice had fully recovered from the glucose tolerance test, which also is a significant stressor to the mice. Nevertheless, in the future, it could be considered to reduce the time lapse between previous fasting and euthanasia. Third, it is possible that the huge effects of the final 16-hour-fast on liver metabolism overruled the much more subtle memory effects of the prior fasts. Accordingly, it could be speculated that a milder metabolic challenge may have better exposed a possible memory effect. However, previous fasting did not influence the results of the glucose tolerance tests. Also, no effect of previous fasting on any metabolic parameters was observed in metabolically unchallenged mice euthanized in the ad libitum fed state. Nevertheless, for future studies, it is recommended to perform measurements throughout the fasting response and not only at the final 16 hour timepoint. Fourth, we only investigated the response to fasting in the liver at the level of mRNA and the metabolome, and did not investigate protein levels or post-translational modifications. Accordingly, any conclusions made are specifically about metabolic and transcriptional memory. Finally, the study was done in healthy mice fed regular chow. Our data do not exclude a possible memory effect of fasting in obese and/or diabetic mice fed a special diet.

Although our study protocol resembles intermittent fasting, it was not intended to model intermittent fasting. Different definitions of intermittent fasting exist, but in general it is described as periods of voluntary abstinence from food and drink, which in practise can vary from complete alternate-day fasting, modified fasting regimes, and time-restricted feeding [25]. In general, individuals and mice practicing intermittent fasting exhibit better metabolic flexibility and improvement in metabolic health parameters compared to a control group [26–28]. However, the major difference between intermittent fasting studies and our study protocol is that intermittent fasting is often associated with loss of bodyweight caused by a chronic caloric deficit [29]. While weight loss is often the primary purpose of intermittent fasting, it represents a huge confounder when studying the possible memory effect of fasting [28,30]. In addition, when fasting intermittently, the limited time between fasting episodes may not allow for a restoration of metabolic homeostasis, which is necessary to be able to detect a veritable memory effect. It should be noted that while some intermittent fasting studies have reported favourable results, mostly concomitant with weight loss, many other studies have failed to find an effect on

metabolic parameters, which is in line with the absence of a metabolic memory effect of fasting [31–35].

Conceptually, the idea of metabolic memory has lots of similarities with metabolic programming. Metabolic programming describes a concept where early adaptations to a nutritional stressor permanently change the physiology and metabolism of the organism and continue to be expressed even in the absence of the stressor that initiated them [36,37]. Nearly all research in this area focuses on early metabolic programming and examines the long-term impact of exposure to nutritional stressors during critical periods in development, which often means in utero [36,38,39]. Many studies performed in animals have provided evidence that exposure to certain stressors in utero or even pre-conception may influence the metabolic phenotype or the response to a nutritional intervention later on in life [40]. The major difference with our study design is that our mice were exposed to the metabolic stressor at the adult stage. In theory, however, in both cases, the long-term effect of the nutritional/metabolic stressor may be mediated by epigenetic mechanism. For our study, we had anticipated to investigate the effect of previous fasting on the liver epigenome (13). However, because we did not detect any effect of prior fasting on the liver transcriptome or metabolome, we decided to not further pursue these analyses. Accordingly, we strictly cannot rule out any effect of previous fasting on the liver epigenome. While perhaps mechanistically interesting, the potential epigenetic changes could be considered less relevant in the absence of any changes in gene expression and in functional metabolic parameters.

To our knowledge, this paper is the first to study the effect of fasting on the liver metabolome. Interestingly, the levels of almost all measured metabolites goes down upon fasting, including many amino acids, intermediates of glycolysis, intermediates of the TCA cycle, and nucleotides. The decrease in amino acid levels during fasting is likely explained by enhanced amino acid degradation, which provides building blocks for gluconeogenesis. Similarly, the decrease in TCA intermediates likely reflects the withdrawal of oxaloacetate from the TCA cycle to serve as substrate for gluconeogenesis. Intriguingly, hepatic levels of ATP and ADP were both decreased by fasting, leading to a modest but statistically significant increase in the ATP/ADP ratio. Only very few metabolites were increased by fasting, including 3-hydroxybutyrate and 3-aminoisobutyric acid (BAIBA). The increased levels of 3-hydroxybutyrate (a.k.a. β -hydroxybutyrate) must be the consequence of enhanced ketogenesis in the liver upon fasting. The origin of the elevated BAIBA levels in the liver is unclear. BAIBA has been suggested to stimulate fatty acid oxidation in liver in vitro and in vivo in a PPAR α -dependent manner [41].

The parallel analysis of the liver transcriptome and liver metabolome allowed us to assess to what extent the changes in liver metabolites upon fasting may be reflected in and are possibly driven by changes in gene expression. The increase in

hepatic levels of 3-hydroxybutyrate by fasting were accompanied by upregulation of the enzymes catalyzing ketone body synthesis, and by upregulation of >20 genes involved in fatty acid oxidation. These data suggest that changes in mRNA expression of relevant enzymes may at least partly explain the fasting-induced increase in liver ketone body levels. Similarly, the decrease in citrate levels by fasting was accompanied by upregulation of the Aconitase 2 enzyme (*Aco2*). Furthermore, the decrease in α -ketoglutarate was paralleled by decreased expression of *Idh1* and increased expression of *Dlst*, which encode the enzymes catalyzing the synthesis and conversion of α -ketoglutarate, respectively. In general, however, the reduction in hepatic levels of numerous metabolites during fasting could not be explained by changes in mRNA levels of enzymes, suggesting that they are likely driven by other factors. For example, fasting caused a marked decrease in hepatic glycogen levels, while at the same time fasting was associated with a significant increase in hepatic expression of glycogen synthase 2 (*Gys2*) and a decrease in expression of glycogen phosphorylase (*Pygl*). As previously suggested, this seemingly counterintuitive regulation may serve to prime the glycogen synthesizing system for when dietary glucose becomes available again [42]. Overall, many changes in liver metabolite levels upon fasting cannot be distilled from the changes in mRNA expression, at least for the set of metabolites measured, suggesting that caution should be exercised when coupling mRNA data to cellular metabolism. Overall, the transcriptome signature of fasting identified in our study is in agreement with and expands on previous studies that have examined the effect of fasting on the liver transcriptome in pigs, rats, and mice [8,43,44]. As summarized in figure 2, fasting upregulated genes involved in gluconeogenesis and in uptake, oxidation, storage, and mobilization of fatty acids, and downregulated genes involved in fatty acid synthesis, fatty acid elongation/desaturation, and cholesterol synthesis.

We provide evidence against a memory effect of fasting on liver gene expression in mice. To what extent these results can be extrapolated to human liver is unclear. To our knowledge, no studies have examined the effect of fasting on gene expression in human liver. Our analysis of a RNAseq dataset of fasted hepatocyte humanized mice revealed modest similarity in the transcriptome response to fasting in human and mouse liver cells. A substantial number of genes was differentially regulated by fasting in human and mouse liver cells. Importantly, the downregulation of genes involved in lipogenesis and cholesterol synthesis, as well as the upregulation of genes involved in various pathways of fatty acid catabolism and storage was generally more modest in human cells than mouse cells, with some clear exceptions. The analysis indicates that caution should be exercised when extrapolating the effect of fasting on gene expression in mouse liver to human liver.

Here, we explored for the first time the possibility that a strong metabolic stimulus such as overnight fasting may elicit a memory effect in the liver. We find that previous exposure to fasting does not influence the metabolic phenotype of mice

and does not influence the liver transcriptome and metabolome. We conclude that previous exposure to fasting in mice does not leave a metabolic mark in the liver, thus arguing against the concept of metabolic memory in the hepatic response to fasting. Collectively, our data provide a useful resource for the study of liver metabolism during fasting.

Acknowledgements

We acknowledge the support from the Netherlands Cardiovascular Research Initiative: an initiative with support of the Dutch Heart Foundation (CVON2014-02 ENERGISE)

Author contribution

M.D and S.K. conceived and planned the research and experiments. M.D carried out the mouse studies and performed the experiments. M.D, G.J.E.J.H. and S.K analyzed the data. M.v.W. performed the lipidomics analysis. M.D and S.K wrote the manuscript. All authors provided critical feedback and helped to shape the research, analysis, and manuscript.

Competing interests

None declared

References

- [1] Secor, S.M., Carey, H. V., 2016. Integrative physiology of fasting. *Comprehensive Physiology* 6(2): 773–825, Doi: 10.1002/cphy.c150013.
- [2] Moitra, J., Mason, M.M., Olive, M., Krylov, D., Gavrilova, O., Marcus-Samuels, B., et al., 1998. Life without white fat: A transgenic mouse. *Genes and Development* 12(20): 3168–81, Doi: 10.1101/gad.12.20.3168.
- [3] Kersten, S., Seydoux, J., Peters, J.M., Gonzalez, F.J., Desvergne, B., Wraahli, W., 1999. Peroxisome proliferator-activated receptor alpha mediates the adaptive response to fasting. *Journal of Clinical Investigation* 103(11): 1489–98, Doi: 10.1172/JCI6223.
- [4] van den Berghe, G., 1991. The role of the liver in metabolic homeostasis: Implications for inborn errors of metabolism. *Journal of Inherited Metabolic Disease* 14(4): 407–20, Doi: 10.1007/BF01797914.
- [5] Alamri, Z.Z., 2018. The role of liver in metabolism: an updated review with physiological emphasis. *International Journal of Basic & Clinical Pharmacology* 7(11): 2271, Doi: 10.18203/2319-2003.ijbcp20184211.
- [6] Owen, O.E., Morgan, A.P., Kemp, H.G., Sullivan, J.M., Herrera, M.G., Cahill, G.F., 1967. Brain metabolism during fasting. *The Journal of Clinical Investigation* 46(10): 1589–95, Doi: 10.1172/JCI105650.
- [7] Kersten, S., 2001. Mechanisms of nutritional and hormonal regulation of lipogenesis. *EMBO Reports* 2(4): 282–6, Doi: 10.1093/embo-reports/kve071.
- [8] Chi, Y., Youn, D.Y., Xiaoli, A.M., Liu, L., Pessin, J.B., Yang, F., et al., 2020. Regulation of gene expression during the fasting-feeding cycle of the liver displays mouse strain specificity. *The Journal of Biological Chemistry* 295(15): 4809–21, Doi: 10.1074/jbc.RA119.012349.
- [9] Besse-Patin, A., Jeromson, S., Levesque-Damphousse, P., Secco, B., Laplante, M., Estall, J.L., 2019. PGC1A regulates the IRS1:IRS2 ratio during fasting to influence hepatic metabolism downstream of insulin. *Proceedings of the National Academy of Sciences of the United States of America* 116(10): 4285–90, Doi: 10.1073/pnas.1815150116.
- [10] Leone, T.C., Weinheimer, C.J., Kelly, D.P., 1999. A critical role for the peroxisome proliferator-activated receptor α (PPAR α) in the cellular fasting response: The PPAR α -null mouse as a model of fatty acid oxidation disorders. *Proceedings of the National Academy of Sciences of the United States of America* 96(13): 7473–8, Doi: 10.1073/pnas.96.13.7473.
- [11] Oh, K.J., Han, H.S., Kim, M.J., Koo, S.H., 2013. CREB and FoxO1: Two transcription factors for the regulation of hepatic gluconeogenesis. *BMB Reports* 46(12): 567–74, Doi: 10.5483/BMBRep.2013.46.12.248.
- [12] Boraschi, D., Italiani, P., 2018. Innate immune memory: Time for adopting a correct terminology. *Frontiers in Immunology* 9(APR): 1–4, Doi: 10.3389/fimmu.2018.00799.
- [13] Rusek, P., Wala, M., Druszczyńska, M., Fol, M., 2018. Infectious agents as stimuli of trained innate immunity. *International Journal of Molecular Sciences* 19(2), Doi: 10.3390/ijms19020456.
- [14] Crisan, T.O., Netea, M.G., Joosten, L.A.B., 2016. Innate immune memory: Implications for host responses to damage-associated molecular patterns. *European Journal of Immunology* 46(4): 817–28, Doi: 10.1002/eji.201545497.

- [15] Dai, M., Wang, P., Boyd, A.D., Kostov, G., Athey, B., Jones, E.G., et al., 2005. Evolving gene/transcript definitions significantly alter the interpretation of GeneChip data. *Nucleic Acids Research* 33(20): 1–9, Doi: 10.1093/nar/gni179.
- [16] Molenaars, M., Janssens, G.E., Williams, E.G., Jongejan, A., Lan, J., Rabot, S., et al., 2020. A Conserved Mito-Cytosolic Translational Balance Links Two Longevity Pathways. *Cell Metabolism* 31(3): 549–563.e7, Doi: 10.1016/j.cmet.2020.01.011.
- [17] Netea, M.G., Quintin, J., Van Der Meer, J.W.M., 2011. Trained immunity: A memory for innate host defense. *Cell Host and Microbe* 9(5): 355–61, Doi: 10.1016/j.chom.2011.04.006.
- [18] van der Meer, J.W.M., Joosten, L.A.B., Riksen, N., Netea, M.G., 2015. Trained immunity: A smart way to enhance innate immune defence. *Molecular Immunology* 68(1): 40–4, Doi: 10.1016/j.molimm.2015.06.019.
- [19] Quintin, J., Saeed, S., Martens, J.H.A., Giamarellos-Bourboulis, E.J., Ifrim, D.C., Logie, C., et al., 2012. *Candida albicans* infection affords protection against reinfection via functional reprogramming of monocytes. *Cell Host and Microbe* 12(2): 223–32, Doi: 10.1016/j.chom.2012.06.006.
- [20] Saeed, S., Quintin, J., Kerstens, H.H.D., Rao, N.A., Aghajani-Refah, A., Matarese, F., et al., 2014. Epigenetic programming of monocyte-to-macrophage differentiation and trained innate immunity. *Science* 345(6204), Doi: 10.1126/science.1251086.
- [21] Van Der Heijden, C.D.C.C., Noz, M.P., Joosten, L.A.B., Netea, M.G., Riksen, N.P., Keating, S.T., 2018. Epigenetics and Trained Immunity. *Antioxidants and Redox Signaling* 29(11): 1023–40, Doi: 10.1089/ars.2017.7310.
- [22] Arts, R.J.W., Carvalho, A., La Rocca, C., Palma, C., Rodrigues, F., Silvestre, R., et al., 2016. Immunometabolic Pathways in BCG-Induced Trained Immunity. *Cell Reports* 17(10): 2562–71, Doi: 10.1016/j.celrep.2016.11.011.
- [23] Tarasco, E., Boyle, C.N., Pellegrini, G., Arnold, M., Steiner, R., Hornemann, T., et al., 2019. Body weight-dependent and independent improvement in lipid metabolism after Roux-en-Y gastric bypass in ApoE*3Leiden.CETP mice. *International Journal of Obesity* 43(12): 2394–406, Doi: 10.1038/s41366-019-0408-y.
- [24] Sánchez-Ramón, S., Conejero, L., Netea, M.G., Sancho, D., Palomares, Ó., Subiza, J.L., 2018. Trained Immunity-Based Vaccines: A New Paradigm for the Development of Broad-Spectrum Anti-infectious Formulations. *Frontiers in Immunology* 9(December): 2936, Doi: 10.3389/fimmu.2018.02936.
- [25] Patterson, R.E., Sears, D.D., 2017. Metabolic Effects of Intermittent Fasting. *Annual Review of Nutrition* 37(1): 371–93, Doi: 10.1146/annurev-nutr-071816-064634.
- [26] Dedual, M.A., Wueest, S., Borsigova, M., Konrad, D., 2019. Intermittent fasting improves metabolic flexibility in short-term high-fat diet-fed mice. *American Journal of Physiology. Endocrinology and Metabolism* 317(5): E773–82, Doi: 10.1152/ajpendo.00187.2019.
- [27] Bray, M.S., Tsai, J.Y., Villegas-Montoya, C., Boland, B.B., Blasier, Z., Egbejimi, O., et al., 2010. Time-of-day-dependent dietary fat consumption influences multiple cardiometabolic syndrome parameters in mice. *International Journal of Obesity* 34(11): 1589–98, Doi: 10.1038/ijo.2010.63.

- [28] Sutton, E.F., Beyl, R., Early, K.S., Cefalu, W.T., Ravussin, E., Peterson, C.M., 2018. Early Time-Restricted Feeding Improves Insulin Sensitivity, Blood Pressure, and Oxidative Stress Even without Weight Loss in Men with Prediabetes. *Cell Metabolism* 27(6): 1212-1221.e3, Doi: 10.1016/j.cmet.2018.04.010.
- [29] Catenacci, V.A., Pan, Z., Ostendorf, D., Brannon, S., Gozansky, W.S., Mattson, M.P., et al., 2016. A randomized pilot study comparing zero-calorie alternate-day fasting to daily caloric restriction in adults with obesity. *Obesity* 24(9): 1874–83, Doi: 10.1002/oby.21581.
- [30] Raab, R.M., Bullen, J., Kelleher, J., Mantzoros, C., Stephanopoulos, G., 2005. Regulation of mouse hepatic genes in response to diet induced obesity, insulin resistance and fasting induced weight reduction. *Nutrition and Metabolism* 2: 1–13, Doi: 10.1186/1743-7075-2-15.
- [31] Rynders, C.A., Thomas, E.A., Zaman, A., Pan, Z., Catenacci, V.A., Melanson, E.L., 2019. Effectiveness of intermittent fasting and time-restricted feeding compared to continuous energy restriction for weight loss. *Nutrients* 11(10): 1–23, Doi: 10.3390/nu11102442.
- [32] Johnstone, A., 2015. Fasting for weight loss: An effective strategy or latest dieting trend? *International Journal of Obesity* 39(5): 727–33, Doi: 10.1038/ijo.2014.214.
- [33] Soeters M, Lammers N M, Dubbelhuis P F, Ackermans M T, Jonkers-Schuitema C F, Fliers E, Sauerwein H P, Aertst J M, S.M.J., 2009. Intermittent fasting does not affect whole-body glucose, lipid, or protein metabolism. *American Journal of Clinical Nutrition*: 1244–51, Doi: 10.3945/ajcn.2008.27327.1.
- [34] Heilbronn, L.K., Civitarese, A.E., Bogacka, I., Smith, S.R., Hulver, M., Ravussin, E., 2005. Glucose tolerance and skeletal muscle gene expression in response to alternate day fasting. *Obesity Research* 13(3): 574–81, Doi: 10.1038/oby.2005.61.
- [35] Joo, J., Cox, C.C., Kindred, E.D., Lashinger, L.M., Young, M.E., Bray, M.S., 2016. The acute effects of time-of-day-dependent high fat feeding on whole body metabolic flexibility in mice. *International Journal of Obesity* 40(9): 1444–51, Doi: 10.1038/ijo.2016.80.
- [36] Block, T., El-Osta, A., 2017. Epigenetic programming, early life nutrition and the risk of metabolic disease. *Atherosclerosis* 266: 31–40, Doi: 10.1016/j.atherosclerosis.2017.09.003.
- [37] Patel, M.S., Srinivasan, M., 2002. Metabolic programming: Causes and consequences. *Journal of Biological Chemistry* 277(3): 1629–32, Doi: 10.1074/jbc.R100017200.
- [38] Barker DJP., 1990. The fetal and infant origins of adult disease The womb may be more important than the home. *Bmj* (156): 1990.
- [39] Hahn, O., Drews, L.F., Nguyen, A., Tatsuta, T., Gkioni, L., Hendrich, O., et al., 2019. A nutritional memory effect counteracts the benefits of dietary restriction in old mice. *Nature Metabolism* 1(11): 1059–73, Doi: 10.1038/s42255-019-0121-0.
- [40] Ozanne, S.E., Hales, C.N., 1999. The long-term consequences of intra-uterine protein malnutrition for glucose metabolism. *Proceedings of the Nutrition Society* 58(3): 615–9, Doi: 10.1017/S0029665199000804.
- [41] Roberts, L.D., Boström, P., O’Sullivan, J.F., Schinzel, R.T., Lewis, G.D., Dejam, A., et al., 2014. β -Aminoisobutyric acid induces browning of white fat and hepatic β -oxidation and is inversely correlated with cardiometabolic risk factors. *Cell Metabolism* 19(1): 96–108, Doi: 10.1016/j.cmet.2013.12.003.

- [42] Mandard, S., Stienstra, R., Escher, P., Tan, N.S., Kim, I., Gonzalez, F.J., et al., 2007. Glycogen synthase 2 is a novel target gene of peroxisome proliferator-activated receptors. *Cellular and Molecular Life Sciences* : CMLS 64(9): 1145–57, Doi: 10.1007/s00018-007-7006-1.
- [43] Lkhagvadorj, S., Qu, L., Cai, W., Couture, O.P., Barb, C.R., Hausman, G.J., et al., 2009. Microarray gene expression profiles of fasting induced changes in liver and adipose tissues of pigs expressing the melanocortin-4 receptor D298N variant. *Physiological Genomics* 38(1): 98–111, Doi: 10.1152/physiolgenomics.90372.2008.
- [44] Li, R.Y., Zhang, Q.H., Liu, Z., Qiao, J., Zhao, S.X., Shao, L., et al., 2006. Effect of short-term and long-term fasting on transcriptional regulation of metabolic genes in rat tissues. *Biochemical and Biophysical Research Communications* 344(2): 562–70, Doi: 10.1016/j.bbrc.2006.03.155.

Supplemental materials

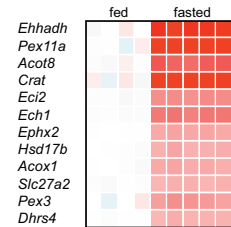
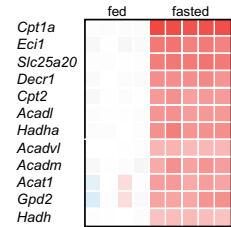
A

NAME	NES	FDR q-val
PPARA_TARGETS	2.800398	0
KEGG_PPARG_SIGNALING_PATHWAY	2.496525	0
WP2316_PPARG_SIGNALING_PATHWAY	2.495677	0
WP1269_FATTY_ACID_BETA_OXIDATION	2.306543	0
KEGG_FATTY_ACID_DEGRADATION	2.227269	0
KEGG_BIOSYNTHESIS_OF_UNSATURATED_FATTY_ACIDS	2.055579	0.002096
KEGG_LYSINE_DEGRADATION	2.033196	0.002306
KEGG_PEROXISOME	1.985299	0.007393
KEGG_FAT_DIGESTION_AND_ABSORPTION	1.971312	0.008334
GLUCONEOGENESIS	1.915318	0.019453
FATTY_ACID_TRIACYLGLYCEROL_AND_KETONE_BODY_METABOLISM	1.903016	0.021893
GLYCEROPHOSPHOLIPID_BIOSYNTHESIS	1.88746	0.023802
PPARA_ACTIVATES_GENE_EXPRESSION	1.866559	0.031855
KEGG_GLYCEROPHOSPHOLIPID_METABOLISM	1.859827	0.032059
REGULATION_OF_LIPID_METABOLISM_BY_PPARG	1.8407	0.039563
SYNTHESIS_OF_PA	1.815876	0.052689

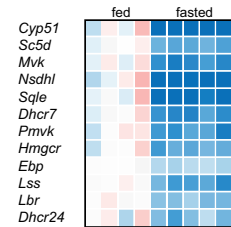
C

NAME	NES	FDR q-val
KEGG_COMPLEMENT_AND_COAGULATION_CASCADES	-2.45205	0
CHOLESTEROL_BIOSYNTHESIS	-2.28112	0
ACTIVATION_OF_GENE_EXPRESSION_BY_SREBF_SREBF	-2.26252	0
KEGG_CHEMICAL_CARCINOGENESIS	-2.25945	0
KEGG_METABOLISM_OF_XENOBIOTICS_BY_CYTOCHROME_P450	-2.23094	2.16E-04
WP449_COMPLEMENT_AND_COAGULATION_CASCADES	-2.22717	1.80E-04
SRP_DEPENDENT_COTRANSLATIONAL_PROTEIN_TARGETING_TO_MEMBRANE	-2.22674	1.54E-04
NRF2_TARGETS	-2.20591	1.35E-04
KEGG_DRUG_METABOLISM_CYTOCHROME_P450	-2.19936	1.20E-04
KEGG_SYSTEMIC_LUPUS_ERYTHEMATOSUS	-2.18486	1.08E-04
KEGG_PROTEIN_EXPORT	-2.1819	9.80E-05
KEGG_STEROID_BIOSYNTHESIS	-2.11907	6.53E-04
KEGG_PROTEIN_PROCESSING_IN_ENDOPLASMIC_RETICULUM	-2.11605	6.03E-04
COMPLEMENT_CASCADE	-2.09421	7.21E-04
KEGG_STEROID_HORMONE_BIOSYNTHESIS	-2.07321	0.001047
KEGG_PRION_DISEASES	-2.0683	0.001054
KEGG_DNA_REPLICATION	-1.99782	0.003632
PHASE_II_CONJUGATION	-1.96292	0.006699
KEGG_PENTOSE_AND_GLUCURONATE_INTERCONVERSIONS	-1.96071	0.006521
KEGG_ASCORBATE_AND_ALDARATE_METABOLISM	-1.94457	0.007975
BIOC_INTRINSIC_PATHWAY	-1.91083	0.012805
BIOLOGICAL_OXIDATIONS	-1.88159	0.019758
KEGG_GLUTATHIONE_METABOLISM	-1.8629	0.023742
REGULATION_OF_COMPLEMENT_CASCADE	-1.84717	0.028113
REGULATION_OF_CHOLESTEROL_BIOSYNTHESIS_BY_SREBF_SREBF	-1.84236	0.028965
WP460_BLOOD_CLOTTING_CASCADE	-1.83309	0.031678
THE_CANONICAL_RETINOID_CYCLE_IN_RODS_TWILIGHT_VISION	-1.81551	0.037675
KEGG_PORPHYRIN_AND_CHLOROPHYLL_METABOLISM	-1.81037	0.038607
KEGG_RETINOL_METABOLISM	-1.8002	0.04153
FATTY_ACYL_COA_BIOSYNTHESIS	-1.79554	0.042424
TRANSLATION	-1.79509	0.04142
IRE1ALPHA_ACTIVATES_CHAPERONES	-1.7919	0.041556
POST_ELONGATION_PROCESSING_OF_INTRONLESS_PRE_MRNA	-1.78977	0.041079
KEGG_TYROSINE_METABOLISM	-1.78139	0.044652
PROCESSING_OF_CAPPED_INTRONLESS_PRE_MRNA	-1.76171	0.053398
FORMATION_OF_FIBRIN_CLOT_CLOTTING_CASCADE	-1.76154	0.052007
KEGG_MISMATCH_REPAIR	-1.75483	0.054657
STEROID_HORMONES	-1.7414	0.062243
METABOLISM_OF_STEROID_HORMONES_AND_VITAMIN_D	-1.73476	0.065652
KEGG_STARCH_AND_SUCROSE_METABOLISM	-1.70642	0.085827
MITOCHONDRIAL_TRANSLATION	-1.7002	0.089042
KEGG_AMINOACYL_TRNA_BIOSYNTHESIS	-1.69349	0.092723

B



D



Supplemental figure 1. Pathway analysis of the effect of fasting on hepatic gene expression.

A) Gene sets positively enriched by fasting according to GSEA (FDR q value > 0.1). Gene sets are ranked according to Normalized Enrichment Score. B) Heatmaps of WP1269.FATTY.ACID.BETA.OXIDATION and PEROXISOME. The heatmap shows the changes in gene expression by fasting for the positively enriched genes in the two gene sets, expressed as signal log ratio. The average signal log ratio of the fed mice was set at 0. Red indicates upregulated, blue indicates downregulated. C) Gene sets negatively enriched by fasting according to GSEA (FDR q value > 0.1). Gene sets are ranked according to Normalized Enrichment Score. D) The heatmap shows the changes in gene expression by fasting for the negatively enriched genes in the gene set CHOLESTEROL.BIOSYNTHESIS. The average signal log ratio of the fed mice was set at 0. Red indicates upregulated, blue indicates downregulated.

Supplemental table 1. Genes significantly increased by 24h fasting in mouse liver (P<0.001)

<i>gene name</i>	FC	P value	<i>gene name</i>	FC	P value
<i>Cyp4a14</i>	55.70	4.4E-16	<i>Slc22a3</i>	4.56	1.9E-11
<i>Cyp4a31</i>	44.94	4.4E-16	<i>Acot4</i>	4.49	6.5E-09
<i>Fgf21</i>	29.43	5.3E-08	<i>Chpf2</i>	4.27	6.4E-09
<i>Cidec</i>	29.13	2.0E-13	<i>Fkbp5</i>	4.25	8.8E-07
<i>Vnn1</i>	27.14	4.4E-11	<i>Fbxo21</i>	4.21	2.5E-09
<i>Mt2</i>	23.60	2.1E-06	<i>Tmem120a</i>	4.19	4.4E-16
<i>Cyp17a1</i>	22.79	2.1E-08	<i>St3gal5</i>	4.18	2.3E-06
<i>Dbp</i>	16.55	1.1E-11	<i>Plin5</i>	4.12	4.6E-07
<i>Rad51b</i>	15.22	1.3E-09	<i>Csad</i>	4.06	2.0E-05
<i>Chrna2</i>	13.82	1.3E-15	<i>Pigp</i>	3.93	6.1E-12
<i>Acot2</i>	12.84	5.1E-12	<i>Cntrl</i>	3.92	4.3E-07
<i>Acot1</i>	12.07	2.7E-17	<i>Cgref1</i>	3.82	4.3E-08
<i>Cyp7a1</i>	10.92	5.1E-06	<i>Zkscan17</i>	3.81	6.0E-08
<i>Ren1</i>	10.86	4.8E-09	<i>Aqp4</i>	3.81	3.4E-05
<i>Cyp2c38</i>	10.63	4.7E-08	<i>Zbed5</i>	3.72	2.8E-11
<i>Txnip</i>	10.17	3.5E-11	<i>Sox6os</i>	3.68	1.4E-12
<i>Lamb3</i>	8.45	1.3E-10	<i>Gadd45b</i>	3.67	5.0E-08
<i>Plin4</i>	8.14	3.1E-05	<i>Lipg</i>	3.66	4.4E-06
<i>Krt23</i>	8.03	1.4E-12	<i>Agpat3</i>	3.63	4.7E-10
<i>Pex11a</i>	7.26	1.6E-14	<i>Qpct</i>	3.51	6.7E-10
<i>Lgals4</i>	7.20	2.4E-09	<i>Atp10d</i>	3.51	7.0E-10
<i>Crat</i>	7.17	3.5E-14	NA	3.48	4.5E-09
<i>Lepr</i>	7.10	6.4E-08	<i>2410022M11Rik</i>	3.48	2.7E-06
<i>Nceh1</i>	7.00	5.7E-13	<i>Cbfa2t3</i>	3.44	1.9E-11
<i>Slc16a5</i>	6.89	1.2E-09	<i>Mfsd7c</i>	3.44	6.0E-10
<i>Cyp39a1</i>	6.86	5.6E-05	<i>Wdr73</i>	3.44	6.6E-11
<i>Fmo2</i>	6.15	1.0E-08	<i>Aldh3a2</i>	3.44	1.7E-09
<i>Pctp</i>	6.08	2.6E-10	<i>Tmem98</i>	3.40	1.4E-07
<i>Abca6</i>	6.01	5.0E-11	<i>Vwa8</i>	3.39	4.6E-11
<i>Por</i>	5.99	1.3E-12	<i>Gpcpd1</i>	3.39	1.4E-05
<i>2010003K11Rik</i>	5.61	1.6E-05	<i>Arl4a</i>	3.39	1.7E-09
<i>Inhbe</i>	5.54	3.7E-04	<i>Slc4a4</i>	3.38	1.1E-14
<i>Bhlhb9</i>	5.41	7.0E-11	<i>Adcy6</i>	3.36	5.3E-09
<i>Psmd9</i>	5.28	4.4E-16	<i>Cpt1a</i>	3.33	2.7E-15
<i>Ehhadh</i>	5.28	6.7E-16	<i>2410006H16Rik</i>	3.33	2.8E-07
<i>Mfsd2a</i>	5.10	2.3E-04	<i>1810055G02Rik</i>	3.28	6.6E-06
<i>Peg3</i>	5.06	1.7E-07	<i>Tdrp</i>	3.27	3.0E-10
<i>4833411C07Rik</i>	5.02	1.2E-08	<i>Paqr3</i>	3.26	2.6E-10
<i>Fam131c</i>	4.92	5.8E-11	<i>Retsat</i>	3.26	3.1E-10
<i>Pdk4</i>	4.89	2.4E-05	<i>Ctse</i>	3.25	1.2E-10
<i>Cirbp</i>	4.81	1.4E-08	<i>Fbxo31</i>	3.16	3.2E-09
<i>Aprt</i>	4.80	5.3E-15	<i>Tmed5</i>	3.16	6.7E-13
<i>4931408D14Rik</i>	4.77	3.4E-06	<i>Cda</i>	3.12	1.7E-06
<i>Tmtc2</i>	4.73	2.2E-11	<i>Slc25a22</i>	3.12	3.1E-08
<i>Unc119</i>	4.64	4.1E-11	<i>Cyp8b1</i>	3.09	1.4E-08
<i>G0s2</i>	4.57	2.4E-04	<i>Pgm3</i>	3.07	8.4E-10

gene name	FC	P value
<i>Slc25a30</i>	3.06	8.0E-05
<i>Grpel2</i>	3.05	6.9E-06
<i>Rusc2</i>	3.03	3.2E-06
<i>Bche</i>	3.01	1.3E-08
<i>Igsf11</i>	2.99	2.7E-11
<i>Agpat9</i>	2.97	2.1E-10
<i>Acot8</i>	2.96	3.1E-13
<i>Cox6b2</i>	2.95	7.0E-09
<i>Eps8</i>	2.95	1.0E-06
<i>Ufd1l</i>	2.89	2.2E-06
<i>Pspc1</i>	2.89	3.1E-07
<i>Arsg</i>	2.89	9.8E-09
<i>Slc16a7</i>	2.88	4.0E-09
<i>2310061J03Rik</i>	2.87	4.2E-11
<i>Rcan2</i>	2.87	4.1E-06
<i>Sel1l3</i>	2.87	8.7E-06
<i>Slco1a4</i>	2.87	1.7E-10
<i>Myliip</i>	2.84	1.8E-06
<i>4930480G23Rik</i>	2.83	3.0E-06
<i>Tef</i>	2.82	2.0E-08
<i>Acot12</i>	2.78	3.8E-13
<i>Sdsl</i>	2.78	9.5E-08
<i>Abcb4</i>	2.77	1.6E-11
<i>Sec22c</i>	2.75	1.1E-07
<i>Elmod3</i>	2.75	2.6E-08
<i>Brcc3</i>	2.73	2.1E-09
<i>Trib3</i>	2.72	1.4E-04
<i>0610040B10Rik</i>	2.72	2.9E-08
<i>Nnmt</i>	2.71	1.4E-04
<i>Hsd12</i>	2.68	4.6E-13
<i>Grn</i>	2.67	0.0E+00
<i>Hsd17b10</i>	2.66	0.0E+00
<i>Pank1</i>	2.66	5.4E-10
<i>Fabp2</i>	2.66	5.4E-08
<i>Tor1b</i>	2.64	3.6E-12
<i>Brap</i>	2.64	3.8E-09
<i>Fgl1</i>	2.64	4.8E-04
<i>Slc25a32</i>	2.63	1.4E-06
<i>Smyd4</i>	2.62	4.8E-09
<i>Oplah</i>	2.62	2.2E-13
<i>Pcx</i>	2.61	2.3E-12
<i>Paqr7</i>	2.60	2.5E-06
<i>Tbx3</i>	2.60	3.9E-04
<i>Nudt18</i>	2.58	7.1E-09
<i>Tor3a</i>	2.58	7.1E-04
<i>Aifm2</i>	2.58	1.5E-07
<i>1810010H24Rik</i>	2.57	5.6E-08

gene name	FC	P value
<i>Rrp36</i>	2.57	4.6E-07
<i>Mzt1</i>	2.55	3.0E-07
<i>Hscb</i>	2.55	2.1E-07
<i>Usp40</i>	2.54	3.0E-04
<i>Csrp3</i>	2.54	9.2E-08
<i>Fam208a</i>	2.49	2.1E-04
<i>Ech1</i>	2.46	3.7E-11
<i>Apoa4</i>	2.46	4.4E-16
<i>Slc25a20</i>	2.46	4.6E-13
<i>Fgfr1</i>	2.45	2.7E-06
<i>Pcsk4</i>	2.44	2.5E-08
<i>5031439G07Rik</i>	2.43	1.6E-09
<i>Baiap2l1</i>	2.41	9.3E-09
<i>Eci1</i>	2.40	2.2E-13
<i>Mtor</i>	2.40	1.1E-12
<i>Fam13a</i>	2.39	3.8E-04
<i>A1cf</i>	2.39	3.3E-07
<i>Alpl</i>	2.38	1.4E-07
<i>Rab34</i>	2.37	1.5E-05
<i>Lhpp</i>	2.37	2.8E-08
<i>Tenc1</i>	2.37	4.3E-06
<i>Pla2g12a</i>	2.37	9.5E-10
<i>Slc6a9</i>	2.36	1.6E-06
<i>Clstn3</i>	2.34	7.1E-10
<i>Plin2</i>	2.34	3.0E-13
<i>Polr1b</i>	2.34	1.7E-05
<i>Dclre1a</i>	2.32	2.6E-05
<i>Atf5</i>	2.32	1.9E-06
<i>Rin2</i>	2.31	3.7E-05
<i>Cyp2j9</i>	2.29	4.9E-06
<i>Tor1a</i>	2.27	4.5E-12
<i>Tlr5</i>	2.27	9.1E-07
<i>Sun2</i>	2.27	9.2E-09
<i>Fam195a</i>	2.23	9.0E-12
<i>Pi4ka</i>	2.22	8.9E-12
<i>Arel1</i>	2.22	2.6E-09
<i>Pdgfra</i>	2.21	7.2E-06
<i>Tmem82</i>	2.20	3.3E-09
<i>Ddhd2</i>	2.20	2.1E-08
<i>Igfbp2</i>	2.20	7.6E-09
<i>D17Wsu92e</i>	2.19	2.0E-04
<i>Slc25a12</i>	2.19	2.8E-09
<i>Slc25a47</i>	2.19	3.4E-08
<i>Tldc1</i>	2.17	6.5E-05
<i>Pcbp2</i>	2.17	1.3E-07
<i>Dnmbp</i>	2.17	1.4E-04
<i>Smim4</i>	2.17	6.9E-09

gene name	FC	P value
<i>Pilp</i>	2.16	7.3E-08
<i>Tmem106b</i>	2.16	7.7E-08
<i>Optn</i>	2.15	2.0E-11
<i>Tmem56</i>	2.15	6.0E-12
<i>Palmd</i>	2.15	5.6E-11
<i>Gpd1</i>	2.15	1.0E-06
<i>Nprl3</i>	2.15	9.7E-05
<i>Aim1</i>	2.14	7.2E-06
<i>Slc52a2</i>	2.14	3.4E-06
<i>Gpatch2l</i>	2.13	1.4E-06
<i>Dync1li1</i>	2.13	2.5E-04
<i>Rogdi</i>	2.12	4.4E-09
<i>Etfdh</i>	2.12	1.4E-11
<i>Ddb2</i>	2.11	2.4E-07
<i>Hadha</i>	2.09	5.8E-11
<i>Zscan21</i>	2.09	6.1E-05
<i>Tenm3</i>	2.09	1.0E-06
<i>Hyal2</i>	2.09	7.0E-09
<i>Paqr9</i>	2.09	3.5E-04
<i>Npc1</i>	2.09	2.2E-10
<i>Eci2</i>	2.09	2.0E-11
<i>Prpf40a</i>	2.08	4.5E-04
<i>Tatdn2</i>	2.08	4.1E-05
<i>Pex14</i>	2.08	1.9E-07
<i>Decr1</i>	2.07	2.1E-13
<i>Snhg5</i>	2.07	8.2E-04
<i>Slc1a2</i>	2.07	8.6E-05
<i>Galnt2</i>	2.07	9.2E-06
<i>Mmp14</i>	2.07	2.1E-04
<i>Ube2e2</i>	2.07	9.3E-10
<i>Tor1aip1</i>	2.06	3.3E-07
<i>Vnn3</i>	2.06	3.2E-07
<i>Scyl2</i>	2.06	3.2E-05
<i>Fzd4</i>	2.06	1.5E-06
<i>Zfp672</i>	2.05	4.1E-05
<i>Clmn</i>	2.05	1.1E-04
<i>Wdr34</i>	2.05	3.3E-06
<i>Asic5</i>	2.05	2.1E-06
<i>Dact2</i>	2.05	1.1E-04
<i>Zfp777</i>	2.04	3.9E-07
<i>Tubgcp2</i>	2.03	9.7E-07
<i>Ldb1</i>	2.03	1.7E-07
<i>Hddc3</i>	2.02	6.1E-08
<i>Ppara</i>	2.02	1.9E-04
<i>Odf3b</i>	2.01	6.5E-06
<i>Polr3gl</i>	2.01	1.2E-04
<i>Bcap29</i>	2.00	1.1E-09

gene name	FC	P value
<i>Fam126b</i>	2.00	7.4E-08
<i>Gpt2</i>	2.00	2.1E-10
<i>Gstt2</i>	1.99	6.3E-12
<i>9130401M01Rik</i>	1.99	2.0E-08
<i>Tmpo</i>	1.98	8.2E-09
<i>Amigo2</i>	1.98	1.4E-06
<i>Ilvbl</i>	1.97	2.2E-07
<i>Taok3</i>	1.97	2.4E-09
<i>Zc3h14</i>	1.97	3.1E-07
<i>Hsd17b11</i>	1.97	2.0E-13
<i>Nrbp2</i>	1.97	1.8E-07
<i>Zfp612</i>	1.97	9.2E-04
<i>Ppap2c</i>	1.97	7.0E-05
<i>Zfp746</i>	1.96	4.3E-05
<i>1190005I06Rik</i>	1.96	6.1E-06
<i>Bin3</i>	1.94	2.8E-07
<i>Acadl</i>	1.94	9.1E-13
<i>Gaa</i>	1.94	1.7E-08
<i>Dhrs13</i>	1.94	3.0E-06
<i>Dgka</i>	1.94	1.5E-05
<i>Smco4</i>	1.94	6.8E-04
<i>Pck1</i>	1.94	1.9E-06
<i>Nr1h4</i>	1.94	3.9E-07
<i>Hykk</i>	1.94	9.8E-05
<i>Haus4</i>	1.93	3.8E-06
<i>Acad10</i>	1.93	3.5E-06
<i>Snhg12</i>	1.93	8.1E-04
<i>Galk1</i>	1.93	4.1E-09
<i>Adora1</i>	1.93	3.9E-05
<i>Xpa</i>	1.93	7.9E-11
<i>Ofd1</i>	1.93	6.2E-06
<i>Mat1a</i>	1.92	1.4E-12
<i>1700008J07Rik</i>	1.92	1.6E-05
<i>Nr1d2</i>	1.92	3.8E-06
<i>Fbxl12</i>	1.92	1.5E-05
<i>BC020402</i>	1.92	1.8E-05
<i>Creb3</i>	1.92	5.2E-07
<i>Uhrf1bp1l</i>	1.91	1.8E-09
<i>Extl1</i>	1.91	3.1E-06
<i>Ifngr2</i>	1.91	5.5E-06
<i>2810013P06Rik</i>	1.91	3.1E-04
<i>Kctd15</i>	1.91	4.5E-05
<i>Smim19</i>	1.91	2.1E-07
<i>Slc25a42</i>	1.91	7.6E-05
<i>Pex3</i>	1.90	4.3E-09
<i>Ivns1abp</i>	1.90	4.8E-05
<i>Cpt2</i>	1.90	5.6E-13

gene name	FC	P value
<i>Phykpl</i>	1.89	4.6E-09
<i>Slc35g1</i>	1.89	2.2E-05
<i>Tspan31</i>	1.89	5.6E-12
<i>Dcun1d4</i>	1.89	1.4E-05
<i>Fam73b</i>	1.88	4.7E-08
<i>Calcoco1</i>	1.88	9.0E-06
<i>Fmo4</i>	1.88	7.0E-05
<i>Acad11</i>	1.88	4.1E-13
<i>Lrp4</i>	1.88	2.7E-05
<i>Abhd1</i>	1.88	4.0E-09
<i>Ttc23</i>	1.88	6.7E-07
<i>Slc41a3</i>	1.88	3.9E-05
<i>Zfp655</i>	1.87	5.7E-04
<i>Cdip1</i>	1.87	3.8E-08
<i>Tmem62</i>	1.87	1.8E-05
<i>Cpsf4l</i>	1.87	3.4E-05
<i>Abhd2</i>	1.87	3.0E-05
<i>Tug1</i>	1.87	2.4E-05
<i>Acadm</i>	1.86	3.2E-09
<i>Rtn4</i>	1.86	4.0E-04
<i>Plekhg3</i>	1.86	1.6E-04
<i>Nmrk1</i>	1.86	2.1E-05
<i>Prune</i>	1.85	3.2E-05
<i>Tmem86a</i>	1.85	3.9E-05
<i>Golt1a</i>	1.85	7.5E-09
<i>Commd5</i>	1.85	3.6E-05
<i>Agpat6</i>	1.84	2.6E-04
<i>Gpd2</i>	1.84	2.2E-07
<i>Pddc1</i>	1.84	5.7E-05
<i>Hmgcs2</i>	1.84	2.0E-08
<i>Dcaf6</i>	1.84	9.0E-07
<i>Adat2</i>	1.84	2.7E-05
<i>Nr1i2</i>	1.84	2.9E-04
<i>Slc17a1</i>	1.83	3.0E-04
<i>Slc25a10</i>	1.83	8.8E-08
<i>Asl</i>	1.83	3.1E-09
<i>Atp5s</i>	1.83	8.4E-06
<i>Ppapdc1b</i>	1.82	3.0E-04
<i>Ptplad1</i>	1.82	7.1E-12
<i>Ece2</i>	1.82	1.3E-06
<i>Plcl2</i>	1.81	5.3E-07
<i>Cblc</i>	1.81	1.1E-05
<i>Mamdc2</i>	1.81	8.8E-04
<i>Als2cl</i>	1.81	5.5E-08
<i>Casp8</i>	1.81	1.8E-05
<i>Kctd9</i>	1.80	5.2E-07
<i>Aig1</i>	1.80	1.9E-04

gene name	FC	P value
<i>Cers6</i>	1.80	3.6E-04
<i>Kdsr</i>	1.80	7.9E-07
<i>Vwce</i>	1.80	9.2E-05
<i>Mmachc</i>	1.80	8.7E-06
<i>Lrrc28</i>	1.80	2.2E-05
<i>Mppe1</i>	1.80	3.8E-04
<i>Acat1</i>	1.79	1.6E-08
<i>Sorbs3</i>	1.79	2.3E-05
<i>Tnfaip8l1</i>	1.79	1.5E-04
<i>Nt5c2</i>	1.79	6.8E-05
<i>Zc3h13</i>	1.78	1.3E-06
<i>Vipas39</i>	1.78	2.5E-05
<i>Il17rb</i>	1.78	3.0E-05
<i>Plbd1</i>	1.78	6.3E-08
<i>Zfp444</i>	1.78	6.9E-05
<i>Mapk1ip1</i>	1.78	6.3E-05
<i>Wbp1l</i>	1.78	2.1E-06
<i>Impact</i>	1.78	2.8E-05
<i>Atxn10</i>	1.77	3.2E-10
<i>Tha1</i>	1.77	8.1E-04
<i>Dlgap4</i>	1.77	2.5E-05
<i>Nle1</i>	1.77	8.0E-05
<i>Flot1</i>	1.76	4.0E-05
<i>Rhot2</i>	1.76	7.4E-05
<i>Adck2</i>	1.76	1.5E-06
<i>Sft2d3</i>	1.76	5.8E-04
<i>Gfra1</i>	1.76	6.1E-08
<i>Il15ra</i>	1.76	1.4E-04
<i>Khdrbs3</i>	1.75	3.6E-05
<i>Odf2</i>	1.75	9.9E-04
<i>Reep4</i>	1.75	4.2E-06
<i>Insig2</i>	1.75	1.6E-09
<i>Ell</i>	1.75	9.1E-06
<i>Cul4b</i>	1.75	1.6E-05
<i>Pex19</i>	1.74	8.2E-04
<i>Reps1</i>	1.74	3.8E-05
<i>Ubr3</i>	1.74	1.2E-09
<i>Klb</i>	1.73	3.2E-04
<i>Zfp956</i>	1.73	8.5E-04
<i>Cdc42bpg</i>	1.73	6.8E-05
<i>Atg2a</i>	1.73	1.2E-04
<i>Lrrc20</i>	1.72	6.8E-06
<i>Trub2</i>	1.72	1.5E-07
<i>Ephx2</i>	1.72	7.7E-13
<i>Tmed4</i>	1.72	1.1E-08
<i>Slc39a2</i>	1.72	9.1E-04
<i>Tbc1d16</i>	1.72	3.8E-05

gene name	FC	P value
<i>Sorbs1</i>	1.72	4.1E-05
<i>Gpatch4</i>	1.72	2.3E-04
<i>Mybbp1a</i>	1.71	6.9E-04
<i>Zcchc11</i>	1.71	8.9E-06
<i>Treh</i>	1.71	3.5E-04
<i>Siah2</i>	1.71	5.8E-04
<i>Mtnr1a</i>	1.70	6.8E-05
<i>Arsa</i>	1.70	1.1E-07
<i>Lmo7</i>	1.70	2.8E-05
<i>Inpp5k</i>	1.70	7.3E-06
<i>Bag4</i>	1.69	1.6E-04
<i>Sgms1</i>	1.69	3.2E-04
<i>Lgals8</i>	1.69	1.2E-07
<i>Aptx</i>	1.69	9.7E-07
<i>Zbtb44</i>	1.69	7.2E-07
<i>Spryd3</i>	1.69	1.7E-05
<i>Ddx28</i>	1.69	8.9E-04
<i>Fas</i>	1.69	3.3E-06
<i>Gyk</i>	1.69	3.1E-06
<i>2010012005Rik</i>	1.69	4.6E-04
<i>Tmem243</i>	1.69	5.6E-09
<i>Uvssa</i>	1.68	8.1E-07
<i>Gpr146</i>	1.68	3.4E-05
<i>Ctsf</i>	1.68	2.8E-05
<i>Atr</i>	1.68	9.9E-06
<i>Ttc3</i>	1.68	1.4E-04
<i>Anxa7</i>	1.68	7.1E-06
<i>Acox1</i>	1.68	1.6E-12
<i>Gys2</i>	1.67	2.6E-06
<i>Ubr5</i>	1.67	3.4E-07
<i>Hook2</i>	1.67	1.8E-04
<i>L3mbtl3</i>	1.67	7.7E-04
<i>Slc43a3</i>	1.67	8.1E-05
<i>Tmem184a</i>	1.67	4.9E-04
<i>Atl2</i>	1.67	2.8E-07
<i>Nat9</i>	1.67	1.3E-07
<i>Slc12a9</i>	1.67	1.0E-06
<i>Cmb1</i>	1.66	1.1E-12
<i>Acaa1b</i>	1.66	3.0E-06
<i>Fam160b2</i>	1.66	1.0E-05
<i>Atg16l1</i>	1.66	3.5E-05
<i>Ankrd16</i>	1.66	7.1E-04
<i>Ssc4d</i>	1.66	1.9E-04
<i>Stamos</i>	1.66	9.6E-05
<i>Nln</i>	1.65	2.2E-05
<i>2310011J03Rik</i>	1.65	7.1E-05
<i>Ranbp10</i>	1.65	7.2E-06

gene name	FC	P value
<i>Cpox</i>	1.65	1.2E-07
<i>Gna12</i>	1.65	4.7E-05
<i>Mocs3</i>	1.65	2.5E-04
<i>4930506M07Rik</i>	1.65	6.4E-05
<i>Bzw1</i>	1.64	3.2E-06
<i>Rabl3</i>	1.64	1.9E-06
<i>Slc25a46</i>	1.64	6.4E-07
<i>Def8</i>	1.64	3.8E-05
<i>Hsd17b4</i>	1.64	2.5E-12
<i>Flnb</i>	1.64	3.7E-04
<i>Klhl7</i>	1.64	5.6E-04
<i>Plscr3</i>	1.64	1.9E-05
<i>Aco2</i>	1.64	8.1E-09
<i>Zxdc</i>	1.64	4.6E-05
<i>Firre</i>	1.63	2.1E-05
<i>Kif21a</i>	1.63	3.5E-04
<i>Guk1</i>	1.63	8.5E-04
<i>Nisch</i>	1.63	3.2E-04
<i>Mrpl9</i>	1.63	1.2E-04
<i>1110054M08Rik</i>	1.63	2.5E-04
<i>Tk2</i>	1.63	7.9E-05
<i>Denr</i>	1.63	6.3E-04
<i>Tmem131</i>	1.63	8.4E-06
<i>Smim20</i>	1.63	5.3E-06
<i>Psap</i>	1.62	2.1E-06
<i>Fam160b1</i>	1.62	5.8E-06
<i>Ltbr</i>	1.62	9.0E-07
<i>Heca</i>	1.62	1.9E-07
<i>Map1lc3a</i>	1.62	9.1E-07
<i>Kif1b</i>	1.62	1.2E-08
<i>Ogdh</i>	1.62	2.8E-09
<i>Lrg1</i>	1.62	8.0E-07
<i>Hgs</i>	1.62	8.3E-06
<i>Sec23a</i>	1.62	9.6E-10
<i>Rapgef1</i>	1.61	1.5E-04
<i>Pawr</i>	1.61	5.2E-04
<i>Ptpn6</i>	1.61	4.1E-05
<i>Brpf3</i>	1.61	1.3E-04
<i>Vkorc1l1</i>	1.61	3.2E-05
<i>Sntb1</i>	1.61	1.1E-04
<i>Setd1b</i>	1.60	4.0E-04
<i>C1qtnf1</i>	1.60	1.2E-04
<i>Ap4m1</i>	1.60	1.2E-05
<i>Vamp2</i>	1.60	4.7E-04
<i>Eno3</i>	1.60	2.4E-04
<i>Ythdc2</i>	1.60	2.3E-04
<i>Ppap2b</i>	1.60	2.3E-06

gene name	FC	P value
<i>Mtg1</i>	1.60	8.3E-05
<i>Tmem30b</i>	1.60	7.0E-09
<i>Arih2</i>	1.59	9.9E-05
<i>Ei24</i>	1.59	4.4E-10
<i>Znf512b</i>	1.59	7.7E-04
<i>Elovl5</i>	1.59	2.2E-08
<i>R3hcc1</i>	1.59	4.2E-05
<i>Fcgrt</i>	1.59	1.3E-08
<i>Srxn1</i>	1.59	5.4E-06
<i>Slc27a2</i>	1.59	2.4E-12
<i>Golga5</i>	1.59	1.5E-05
<i>Sbds</i>	1.59	1.3E-04
<i>Zahhc13</i>	1.59	7.8E-04
<i>Tmem135</i>	1.59	1.5E-06
<i>Cpd</i>	1.59	2.2E-04
<i>O610005C13Rik</i>	1.58	1.6E-07
<i>Z310039H08Rik</i>	1.58	3.5E-08
<i>Slc25a13</i>	1.58	5.5E-08
<i>Gatad2a</i>	1.58	1.6E-07
<i>Usp22</i>	1.58	2.7E-06
<i>Ctf1</i>	1.58	3.0E-04
<i>Pqhc2</i>	1.58	2.1E-05
<i>Ermp1</i>	1.58	5.7E-04
<i>Dhrs4</i>	1.58	1.4E-09
<i>Dusp22</i>	1.58	7.5E-05
<i>Eif1</i>	1.58	4.3E-06
<i>Tspo</i>	1.57	1.1E-08
<i>Gtdc1</i>	1.57	8.9E-04
<i>Ccdc82</i>	1.57	4.6E-04
<i>Cnst</i>	1.57	6.5E-04
<i>Dusp3</i>	1.57	2.4E-06
<i>Zwint</i>	1.57	1.9E-05
<i>Arl15</i>	1.56	1.9E-05
<i>Fra10ac1</i>	1.56	6.1E-05
<i>Prkrir</i>	1.56	2.2E-05
<i>Acsm3</i>	1.56	1.0E-07
<i>Elovl2</i>	1.56	5.1E-09
<i>Ccnd3</i>	1.56	8.1E-06
<i>Gltscr2</i>	1.56	1.4E-04
<i>Usp38</i>	1.56	4.7E-04
<i>Coq3</i>	1.56	6.5E-04
<i>Samm50</i>	1.56	8.3E-08
<i>Txnac8</i>	1.56	7.2E-06
<i>Trim25</i>	1.55	2.0E-04
<i>Rbms1</i>	1.55	5.7E-05
<i>Mapre3</i>	1.55	2.3E-04
<i>Pqbp1</i>	1.55	3.0E-05
<i>Creb3l3</i>	1.55	6.1E-07

gene name	FC	P value
<i>Fkbp15</i>	1.55	3.2E-05
<i>Pbld1</i>	1.55	2.5E-06
<i>Tesk1</i>	1.55	2.6E-05
<i>Nfx1</i>	1.55	9.4E-05
<i>Klhdc3</i>	1.54	1.3E-06
<i>Psmc4</i>	1.54	1.1E-08
<i>Mtm1</i>	1.54	6.9E-04
<i>1500012F01Rik</i>	1.54	6.4E-04
<i>Lbp</i>	1.54	9.7E-08
<i>Ermard</i>	1.54	1.5E-04
<i>Acadvl</i>	1.54	2.8E-10
<i>Pcyt1a</i>	1.54	9.8E-05
<i>Dlst</i>	1.54	1.4E-09
<i>Eftud1</i>	1.54	1.6E-04
<i>Itga7</i>	1.54	2.8E-04
<i>lkbkap</i>	1.54	9.6E-04
<i>Slc37a4</i>	1.54	1.8E-06
<i>Afg3l2</i>	1.53	2.1E-05
<i>Eif4b</i>	1.53	5.3E-04
<i>Entpd5</i>	1.53	4.1E-10
<i>Sycp3</i>	1.53	4.6E-04
<i>Mbtps2</i>	1.53	7.1E-05
<i>Aaed1</i>	1.53	3.2E-07
<i>Mpdu1</i>	1.53	1.1E-08
<i>Clip1</i>	1.53	1.7E-05
<i>Nek3</i>	1.52	6.4E-04
<i>Cdk6</i>	1.52	1.6E-04
<i>Aass</i>	1.52	6.1E-06
<i>Adam23</i>	1.52	2.5E-04
<i>Wsb2</i>	1.52	3.8E-05
<i>Zc3h7b</i>	1.52	2.8E-04
<i>Pex1</i>	1.51	6.8E-06
<i>Phka2</i>	1.51	9.2E-04
<i>Apoa5</i>	1.51	5.6E-06
<i>Tmem41a</i>	1.51	7.5E-04
<i>lpo5</i>	1.51	1.3E-04
<i>Minpp1</i>	1.51	5.8E-06
<i>Zfp362</i>	1.51	6.4E-05
<i>Ptpmt1</i>	1.50	3.6E-09
<i>Naa50</i>	1.50	2.8E-06
<i>Gpr116</i>	1.50	1.3E-04
<i>Snx33</i>	1.50	7.5E-04
<i>Crbn</i>	1.50	3.8E-05
<i>Atad3a</i>	1.50	1.4E-07
<i>Araf</i>	1.50	2.7E-07
<i>Trim23</i>	1.50	1.3E-04
<i>Fam102a</i>	1.50	9.9E-04
<i>Copz2</i>	1.50	2.4E-05

gene name	FC	P value
<i>Mri1</i>	1.50	6.4E-04
<i>D5Erttd579e</i>	1.49	2.8E-04
<i>Cttnnb1</i>	1.49	7.4E-04
<i>Ifnar2</i>	1.49	7.3E-09
<i>Snta1</i>	1.49	9.3E-04
<i>1600012H06Rik</i>	1.49	3.2E-07
<i>Fads2</i>	1.49	6.7E-04
<i>Ttc19</i>	1.49	6.5E-05
<i>Tmem259</i>	1.49	2.9E-06
<i>Atp1a1</i>	1.49	2.8E-05
<i>Cnppd1</i>	1.49	1.4E-04
<i>Rad51d</i>	1.48	6.5E-04
<i>Wdr36</i>	1.48	9.9E-05
<i>Ddx52</i>	1.48	4.2E-04
<i>Crot</i>	1.48	8.2E-05
<i>Fam98c</i>	1.48	8.7E-05
<i>Perp</i>	1.48	2.4E-06
<i>Ttpa</i>	1.48	6.2E-11
<i>Btbd6</i>	1.48	2.9E-04
<i>Xrn2</i>	1.48	3.0E-05
<i>Ncl</i>	1.48	8.0E-04
<i>Rad23a</i>	1.48	5.4E-05
<i>Abi1</i>	1.47	4.3E-04
<i>Fez2</i>	1.47	1.7E-05
<i>Cenpb</i>	1.47	1.7E-04
<i>Slc25a28</i>	1.47	3.5E-05
<i>Timm10</i>	1.47	1.4E-04
<i>Scand1</i>	1.47	1.8E-04
<i>Phf14</i>	1.47	1.1E-05
<i>Phb2</i>	1.47	7.5E-10
<i>BC048403</i>	1.46	4.9E-05
<i>Apmap</i>	1.46	1.9E-05
<i>Josd1</i>	1.46	2.3E-04
<i>2610008E11Rik</i>	1.46	2.8E-04
<i>Tango2</i>	1.46	1.4E-04
<i>Gnl2</i>	1.46	2.3E-04
<i>Med15</i>	1.46	3.5E-04
<i>Abcc3</i>	1.46	3.5E-06
<i>Vps11</i>	1.46	5.4E-04
<i>Fastk</i>	1.46	8.0E-06
<i>Tsks</i>	1.46	1.2E-04
<i>Hmgcl</i>	1.46	3.9E-09
<i>Myd88</i>	1.46	4.9E-04
<i>Paip1</i>	1.45	1.1E-04
<i>R3hdm2</i>	1.45	8.7E-07
<i>Eme2</i>	1.45	5.6E-04
<i>Ssx2ip</i>	1.45	4.4E-04

gene name	FC	P value
<i>Sgk3</i>	1.45	8.6E-04
<i>Accs</i>	1.45	6.3E-04
<i>Lmbrd1</i>	1.45	2.3E-05
<i>Hadh</i>	1.45	1.2E-07
<i>Orc3</i>	1.45	2.7E-04
<i>Hprt</i>	1.45	1.2E-07
<i>Zfp266</i>	1.45	2.7E-04
<i>Slc16a1</i>	1.45	2.8E-07
<i>Cr1s1</i>	1.44	2.8E-07
<i>Arl2</i>	1.44	7.8E-04
<i>Acads</i>	1.44	9.2E-05
<i>Xpot</i>	1.44	4.7E-07
<i>Got1</i>	1.44	1.5E-04
<i>Ppp2r2d</i>	1.43	8.4E-04
<i>Ubxn6</i>	1.43	1.7E-05
<i>Cluh</i>	1.43	2.4E-07
<i>Narf1</i>	1.43	5.1E-04
<i>Fyco1</i>	1.43	2.3E-04
<i>Add3</i>	1.43	8.8E-04
<i>Dram2</i>	1.43	3.0E-06
<i>Yif1a</i>	1.43	2.9E-05
<i>Gch1</i>	1.42	2.6E-04
<i>Ccni</i>	1.42	6.9E-07
<i>Rnf149</i>	1.42	1.5E-07
<i>Wrnip1</i>	1.42	7.6E-06
<i>Rabggtb</i>	1.42	1.2E-05
<i>Hsd17b13</i>	1.42	2.1E-07
<i>Ppa1</i>	1.42	7.8E-07
<i>Nsd1</i>	1.42	3.8E-04
<i>Pxmp4</i>	1.42	2.2E-04
<i>Elac1</i>	1.42	8.1E-04
<i>Esrp2</i>	1.42	8.8E-05
<i>Scyl3</i>	1.41	1.1E-05
<i>Use1</i>	1.41	1.6E-06
<i>Agtr1a</i>	1.41	1.2E-05
<i>Ftsj3</i>	1.41	7.4E-04
<i>Pnpla8</i>	1.41	1.2E-08
<i>Psmd3</i>	1.41	4.4E-06
<i>Kiz</i>	1.41	6.8E-04
<i>Lrrfip1</i>	1.41	4.4E-05
<i>Cmip</i>	1.41	9.9E-04
<i>Arhgap23</i>	1.41	2.4E-04
<i>Slc35b2</i>	1.41	6.1E-04
<i>Dtnbp1</i>	1.41	3.6E-05
<i>Pus10</i>	1.41	8.4E-05
<i>Spast</i>	1.41	7.1E-04
<i>Eif4ebp1</i>	1.40	9.1E-04

gene name	FC	P value
<i>Fam63a</i>	1.40	1.9E-04
<i>Map11c3b</i>	1.40	5.9E-05
<i>Prpf39</i>	1.40	6.5E-04
<i>G3bp2</i>	1.40	3.0E-04
<i>Poldip2</i>	1.40	2.4E-06
<i>Tbp</i>	1.40	9.9E-04
<i>Tmem134</i>	1.40	3.1E-04
<i>Gm5617</i>	1.40	2.8E-04
<i>Lrrc8a</i>	1.39	2.9E-04
<i>Cisd3</i>	1.39	7.4E-04
<i>Dcaf13</i>	1.39	1.8E-05
<i>Tomm40</i>	1.39	9.4E-05
<i>Trak1</i>	1.39	1.8E-04
<i>Alkbh6</i>	1.39	3.5E-04
<i>Aqp9</i>	1.39	3.1E-05
<i>Apon</i>	1.39	3.7E-08
<i>Mmadhc</i>	1.39	3.9E-07
<i>Tbrg1</i>	1.39	2.4E-04
<i>Trip6</i>	1.39	9.4E-04
<i>Slk</i>	1.39	2.9E-04
<i>Mtch2</i>	1.39	6.0E-05
<i>Timm17a</i>	1.38	2.7E-05
<i>Mfn2</i>	1.38	1.8E-06
<i>Hnrnp1</i>	1.38	5.6E-05
<i>Zswim7</i>	1.38	3.1E-04
<i>Serpina3n</i>	1.38	2.2E-05
<i>Mkrn2</i>	1.38	5.0E-04
<i>Grpel1</i>	1.37	1.3E-07
<i>Psmg7</i>	1.37	1.3E-06
<i>Mon2</i>	1.37	1.0E-04
<i>Creg1</i>	1.37	2.1E-07
<i>Mttp</i>	1.37	1.4E-05
<i>Slc27a4</i>	1.37	3.2E-04
<i>Slc17a5</i>	1.37	7.9E-04
<i>Uimc1</i>	1.37	6.7E-04
<i>Ubp1</i>	1.37	2.0E-05
<i>Ddx42</i>	1.37	5.4E-04
<i>Fgf1</i>	1.36	9.6E-04
<i>Manea</i>	1.36	4.1E-04
<i>Rab9</i>	1.36	2.4E-06
<i>Krcc1</i>	1.36	8.9E-05
<i>Ubac1</i>	1.36	5.3E-05
<i>Nnt</i>	1.36	2.5E-04
<i>Smlr1</i>	1.36	3.8E-05
<i>Btd</i>	1.36	3.5E-04
<i>Pigx</i>	1.36	2.3E-04
<i>Gsto1</i>	1.36	5.5E-05

gene name	FC	P value
<i>Sec16b</i>	1.35	1.8E-05
<i>Slc20a2</i>	1.35	1.1E-04
<i>Smpd13a</i>	1.35	2.6E-04
<i>Rtfdc1</i>	1.35	1.5E-04
<i>Gpr180</i>	1.35	5.3E-04
<i>Adtrp</i>	1.35	8.4E-04
<i>Cd1d1</i>	1.35	6.6E-08
<i>Ipo4</i>	1.34	3.4E-04
<i>Vdac2</i>	1.34	1.2E-07
<i>Eif3k</i>	1.34	9.0E-06
<i>Pgm2</i>	1.34	3.1E-06
<i>Ostf1</i>	1.34	1.4E-04
<i>1810044D09Rik</i>	1.34	1.0E-03
<i>Tgoln1</i>	1.34	4.3E-05
<i>Glyr1</i>	1.34	2.7E-05
<i>Aimp1</i>	1.34	3.0E-04
<i>Abcf3</i>	1.34	5.7E-04
<i>Lpcat3</i>	1.34	2.0E-04
<i>F11r</i>	1.34	2.4E-04
<i>Ak2</i>	1.33	8.3E-07
<i>Ccdc6</i>	1.33	6.3E-04
<i>Emc8</i>	1.33	9.1E-04
<i>Matr3</i>	1.33	1.3E-05
<i>Sidt2</i>	1.33	3.2E-05
<i>Prpsap1</i>	1.33	1.3E-05
<i>Phb</i>	1.33	6.8E-04
<i>Rdh14</i>	1.33	1.7E-05
<i>Syap1</i>	1.32	1.5E-06
<i>Chdh</i>	1.32	4.7E-04
<i>Bri3</i>	1.32	5.2E-04
<i>Coa7</i>	1.32	2.7E-04
<i>Cyp3a25</i>	1.32	5.8E-06
<i>Suclg1</i>	1.32	6.8E-08
<i>Cops6</i>	1.32	4.6E-06
<i>Orc5</i>	1.32	9.5E-04
<i>Lcat</i>	1.32	9.8E-07
<i>Reep6</i>	1.31	7.3E-07
<i>Gns</i>	1.31	5.8E-07
<i>Aadat</i>	1.31	1.4E-04
<i>Pgrmc2</i>	1.31	2.1E-04
<i>Napa</i>	1.31	1.8E-04
<i>Mxi1</i>	1.31	2.0E-04
<i>Naprt</i>	1.31	5.6E-04
<i>Cisd1</i>	1.31	2.8E-05
<i>Zranb1</i>	1.31	5.8E-04
<i>Setd2</i>	1.31	7.1E-04
<i>Oxr1</i>	1.31	2.6E-06

gene name	FC	P value
<i>Mertk</i>	1.31	8.0E-04
<i>Txn2</i>	1.30	1.6E-04
<i>Glt25d1</i>	1.30	2.8E-04
<i>Fxr2</i>	1.30	5.5E-04
<i>Ptbp3</i>	1.30	1.3E-04
<i>Cdk17</i>	1.30	4.6E-04
<i>Mrpl40</i>	1.30	8.3E-04
<i>Phax</i>	1.30	2.7E-04
<i>Ehmt2</i>	1.30	8.0E-04
<i>Hspa4</i>	1.30	2.5E-05
<i>Pdxdc1</i>	1.29	7.2E-04
<i>Ctsa</i>	1.29	5.2E-05
<i>Mrps26</i>	1.29	3.5E-04
<i>Polr3c</i>	1.29	4.5E-04
<i>Ccpg1</i>	1.29	2.7E-04
<i>Lims2</i>	1.29	3.8E-04
<i>Prodh2</i>	1.29	1.6E-04
<i>Vamp8</i>	1.29	1.9E-06
<i>Coa5</i>	1.28	4.0E-04
<i>Rabac1</i>	1.28	7.4E-05
<i>Wdr45</i>	1.28	9.5E-04
<i>Mtfr1</i>	1.28	5.5E-05
<i>Cenpv</i>	1.28	8.7E-04
<i>Vps53</i>	1.28	6.9E-04
<i>Copb2</i>	1.28	5.0E-04
<i>Sult1a1</i>	1.28	4.2E-04
<i>Nt5dc1</i>	1.28	6.1E-04
<i>Tm7sf3</i>	1.28	6.8E-04
<i>Cnot7</i>	1.28	1.8E-04
<i>Dpy19l1</i>	1.28	6.1E-04
<i>Slc25a11</i>	1.27	5.2E-04
<i>Chchd2</i>	1.27	1.1E-06
<i>Scarb1</i>	1.27	4.1E-06
<i>Uqcc3</i>	1.27	6.6E-04
<i>Gjb2</i>	1.27	8.1E-04
<i>Pdcd6</i>	1.27	3.6E-07
<i>March8</i>	1.27	4.2E-04
<i>Mtx2</i>	1.26	2.7E-05
<i>Ubqln2</i>	1.26	5.9E-04
<i>Sap30l</i>	1.26	3.2E-04
<i>Tcp1</i>	1.26	4.9E-04
<i>Cbr4</i>	1.26	5.5E-04
<i>Copb1</i>	1.26	4.1E-04
<i>Pa2g4</i>	1.26	6.9E-05
<i>Mtus1</i>	1.26	5.8E-04
<i>Igbbp1</i>	1.26	3.4E-04
<i>Dag1</i>	1.26	6.8E-04

gene name	FC	P value
<i>Chchd10</i>	1.25	1.4E-08
<i>Txndc17</i>	1.25	4.9E-05
<i>Psmc12</i>	1.25	1.7E-05
<i>Psmc4</i>	1.25	1.2E-04
<i>Man2a1</i>	1.25	3.8E-05
<i>Psmb4</i>	1.25	8.1E-06
<i>Eif5</i>	1.24	4.2E-05
<i>Fbp1</i>	1.24	7.3E-07
<i>Hnrnpk</i>	1.24	1.2E-04
<i>Ctage5</i>	1.24	2.2E-06
<i>Insr</i>	1.24	3.7E-04
<i>Nek7</i>	1.23	3.6E-04
<i>Slc38a4</i>	1.23	9.4E-06
<i>Bckdha</i>	1.23	1.1E-04
<i>Eif3e</i>	1.23	4.6E-04
<i>Nploc4</i>	1.23	5.4E-04
<i>Ctsd</i>	1.23	1.2E-04
<i>Etfb</i>	1.23	4.6E-06
<i>Ccs</i>	1.22	2.6E-04
<i>Dynlrb1</i>	1.22	1.9E-05
<i>Apoc4</i>	1.22	4.3E-06
<i>Drg1</i>	1.22	3.3E-04
<i>Pex13</i>	1.22	9.6E-05
<i>Amy1</i>	1.21	2.0E-05
<i>Ctsz</i>	1.21	5.3E-04
<i>Serinc1</i>	1.21	1.6E-05
<i>Rp9</i>	1.21	4.0E-04
<i>Aldh9a1</i>	1.21	5.1E-04
<i>Tecr</i>	1.21	1.7E-04
<i>Grina</i>	1.21	8.2E-04
<i>Tfam</i>	1.20	7.7E-05
<i>Abhd17a</i>	1.20	3.5E-04
<i>Dctn2</i>	1.20	6.9E-04
<i>Sec24a</i>	1.20	4.6E-05
<i>Eif3g</i>	1.19	7.4E-04
<i>Glrx5</i>	1.19	7.3E-04
<i>Psmc3</i>	1.19	6.9E-05
<i>Rab1</i>	1.18	3.6E-04
<i>Pnpo</i>	1.18	8.5E-04
<i>Hp</i>	1.16	9.4E-05
<i>Cdo1</i>	1.15	2.9E-04
<i>Acaa2</i>	1.15	2.8E-04
<i>Slc10a1</i>	1.14	4.0E-04

Supplemental table 2. Genes significantly decreased by 24h fasting in mouse liver (P<0.001)

<i>gene name</i>	FC	P value	<i>gene name</i>	FC	P value
<i>Serpina4-ps1</i>	-27.22	7.7E-07	<i>Aqp8</i>	-4.30	1.3E-08
<i>Sdf2l1</i>	-23.88	2.7E-08	<i>Adra1b</i>	-4.27	9.3E-09
<i>Hsd3b2</i>	-22.78	9.3E-15	<i>Gna14</i>	-4.24	3.3E-09
<i>Hsd3b5</i>	-21.64	5.3E-10	<i>Il13ra1</i>	-4.20	3.8E-10
<i>Gck</i>	-20.57	4.0E-11	<i>Slc17a4</i>	-4.15	3.4E-11
<i>Dpy19l3</i>	-18.00	1.3E-17	<i>Lect1</i>	-4.15	3.7E-08
<i>Cyp26a1</i>	-15.62	2.0E-05	<i>Enho</i>	-4.10	1.2E-08
<i>Srebf1</i>	-14.50	1.0E-10	<i>Ido2</i>	-4.09	3.6E-10
<i>Slc41a2</i>	-13.55	1.0E-09	<i>Ero1lb</i>	-4.06	1.2E-06
<i>Cyp51</i>	-13.41	5.3E-11	<i>Pold2</i>	-4.01	2.1E-09
<i>Thrsp</i>	-13.35	2.7E-08	<i>Cyp2r1</i>	-3.93	1.9E-11
<i>Gstm3</i>	-11.86	4.2E-12	<i>Mvk</i>	-3.93	4.6E-09
<i>Sqle</i>	-11.84	8.6E-09	<i>Fam47e</i>	-3.90	1.7E-06
<i>Slc22a7</i>	-11.52	6.4E-08	<i>Bst2</i>	-3.90	1.4E-10
<i>Olfrl202</i>	-8.99	1.6E-14	<i>Dhcr7</i>	-3.70	8.1E-09
<i>Cyp2c70</i>	-8.99	4.0E-15	<i>Manf</i>	-3.66	1.0E-06
<i>Keg1</i>	-8.95	2.3E-09	<i>Sucnr1</i>	-3.59	8.3E-07
<i>Pdia6</i>	-8.85	6.6E-10	<i>Wwox</i>	-3.52	6.3E-07
<i>Slc3a1</i>	-8.66	1.5E-11	<i>Wdr53</i>	-3.52	2.2E-04
<i>Egfr</i>	-8.63	3.1E-07	<i>Slc46a3</i>	-3.49	2.8E-09
<i>Cela1</i>	-8.49	6.2E-15	<i>Steap4</i>	-3.47	5.8E-08
<i>Serpina12</i>	-7.77	3.4E-06	<i>Hspa13</i>	-3.47	1.3E-08
<i>Mid1ip1</i>	-7.22	9.8E-09	<i>Lin7a</i>	-3.46	3.3E-12
<i>Nsdhl</i>	-6.95	7.3E-09	<i>Slc13a3</i>	-3.45	1.8E-06
<i>Bcl6</i>	-6.59	3.1E-04	<i>Pmvk</i>	-3.40	3.8E-08
<i>Bdh2</i>	-6.08	3.6E-10	<i>Prg4</i>	-3.37	6.9E-11
<i>Cxcl1</i>	-6.01	1.9E-05	<i>Stard4</i>	-3.36	9.9E-11
<i>Ppp1r14a</i>	-5.60	3.2E-10	<i>Ppard</i>	-3.31	6.6E-05
<i>Acmsd</i>	-5.59	2.3E-05	<i>Serpina7</i>	-3.28	1.1E-04
<i>Cml1</i>	-5.51	4.1E-11	<i>Aox3</i>	-3.24	1.2E-10
<i>Hyou1</i>	-5.37	9.0E-08	<i>Nat8</i>	-3.22	5.7E-10
<i>Serpina9</i>	-5.32	1.3E-07	<i>Ppp1r3b</i>	-3.19	9.4E-07
<i>Pcsk9</i>	-5.32	1.2E-11	<i>Hist1h4i</i>	-3.19	1.9E-06
<i>Ikbke</i>	-5.31	1.9E-08	<i>Xkr9</i>	-3.19	6.9E-10
<i>Cyp4f14</i>	-5.17	5.6E-15	<i>Cyp7b1</i>	-3.17	1.4E-08
<i>Rdh11</i>	-5.01	1.9E-11	<i>Papss1</i>	-3.17	3.8E-07
<i>Car3</i>	-4.87	1.5E-05	<i>Spsb4</i>	-3.13	9.5E-07
<i>Aacs</i>	-4.78	1.4E-08	<i>Tmem14a</i>	-3.12	2.4E-09
<i>Acly</i>	-4.74	1.5E-11	<i>Sntg2</i>	-3.11	2.0E-07
<i>Scara5</i>	-4.70	7.7E-04	<i>Ttc39c</i>	-3.11	3.5E-08
<i>Abca8a</i>	-4.70	8.8E-10	<i>2200002D01Rik</i>	-3.08	1.5E-09
<i>Dexi</i>	-4.62	5.0E-11	<i>C6</i>	-3.05	2.5E-08
<i>Nr0b2</i>	-4.62	7.2E-07	<i>Gstm6</i>	-3.04	1.9E-05
<i>Fasn</i>	-4.48	1.1E-08	<i>Bhlhe40</i>	-3.02	1.3E-04
<i>Hes6</i>	-4.42	2.7E-12	<i>Slco1a1</i>	-3.02	1.3E-08
<i>Elovl3</i>	-4.40	7.5E-09	<i>Lss</i>	-3.02	1.9E-06

gene name	FC	P value
<i>Acot11</i>	-3.01	4.9E-06
<i>Slc35b1</i>	-3.00	1.2E-10
<i>Elovl6</i>	-2.99	3.0E-06
<i>Cry1</i>	-2.95	3.1E-06
<i>Mlec</i>	-2.95	2.9E-04
<i>BC029214</i>	-2.94	3.9E-08
<i>Aldh1b1</i>	-2.94	2.4E-09
<i>Ropn1l</i>	-2.93	7.8E-07
<i>Srd5a1</i>	-2.90	4.6E-05
<i>Slc22a29</i>	-2.89	8.2E-09
<i>Tmem107</i>	-2.88	5.0E-06
<i>Polr3k</i>	-2.88	6.0E-09
<i>Cetn2</i>	-2.87	4.2E-09
<i>Exph5</i>	-2.87	1.7E-06
<i>Cmah</i>	-2.86	7.1E-08
<i>Insc</i>	-2.83	8.6E-06
<i>Uba5</i>	-2.83	3.0E-07
<i>Igfals</i>	-2.83	7.2E-07
<i>Creb3l2</i>	-2.82	3.6E-05
<i>Bach2</i>	-2.82	2.2E-04
<i>Tlcd2</i>	-2.81	3.6E-09
<i>Dnajb11</i>	-2.80	1.1E-07
<i>Tmem258</i>	-2.80	4.0E-08
<i>Osgin1</i>	-2.79	4.6E-05
<i>Ly6a</i>	-2.78	6.6E-05
<i>Gamt</i>	-2.76	4.9E-06
<i>Ssr1</i>	-2.75	9.4E-08
<i>Irf2bp2</i>	-2.75	3.6E-05
<i>Slc25a17</i>	-2.75	3.1E-11
<i>Elovl1</i>	-2.73	3.8E-08
<i>Slc26a1</i>	-2.73	5.9E-04
<i>Uggt1</i>	-2.72	2.6E-08
<i>Saa4</i>	-2.69	6.6E-04
<i>Rab20</i>	-2.69	1.4E-04
<i>Cwlf19l1</i>	-2.69	2.5E-10
<i>Nqo2</i>	-2.69	2.1E-08
<i>Cnp</i>	-2.68	6.7E-09
<i>Hmgcr</i>	-2.67	2.1E-07
<i>Ddost</i>	-2.66	7.2E-10
<i>Cyb5b</i>	-2.66	1.1E-12
<i>Slc25a37</i>	-2.66	1.8E-08
<i>F11</i>	-2.66	1.1E-13
<i>Mmab</i>	-2.65	5.6E-07
<i>Sc5d</i>	-2.64	2.3E-10
<i>Pdia4</i>	-2.63	5.7E-05
<i>Orm3</i>	-2.61	4.0E-04
<i>Frmd4b</i>	-2.59	1.0E-05

gene name	FC	P value
<i>Ahsa2</i>	-2.58	2.3E-09
<i>Tuba4a</i>	-2.54	5.7E-13
<i>Ptgr1</i>	-2.53	7.6E-08
<i>P4ha1</i>	-2.53	9.9E-04
<i>Nrep</i>	-2.53	2.2E-06
<i>Slc25a23</i>	-2.52	1.4E-08
<i>Chid1</i>	-2.52	9.6E-09
<i>Syt1</i>	-2.52	3.5E-06
<i>Magt1</i>	-2.52	3.7E-09
<i>Ijf147</i>	-2.52	6.7E-06
<i>Wbp1</i>	-2.51	1.5E-09
<i>Ptprf</i>	-2.50	2.1E-07
<i>Pdilt</i>	-2.50	9.3E-05
<i>Ostc</i>	-2.47	1.4E-05
<i>Casp3</i>	-2.47	5.7E-09
<i>Cadps2</i>	-2.47	2.0E-07
<i>Gsta4</i>	-2.46	3.9E-06
<i>Dnph1</i>	-2.46	2.2E-07
<i>Pggt1b</i>	-2.46	1.2E-05
<i>Gsta3</i>	-2.46	1.0E-09
<i>Slc33a1</i>	-2.46	1.0E-10
<i>Ethe1</i>	-2.43	3.5E-10
<i>Thap1</i>	-2.43	1.1E-06
<i>Meg3</i>	-2.42	6.5E-05
<i>Zfp101</i>	-2.42	9.5E-06
<i>Hsph1</i>	-2.40	4.0E-04
<i>Abcb11</i>	-2.40	2.6E-10
<i>Plxna2</i>	-2.40	2.7E-05
<i>Nrn1</i>	-2.38	1.5E-11
<i>Irf5</i>	-2.38	1.5E-08
<i>Pter</i>	-2.38	7.2E-04
<i>Lsm6</i>	-2.38	9.9E-07
<i>Cyp2c29</i>	-2.37	8.0E-12
<i>Psmb9</i>	-2.37	4.0E-05
<i>Ube2u</i>	-2.36	6.1E-06
<i>Ormdl1</i>	-2.36	3.7E-05
<i>BC021614</i>	-2.35	9.9E-07
<i>Ppp1r1b</i>	-2.34	9.5E-06
<i>Spcs2</i>	-2.33	5.5E-09
<i>Npas2</i>	-2.33	7.1E-05
<i>Bmyc</i>	-2.33	2.2E-04
<i>Pdgfc</i>	-2.32	3.0E-05
<i>Slc39a10</i>	-2.32	8.5E-06
<i>Cutal</i>	-2.30	1.5E-04
<i>Serpina6</i>	-2.30	4.1E-06
<i>Ifitm3</i>	-2.30	4.0E-13
<i>Tpqs2</i>	-2.30	1.4E-04

gene name	FC	P value
<i>TK1</i>	-2.28	5.6E-04
<i>Ube2n</i>	-2.28	6.9E-05
<i>Cdk2ap2</i>	-2.27	1.3E-08
<i>Col27a1</i>	-2.27	7.1E-07
<i>Ccnd2</i>	-2.27	6.4E-08
<i>Susd4</i>	-2.27	7.3E-06
<i>Ces2g</i>	-2.26	2.2E-09
<i>Gsta2</i>	-2.26	1.5E-06
<i>Tmed3</i>	-2.25	9.7E-05
<i>Fbxo33</i>	-2.25	6.0E-07
<i>Sqrdl</i>	-2.25	3.6E-12
<i>Tmem141</i>	-2.24	7.7E-06
<i>F2r</i>	-2.23	2.3E-07
<i>Tmem86b</i>	-2.23	1.6E-07
<i>Lsr</i>	-2.23	2.4E-10
<i>Trhde</i>	-2.23	2.1E-05
<i>I7Rn6</i>	-2.23	1.6E-07
<i>Tsc22d3</i>	-2.23	8.1E-05
<i>Klf12</i>	-2.22	2.9E-06
<i>Hao1</i>	-2.22	8.4E-09
<i>Pdia3</i>	-2.21	1.2E-06
<i>Sult1c2</i>	-2.21	7.8E-06
<i>Hspa5</i>	-2.21	2.2E-06
<i>Camk1d</i>	-2.21	4.2E-05
<i>Mtmr7</i>	-2.21	1.7E-06
<i>Pklr</i>	-2.21	6.1E-06
<i>Tmem150a</i>	-2.20	2.1E-06
<i>Acss2</i>	-2.20	5.1E-06
<i>Haus3</i>	-2.20	6.9E-07
<i>Ugt2b34</i>	-2.20	6.8E-08
<i>Wdr91</i>	-2.20	1.5E-07
<i>Abca2</i>	-2.19	1.2E-08
<i>Krtcap2</i>	-2.19	2.0E-09
<i>Mrps27</i>	-2.19	8.9E-07
<i>Mfhas1</i>	-2.18	8.0E-07
<i>Acaca</i>	-2.18	5.2E-06
<i>Svip</i>	-2.17	1.3E-07
<i>Rfxap</i>	-2.17	7.4E-05
<i>Vps25</i>	-2.16	3.5E-06
<i>Gmppb</i>	-2.16	6.1E-04
<i>2610002M06Rik</i>	-2.16	1.3E-05
<i>Olfml1</i>	-2.15	1.5E-09
<i>Mlxipl</i>	-2.15	2.0E-08
<i>Nup155</i>	-2.15	2.0E-06
<i>Bco2</i>	-2.15	2.0E-08
<i>Dock6</i>	-2.14	4.6E-08
<i>Dhcr24</i>	-2.14	7.7E-04

gene name	FC	P value
<i>Apcs</i>	-2.14	7.5E-06
<i>Nudt2</i>	-2.14	9.0E-08
<i>Sec23b</i>	-2.13	4.6E-07
<i>Frrs1</i>	-2.13	3.6E-07
<i>Scnn1a</i>	-2.12	3.1E-08
<i>Sod3</i>	-2.12	1.2E-04
<i>Tubb5</i>	-2.11	4.2E-04
<i>Tcaim</i>	-2.11	1.7E-08
<i>Dcps</i>	-2.11	1.1E-08
<i>C8a</i>	-2.11	1.6E-11
<i>Ppib</i>	-2.11	8.8E-12
<i>Tmtc4</i>	-2.11	7.2E-06
<i>Ociad2</i>	-2.11	8.7E-07
<i>Gstm7</i>	-2.11	4.7E-07
<i>Ndufaf6</i>	-2.11	8.5E-09
<i>Ivd</i>	-2.11	2.5E-05
<i>Kdelc2</i>	-2.10	7.1E-06
<i>Acsm1</i>	-2.10	5.4E-11
<i>Ogfrl1</i>	-2.10	4.5E-08
<i>Ndst1</i>	-2.10	5.6E-05
<i>Il18</i>	-2.10	1.2E-07
<i>Sdr9c7</i>	-2.10	4.1E-04
<i>Inmt</i>	-2.10	4.0E-05
<i>Echdc1</i>	-2.10	1.0E-11
<i>Gclc</i>	-2.09	1.7E-08
<i>Folr2</i>	-2.09	7.2E-04
<i>C8b</i>	-2.09	2.5E-10
<i>Zfand4</i>	-2.09	1.0E-04
<i>Acy1</i>	-2.08	4.2E-04
<i>Iffitm1</i>	-2.08	2.1E-05
<i>Cxadr</i>	-2.08	3.7E-05
<i>Slc9a3r1</i>	-2.07	7.9E-07
<i>Ppil1</i>	-2.07	2.8E-04
<i>Rfc5</i>	-2.06	3.1E-06
<i>Fam213b</i>	-2.06	3.3E-05
<i>Aox1</i>	-2.04	7.8E-08
<i>Spcs3</i>	-2.04	5.7E-10
<i>Tmem19</i>	-2.04	1.0E-05
<i>Tpst1</i>	-2.04	5.1E-06
<i>Gale</i>	-2.03	1.7E-05
<i>Slc17a3</i>	-2.03	3.7E-06
<i>Memo1</i>	-2.03	3.9E-06
<i>Cmtm6</i>	-2.02	4.8E-08
<i>Lbr</i>	-2.01	3.1E-06
<i>Dusp19</i>	-2.01	1.2E-04
<i>Dnajb14</i>	-2.00	3.2E-05
<i>C9</i>	-2.00	7.0E-09

gene name	FC	P value
<i>Zfp692</i>	-2.00	1.7E-05
<i>Stra6l</i>	-1.99	3.5E-11
<i>Mmp19</i>	-1.99	3.0E-04
<i>Stip1</i>	-1.99	1.6E-06
<i>Cyp1a2</i>	-1.98	9.7E-11
<i>Rtp3</i>	-1.98	9.1E-06
<i>Traf3</i>	-1.98	2.7E-06
<i>Nit2</i>	-1.97	5.3E-08
<i>Fam149a</i>	-1.96	3.9E-06
<i>Cyhr1</i>	-1.96	2.2E-07
<i>Gpr155</i>	-1.96	1.1E-05
<i>Dnajc3</i>	-1.96	2.0E-08
<i>Adh4</i>	-1.95	7.9E-05
<i>Ap3m1</i>	-1.95	8.8E-04
<i>Calm3</i>	-1.95	1.2E-07
<i>Slc39a11</i>	-1.95	2.8E-07
<i>Psmb10</i>	-1.95	9.4E-06
<i>Wfdc17</i>	-1.94	5.6E-04
<i>Polb</i>	-1.94	2.5E-07
<i>Hn1l</i>	-1.94	1.6E-04
<i>Arhgdia</i>	-1.94	7.2E-06
<i>Tmem29</i>	-1.93	8.2E-06
<i>Crem</i>	-1.93	7.9E-06
<i>Psmb8</i>	-1.93	7.0E-06
<i>Mettl7a1</i>	-1.92	1.3E-09
<i>Prps2</i>	-1.92	1.2E-05
<i>Slco2b1</i>	-1.91	5.8E-09
<i>Sult1b1</i>	-1.91	2.2E-06
<i>Stt3a</i>	-1.91	3.5E-04
<i>Dck</i>	-1.91	2.7E-04
<i>Klhl13</i>	-1.91	1.6E-06
<i>Fgfr2</i>	-1.89	3.6E-04
<i>Snd1</i>	-1.89	8.4E-08
<i>Ugt2b1</i>	-1.89	1.5E-09
<i>Alcam</i>	-1.89	5.5E-08
<i>Pla1a</i>	-1.88	2.6E-04
<i>Gcat</i>	-1.88	2.3E-08
<i>9030617O03Rik</i>	-1.88	4.2E-07
<i>Cyp2c44</i>	-1.88	1.1E-09
<i>Rpe</i>	-1.87	1.2E-04
<i>Adam11</i>	-1.87	3.5E-04
<i>Yif1b</i>	-1.87	1.1E-08
<i>Commd10</i>	-1.87	5.9E-06
<i>Polr3g</i>	-1.87	4.4E-04
<i>Serp1</i>	-1.87	1.5E-10
<i>Rhobtb1</i>	-1.87	5.6E-05
<i>1700066M21Rik</i>	-1.86	1.6E-06

gene name	FC	P value
<i>Car1</i>	-1.86	2.7E-04
<i>Arhgap26</i>	-1.86	1.3E-05
<i>Abtb2</i>	-1.86	9.1E-05
<i>Pik3r1</i>	-1.86	2.8E-05
<i>Nox4</i>	-1.85	4.8E-08
<i>Kmo</i>	-1.85	1.3E-08
<i>Ahctf1</i>	-1.85	7.5E-05
<i>2700029M09Rik</i>	-1.85	1.3E-05
<i>Psph</i>	-1.84	3.8E-04
<i>Ngfr</i>	-1.84	8.7E-06
<i>Mn1</i>	-1.84	1.2E-05
<i>Rap2a</i>	-1.84	5.2E-06
<i>2310040G24Rik</i>	-1.84	1.7E-05
<i>Lifr</i>	-1.83	1.9E-06
<i>Nostrin</i>	-1.83	1.5E-05
<i>Sec61a1</i>	-1.82	4.6E-09
<i>1810011O10Rik</i>	-1.82	2.6E-05
<i>Pde9a</i>	-1.82	4.8E-04
<i>Dhx29</i>	-1.82	1.7E-04
<i>Hnmt</i>	-1.82	6.3E-06
<i>Slc35a1</i>	-1.82	7.7E-05
<i>lfih1</i>	-1.82	2.7E-06
<i>Akr1c14</i>	-1.82	6.5E-06
<i>Rsu1</i>	-1.82	9.1E-07
<i>Rp2h</i>	-1.82	4.1E-04
<i>Tcea3</i>	-1.82	1.4E-04
<i>Cndp2</i>	-1.82	1.3E-08
<i>lfi35</i>	-1.81	5.0E-07
<i>Jmjd8</i>	-1.81	2.5E-06
<i>Nme1</i>	-1.81	1.0E-10
<i>Raph1</i>	-1.81	2.4E-07
<i>Gm2a</i>	-1.80	1.0E-05
<i>Mmaa</i>	-1.80	6.0E-05
<i>Osgep</i>	-1.80	6.1E-04
<i>Anks4b</i>	-1.80	9.9E-04
<i>Slc25a44</i>	-1.80	1.0E-06
<i>Akr1c20</i>	-1.80	7.4E-07
<i>Srprb</i>	-1.80	7.7E-04
<i>Rgn</i>	-1.80	2.5E-09
<i>Vwa5a</i>	-1.79	2.7E-04
<i>Pigf</i>	-1.79	3.0E-04
<i>Dap</i>	-1.79	3.6E-09
<i>Cars</i>	-1.79	3.8E-05
<i>Pygl</i>	-1.78	7.2E-11
<i>Snrpd1</i>	-1.78	5.5E-05
<i>Uqcc2</i>	-1.78	1.9E-07
<i>Dars2</i>	-1.78	3.0E-05

gene name	FC	P value
<i>Pfkfb1</i>	-1.78	6.9E-04
<i>Sgpl1</i>	-1.77	1.3E-05
<i>Tram1</i>	-1.77	3.7E-08
<i>Fars2</i>	-1.77	1.3E-05
<i>Selt</i>	-1.77	1.6E-04
<i>Avpr1a</i>	-1.77	1.2E-05
<i>Tbcel</i>	-1.76	1.4E-05
<i>Ccbl2</i>	-1.76	3.0E-05
<i>Pfdn1</i>	-1.76	4.9E-07
<i>Med19</i>	-1.76	1.4E-05
<i>Rnf181</i>	-1.76	2.2E-06
<i> Tubgcp5</i>	-1.76	7.3E-04
<i>Haao</i>	-1.75	1.2E-08
<i>Actb</i>	-1.75	1.5E-10
<i>Ptms</i>	-1.75	1.9E-07
<i>Slc10a2</i>	-1.75	6.2E-04
<i>Fgfr3</i>	-1.75	1.9E-05
<i>Mkrn2os</i>	-1.75	7.4E-04
<i>Exosc8</i>	-1.75	1.7E-04
<i>Rnf141</i>	-1.75	6.1E-04
<i>Gsdmd</i>	-1.75	6.0E-05
<i>Bcs1l</i>	-1.74	2.3E-05
<i>Bet1</i>	-1.74	1.6E-06
<i>Ddc</i>	-1.74	2.3E-08
<i>Tfpi2</i>	-1.74	4.3E-08
<i>Tmem218</i>	-1.74	2.1E-04
<i>Hars2</i>	-1.74	1.4E-04
<i>Sfxn5</i>	-1.73	1.3E-05
<i>Smchd1</i>	-1.73	1.3E-05
<i>Gm17296</i>	-1.73	4.3E-05
<i>Slc11a2</i>	-1.73	7.1E-05
<i>Igf1</i>	-1.73	5.8E-06
<i>Adam17</i>	-1.73	5.1E-05
<i>Akr1c6</i>	-1.73	1.7E-07
<i>Clec4g</i>	-1.73	4.5E-06
<i>Rnaseh2c</i>	-1.73	1.1E-05
<i>D17Wsu104e</i>	-1.73	3.4E-07
<i>Ninj1</i>	-1.72	1.9E-06
<i>Ssr3</i>	-1.72	2.3E-09
<i>Cpb2</i>	-1.72	1.7E-12
<i>Derl2</i>	-1.72	3.7E-09
<i>Sec63</i>	-1.72	7.1E-07
<i>Tstd1</i>	-1.72	6.9E-06
<i>Arf5</i>	-1.72	7.7E-06
<i>Msh6</i>	-1.71	1.3E-04
<i>Fgfr1op</i>	-1.71	4.3E-06
<i>Mr1</i>	-1.70	9.8E-05
<i>Edem1</i>	-1.70	4.4E-09

gene name	FC	P value
<i>Smek1</i>	-1.70	4.8E-06
<i>Mal2</i>	-1.70	2.9E-05
<i>Pigh</i>	-1.70	9.0E-04
<i>Chmp3</i>	-1.70	1.2E-05
<i>Actr10</i>	-1.70	1.6E-04
<i>Impa1</i>	-1.70	7.5E-07
<i>Atf6b</i>	-1.69	1.9E-04
<i>Acy3</i>	-1.69	2.1E-04
<i>Stra13</i>	-1.69	1.0E-08
<i>Lgalsl</i>	-1.69	1.5E-04
<i>LOC100503676</i>	-1.68	7.5E-04
<i>Tmem50a</i>	-1.68	5.9E-08
<i>Arhgap18</i>	-1.68	1.1E-04
<i>Iws1</i>	-1.68	1.7E-05
<i>Ubr2</i>	-1.68	1.4E-04
<i>Gimap4</i>	-1.68	4.6E-04
<i>Rmdn2</i>	-1.68	4.1E-05
<i>Klf13</i>	-1.68	5.0E-04
<i>Serpind1</i>	-1.68	3.4E-08
<i>Mettl17</i>	-1.67	5.5E-04
<i>Slc39a8</i>	-1.67	3.2E-04
<i>Tbcb</i>	-1.67	3.3E-05
<i>Slc44a1</i>	-1.67	6.8E-06
<i>Ccl9</i>	-1.67	1.2E-06
<i>Cdk5rap3</i>	-1.67	1.0E-05
<i>Cars2</i>	-1.66	4.9E-04
<i>Gm20300</i>	-1.66	2.5E-06
<i>Herc6</i>	-1.66	2.2E-04
<i>Nhsl1</i>	-1.66	6.5E-04
<i>Usp39</i>	-1.66	8.0E-05
<i>Smcr8</i>	-1.66	2.6E-04
<i>St3gal1</i>	-1.66	4.8E-06
<i>Tirap</i>	-1.66	2.8E-06
<i>Gstm5</i>	-1.66	1.8E-07
<i>Adck3</i>	-1.65	1.4E-06
<i>Uxs1</i>	-1.65	6.2E-04
<i>Txndc5</i>	-1.65	3.2E-05
<i>Ppm1b</i>	-1.65	1.5E-07
<i>Canx</i>	-1.65	7.1E-07
<i>Hapln4</i>	-1.65	6.5E-06
<i>Orm1</i>	-1.65	8.4E-09
<i>Mccc1</i>	-1.64	1.1E-06
<i>Cdc37l1</i>	-1.64	4.7E-05
<i>Cnpy4</i>	-1.64	1.1E-04
<i>Gucy1b3</i>	-1.64	1.8E-04
<i>Tars</i>	-1.64	5.8E-09
<i>Rai14</i>	-1.64	1.2E-04
<i>Rnf121</i>	-1.64	2.2E-04

gene name	FC	P value
<i>Ick</i>	-1.64	3.3E-04
<i>Abcc6</i>	-1.63	3.2E-05
<i>Tcl1b3</i>	-1.63	3.4E-05
<i>Ormdl2</i>	-1.63	1.6E-07
<i>Glo1</i>	-1.63	7.3E-09
<i>Galk2</i>	-1.63	2.6E-04
<i>Trim12c</i>	-1.63	5.2E-04
<i>Mtss1</i>	-1.62	4.7E-04
<i>Mrps25</i>	-1.62	1.9E-04
<i>Myo1e</i>	-1.62	3.2E-05
<i>Ssr2</i>	-1.62	7.0E-07
<i>Rrbp1</i>	-1.62	2.2E-06
<i>Erp44</i>	-1.62	3.5E-09
<i>Lmf1</i>	-1.62	2.5E-06
<i>Tars2</i>	-1.62	6.5E-06
<i>Erlin1</i>	-1.62	1.1E-05
<i>Klhl22</i>	-1.62	3.5E-05
<i>Mipep</i>	-1.62	1.8E-05
<i>Stat5b</i>	-1.61	1.6E-04
<i>Mpnd</i>	-1.61	3.1E-09
<i>Acad5b</i>	-1.61	3.8E-08
<i>Casp7</i>	-1.61	4.1E-05
<i>Abcb10</i>	-1.61	7.9E-06
<i>Nt5c</i>	-1.61	2.9E-05
<i>Sdc2</i>	-1.61	5.7E-07
<i>Serpina10</i>	-1.61	1.6E-06
<i>Blvra</i>	-1.61	3.0E-05
<i>Dhrs11</i>	-1.61	1.6E-05
<i>Apip</i>	-1.61	1.4E-05
<i>Ube2a</i>	-1.60	1.6E-04
<i>H2afv</i>	-1.60	4.6E-05
<i>Wrap73</i>	-1.60	8.7E-05
<i>Gpc4</i>	-1.60	1.1E-06
<i>Tubgcp4</i>	-1.60	9.7E-05
<i>Cib2</i>	-1.59	3.4E-04
<i>Mbd3</i>	-1.59	7.5E-05
<i>Med21</i>	-1.59	8.3E-06
<i>Tbc1d9b</i>	-1.59	3.4E-06
<i>Fndc3a</i>	-1.59	2.4E-05
<i>Fam188a</i>	-1.59	1.6E-07
<i>Cse1l</i>	-1.59	8.8E-06
<i>Gls2</i>	-1.59	6.2E-07
<i>Abca3</i>	-1.59	1.1E-05
<i>Stap2</i>	-1.58	5.6E-07
<i>Snrpd3</i>	-1.58	4.8E-09
<i>Rbms3</i>	-1.58	5.1E-04
<i>Stk38l</i>	-1.58	7.8E-05
<i>Mrpl39</i>	-1.58	2.6E-05

gene name	FC	P value
<i>Arl3</i>	-1.58	3.0E-06
<i>Coa3</i>	-1.58	5.4E-04
<i>Foxo4</i>	-1.58	7.9E-04
<i>Noa1</i>	-1.57	6.5E-04
<i>Pigyl</i>	-1.57	1.3E-05
<i>Hagh</i>	-1.57	1.7E-09
<i>Cuta</i>	-1.57	2.5E-06
<i>Slc39a4</i>	-1.57	8.4E-04
<i>Tkt</i>	-1.57	1.1E-07
<i>Mbl2</i>	-1.57	7.2E-09
<i>Cyp2f2</i>	-1.57	2.6E-08
<i>Slc35d2</i>	-1.57	5.0E-05
<i>Map3k4</i>	-1.57	7.1E-04
<i>Dhrs3</i>	-1.56	1.6E-06
<i>Thns12</i>	-1.56	6.8E-07
<i>Fgfr4</i>	-1.56	2.1E-04
<i>Prkra</i>	-1.56	3.5E-07
<i>Tmed10</i>	-1.56	4.8E-04
<i>Gpr125</i>	-1.56	8.0E-04
<i>Smc5</i>	-1.55	2.8E-04
<i>Pip4k2b</i>	-1.55	1.9E-04
<i>F7</i>	-1.55	2.4E-07
<i>Fastkd2</i>	-1.55	5.8E-05
<i>Naglu</i>	-1.55	5.4E-05
<i>Slc22a18</i>	-1.55	2.0E-06
<i>Cbs</i>	-1.55	3.0E-07
<i>Pgd</i>	-1.55	3.3E-05
<i>Oma1</i>	-1.55	5.1E-05
<i>Rell1</i>	-1.55	3.0E-04
<i>Rbm33</i>	-1.55	1.8E-04
<i>Psd3</i>	-1.55	7.2E-06
<i>Uap1</i>	-1.55	1.2E-04
<i>Stim2</i>	-1.55	3.2E-04
<i>Mrpl1</i>	-1.54	6.3E-04
<i>Itgb1bp1</i>	-1.54	2.5E-04
<i>Dtymk</i>	-1.54	9.9E-04
<i>Stxbp5</i>	-1.54	6.1E-04
<i>Galm</i>	-1.54	3.6E-05
<i>Nudt16l1</i>	-1.54	3.6E-04
<i>Cyp2c54</i>	-1.54	5.3E-06
<i>Slc46a1</i>	-1.54	4.3E-05
<i>Edem2</i>	-1.54	1.8E-05
<i>Sort1</i>	-1.53	6.2E-05
<i>1110057K04Rik</i>	-1.53	8.2E-06
<i>Rce1</i>	-1.53	6.9E-05
<i>Mief2</i>	-1.53	4.5E-05
<i>Ociad1</i>	-1.52	5.6E-04
<i>Luc7l3</i>	-1.52	9.9E-04

gene name	FC	P value
<i>Sil1</i>	-1.52	9.6E-08
<i>Mfsd1</i>	-1.52	1.5E-06
<i>Abca8b</i>	-1.52	3.0E-04
<i>Haus7</i>	-1.52	6.5E-04
<i>Dcaf12</i>	-1.52	5.2E-04
<i>Ints7</i>	-1.52	2.8E-05
<i>Arhgap42</i>	-1.52	3.1E-04
<i>Taldo1</i>	-1.51	9.3E-09
<i>Ergic1</i>	-1.51	4.0E-04
<i>Ugp2</i>	-1.51	2.2E-05
<i>Lactb</i>	-1.51	8.7E-06
<i>Zfp35</i>	-1.51	1.7E-04
<i>Lace1</i>	-1.51	9.6E-04
<i>Prnp</i>	-1.51	5.4E-06
<i>Ikbkb</i>	-1.51	2.2E-07
<i>Ebp</i>	-1.51	1.9E-08
<i>Bcar3</i>	-1.51	9.0E-04
<i>Commd1</i>	-1.51	6.6E-06
<i>Dnajc4</i>	-1.51	9.6E-05
<i>Trappc9</i>	-1.51	6.0E-04
<i>Pid1</i>	-1.51	1.6E-10
<i>Rdh5</i>	-1.51	1.7E-04
<i>Arsb</i>	-1.51	2.4E-04
<i>Tpst2</i>	-1.51	4.0E-05
<i>Aes</i>	-1.51	1.1E-08
<i>Slco2a1</i>	-1.51	4.2E-04
<i>Prr16</i>	-1.51	1.9E-04
<i>BC026585</i>	-1.51	1.9E-04
<i>Selenof</i>	-1.51	4.4E-09
<i>Ugt2b35</i>	-1.50	6.8E-07
<i>Cnih1</i>	-1.50	7.6E-07
<i>Gda</i>	-1.50	1.6E-04
<i>Calu</i>	-1.50	2.0E-06
<i>Acsf4</i>	-1.50	3.3E-05
<i>Hs3st3b1</i>	-1.50	3.4E-05
<i>Tubg1</i>	-1.50	1.4E-04
<i>Tmcc1</i>	-1.49	3.1E-04
<i>Smim14</i>	-1.49	4.8E-06
<i>Copz1</i>	-1.49	3.2E-08
<i>Commd7</i>	-1.49	1.6E-04
<i>Cfi</i>	-1.49	1.3E-08
<i>Galnt4</i>	-1.49	1.7E-05
<i>Afm</i>	-1.49	2.5E-06
<i>Ints12</i>	-1.48	3.2E-04
<i>Aadac</i>	-1.48	1.4E-08
<i>Hsd17b2</i>	-1.48	8.7E-07
<i>Gm4788</i>	-1.48	6.8E-05

gene name	FC	P value
<i>Rab32</i>	-1.48	2.2E-04
<i>Gpr89</i>	-1.48	2.1E-05
<i>Ehd3</i>	-1.48	1.2E-04
<i>Qdpr</i>	-1.48	8.0E-09
<i>Ulk2</i>	-1.48	5.8E-04
<i>Lman2l</i>	-1.47	8.3E-04
<i>Mrps22</i>	-1.47	3.4E-07
<i>Slirp</i>	-1.47	5.9E-07
<i>Hc</i>	-1.47	2.7E-07
<i>Ttc17</i>	-1.47	2.6E-04
<i>Leo1</i>	-1.47	2.9E-04
<i>Slc36a1</i>	-1.47	6.7E-04
<i>Slc30a10</i>	-1.47	2.6E-04
<i>Myh9</i>	-1.47	1.2E-04
<i>C4bp</i>	-1.47	1.7E-07
<i>Lman2</i>	-1.47	2.2E-06
<i>Dnm1l</i>	-1.47	6.1E-04
<i>Ces2a</i>	-1.47	5.4E-05
<i>Fermt2</i>	-1.46	1.5E-07
<i>Naa10</i>	-1.46	9.6E-04
<i>Wdr83os</i>	-1.46	2.8E-04
<i>Lamtor2</i>	-1.46	2.9E-08
<i>Ufl1</i>	-1.46	1.2E-04
<i>Cdad1</i>	-1.46	1.5E-04
<i>Abhd17c</i>	-1.46	1.9E-05
<i>Atxn1</i>	-1.46	1.8E-04
<i>Hist1h2bc</i>	-1.46	5.6E-06
<i>Pdcd6ip</i>	-1.46	1.6E-05
<i>Rpa3</i>	-1.45	9.9E-04
<i>Tmem14c</i>	-1.45	3.6E-06
<i>Ugt2a3</i>	-1.45	6.5E-06
<i>Smdt1</i>	-1.45	1.0E-06
<i>Adh1</i>	-1.45	3.2E-11
<i>Gatb</i>	-1.45	5.2E-04
<i>Tmem160</i>	-1.45	3.3E-05
<i>Mocs2</i>	-1.44	3.2E-04
<i>Atp2b1</i>	-1.44	4.2E-04
<i>Slc23a1</i>	-1.44	9.6E-05
<i>Mpi</i>	-1.44	9.1E-04
<i>1110008P14Rik</i>	-1.44	1.1E-04
<i>Gng10</i>	-1.44	4.0E-04
<i>BC025446</i>	-1.44	1.2E-04
<i>Cpn2</i>	-1.44	7.4E-07
<i>Gadd45gip1</i>	-1.43	7.8E-06
<i>Zfyve1</i>	-1.43	3.5E-04
<i>Smpd1</i>	-1.43	1.2E-04
<i>Ces1c</i>	-1.43	5.5E-06

gene name	FC	P value
<i>ldh1</i>	-1.43	9.1E-09
<i>Clcn7</i>	-1.43	3.1E-04
<i>Slc31a1</i>	-1.43	9.2E-06
<i>Aagab</i>	-1.43	7.1E-04
<i>Tmem176a</i>	-1.43	1.0E-05
<i>Ptpn3</i>	-1.43	2.9E-04
<i>Sema4a</i>	-1.43	6.5E-05
<i>H13</i>	-1.42	1.4E-08
<i>Dnajb2</i>	-1.42	2.3E-04
<i>Zfp148</i>	-1.42	4.0E-05
<i>Idnk</i>	-1.42	9.6E-05
<i>Sh3glb2</i>	-1.42	3.3E-04
<i>Mien1</i>	-1.42	1.6E-06
<i>Hdhd2</i>	-1.42	4.9E-04
<i>Taf12</i>	-1.41	4.3E-04
<i>Yars</i>	-1.41	2.6E-04
<i>Fdx1</i>	-1.41	7.6E-08
<i>Cers2</i>	-1.41	6.2E-09
<i>Zmpste24</i>	-1.41	2.1E-07
<i>Kynu</i>	-1.41	1.5E-04
<i>Usp7</i>	-1.41	7.9E-04
<i>Polr2d</i>	-1.41	8.1E-04
<i>Mrpl14</i>	-1.40	4.2E-04
<i>Phkb</i>	-1.40	3.9E-04
<i>Snx27</i>	-1.40	6.7E-04
<i>Rnpep</i>	-1.40	8.8E-04
<i>U2af114</i>	-1.40	5.1E-04
<i>Fam173a</i>	-1.40	7.6E-07
<i>Ckap5</i>	-1.40	5.9E-05
<i>2310030G06Rik</i>	-1.40	4.1E-04
<i>Rpn2</i>	-1.40	6.1E-08
<i>Josd2</i>	-1.40	3.7E-04
<i>Gulo</i>	-1.40	1.5E-09
<i>Kif13b</i>	-1.40	9.9E-04
<i>Pls3</i>	-1.40	4.0E-04
<i>Cpne3</i>	-1.40	3.3E-06
<i>Pomp</i>	-1.39	2.1E-06
<i>Eps8l2</i>	-1.39	5.2E-04
<i>Isoc1</i>	-1.39	1.1E-04
<i>Ndufs8</i>	-1.39	3.1E-06
<i>Poglut1</i>	-1.38	6.5E-04
<i>Peptd</i>	-1.38	4.1E-05
<i>Srp9</i>	-1.38	2.3E-04
<i>Rps19bp1</i>	-1.38	9.6E-05
<i>Nsun2</i>	-1.38	1.0E-05
<i>Pcbd1</i>	-1.38	1.7E-07
<i>Ctnnb1</i>	-1.38	5.8E-04

gene name	FC	P value
<i>Hnrnpc</i>	-1.38	1.5E-04
<i>Dad1</i>	-1.38	2.1E-07
<i>Rnasek</i>	-1.38	2.2E-04
<i>Cstf2</i>	-1.38	2.6E-04
<i>Top1</i>	-1.37	1.1E-04
<i>Gbf1</i>	-1.37	7.7E-04
<i>Slc6a13</i>	-1.37	6.1E-07
<i>Enpep</i>	-1.37	1.4E-04
<i>Ythdf1</i>	-1.37	4.6E-04
<i>Gbe1</i>	-1.37	4.6E-06
<i>Gstm1</i>	-1.37	4.0E-09
<i>Clcn4-2</i>	-1.37	7.8E-04
<i>Psmd5</i>	-1.37	3.8E-04
<i>Sec11a</i>	-1.36	5.6E-05
<i>Vimp</i>	-1.36	6.6E-04
<i>Acp5</i>	-1.36	4.7E-04
<i>Itih4</i>	-1.36	1.0E-07
<i>Ergic3</i>	-1.36	9.9E-06
<i>Ggact</i>	-1.36	9.7E-04
<i>D930016D06Rik</i>	-1.36	4.7E-04
<i>Lman1</i>	-1.36	1.3E-05
<i>Aldh4a1</i>	-1.36	2.9E-04
<i>Saraf</i>	-1.36	5.9E-06
<i>Serpina11</i>	-1.36	3.8E-04
<i>Hibadh</i>	-1.36	3.8E-07
<i>Osbp</i>	-1.36	9.4E-04
<i>Dynlt3</i>	-1.35	3.8E-06
<i>Lipc</i>	-1.35	6.7E-06
<i>Acsn5</i>	-1.35	5.4E-06
<i>Kdelr2</i>	-1.35	3.8E-04
<i>Lyplal1</i>	-1.35	1.1E-04
<i>Lap3</i>	-1.35	4.3E-07
<i>Zdhhc18</i>	-1.35	1.5E-04
<i>Cacul1</i>	-1.35	9.7E-05
<i>Cacybp</i>	-1.35	9.8E-04
<i>Cyp2d40</i>	-1.35	5.6E-04
<i>Ganab</i>	-1.35	2.0E-05
<i>Ugdh</i>	-1.35	1.4E-05
<i>Prps1l3</i>	-1.35	3.5E-04
<i>Timd2</i>	-1.35	3.2E-05
<i>Gltpd2</i>	-1.35	7.7E-04
<i>Slc16a2</i>	-1.34	6.2E-04
<i>Pnp</i>	-1.34	4.5E-05
<i>Cox18</i>	-1.34	2.4E-04
<i>Bnip2</i>	-1.34	7.4E-04
<i>Pmpcb</i>	-1.34	4.7E-06
<i>Mocos</i>	-1.34	5.0E-05

gene name	FC	P value
<i>C2</i>	-1.34	1.2E-04
<i>Prdx4</i>	-1.34	2.4E-06
<i>Nipsnap1</i>	-1.34	3.5E-05
<i>Crp</i>	-1.34	7.6E-06
<i>Gjb1</i>	-1.34	8.8E-05
<i>Fgb</i>	-1.34	1.0E-10
<i>Selenbp1</i>	-1.33	3.0E-07
<i>Ddx5</i>	-1.33	2.5E-05
<i>Uevld</i>	-1.33	9.2E-04
<i>Pop5</i>	-1.33	1.8E-05
<i>Foxn3</i>	-1.33	8.5E-05
<i>Fgg</i>	-1.33	1.5E-10
<i>Cetn3</i>	-1.33	3.7E-04
<i>Ndufaf1</i>	-1.33	4.1E-04
<i>Gstt1</i>	-1.32	3.7E-04
<i>Tmem176b</i>	-1.32	5.3E-05
<i>Mvb12a</i>	-1.32	2.5E-04
<i>BC031181</i>	-1.32	2.9E-05
<i>Casd1</i>	-1.32	3.0E-04
<i>Gnai3</i>	-1.32	8.1E-07
<i>Akr1a1</i>	-1.32	2.7E-07
<i>Camk2n1</i>	-1.32	3.7E-04
<i>Gramd1c</i>	-1.32	6.9E-04
<i>Cd82</i>	-1.31	2.0E-05
<i>Pipax</i>	-1.31	7.0E-05
<i>Sec22b</i>	-1.31	3.7E-04
<i>Snap47</i>	-1.31	3.1E-06
<i>Khk</i>	-1.31	9.1E-05
<i>Apeh</i>	-1.31	1.2E-04
<i>Ugt2b5</i>	-1.31	1.0E-07
<i>Dpm3</i>	-1.30	9.6E-04
<i>Lrp1</i>	-1.30	9.9E-04
<i>Arl6ip1</i>	-1.30	7.2E-05
<i>Sdcbp</i>	-1.30	1.9E-04
<i>Aco1</i>	-1.30	6.0E-05
<i>Slc25a1</i>	-1.30	3.3E-05
<i>lyd</i>	-1.29	2.0E-05
<i>Pecr</i>	-1.29	8.5E-04
<i>Setd6</i>	-1.29	4.8E-04
<i>Pemt</i>	-1.29	1.9E-05
<i>Rdx</i>	-1.29	1.3E-06
<i>Cope</i>	-1.28	4.3E-04
<i>Prodh</i>	-1.28	7.0E-04
<i>Ndfip1</i>	-1.28	7.7E-06
<i>Pah</i>	-1.28	1.3E-06
<i>Znhit1</i>	-1.28	4.8E-04
<i>Oard1</i>	-1.28	7.9E-04

gene name	FC	P value
<i>Arpc5l</i>	-1.28	9.7E-05
<i>Chmp7</i>	-1.27	5.6E-04
<i>Spint2</i>	-1.27	4.5E-05
<i>Msrb1</i>	-1.27	3.6E-06
<i>Zbtb33</i>	-1.27	2.2E-04
<i>Serpinf2</i>	-1.27	3.2E-05
<i>Fkbp2</i>	-1.26	1.1E-05
<i>Slc30a9</i>	-1.26	5.8E-04
<i>Sep-07</i>	-1.26	1.4E-04
<i>Glud1</i>	-1.26	4.7E-06
<i>Nop10</i>	-1.26	1.4E-04
<i>Tmem205</i>	-1.25	2.7E-06
<i>Paip2</i>	-1.25	4.6E-05
<i>Hsd17b12</i>	-1.25	8.8E-05
<i>Txn1</i>	-1.25	3.5E-05
<i>St13</i>	-1.25	7.3E-04
<i>Tst</i>	-1.25	1.6E-05
<i>D10Jhu81e</i>	-1.25	3.5E-04
<i>Uox</i>	-1.24	7.7E-04
<i>Akr1c13</i>	-1.24	2.0E-04
<i>Rpl26</i>	-1.24	8.1E-04
<i>Tmem208</i>	-1.23	3.5E-04
<i>Ugt2b36</i>	-1.23	8.0E-06
<i>Prr13</i>	-1.23	4.0E-04
<i>Snx3</i>	-1.23	1.6E-04
<i>Nars</i>	-1.22	7.0E-04
<i>Tmed7</i>	-1.22	3.2E-05
<i>lfitm2</i>	-1.21	3.0E-05
<i>Aifm1</i>	-1.21	1.4E-05
<i>Rpl15</i>	-1.20	9.8E-04
<i>Il1rap</i>	-1.20	6.7E-04
<i>Bcap31</i>	-1.20	9.1E-05
<i>Cyp2a12</i>	-1.20	1.0E-06
<i>Nfs1</i>	-1.20	6.0E-04
<i>Fah</i>	-1.19	3.7E-06
<i>Hrsp12</i>	-1.18	6.6E-04
<i>Dbi</i>	-1.17	2.7E-04
<i>Pgrmc1</i>	-1.17	3.3E-05
<i>Fggy</i>	-1.16	7.3E-04
<i>Higd2a</i>	-1.16	2.8E-04
<i>Txndc15</i>	-1.16	8.0E-04

Supplemental table 3. Human genes significantly increased by fasting in hepatocyte humanized liver (P<0.001)

gene name	FC	P value
<i>APOA4</i>	64.65	6.06E-04
<i>IGFBP1</i>	50.55	2.64E-10
<i>PPP1R3G</i>	22.26	2.36E-04
<i>PCK1</i>	20.45	1.47E-04
<i>TXNIP</i>	12.26	1.71E-06
<i>G6PC</i>	8.79	4.10E-05
<i>ANGPTL4</i>	7.29	1.18E-05
<i>CYP17A1</i>	6.76	1.88E-04
<i>LEPR</i>	6.40	4.81E-05
<i>PLIN2</i>	5.73	8.02E-05
<i>MYCL</i>	5.51	9.04E-05
<i>CPT1A</i>	5.40	3.21E-04
<i>IRS2</i>	5.38	1.01E-06
<i>DEPP1</i>	4.95	8.64E-04
<i>SSBP2</i>	4.84	4.49E-04
<i>PPARGC1A</i>	4.43	7.80E-07
<i>SLC25A47</i>	3.97	7.09E-04
<i>GADD45B</i>	3.93	6.42E-05
<i>RBMS1</i>	3.79	9.44E-04
<i>BSN</i>	3.76	2.81E-05
<i>VNN1</i>	3.56	6.23E-05
<i>PDK4</i>	3.53	1.80E-05
<i>GPT2</i>	3.49	2.49E-07
<i>SLC16A1</i>	3.33	1.24E-05
<i>FBP1</i>	3.19	1.61E-04
<i>TRAF3IP2</i>	3.03	5.67E-04
<i>FAM102A</i>	2.99	5.12E-05
<i>HMGCS2</i>	2.66	2.23E-04
<i>PRKAG2</i>	2.62	2.93E-04
<i>LTBP1</i>	2.47	8.23E-04
<i>MEF2D</i>	2.37	3.38E-04
<i>PNPLA2</i>	2.31	4.99E-04
<i>HSD17B13</i>	2.27	3.22E-05
<i>GK</i>	2.25	6.89E-04
<i>SORL1</i>	2.23	1.19E-04
<i>SLC1A2</i>	2.23	2.42E-05
<i>SIK2</i>	2.20	8.64E-05
<i>PLCG2</i>	2.19	4.71E-04
<i>SLC23A2</i>	2.19	1.08E-04
<i>DUSP1</i>	2.01	3.09E-04
<i>POR</i>	1.96	9.23E-04
<i>PRLR</i>	1.93	5.44E-04
<i>CNKS3</i>	1.93	1.84E-04
<i>ABHD2</i>	1.88	9.48E-04
<i>ACOX1</i>	1.88	6.80E-04
<i>PANK1</i>	1.76	5.44E-04

Supplemental table 4. Mouse genes significantly increased by fasting in hepatocyte humanized liver (P<0.001)

<i>gene name</i>	FC	P value	<i>gene name</i>	FC	P value
<i>Cyp8b1</i>	47.79	6.93E-05	<i>Zbtb16</i>	3.27	6.70E-04
<i>Igfbp1</i>	25.29	9.35E-05	<i>Fam166b</i>	3.27	5.50E-04
<i>Angptl4</i>	8.50	5.03E-05	<i>Acs1l</i>	3.26	2.37E-06
<i>Irs2</i>	8.33	9.40E-07	<i>Slc25a34</i>	3.22	9.33E-06
<i>Lepr</i>	7.74	3.84E-09	<i>Hsd17b11</i>	3.11	1.55E-07
<i>Lgals4</i>	7.62	4.69E-07	<i>Mycl</i>	3.09	2.81E-06
<i>Vnn1</i>	7.51	1.41E-07	<i>Pex11a</i>	3.05	8.37E-06
<i>Cux2</i>	7.50	3.72E-06	<i>Myom1</i>	3.00	1.08E-04
<i>Acot1</i>	7.26	1.80E-05	<i>Myo15b</i>	2.93	1.16E-06
<i>Slc27a1</i>	6.32	3.18E-09	<i>Atf5</i>	2.93	5.87E-05
<i>Slc25a47</i>	6.21	2.13E-04	<i>Slc7a2</i>	2.92	8.81E-07
<i>Peg3</i>	6.12	1.57E-09	<i>Fam13a</i>	2.90	2.93E-04
<i>Gpcpd1</i>	5.93	4.97E-09	<i>Fmo3</i>	2.88	4.21E-04
<i>Cidec</i>	5.52	5.57E-05	<i>Epor</i>	2.88	2.70E-04
<i>Ppargc1a</i>	5.49	4.78E-06	<i>Slc25a20</i>	2.87	1.63E-06
<i>Acot2</i>	5.25	4.54E-07	<i>Ackr4</i>	2.86	2.54E-06
<i>Retsat</i>	5.22	1.89E-08	<i>Por</i>	2.85	2.30E-06
<i>Fbxo21</i>	5.12	5.29E-06	<i>Slc25a42</i>	2.84	8.85E-06
<i>Rab30</i>	5.02	1.61E-07	<i>Fgl1</i>	2.83	9.12E-04
<i>Slc25a30</i>	4.92	1.71E-05	<i>Dcaf6</i>	2.80	1.79E-06
<i>Pck1</i>	4.86	1.21E-07	<i>Slc8b1</i>	2.79	3.88E-06
<i>Lpin1</i>	4.86	6.70E-05	<i>Nceh1</i>	2.77	3.84E-06
<i>Nipal1</i>	4.78	3.12E-04	<i>Brap</i>	2.77	7.06E-07
<i>Plin4</i>	4.69	1.56E-05	<i>Acot4</i>	2.72	2.94E-05
<i>Apoa4</i>	4.59	8.73E-07	<i>Slc41a3</i>	2.72	3.71E-05
<i>G6pc</i>	4.49	2.79E-05	<i>Oplah</i>	2.72	1.59E-06
<i>Ip6k2</i>	4.42	4.35E-04	<i>Rnf125</i>	2.71	1.92E-04
<i>Ehhadh</i>	4.32	9.96E-07	<i>Gpt2</i>	2.71	5.72E-07
<i>Trib3</i>	4.24	5.87E-06	<i>Arl4d</i>	2.70	4.57E-04
<i>Smad9</i>	4.21	1.76E-07	<i>Hsd17b10</i>	2.69	1.21E-06
<i>Trpm4</i>	4.12	3.61E-07	<i>Cyp1b1</i>	2.69	1.86E-04
<i>Cpt1a</i>	4.07	1.22E-07	<i>Sun2</i>	2.66	1.32E-05
<i>Ppm1k</i>	4.05	9.67E-09	<i>Tbc1d8</i>	2.64	3.80E-04
<i>Slc27a2</i>	3.90	4.25E-07	<i>Pcsk4</i>	2.64	3.03E-06
<i>Fbxo31</i>	3.86	9.15E-06	<i>Slc25a33</i>	2.64	1.92E-05
<i>Pnpla2</i>	3.77	8.58E-08	<i>Gfra1</i>	2.63	5.28E-06
<i>Zbed5</i>	3.75	1.23E-06	<i>Sesn2</i>	2.57	1.54E-06
<i>Lpin2</i>	3.71	2.12E-04	<i>Cyp17a1</i>	2.57	1.85E-04
<i>St3gal5</i>	3.70	2.29E-07	<i>Nr1i3</i>	2.57	2.02E-04
<i>Got1</i>	3.66	8.46E-04	<i>Bnip3</i>	2.55	1.33E-06
<i>Sorbs3</i>	3.65	4.36E-07	<i>Eif1</i>	2.54	6.54E-06
<i>Hmgcs2</i>	3.64	1.41E-07	<i>Acox1</i>	2.53	2.99E-05
<i>Mat1a</i>	3.48	2.79E-06	<i>Wnt2b</i>	2.52	5.49E-04
<i>Txnip</i>	3.42	3.23E-08	<i>Igfbp2</i>	2.51	1.46E-04
<i>Slc22a5</i>	3.37	1.11E-06	<i>Arrdc4</i>	2.49	2.05E-05
<i>Pmm1</i>	3.32	7.71E-04	<i>Gpr17</i>	2.49	1.66E-04

gene name	FC	P value
<i>Fitm2</i>	2.48	6.12E-05
<i>Ahcy</i>	2.47	5.71E-05
<i>Ccng2</i>	2.47	2.91E-05
<i>Arl4a</i>	2.46	1.11E-05
<i>Chkb</i>	2.46	4.84E-04
<i>Acot12</i>	2.45	2.02E-05
<i>Slc25a22</i>	2.45	2.48E-04
<i>Acadl</i>	2.45	1.81E-05
<i>Pank1</i>	2.44	1.99E-05
<i>Crot</i>	2.44	3.39E-04
<i>Gal3st1</i>	2.44	9.68E-04
<i>Nrbp2</i>	2.44	5.94E-06
<i>Hacl1</i>	2.43	2.09E-04
<i>Erbp3</i>	2.43	1.64E-05
<i>Il1rn</i>	2.42	1.42E-04
<i>Fkbp5</i>	2.41	2.08E-05
<i>Crat</i>	2.41	1.31E-05
<i>Bcl2l11</i>	2.39	2.21E-05
<i>Abhd6</i>	2.39	3.63E-05
<i>Rbpms</i>	2.36	7.40E-06
<i>Acadm</i>	2.36	6.56E-06
<i>Enc1</i>	2.34	5.02E-06
<i>Eci2</i>	2.34	6.10E-05
<i>Glt1d1</i>	2.34	6.64E-05
<i>Vwa8</i>	2.34	9.80E-06
<i>Cbx7</i>	2.33	7.58E-05
<i>Aldh3a2</i>	2.33	3.74E-04
<i>Ubald1</i>	2.32	1.26E-04
<i>Csad</i>	2.32	1.75E-04
<i>Ech1</i>	2.30	1.22E-05
<i>Eci1</i>	2.28	3.35E-05
<i>Asl</i>	2.28	5.93E-04
<i>Klf9</i>	2.27	6.54E-05
<i>Mid1</i>	2.27	3.66E-04
<i>Mgll</i>	2.26	7.98E-05
<i>Atg2a</i>	2.25	8.62E-06
<i>Pros1</i>	2.25	1.12E-05
<i>Egfr</i>	2.24	2.69E-05
<i>Mpzl1</i>	2.24	3.65E-04
<i>Tmem140</i>	2.24	1.27E-05
<i>Hadhb</i>	2.24	1.77E-05
<i>Cln8</i>	2.23	1.15E-04
<i>Ypel3</i>	2.22	3.34E-05
<i>Lims2</i>	2.22	1.36E-05
<i>Baiap2l1</i>	2.22	3.17E-04
<i>Klh24</i>	2.21	2.51E-04
<i>Calcoco1</i>	2.19	1.26E-05

gene name	FC	P value
<i>Elmod3</i>	2.19	8.75E-05
<i>Slc25a32</i>	2.19	1.88E-04
<i>Crebrf</i>	2.18	2.49E-04
<i>Tmem120a</i>	2.17	6.99E-06
<i>Tango2</i>	2.17	2.06E-04
<i>Gk</i>	2.17	7.81E-04
<i>Tram2</i>	2.15	3.09E-05
<i>F2rl2</i>	2.15	9.29E-04
<i>Hsd1l2</i>	2.15	2.79E-04
<i>Cntrl</i>	2.14	6.56E-06
<i>Abhd2</i>	2.14	9.95E-06
<i>Ephx2</i>	2.13	5.24E-05
<i>Adck5</i>	2.13	2.50E-04
<i>Eif4ebp1</i>	2.13	1.11E-04
<i>Dnmbp</i>	2.13	4.17E-05
<i>Rsad1</i>	2.13	3.33E-04
<i>Etfdh</i>	2.12	6.15E-05
<i>Plin5</i>	2.12	6.82E-04
<i>Tmed5</i>	2.11	8.93E-05
<i>Gpx3</i>	2.11	3.38E-04
<i>Kcnb1</i>	2.11	2.66E-04
<i>Smim13</i>	2.11	5.14E-05
<i>Zfand6</i>	2.10	5.18E-05
<i>Cdip1</i>	2.10	4.41E-05
<i>Slc16a7</i>	2.09	8.45E-06
<i>Chpt1</i>	2.09	2.08E-05
<i>Mknk2</i>	2.09	9.27E-05
<i>Map1lc3b</i>	2.08	3.64E-05
<i>Cyp2e1</i>	2.08	5.64E-04
<i>Psmc9</i>	2.08	1.79E-04
<i>Slc4a4</i>	2.07	2.61E-05
<i>Mtx3</i>	2.07	4.77E-05
<i>Tlcd4</i>	2.07	1.35E-04
<i>Rusc2</i>	2.06	6.16E-05
<i>Retreg1</i>	2.06	3.31E-04
<i>Cblb</i>	2.05	1.72E-04
<i>Lrfn4</i>	2.04	4.18E-04
<i>Zbtb44</i>	2.04	8.16E-05
<i>Slc10a1</i>	2.03	2.31E-05
<i>Ppargc1b</i>	2.03	2.68E-04
<i>Zbtb45</i>	2.03	1.07E-04
<i>Fosl2</i>	2.02	6.62E-05
<i>Apoa5</i>	2.01	2.02E-04
<i>Ldlrad4</i>	2.01	8.76E-05
<i>Sec22c</i>	2.01	5.14E-04
<i>Cpeb2</i>	2.01	1.93E-04
<i>Slc23a2</i>	2.01	3.96E-05

<i>gene name</i>	FC	P value
<i>Tmem134</i>	2.00	3.54E-05
<i>Sphk2</i>	2.00	1.84E-05
<i>Prdm11</i>	1.99	6.34E-04
<i>Dpyd</i>	1.99	2.71E-04
<i>Decr2</i>	1.99	1.40E-04
<i>Il15ra</i>	1.98	4.79E-05
<i>Klhl21</i>	1.98	5.71E-04
<i>Slc37a4</i>	1.98	5.16E-04
<i>Trim24</i>	1.98	1.05E-04
<i>Itga7</i>	1.98	2.86E-04
<i>Npc1</i>	1.97	5.32E-05
<i>Zfp36l2</i>	1.97	7.78E-05
<i>Hyal1</i>	1.96	6.03E-04
<i>Ldb1</i>	1.96	8.05E-05
<i>Gabarapl1</i>	1.96	5.05E-04
<i>Nr2c1</i>	1.96	8.69E-04
<i>Atxn2</i>	1.96	3.74E-05
<i>Fry</i>	1.95	3.81E-04
<i>Insr</i>	1.95	8.77E-05
<i>Usp38</i>	1.94	7.29E-05
<i>Dhtkd1</i>	1.94	7.26E-05
<i>Izumo4</i>	1.94	3.15E-04
<i>Stard5</i>	1.94	2.35E-05
<i>Jmy</i>	1.93	3.06E-04
<i>Ppp2r2d</i>	1.93	3.44E-04
<i>Sdc4</i>	1.92	7.70E-05
<i>Ackr2</i>	1.92	8.37E-04
<i>Ulk1</i>	1.92	7.06E-05
<i>Gpc1</i>	1.92	6.58E-04
<i>Mef2d</i>	1.91	7.61E-05
<i>Idua</i>	1.90	9.43E-05
<i>Agpat3</i>	1.90	1.21E-04
<i>Pdk2</i>	1.90	1.28E-04
<i>Acat1</i>	1.90	1.77E-04
<i>Hadha</i>	1.90	1.91E-04
<i>Ralgapa2</i>	1.90	7.51E-05
<i>Pde4d</i>	1.89	2.11E-04
<i>Slc38a4</i>	1.89	1.65E-04
<i>Ppp1r15a</i>	1.89	1.80E-04
<i>Cmb1</i>	1.88	2.06E-04
<i>Chst15</i>	1.88	3.68E-05
<i>Cobll1</i>	1.88	4.52E-04
<i>Btg1</i>	1.88	4.59E-04
<i>Taok3</i>	1.88	1.10E-04
<i>Apex2</i>	1.87	4.53E-04
<i>Plekhg3</i>	1.87	1.69E-04
<i>Fbxl17</i>	1.87	4.65E-04
<i>Klhl3</i>	1.87	5.12E-04

<i>gene name</i>	FC	P value
<i>Inca1</i>	1.86	5.65E-04
<i>Wrnip1</i>	1.86	8.08E-04
<i>Ei24</i>	1.85	4.61E-04
<i>Ddhd2</i>	1.85	8.47E-04
<i>Chchd10</i>	1.85	2.90E-04
<i>Mllt6</i>	1.85	1.33E-04
<i>Prkd3</i>	1.85	5.18E-04
<i>Cnppd1</i>	1.85	1.94E-04
<i>Atp10d</i>	1.84	1.95E-04
<i>Ctdsp2</i>	1.84	1.30E-04
<i>Ccs</i>	1.84	3.71E-04
<i>Clmn</i>	1.84	2.77E-04
<i>Decr1</i>	1.84	4.65E-04
<i>Lbp</i>	1.84	6.90E-04
<i>Hps4</i>	1.84	4.97E-04
<i>Josd1</i>	1.84	3.77E-04
<i>Elac1</i>	1.83	2.27E-04
<i>Pxmp4</i>	1.83	7.66E-04
<i>Mbd6</i>	1.83	2.89E-04
<i>Heca</i>	1.83	2.45E-04
<i>Gpld1</i>	1.83	4.42E-04
<i>Tet3</i>	1.82	9.68E-05
<i>Adcy6</i>	1.82	2.07E-04
<i>Acsm3</i>	1.82	1.30E-04
<i>Gys2</i>	1.82	2.00E-04
<i>Cd36</i>	1.81	6.99E-05
<i>Ell</i>	1.81	3.32E-04
<i>H6pd</i>	1.80	4.66E-04
<i>Gigyf1</i>	1.80	2.27E-04
<i>Tacc2</i>	1.80	1.93E-04
<i>Zmym5</i>	1.80	1.45E-04
<i>Ranbp10</i>	1.80	3.47E-04
<i>Aifm2</i>	1.80	2.33E-04
<i>Cirbp</i>	1.80	7.96E-04
<i>Dennd4a</i>	1.79	3.15E-04
<i>Slc19a1</i>	1.79	6.34E-04
<i>Abca6</i>	1.79	5.81E-04
<i>Tdrp</i>	1.79	7.19E-04
<i>Rtf2</i>	1.79	3.76E-04
<i>Sirt3</i>	1.78	6.76E-04
<i>Rnf169</i>	1.78	6.01E-04
<i>Tns2</i>	1.78	6.37E-04
<i>Aass</i>	1.78	6.34E-04
<i>Bmp1</i>	1.78	2.91E-04
<i>Atl2</i>	1.78	4.26E-04
<i>Tle1</i>	1.77	6.38E-04
<i>Flvcr2</i>	1.77	7.12E-04
<i>Setd1b</i>	1.76	1.97E-04

gene name	FC	P value
<i>Il1r1</i>	1.76	7.49E-04
<i>Epb41</i>	1.76	1.10E-04
<i>Arid5b</i>	1.75	6.92E-04
<i>Hacd3</i>	1.75	5.68E-04
<i>Selenop</i>	1.75	9.96E-04
<i>Hectd1</i>	1.74	6.42E-04
<i>Hsd17b13</i>	1.74	9.25E-04
<i>Rogdi</i>	1.73	5.33E-04
<i>Azgp1</i>	1.73	5.98E-04
<i>Rere</i>	1.73	2.58E-04
<i>Optn</i>	1.73	3.04E-04
<i>Mast3</i>	1.73	6.73E-04
<i>Chp1</i>	1.72	4.49E-04
<i>Nt5c2</i>	1.72	3.36E-04
<i>Pi4ka</i>	1.72	4.30E-04
<i>Pdpr</i>	1.72	6.75E-04
<i>Maf1</i>	1.72	5.41E-04
<i>Mcc</i>	1.72	5.58E-04
<i>Tfb2m</i>	1.72	6.07E-04
<i>Lpgat1</i>	1.72	2.94E-04
<i>Ppp1cc</i>	1.72	5.30E-04
<i>Spryd3</i>	1.71	7.81E-04
<i>Fam210b</i>	1.71	4.20E-04
<i>Fcgrt</i>	1.71	5.31E-04
<i>Rbl2</i>	1.70	7.52E-04
<i>Wdr81</i>	1.70	8.02E-04
<i>Slc47a1</i>	1.70	3.88E-04
<i>Tns1</i>	1.70	7.66E-04
<i>Bace1</i>	1.69	8.79E-04
<i>Tmem131</i>	1.68	3.60E-04
<i>Klhdc3</i>	1.68	5.59E-04
<i>Hhex</i>	1.67	9.00E-04
<i>Grn</i>	1.67	5.15E-04
<i>Rab11fip2</i>	1.67	6.07E-04
<i>Rbm3</i>	1.66	8.78E-04
<i>Ylpm1</i>	1.66	6.11E-04
<i>Crtc2</i>	1.65	9.00E-04
<i>Gab1</i>	1.65	5.19E-04
<i>Clk1</i>	1.64	1.00E-03
<i>Tmem86a</i>	1.63	5.16E-04
<i>Crybg1</i>	1.63	9.53E-04
<i>Nudt4</i>	1.63	9.25E-04
<i>Rbms1</i>	1.62	4.54E-04
<i>Chd7</i>	1.62	8.39E-04
<i>Smg6</i>	1.62	8.93E-04
<i>Ank3</i>	1.59	5.92E-04

Supplemental table 5. Human genes significantly decreased by fasting in hepatocyte humanized liver (P<0.001)

<i>gene name</i>	FC	P value	<i>gene name</i>	FC	P value
<i>IGF1</i>	0.02	1.03E-04	<i>UQCC2</i>	0.38	3.92E-04
<i>CYP1A1</i>	0.04	2.63E-06	<i>FRAT2</i>	0.38	1.88E-04
<i>CSF1</i>	0.04	9.26E-04	<i>PLD1</i>	0.38	7.98E-04
<i>DDIT4</i>	0.08	7.20E-06	<i>EPHA1</i>	0.38	1.00E-04
<i>PPP1R3C</i>	0.12	7.13E-08	<i>CDKN1A</i>	0.38	7.25E-06
<i>ANGPTL8</i>	0.15	9.64E-07	<i>RAPH1</i>	0.38	3.48E-04
<i>MID1IP1</i>	0.16	3.50E-05	<i>ELOVL6</i>	0.39	1.50E-04
<i>TUBB2A</i>	0.17	1.07E-05	<i>UBXN2B</i>	0.39	3.70E-05
<i>CYP1A2</i>	0.18	6.40E-06	<i>CARD10</i>	0.39	6.90E-05
<i>SOX9</i>	0.20	4.56E-05	<i>ZYX</i>	0.39	2.12E-04
<i>PEG10</i>	0.21	5.67E-05	<i>TSC22D1</i>	0.39	4.02E-05
<i>ARMC8</i>	0.22	9.42E-05	<i>LGALS4</i>	0.39	2.70E-04
<i>FADS2</i>	0.23	1.24E-07	<i>SMC6</i>	0.40	4.86E-04
<i>CYP1B1</i>	0.23	9.07E-06	<i>GLDC</i>	0.40	1.83E-04
<i>BICC1</i>	0.24	7.41E-04	<i>PPARGC1B</i>	0.41	2.37E-04
<i>AKR1B10</i>	0.24	3.00E-07	<i>TTPAL</i>	0.41	4.60E-04
<i>MBL2</i>	0.25	1.77E-04	<i>KANK2</i>	0.41	8.94E-05
<i>PITPNM2</i>	0.25	5.91E-04	<i>HMGCR</i>	0.42	1.88E-04
<i>TSKU</i>	0.25	3.55E-07	<i>SLC35C1</i>	0.42	5.81E-04
<i>MPV17L</i>	0.26	2.38E-04	<i>HYOU1</i>	0.42	9.05E-05
<i>RASSF3</i>	0.27	2.80E-04	<i>CUX2</i>	0.42	7.81E-05
<i>DOCK6</i>	0.27	2.22E-05	<i>GBP3</i>	0.42	7.13E-04
<i>ACTB</i>	0.27	8.51E-07	<i>GEMIN5</i>	0.42	2.22E-04
<i>HSPA13</i>	0.28	4.34E-04	<i>LACTB2</i>	0.42	2.66E-04
<i>PLK2</i>	0.28	1.30E-05	<i>TRIM21</i>	0.42	6.59E-04
<i>BHLHE40</i>	0.28	2.13E-04	<i>PGM3</i>	0.43	1.19E-04
<i>ETNPPL</i>	0.29	2.86E-04	<i>USH2A</i>	0.43	5.68E-04
<i>ACTG1</i>	0.30	2.34E-04	<i>WDR12</i>	0.43	8.77E-04
<i>SMAD6</i>	0.31	4.35E-05	<i>CTNNB1</i>	0.43	9.31E-04
<i>TGM2</i>	0.31	1.15E-04	<i>CYP7A1</i>	0.43	1.39E-04
<i>MANF</i>	0.32	9.39E-05	<i>TUBA1C</i>	0.43	1.77E-04
<i>EHD4</i>	0.32	1.82E-04	<i>PGD</i>	0.43	2.12E-04
<i>SEC14L4</i>	0.33	1.90E-04	<i>TUBB4B</i>	0.44	5.16E-05
<i>RND2</i>	0.33	4.58E-04	<i>CACYBP</i>	0.44	7.43E-04
<i>NROB2</i>	0.33	2.05E-04	<i>SNX4</i>	0.44	3.89E-04
<i>FRAT1</i>	0.34	8.63E-04	<i>GSTA2</i>	0.44	1.05E-05
<i>ANO1</i>	0.34	5.17E-05	<i>ABCA1</i>	0.44	5.72E-04
<i>HEATR3</i>	0.35	5.77E-04	<i>VPS18</i>	0.44	1.85E-04
<i>DNAJB11</i>	0.35	9.70E-05	<i>NME1</i>	0.44	3.27E-04
<i>BCL3</i>	0.35	8.27E-04	<i>CDK2AP2</i>	0.44	6.79E-04
<i>NSDHL</i>	0.35	1.87E-04	<i>PITHD1</i>	0.45	2.70E-04
<i>PPIB</i>	0.35	7.35E-05	<i>AGFG1</i>	0.45	4.02E-04
<i>MIR22HG</i>	0.35	2.30E-04	<i>CYB5B</i>	0.45	4.63E-04
<i>FADS1</i>	0.35	1.50E-05	<i>PPP1R3B</i>	0.45	2.33E-05
<i>CLIC4</i>	0.35	2.30E-05	<i>UBE2L6</i>	0.45	4.50E-04
<i>TUBA4A</i>	0.35	2.61E-05	<i>PDIA6</i>	0.45	3.10E-04
<i>TTC39C</i>	0.36	1.60E-05	<i>ABCA5</i>	0.46	6.86E-04
<i>DIO1</i>	0.36	1.19E-05	<i>ANAPC7</i>	0.46	8.18E-04
<i>FASN</i>	0.36	2.87E-04	<i>AMD1</i>	0.46	2.75E-04
<i>NAT8</i>	0.37	6.77E-04	<i>KLHL5</i>	0.46	4.11E-04
<i>STARD4</i>	0.37	5.37E-04	<i>ESR1</i>	0.46	2.34E-04
<i>ELP1</i>	0.38	1.25E-05	<i>ENO3</i>	0.47	3.97E-04
<i>ALAS1</i>	0.38	3.53E-04	<i>SEC61B</i>	0.47	5.04E-04
<i>ACLY</i>	0.38	7.48E-05	<i>LRRCS9</i>	0.47	6.83E-04

gene name	FC	P value
<i>CALR</i>	0.47	8.46E-04
<i>ATG101</i>	0.47	7.72E-04
<i>MYO7A</i>	0.47	3.15E-04
<i>HSPB1</i>	0.47	7.90E-05
<i>HSPA8</i>	0.48	1.61E-04
<i>PDIA3</i>	0.48	8.72E-04
<i>EMC1</i>	0.48	1.02E-04
<i>SEC61A1</i>	0.49	1.28E-04
<i>CDC42EP1</i>	0.49	2.14E-04
<i>CAPN5</i>	0.49	1.33E-04
<i>PIK3R1</i>	0.49	3.05E-04
<i>FDPS</i>	0.49	1.15E-04
<i>NFKB1</i>	0.49	9.00E-04
<i>ACSS2</i>	0.49	6.76E-04
<i>SRPRB</i>	0.50	6.15E-04
<i>XBP1</i>	0.50	6.91E-05
<i>RFX5</i>	0.50	9.20E-04
<i>RRBP1</i>	0.50	1.51E-04
<i>SELENOT</i>	0.50	3.75E-04
<i>BIN1</i>	0.50	7.68E-04
<i>LIMD1</i>	0.51	2.98E-04
<i>SEC23B</i>	0.51	5.16E-04
<i>SCCPDH</i>	0.51	8.91E-04
<i>RDH11</i>	0.51	8.35E-04
<i>APCS</i>	0.51	5.92E-04
<i>HSPA5</i>	0.52	1.47E-04
<i>SERP1</i>	0.52	7.70E-04
<i>FAM162A</i>	0.52	6.62E-04
<i>UGDH</i>	0.52	1.41E-04
<i>SLC3A2</i>	0.52	9.05E-04
<i>MLEC</i>	0.52	3.63E-04
<i>CMTM6</i>	0.52	4.92E-04
<i>CNN3</i>	0.53	4.05E-04
<i>PTPRJ</i>	0.53	4.86E-04
<i>DNAJB9</i>	0.53	6.46E-04
<i>HACD2</i>	0.53	6.96E-04
<i>ANTXR2</i>	0.54	7.05E-04
<i>RPS7</i>	0.54	5.56E-04
<i>HABP2</i>	0.54	7.79E-04
<i>ALCAM</i>	0.54	7.27E-04
<i>PRDX1</i>	0.55	3.89E-04
<i>VIL1</i>	0.55	7.35E-04
<i>FGB</i>	0.55	4.91E-04
<i>IDI1</i>	0.55	8.14E-04
<i>RPL36AL</i>	0.55	9.44E-04
<i>RHOB</i>	0.55	6.74E-04
<i>FGA</i>	0.57	7.93E-04
<i>HSP90AB1</i>	0.57	5.50E-04
<i>A1CF</i>	0.57	6.18E-04
<i>SLC25A3</i>	0.57	7.42E-04
<i>SLC39A14</i>	0.58	2.89E-04
<i>FGG</i>	0.58	6.54E-04
<i>UBC</i>	0.59	7.93E-04
<i>METTL7B</i>	0.60	7.93E-04

Supplemental table 6. Mouse genes significantly decreased by fasting in hepatocyte humanized liver (P<0.001)

<i>gene name</i>	FC	P value	<i>gene name</i>	FC	P value
<i>Ctnna3</i>	0.02	9.77E-05	<i>Slc3a1</i>	0.39	1.01E-04
<i>Chrna4</i>	0.02	4.96E-04	<i>Spc24</i>	0.40	4.11E-05
<i>Thrsp</i>	0.07	1.16E-04	<i>Serpina6</i>	0.40	7.79E-06
<i>Angptl8</i>	0.08	8.25E-12	<i>Leap2</i>	0.40	1.97E-05
<i>Gck</i>	0.09	2.12E-11	<i>Gmppb</i>	0.40	1.32E-04
<i>Fdps</i>	0.11	1.02E-04	<i>Ccnd1</i>	0.42	3.00E-04
<i>Pcsk9</i>	0.12	8.11E-05	<i>Ldlr</i>	0.42	2.31E-06
<i>Insig1</i>	0.13	1.81E-06	<i>Anks4b</i>	0.42	2.92E-06
<i>Srebfl1</i>	0.15	1.93E-08	<i>Sc5d</i>	0.43	5.86E-06
<i>Fasn</i>	0.15	1.17E-05	<i>Sec61b</i>	0.43	2.61E-05
<i>Adgrd1</i>	0.15	6.51E-04	<i>Cyb5b</i>	0.43	3.09E-05
<i>Gstm3</i>	0.19	1.65E-04	<i>Pold2</i>	0.43	3.90E-04
<i>Mid1ip1</i>	0.22	2.31E-06	<i>Fam83f</i>	0.44	5.04E-04
<i>Fam47e</i>	0.23	3.30E-05	<i>Sec23b</i>	0.44	2.05E-05
<i>Sdf2l1</i>	0.26	2.23E-07	<i>Jpt2</i>	0.44	3.76E-06
<i>Mybl1</i>	0.26	9.54E-04	<i>Adra1b</i>	0.44	5.69E-06
<i>Uhrf1</i>	0.27	1.20E-05	<i>Sucnr1</i>	0.45	6.52E-06
<i>Nsdhl</i>	0.27	5.37E-06	<i>Pls1</i>	0.45	6.80E-04
<i>Tuba1b</i>	0.28	9.48E-06	<i>Gstm4</i>	0.45	1.83E-04
<i>Tuba1c</i>	0.28	3.83E-05	<i>Hspa13</i>	0.45	1.63E-04
<i>Gale</i>	0.29	9.15E-06	<i>Dpy19l3</i>	0.45	1.07E-05
<i>Atp2b2</i>	0.30	1.02E-04	<i>Pter</i>	0.46	1.12E-05
<i>Cdc20</i>	0.31	1.32E-04	<i>Tmem258</i>	0.46	1.22E-04
<i>Serpina7</i>	0.31	7.43E-04	<i>Tmem141</i>	0.47	3.28E-05
<i>Mcm5</i>	0.31	6.11E-06	<i>Tuba4a</i>	0.47	3.24E-05
<i>Acly</i>	0.31	2.23E-07	<i>Id3</i>	0.47	6.43E-05
<i>Isg15</i>	0.32	1.88E-04	<i>Lss</i>	0.48	2.64E-04
<i>Cyp2r1</i>	0.32	5.63E-04	<i>Gbe1</i>	0.48	8.20E-05
<i>Slc22a7</i>	0.32	6.50E-06	<i>Tsc22d1</i>	0.48	7.11E-05
<i>Mcm6</i>	0.32	3.10E-06	<i>Pgd</i>	0.48	4.32E-04
<i>Cks1b</i>	0.33	2.59E-04	<i>Akr1d1</i>	0.48	2.41E-05
<i>Slc41a2</i>	0.33	2.93E-04	<i>Prxl2b</i>	0.48	6.68E-05
<i>Hdhd3</i>	0.34	5.06E-06	<i>Gas2</i>	0.49	7.54E-05
<i>Slc1a4</i>	0.34	1.88E-05	<i>Top2a</i>	0.49	9.61E-04
<i>Cxcl10</i>	0.34	4.05E-05	<i>Elovl6</i>	0.49	3.94E-04
<i>Dnah5</i>	0.34	6.36E-04	<i>Serpinh1</i>	0.49	1.37E-04
<i>lhh</i>	0.35	3.15E-05	<i>Mcm2</i>	0.49	2.80E-04
<i>Nudt7</i>	0.35	1.96E-06	<i>Mmab</i>	0.49	4.56E-05
<i>Ppp1r3b</i>	0.35	8.10E-06	<i>Krt18</i>	0.49	5.71E-05
<i>Stard4</i>	0.36	5.97E-04	<i>Ostc</i>	0.49	2.56E-04
<i>E2f2</i>	0.36	1.04E-05	<i>Pdia6</i>	0.49	1.31E-04
<i>Mvd</i>	0.37	5.83E-05	<i>Adh4</i>	0.49	1.78E-04
<i>Aacs</i>	0.38	5.50E-04	<i>Anxa2</i>	0.49	2.44E-04
<i>Chst13</i>	0.39	2.23E-04	<i>Actg1</i>	0.50	2.50E-05
<i>Krt8</i>	0.39	2.09E-06	<i>Pklr</i>	0.50	2.31E-04
<i>Pmvk</i>	0.39	2.20E-05	<i>S1pr1</i>	0.50	1.98E-05

<i>gene name</i>	FC	P value
<i>Slc35b1</i>	0.51	1.47E-04
<i>Ugdh</i>	0.51	2.51E-04
<i>ler5</i>	0.51	4.32E-04
<i>Dtymk</i>	0.51	7.08E-04
<i>Slc46a3</i>	0.51	6.97E-05
<i>Kpna2</i>	0.52	2.28E-04
<i>Alad</i>	0.52	5.99E-05
<i>Gclc</i>	0.52	5.52E-04
<i>Leo1</i>	0.52	6.75E-04
<i>Abcb11</i>	0.52	1.13E-04
<i>Fkbp4</i>	0.52	7.33E-05
<i>Actb</i>	0.52	3.85E-05
<i>Gsta4</i>	0.52	4.39E-05
<i>Cnp</i>	0.53	1.05E-04
<i>Mvk</i>	0.53	1.59E-04
<i>Nans</i>	0.53	1.20E-04
<i>Qdpr</i>	0.53	7.35E-04
<i>Lect2</i>	0.53	2.74E-04
<i>Rpn1</i>	0.53	4.09E-05
<i>Ddc</i>	0.53	3.09E-04
<i>Hes1</i>	0.53	6.64E-04
<i>Tbcel</i>	0.53	1.67E-04
<i>Slc23a1</i>	0.54	2.29E-04
<i>Manf</i>	0.54	3.21E-04
<i>Hyou1</i>	0.54	9.69E-04
<i>Pdgfa</i>	0.54	5.07E-04
<i>Uba5</i>	0.55	4.21E-04
<i>Iffo2</i>	0.55	9.69E-05
<i>Ssr1</i>	0.55	8.46E-04
<i>Xdh</i>	0.55	2.29E-04
<i>Dhcr7</i>	0.56	3.38E-04
<i>Acaca</i>	0.56	3.01E-04
<i>Calr</i>	0.56	7.27E-04
<i>Tkt</i>	0.56	1.26E-04
<i>Dynll1</i>	0.56	1.80E-04
<i>Slc9a3r1</i>	0.56	1.71E-04
<i>Acat2</i>	0.56	3.74E-04
<i>Tcea3</i>	0.57	2.14E-04
<i>Afm</i>	0.58	5.10E-04
<i>Ddost</i>	0.59	1.56E-04
<i>Tmem86b</i>	0.59	2.48E-04
<i>Pygl</i>	0.59	3.38E-04
<i>Tgm2</i>	0.59	2.43E-04
<i>Nqo2</i>	0.59	6.97E-04
<i>Gsap</i>	0.60	5.26E-04
<i>Asap3</i>	0.60	5.12E-04
<i>Tpm1</i>	0.60	3.31E-04

<i>gene name</i>	FC	P value
<i>Fam149a</i>	0.60	5.61E-04
<i>Ifftm3</i>	0.60	7.93E-04
<i>Kifc3</i>	0.60	4.31E-04
<i>Ppib</i>	0.61	7.82E-04
<i>Calm1</i>	0.61	5.40E-04
<i>Lasp1</i>	0.64	8.48E-04

Supplemental table 7. Genes for which the difference in Signal Log Ratio for the effect of fasting in human and mouse cells exceeded 2. Values are fold changes.

<i>gene name</i>	human	mouse	<i>gene name</i>	human	mouse
<i>IGF1</i>	-53.97	1.36	<i>TNFRSF25</i>	-5.29	1.25
<i>CYP8B1</i>	1.13	47.79	<i>MOB3B</i>	-6.09	1.03
<i>KCNT2</i>	-20.30	1.68	<i>MARCKSL1</i>	-5.50	1.13
<i>PARL</i>	-22.26	1.20	<i>FERMT3</i>	-5.46	1.13
<i>PYCARD</i>	-18.59	1.30	<i>PLCE1</i>	-4.52	1.35
<i>NCEH1</i>	-8.52	2.77	<i>SLC16A7</i>	-2.89	2.09
<i>CSF1</i>	-24.85	-1.24	<i>RILPL2</i>	-4.80	1.23
<i>LGALS4</i>	-2.55	7.62	<i>SOAT2</i>	-6.45	-1.11
<i>NLRCS</i>	-13.92	1.36	<i>ABCB6</i>	-3.43	1.69
<i>CUX2</i>	-2.38	7.50	<i>CLP1</i>	-5.37	1.07
<i>RALGDS</i>	-14.06	1.24	<i>CEP72</i>	-6.75	-1.18
<i>WNT2B</i>	-6.90	2.52	<i>SLC27A1</i>	1.11	6.32
<i>PEG3</i>	-2.79	6.12	<i>CHAC1</i>	-2.64	2.15
<i>DDIT4</i>	-13.07	1.17	<i>SMIM13</i>	-2.63	2.11
<i>GPCPD1</i>	-2.36	5.93	<i>HILPDA</i>	-2.89	1.90
<i>BEX1</i>	-1.10	12.58	<i>TMA16</i>	-5.49	1.00
<i>AQP1</i>	-11.22	1.02	<i>PLIN4</i>	-1.17	4.69
<i>CYP1B1</i>	-4.28	2.69	<i>BZW2</i>	-5.54	-1.03
<i>CYP1A1</i>	-25.52	-2.32	<i>F8</i>	-5.33	1.01
<i>FBXO10</i>	-5.47	1.79	<i>FRAT1</i>	-2.97	1.81
<i>DNAH6</i>	1.22	11.93	<i>ATPCKMT</i>	-4.81	1.10
<i>PPM1K</i>	-2.33	4.05	<i>STARD5</i>	-2.71	1.94
<i>TRIB3</i>	-2.14	4.24	<i>TAGLN</i>	-2.88	1.82
<i>IL15RA</i>	-4.49	1.98	<i>ENPP3</i>	-3.91	1.33
<i>MSTO1</i>	-9.40	-1.08	<i>ADAT2</i>	-5.42	-1.04
<i>APBB1IP</i>	-6.69	1.30	<i>BOLA3</i>	-5.34	-1.04
<i>SERPINI1</i>	-6.38	1.35	<i>ALAS1</i>	-2.65	1.95
<i>WDR53</i>	-7.15	1.16	<i>SYDE2</i>	-4.08	1.26
<i>SMAD9</i>	-1.93	4.21	<i>NTN4</i>	-3.53	1.46
<i>ARL4D</i>	-2.95	2.70	<i>EEF1AKNMT</i>	-5.12	1.00
<i>OSBPL6</i>	-2.47	3.22	<i>DBF4</i>	-8.30	-1.63
<i>PEG10</i>	-4.68	1.68	<i>ITGA10</i>	-2.23	2.28
<i>FGF2</i>	-6.58	1.18	<i>FAM166B</i>	-1.56	3.27
<i>MLLT11</i>	-5.81	1.34	<i>GIN1</i>	-4.19	1.20
<i>ZBED5</i>	-2.04	3.75	<i>BICC1</i>	-4.25	1.18
<i>IRF8</i>	-6.48	1.17	<i>MAMLD1</i>	-3.45	1.45
<i>NOC3L</i>	-6.63	1.13	<i>PPARGC1B</i>	-2.46	2.03
<i>TIMM9</i>	-5.38	1.37	<i>PITPNM2</i>	-3.99	1.25
<i>CEP55</i>	-12.97	-1.78	<i>ZMYND10</i>	-1.77	2.77
<i>IP6K2</i>	-1.63	4.42	<i>KCTD15</i>	-3.40	1.43
<i>TENM1</i>	-1.32	5.38	<i>RETSAT</i>	1.08	5.22
<i>LPIN1</i>	-1.45	4.86	<i>ABHD17B</i>	-4.86	-1.01
<i>CCDC86</i>	-7.56	-1.07	<i>SOX9</i>	-4.99	-1.04
<i>NUDT1</i>	-6.76	1.03	<i>FCAMR</i>	-4.01	1.20
<i>NUMBL</i>	-4.48	1.49	<i>CYP7A1</i>	-2.34	2.06
<i>ACOT1</i>	1.10	7.26	<i>CEP83</i>	-5.68	-1.18

<i>gene name</i>	human	mouse
ZKSCAN4	-1.37	3.51
ARHGAP18	-5.99	-1.25
LGALS1	-6.90	-1.45
HACL1	-1.95	2.43
FRAT2	-2.63	1.79
FBXO4	-3.96	1.19
RBM4	-2.83	1.66
ZMYND12	-1.99	2.34
OSBPL3	-2.90	1.59
ST3GAL5	-1.25	3.70
TTC39C	-2.81	1.64
STYXL1	-2.28	2.02
MPZL1	-2.04	2.24
LRRC1	-4.13	1.10
ZCCHC10	-2.81	1.61
TDRP	-2.54	1.79
SNAI2	-2.39	1.89
CFAP298	-4.77	-1.06
FADS2	-4.37	1.03
METTL25	-4.19	1.07
SYT12	-4.22	1.06
PLCXD2	-2.67	1.66
IZUMO4	-2.29	1.94
SLC22A5	-1.31	3.37
OGFOD2	-3.32	1.33
BMERB1	-2.28	1.93
ACOT2	1.20	5.25
FBXO21	1.17	5.12
SORBS3	-1.19	3.65
CD38	-3.93	1.10
PHC1	-3.42	1.27
SATB2	-2.11	2.05
CRACR2A	-3.96	1.09
POP1	-3.35	1.27
ARHGAP19	-3.52	1.20
USH2A	-2.35	1.79
SNRNP25	-4.09	1.02
SLC25A30	1.18	4.92
PANX2	-1.01	4.12
CAPN12	1.70	7.06
SPP1	-4.28	-1.03
RAB30	1.21	5.02
AGBL3	-2.56	1.59
AP4M1	-2.97	1.37
GPD1L	-3.97	1.02
DNAJB3	-4.06	-1.00
OXLD1	-2.97	1.36
POU5F2	-1.88	2.15

<i>gene name</i>	human	mouse
PPP1R3C	-8.08	-2.01
EHHADH	1.07	4.32
DIO1	-2.80	1.43
GPAT3	7.18	1.72
PCK1	20.45	4.86
HSPBAP1	2.97	-1.42
MORN4	2.37	-1.80
VXN	1.65	-2.65
PRODH	4.28	-1.03
INSIG1	-1.64	-7.45
FDPS	-2.04	-9.30
C1QL3	2.63	-1.75
OLFML1	3.95	-1.16
SSBP2	4.84	1.04
PSTPIP2	-1.21	-5.98
MEGF6	4.14	-1.23
SYT9	4.83	-1.07
PKHD1L1	1.61	-3.81
THRSP	-2.26	-13.95
ADRA1B	2.80	-2.25
SFXN4	-1.21	-7.82
FZD3	1.63	-3.99
DNAH5	2.23	-2.96
H2BC11	-1.03	-9.06
FAM122B	10.41	1.17
CLDN15	1.23	-8.76
APOA4	64.65	4.59
PNPLA3	-1.60	-25.08
ADGRD1	2.47	-6.48
CHRNA4	-1.66	-46.15
CTNNA3	2.28	-56.74

CHAPTER 7



General Discussion

In this thesis, we had a deeper look into several players of energy metabolism during different metabolic challenges. Disturbances in energy metabolism are the root cause of metabolic diseases. These diseases include, and are often a combination of, central obesity, insulin resistance and type 2 diabetes, atherogenic dyslipidemia (increased serum triglycerides, decreased high-density lipoproteins, and increased, smaller, low-density lipoproteins), nonalcoholic fatty liver disease, hypertension and cardiovascular diseases. The combination of hypertension, central obesity, insulin resistance and atherogenic dyslipidemia is referred to as the metabolic syndrome [1–3]. Interestingly, PPARs have been shown to be at the crossroad of glucose metabolism, lipid metabolism, and inflammation, which play crucial roles in the development of these metabolic diseases [4,5].

PPAR as a target to tackle metabolic diseases

PPAR as a direct therapeutic target

Over the years, several treatments for metabolic diseases that specifically target PPARs have been developed. To date, different PPAR-related strategies have been used to tackle one or more metabolic diseases. First, fibrates such as fenofibrate, bezafibrate, and gemfibrozil are PPAR α agonists used to improve dyslipidemia. More specifically, they decrease triglyceride levels, moderately increase HDL levels, increase LDL particle size, and reduce inflammation [4,6–8]. Functionally, fibrates have an effect on the metabolism of TG-rich lipoproteins via stimulation of the activity of lipoprotein lipase. Additionally, fibrates stimulate apolipoprotein A-V and inhibit apolipoprotein C-III expression via a mechanism dependent of PPAR α [9]. The use of fibrates may be particularly valuable in patients with the metabolic syndrome in order to combat cardiovascular diseases [10–12]. Second, thiazolidinediones (TZDs), or glitazones, are PPAR γ agonists that improve insulin resistance in type 2 diabetic patients [13]. TZDs have less pronounced effects on plasma lipoproteins compared to the above mentioned fibrates [14]. Since insulin resistance and atherogenic dyslipidemia very often co-exist in patients, agonists that combine the therapeutic effects of both PPAR α and PPAR γ agonists have been developed. Among these dual PPAR α/γ agonists are compounds belonging to the glitazars class [15–17].

Due to the numerous targets of the PPARs, activation of these nuclear receptors not only carries a potential therapeutic benefit but can also trigger adverse effects such as weight gain, increased plasma creatinine, gallstone formation, and myopathy [17,18]. Long term administration of fibrates in mice results in development of hepatic cancers. However, humans appear to be exempt from this effect of PPAR α activation [19]. Despite the therapeutic benefits of fibrates, the use of fibrates is rather limited since they only seem to be beneficial in a specific type of atherogenic dyslipidemia [20]. For the glitazars, several promising candidates were halted because of adverse effects [17,21,22]. So even though PPARs seem to be very suitable

therapeutic targets, the adverse effects and the lack of specificity due to the many target genes can be considered major drawbacks for their clinical use. Accordingly, therapeutic targeting of genes and proteins that are downstream of PPAR may be a more viable approach. Examples of proteins that are under transcriptional control of PPAR and that are currently being explored as targets for different aspects of the metabolic syndrome include FGF21 and ANGPTL4 [23–25]. The characterization of the molecular and physiological function of novel PPAR target genes may pave the way for novel therapeutic strategies for metabolic diseases. With that in mind, in **chapter 2** and **chapter 3** we identified and characterized two novel PPAR-regulated genes: *Adtrp* and *Tmed5*. By selecting putative target genes of PPAR α , we aimed to identify potential novel players in lipid metabolism. Even though this strategy has resulted in the discovery of a number of important players in lipid metabolism [26–28], this approach has several downsides and might be considered a bit risky. Many target genes with a very distinct and crucial function in lipid metabolism were already identified several years ago. These genes could be considered the “low-hanging fruits”. The remaining genes are likely to have more obscure functions in lipid metabolism that require very lengthy investigation. In addition, the complexity of lipid metabolism and the diverse regulation of target genes over different tissues makes it complicated to unravel the function of 1 specific gene. Multiple genes may cover the same function. Also, ablation of genes may trigger compensatory mechanisms, where in order to maintain homeostasis other genes take over upon blockage or absence of the targeted gene. Next to its dominant role in the regulation of hepatic lipid metabolism, PPAR α also regulates genes involved in other pathways, including glucose homeostasis, inflammation, and cell proliferation [29,30]. The pleiotropic role of PPAR α challenges our current working hypothesis “when it is regulated by PPAR α it is probably involved in lipid metabolism”. Indeed, based on the literature and our own data in **chapter 2**, we propose that ADTRP is only marginally involved in lipid metabolism in the liver [31]. We reached this conclusion based on the fact that neither upon overexpression in our own study, neither upon absence of *Adtrp*, a metabolic phenotype could be detected [32]. According to the literature, ADTRP is a hydrolase for a recently discovered class of lipids named the branched fatty acid esters of hydroxy fatty acids (FAHFAs) [31–33]. However, hepatic FAHFA content was not altered upon absence or overexpression of *Adtrp*, questioning its role as hydrolytic enzyme in the liver specifically [32]. Hydrolysis of FAHFAs does not seem to be very enzyme-specific, as not only ADTRP seems to have hydrolytic capacities but also Androgen-induced gene 1 protein (AIG1) and carboxyl ester lipase (CEL) were shown to be able to hydrolyze FAHFAs [32,34,35]. We propose ADTRP to have an alternative function in the liver. We are unable to draw any conclusions about ADTRP linked to FAHFAs in other tissues since our model is liver-specific. Patel et al. proposed that ADTRP is involved in vascular development and remodeling, as well as vessel integrity [36]. Taking into consideration that also PPAR α itself is linked to cardiac inflammation, extracellular matrix remodeling, oxidative stress, regulation

of cardiac hypertrophy, regulation of cardiac cell cycle, and angiogenesis, the main function of ADTRP should possibly be sought in these fields [4,5,37,38].

As a side note: FAHFAs, the holy grail?

Presently, not much is known about ADTRP, except for its proposed enzymatic function as one of the key enzymes for the hydrolysis of FAHFAs. FAHFAs are a recently discovered class of lipids that were first described in 2014 by Yore et al [39]. Fatty Acid esters of Hydroxy Fatty Acids are ester derivatives of fatty acids (FAs) with hydroxy fatty acids (HFAs). The hydroxy fatty acids can carry the hydroxyl group at different positions. The major classes of FAHFAs that have been detected are dimers of palmitic acid (PA), stearic acid (SA), oleic acid (OA), or palmitoleic acid (PO) with their corresponding hydroxy fatty acids (HPA, HSA, HOA, HPO), resulting in for example PAHSA and OAHSA. But in principle virtually every fatty acid can be incorporated in FAHFAs [40,41]. Additionally, each of these combinations consists of multiple isomers in which the branched ester is at different positions [42]. The large number of possible combinations combined with all possible positional isomers makes the analysis of FAHFAs very challenging.

Yore et al. revealed the existence of endogenous FAHFAs by overexpressing the GLUT4 transporter in adipocytes followed by lipidomic-analysis [39]. Additionally, they showed that PAHSA levels specifically correlate with insulin sensitivity and are reduced in adipose tissue and serum of insulin-resistant humans. Oral PAHSA administration in mice was shown to improve glucose tolerance via stimulation of GLP-1 and insulin secretion and appears to be protective against adipose tissue inflammation [39,43,44]. In adipose tissue, PAHSAs have been suggested to signal through GPR120, a PPAR γ target, to enhance glucose uptake [39,45]. FAHFAs may also carry therapeutic value beyond insulin resistance and type 2 diabetes. They are proposed to prevent against mucosal damage, colitis, and type 1 diabetes [46,47]. Additionally, their production seems to be induced in adipose tissue upon exercise [48]. The last couple of years, the structure, regulation, occurrence in triglycerides, and possible combinations of fatty acids and hydroxy fatty acids were explored extensively [40,49]. Recently, Pflimlin et al. questioned the finding that PAHSAs have beneficial metabolic effects, which resulted in a scientific discussion highlighting the difficulties in FAHFA research [49–51]. Indeed, multiple difficulties have arisen concerning accurately measuring FAHFAs in plasma and tissues. A clear example is the vehicle, which could make the FAHFAs more or less available. For example, in the study of Pflimlin et al., olive oil is used, which has insulin-sensitizing effects on its own and supposedly contains FAHFAs itself [49]. Here, the vehicle could have masked to beneficial effects of the FAHFAs. The analytical measurement of FAHFAs also poses a

challenge. The levels of FAHFAs in human plasma and tissues are as low as nanomolar concentrations [52] as confirmed in our own data in **chapter 2**. Different groups report ceramide contaminants overlapping 5-PAHSAs and high background contamination with lot of variation in all isoforms of PAHSA-measurements, which makes measurements and interpretation difficult, especially in samples with low concentrations [39,42,53,54]. Due to the many different FAHFAs, interpretation of the results obtained via LC-MS is challenging. In our own data, we find very low concentrations with a lot of variation, casting doubt on the absolute accuracy of the present measurement methods.

PAHSAs are at this moment the most studied group of FAHFAs, and are relatively highly abundant in human plasma and tissues. Different FAHFAs can possibly have different effects, which can be both beneficial and detrimental for human health. For example in a study using 9-PAHPA and 9-OAHPA, detrimental effects on liver were found in part of the mice [55]. These differential effects of FAHFAs are in line with different effects of saturated and trans- and cis-unsaturated fatty acids on human health, and even within those classifications fatty acids have different impacts in the body. This highlights the need for a detailed comparison of the effects of the different FAHFAs present. Administration of PAHSAs, at supposedly physiological concentrations, resulted in improvements in insulin sensitivity [39]. By contrast, upon absence of ADTRP, PAHSA levels in the adipose tissue were reduced, but no metabolic effect could be found at the whole body level [32]. It is possible that endogenous PAHSAs do not have the same effect on insulin sensitivity compared to exogenous PAHSAs, even though the PAHSAs are administered in physiological concentrations. The field of FAHFAs is in my opinion a very exciting field, with possibly novel therapeutic values, but caution should be taken when drawing conclusions. Many questions are still unanswered and many more questions might rise in the coming years.

Physiological PPAR related strategies to tackle metabolic diseases

Cold exposure as a therapy for metabolic diseases

After the first description of the existence of BAT in human adults, cold exposure was proposed to be a promising candidate as a therapy for obesity and insulin sensitivity. Consistent with this notion, cold exposure was shown to increase energy expenditure in healthy individuals and improve insulin sensitivity in type 2 diabetic patients. However, there are also growing concerns about targeting BAT to correct metabolic diseases. First, overweight and obese men were shown to have reduced brown adipose tissue activity, which may make it difficult to stimulate BAT activity in overweight individuals [56,57]. Second, BAT and beige adipose tissue only seem

to contribute a small amount to the overall energy expenditure [58]. Third, there is quite some heterogeneity in outcomes between different studies [58]. To this date, the contribution of browning to the improvement in glucose metabolism in humans is unclear since cold-exposure has not been shown to result in browning of human adipose tissue. Alternatively, the cold-induced improvements in insulin sensitivity may be due higher glucose uptake in the muscle [59]. A better understanding of the specific regulation of cold-induced browning in humans could be helpful in order to elucidate its potential role as therapeutic target for metabolic diseases.

In the process of browning, the nuclear receptor PPAR α seems to be involved, as PPAR α is highly expressed in BAT and is highly induced upon adipose tissue browning. Moreover, agonists of PPAR α were shown to induce the expression of thermogenic genes in WAT [60,61]. Importantly, when identifying the role of nuclear receptors under specific conditions, we should make a distinction between the role of a nuclear receptor under *in vivo* physiological conditions, and the effects of any given pharmacological agonist that targets that receptor. A variety of studies were performed in the past years showing that pharmacological activation of PPAR α result in browning of subcutaneous WAT [62–67]. Additionally, no browning characteristics are seen in WAT of PPAR α ^{-/-} mice upon pharmacological activation of browning via the β 3-adrenergic agonist CL316,243, strengthening the idea of the requirement of PPAR α in the browning process [66]. However, in **chapter 4**, we showed PPAR α to be dispensable for cold-induced browning, as adipose tissue browning was indistinguishable between WT and PPAR α ^{-/-} mice. The only distinction between the study of Li et al. and our study was the use of a pharmacological trigger (CL316,243) versus the use of a physiological stimulus (cold exposure) [66].

Since PPAR α is seemingly dispensable for cold-induced browning but not for pharmacologically induced browning, it could be hypothesized that during cold a compensatory mechanism is activated which is not triggered via specific β 3-adrenergic receptor activation. The observation that the absence of PPAR α during cold does not impair WAT-browning does not exclude a role for PPAR α in the browning process under normal conditions. It is conceivable that in the absence of PPAR α , the normal function of PPAR α is taken over by for example PPAR γ . Indeed, activation of PPAR γ also results in induction of browning in adipocytes, possibly via accumulation of PRDM16 [68–70]. Combining PPAR α and PPAR γ activation, via the use of the above-mentioned glitazars, has greater capacity to induce *Ucp1* expression in adipose tissue compared to activation of PPAR γ alone [71]. Metabolites and side products of pathways activated by PPAR, such as β -hydroxybutyrate and lactate, are shown to induce browning *in vivo* [72]. Possibly, metabolites that induce browning can be produced independently from PPAR upon cold-exposure and still stimulate the conversion of white to beige adipose tissue. For now, our data lead to the conclusion that PPAR α is dispensable for cold-induced browning, but we cannot completely exclude a role for PPAR α in the normal browning process.

Fasting - repeatedly - as a therapy for metabolic diseases

Many systems in the human body adapt their response to a stimulus. The major system in the body known for its adaptive ability is the adaptive branch of the immune system. Adaptive immunity is mainly conferred by the action of B and T lymphocytes, creating immune memory and long term protection against a pathogen. Recently, innate immune cells were also hypothesized to “remember” previous episodes of inflammatory response, thereby altering their response to a subsequent exposure to an antigen [73–75].

Fasting, mainly in the form of intermittent fasting and time-restricted feeding, is currently highly popular as a therapy to tackle overweight and obesity, and metabolic diseases [76]. During evolution, humans were likely repeatedly exposed to periods of fasting or food deprivation. As a consequence, fasting has been a strong evolutionary pressure shaping human energy metabolism. Borrowing from the immune system, in **chapter 5** we hypothesized a similar type of memory or training for the metabolic response to fasting in the liver. In *Drosophila*, an altered response to starvation following exposure to one or more starvation events has been observed, but there is no scientific evidence for such a memory effect in mammals [77]. Similarly, it is commonly believed that caloric restriction may lead to activation of energy conserving mechanisms but the actual evidence in support of this fasting-induced hypometabolism in humans is very limited [78]. Indeed, studies looking into body weight loss upon repeated fasting periods in different species were not able to draw a consistent conclusion [77].

We experimentally explored a possible memory effect of fasting in the liver by exposing mice to a 16 hour period of fasting for 3 consecutive times and comparing their fasting response to mice that only fasted once. Unfortunately, in our study we were not able to detect any effect of repeated fasting. However, it should be realized that our study protocol of 3 consecutive periods of fasting for 16 hours was designed based on a combination of estimation and ethical considerations. In hindsight, or as a recommendation for future research, we need to consider the differences between a *memory* response and a *training* regime. To go deeper into this difference, I will make the analogy with the adaptations of skeletal muscles to repeated episodes of physical exercise. When a muscle is challenged repeatedly, it undergoes a *training* response. Following an endurance exercise training protocol, the skeletal muscle increases the mitochondrial and capillary density, as well as the oxidative capacity [79,80]. When training is halted, these alterations in the muscle are reversed, which is referred to as a detraining effect [81,82]. However, when training is resumed, there seems to be a residual *memory* in the muscles. The training adaptations seem to go much faster this second time [83–86]. If this difference between *training* and *memory* holds true for the fasting response in the liver, an alternative research design should have been used in the current study. To study the *training* effect, animals should be fasted more often in order to pick up the

effect of this training. While for studying the *memory* effect the study-design should be changed. Possibly, first a period of training is necessary in order to mark the long term memory effect. Alternatively, to arrive at a more robust memory effect, it may be necessary to fast the mice for a longer period of time. Overall, these ideas provide an excellent basis for an exciting, yet risky future research proposal.

Apart from the number of times that the mice were fasted and the duration of each fast to leave a lasting footprint on metabolism, it is possible that we did not measure our outcome at the right moment of the fasting response. We only performed analyses at the end of the 16 hour fasting period and did not do any measurements during this 16 hour period. It is possible that repeated fasting causes mice to become more metabolically flexible, which is not necessarily visible at the endpoint but may be detectable during the 16 hour fast. For future studies, it would be interesting to follow the entire fasting response by measuring real-time ketone body production or the switch of fuel-use over time by the use of fluxomic techniques. Moreover, sacrificing mice at an earlier moment in the fasting response would make it possible to look at changes in the very-early fasting response upon repeated fasting. As a final note, muscle, liver and adipose tissue should be analyzed for possible enhanced storage of energy in the form of glycogen or fat as a training effect of repeated fasting.

On a side note - Mouse as model system for humans?

In this thesis we aimed to look into energy metabolism by using mice as a model for human. To borrow a quote from the English poet Alexander Pope, "*the proper study of mankind is man*" [87]. Even though this quote has a slightly different meaning in the original poem, it draws attention to the importance of translational research, which describes research that transcends from cell culture and animal studies (bench) to patient (bedside). Using model systems to study human metabolism should be done with care. Extensive validation of the model system is of major importance before conclusions for the general public and patients can be drawn. Therefore, in **chapter 6**, we looked into the differences and similarities in the fasting response in adipose tissue between mice and humans. Our major conclusion is that despite many similarities in the transcriptional regulation of fasting in human and mouse adipose tissue, still many genes show distinct responses to fasting between the two species. Especially the genes involved in insulin signaling, PPAR signaling, glycogen metabolism, and lipid droplets seem to respond differently upon fasting. Even though our comparative analysis was performed on adipose tissue and not on liver, we might assume the fasting response in the liver, and specifically the PPAR-pathway, might deviate between humans and mice too. However, analysis of the fasting response in hepatocyte humanized mice revealed large similarities in gene regulation between the human and mouse hepatocytes

[88]. Although hepatocyte humanized mice are not humans, they represent a very valuable *in vivo* model for studying human hepatocytes.

Nevertheless, it should be emphasized that outcomes of studies performed in mice often do not directly translate to humans. The limited translation of research findings from mice to humans is especially problematic for drug development. Indeed, many candidate drugs that show positive effects in mice and other animals are ultimately discontinued. It has been estimated that currently only 1 in 9 drugs entering human trials will eventually succeed [89,90]. The poor translation of mouse data to human patients does not only apply to therapeutic benefits but also holds true for potential side effects. For example, fibrates are hepatocarcinogenic in mice but most likely not in humans [91–93]. This type of property usually causes the drug of interest to be abandoned already at the preclinical level. This difference between mice and humans not only exists because of the obvious fact that mice are not “tiny furry humans”, but also because in animal experiments all parameters are kept as stable and controlled as possible. This gives little to no room for interindividual variation, which is huge in humans. There are some artificial ways to circumvent part of this problem, including the use of genetically outbred mice, but this only tackles part of the issue [94]. In 2017, Garner et al. proposed a new field of study named “Therioepistemology”, which investigates what type of knowledge can be gained from animal research [90]. Therioepistemology starts from the idea that “all models are imperfect: how that imperfection affects inference is what matters” [90]. They nicely describe the very big advantages of animal models, and why we should not discard animal research, but they point out there is a need for a critical view in order to improve the validity, reproducibility and translatability of animal work by asking ourselves a couple of key questions such as “What features of human/model biology are ignored?” and “What features of measures/methodology are ignored”. As an example of a possible “ignored feature of the mouse model” is murine plasma triglyceride metabolism. In mice, apolipoprotein E3 regulation is very distinct from humans, resulting in a more efficient clearance of triglyceride-rich lipoproteins and thus limited triglyceride accumulation in the blood [95]. Using “normal” mice to study drugs targeting triglyceride metabolism without acknowledging this major difference possibly results in the development of irrelevant drugs. In order to take this “ignored feature of the model” into consideration, mice with a humanized lipid profile were developed, for example the apoE*3-Leiden.CETP mouse [96]. A second example, which might be important for the current work, is the use of genetically modified mice silencing or overexpressing certain genes. While developing these systems, the aim is to target only the gene of interest. However, unintentional loss of function of another gene due to for example overlapping open reading frames is important to take into

consideration. Ignoring this risk could result in a phenotype in mice which is absent in humans, since the change in mouse phenotype is not due to the targeted gene [90]. A possibly “ignored feature of measurement”, which also applies for the current work, is in the experimental background. For many years, the same bedding, cage-enrichment and (chow) diet has been used to increase reproducibility. Therioepistemology points us towards the fact that if these variables are blunting the measured outcome, the model system or readout used might not be valid anyhow [90]. Additionally, basal body temperature of mice and humans is both around 37°C. However to maintain this temperature mice require more heat-generating capacity. Where in humans only a very small fraction of total energy expenditure can be attributed to cold-induced thermogenesis, for mice at room temperature this counts up to one-third of their total energy expenditure [97]. Indeed many, but not all [98], studies point towards differences in outcome in mice housed at conventional room temperature compared to mice in thermoneutral living environments [99–104]. For better translatability of the results, mice should thus be housed at thermoneutral housing temperature in order to minimize the contribution of cold-induced thermogenesis on the measured outcome, but for now the optimal temperature is debated [105].

It should be noted that there is no perfect model system to study humans, and to continue with animal studies accepting part of these “ignored features” will be necessary, since there are no alternatives to mimic the complex interplay of organs in the body [106]. By using the field of Therioepistemology while designing a study and again when translating it to the human population, the translatability of the outcomes should increase, making animal studies even more valuable than before.

Looking at the work presented in this thesis, we should not only focus on identifying novel target genes in mice, but we should put effort in translational metabolic research in order to develop functional therapies specifically for humans to tackle the worldwide burden of obesity, diabetes and the metabolic syndrome. This could be done by using the inbred, perfectly controlled mice only as hypothesis generating models, the first step in basic research, and confirming findings in outbred mice and humanized mouse models.

Conclusion

In this thesis we identified *Adtrp* and *Tmed* as novel PPAR target genes in murine liver and adipose tissue. Hepatic overexpression of *Adtrp* had no major impact on the metabolic response to a high fat diet, nor to fasting. In line with the literature showing no effect of deletion of ADTRP on the metabolic phenotype, we propose that ADTRP has a non-metabolic function in the body. Hepatic overexpression of TMED5 did not result in any phenotypical changes either, keeping the function of TMED5 still obscure. We focused on the role of PPAR α during cold-induced browning, showing that browning still occurs when PPAR α is absent. Lastly, we had a deeper look into the physiology of fasting. First, we compared the fasting response in the adipose tissue of mice and humans, showing clear distinctions but also similarities between the two species. Secondly, we proposed that the liver may develop a memory to metabolic stressors. However, we were unable to collect experimental support for this concept. To recapitulate, the identification of novel PPAR α target genes can be used as a strategy to find novel therapeutic candidates for cardiovascular diseases, obesity, and the metabolic syndrome. As a general recommendation for future research, more attention should be directed towards the translational relevance of research findings from mice to humans, keeping in mind that (the regulation of) pathways may be distinct between mice and humans.

References

- [1] Samson, S.L., Garber, A.J., 2014. Metabolic syndrome. *Endocrinology and Metabolism Clinics of North America* 43(1): 1–23, Doi: 10.1016/j.ecl.2013.09.009.
- [2] Saklayen, M.G., 2018. The Global Epidemic of the Metabolic Syndrome. *Current Hypertension Reports* 20(2): 12, Doi: 10.1007/s11906-018-0812-z.
- [3] Nilsson, P.M., Tuomilehto, J., Rydén, L., 2019. The metabolic syndrome - What is it and how should it be managed? *European Journal of Preventive Cardiology* 26(2_suppl): 33–46, Doi: 10.1177/2047487319886404.
- [4] Staels, B., 2007. PPAR agonists and the metabolic syndrome. *Thérapie* 62(4): 319–26, Doi: 10.2515/therapie:2007051.
- [5] Han, L., Shen, W.-J., Bittner, S., Kraemer, F.B., Azhar, S., 2017. PPARs: regulators of metabolism and as therapeutic targets in cardiovascular disease. Part II: PPAR- β/δ and PPAR- γ . *Future Cardiology* 13(3): 279–96, Doi: 10.2217/fca-2017-0019.
- [6] Brown, W. V., 1987. Potential use of fenofibrate and other fibric acid derivatives in the clinic. *The American Journal of Medicine* 83(5B): 85–9, Doi: 10.1016/0002-9343(87)90876-x.
- [7] Rössner, S., Orö, L., 1981. Fenofibrate therapy of hyperlipoproteinaemia. A dose-response study and a comparison with clofibrate. *Atherosclerosis* 38(3–4): 273–82, Doi: 10.1016/0021-9150(81)90043-5.
- [8] Goldenberg, I., Benderly, M., Goldbourt, U., 2008. Update on the use of fibrates: focus on bezafibrate. *Vascular Health and Risk Management* 4(1): 131–141, Doi: 10.2147/vhrm.2008.04.01.131.
- [9] Fruchart, J.-C., Duriez, P., 2006. Mode of action of fibrates in the regulation of triglyceride and HDL-cholesterol metabolism. *Drugs of Today (Barcelona, Spain : 1998)* 42(1): 39–64, Doi: 10.1358/dot.2006.42.1.963528.
- [10] Tenenbaum, A., Fisman, E.Z., 2012. Fibrates are an essential part of modern anti-dyslipidemic arsenal: spotlight on atherogenic dyslipidemia and residual risk reduction. *Cardiovascular Diabetology* 11: 125, Doi: 10.1186/1475-2840-11-125.
- [11] Shipman, K.E., Strange, R.C., Ramachandran, S., 2016. Use of fibrates in the metabolic syndrome: A review. *World Journal of Diabetes* 7(5): 74–88, Doi: 10.4239/wjd.v7.i5.74.
- [12] Tarantino, N., Santoro, F., Correale, M., De Gennaro, L., Romano, S., Di Biase, M., et al., 2018. Fenofibrate and Dyslipidemia: Still a Place in Therapy? *Drugs* 78(13): 1289–96, Doi: 10.1007/s40265-018-0965-8.
- [13] Reginato, M.J., Lazar, M.A., 1999. Mechanisms by which Thiazolidinediones Enhance Insulin Action. *Trends in Endocrinology and Metabolism: TEM* 10(1): 9–13, Doi: 10.1016/s1043-2760(98)00110-6.
- [14] Rigato, M., Avogaro, A., Vigili de Kreutzenberg, S., Fadini, G.P., 2020. Effects of Basal Insulin on Lipid Profile Compared to Other Classes of Antihyperglycemic Agents in Type 2 Diabetic Patients. *The Journal of Clinical Endocrinology and Metabolism* 105(7), Doi: 10.1210/clinem/dgaa178.

- [15] Kendall, D.M., Rubin, C.J., Mohideen, P., Ledezine, J.-M., Belder, R., Gross, J., et al., 2006. Improvement of glycemic control, triglycerides, and HDL cholesterol levels with muraglitazar, a dual (alpha/gamma) peroxisome proliferator-activated receptor activator, in patients with type 2 diabetes inadequately controlled with metformin monotherapy: . *Diabetes Care* 29(5): 1016–23, Doi: 10.2337/diacare.2951016.
- [16] Jain, M.R., Giri, S.R., Trivedi, C., Bhoi, B., Rath, A., Vanage, G., et al., 2015. Saroglitazar, a novel PPAR α / γ agonist with predominant PPAR α activity, shows lipid-lowering and insulin-sensitizing effects in preclinical models. *Pharmacology Research & Perspectives* 3(3): e00136, Doi: 10.1002/prp2.136.
- [17] Lalloyer, F., Staels, B., 2010. Fibrates, glitazones, and peroxisome proliferator-activated receptors. *Arteriosclerosis, Thrombosis, and Vascular Biology* 30(5): 894–9, Doi: 10.1161/ATVBAHA.108.179689.
- [18] Shearer, B.G., Billin, A.N., 2007. The next generation of PPAR drugs: do we have the tools to find them? *Biochimica et Biophysica Acta* 1771(8): 1082–93, Doi: 10.1016/j.bbali.2007.05.005.
- [19] Roberts, W.C., 1989. Safety of fenofibrate--US and worldwide experience. *Cardiology* 76(3): 169–79, Doi: 10.1159/000174488.
- [20] Wierzbicki, A.S., 2010. Fibrates: no ACCORD on their use in the treatment of dyslipidaemia. *Current Opinion in Lipidology* 21(4): 352–8, Doi: 10.1097/MOL.0b013e32833c1e74.
- [21] Shah, P., Mudaliar, S., 2010. Pioglitazone: side effect and safety profile. *Expert Opinion on Drug Safety* 9(2): 347–54, Doi: 10.1517/14740331003623218.
- [22] Fiévet, C., Fruchart, J.-C., Staels, B., 2006. PPAR α and PPAR γ dual agonists for the treatment of type 2 diabetes and the metabolic syndrome. *Current Opinion in Pharmacology* 6(6): 606–14, Doi: 10.1016/j.coph.2006.06.009.
- [23] Ruscica, M., Zimetti, F., Adorni, M.P., Sirtori, C.R., Lupo, M.G., Ferri, N., 2020. Pharmacological aspects of ANGPTL3 and ANGPTL4 inhibitors: New therapeutic approaches for the treatment of atherogenic dyslipidemia. *Pharmacological Research* 153: 104653, Doi: 10.1016/j.phrs.2020.104653.
- [24] Geng, L., Lam, K.S.L., Xu, A., 2020. The therapeutic potential of FGF21 in metabolic diseases: from bench to clinic. *Nature Reviews. Endocrinology* 16(11): 654–67, Doi: 10.1038/s41574-020-0386-0.
- [25] Sonoda, J., Chen, M.Z., Baruch, A., 2017. FGF21-receptor agonists: an emerging therapeutic class for obesity-related diseases. *Hormone Molecular Biology and Clinical Investigation* 30(2), Doi: 10.1515/hmbci-2017-0002.
- [26] Kersten, S., Mandard, S., Tan, N.S., Escher, P., Metzger, D., Chambon, P., et al., 2000. Characterization of the fasting-induced adipose factor FIAF, a novel peroxisome proliferator-activated receptor target gene. *The Journal of Biological Chemistry* 275(37): 28488–93, Doi: 10.1074/jbc.M004029200.
- [27] Mattijssen, F., Georgiadi, A., Andasarie, T., Szalowska, E., Zota, A., Krones-Herzig, A., et al., 2014. Hypoxia-inducible Lipid Droplet-associated (HILPDA) is a novel Peroxisome Proliferator-activated Receptor (PPAR) target involved in hepatic triglyceride secretion. *Journal of Biological Chemistry* 289(28): 19279–93, Doi: 10.1074/jbc.M114.570044.

- [28] Zandbergen, F., Mandard, S., Escher, P., Tan, N.S., Patsouris, D., Jatkoje, T., et al., 2005. The G0/G1 switch gene 2 is a novel PPAR target gene. *The Biochemical Journal* 392(Pt 2): 313–24, Doi: 10.1042/BJ20050636.
- [29] Bougarne, N., Weyers, B., Desmet, S.J., Deckers, J., Ray, D.W., Staels, B., et al., 2018. Molecular Actions of PPAR α in Lipid Metabolism and Inflammation. *Endocrine Reviews* 39(5): 760–802, Doi: 10.1210/er.2018-00064.
- [30] Chen, Y., Wang, Y., Huang, Y., Zeng, H., Hu, B., Guan, L., et al., 2017. PPAR α regulates tumor cell proliferation and senescence via a novel target gene carnitine palmitoyltransferase 1C. *Carcinogenesis* 38(4): 474–83, Doi: 10.1093/carcin/bgx023.
- [31] Lupu, C., Patel, M.M., Lupu, F., 2021. Insights into the Functional Role of ADTRP (Androgen-Dependent TFPI-Regulating Protein) in Health and Disease. *International Journal of Molecular Sciences* 22(9), Doi: 10.3390/ijms22094451.
- [32] Eriksi Ertunc, M., Kok, B.P., Parsons, W.H., Wang, J.G., Tan, D., Donaldson, C.J., et al., 2020. AIG1 and ADTRP are endogenous hydrolases of fatty acid esters of hydroxy fatty acids (FAHFAs) in mice. *The Journal of Biological Chemistry* 295(18): 5891–905, Doi: 10.1074/jbc.RA119.012145.
- [33] Parsons, W.H., Kolar, M.J., Kamat, S.S., III, A.B.C., Hulce, J.J., Saez, E., et al., 2016. AIG1 and ADTRP are atypical integral membrane hydrolases that degrade bioactive FAHFAs. *Nature Chemical Biology* (March): 1–8, Doi: 10.1038/nchembio.2051.
- [34] Kolar, M.J., Kamat, S.S., Parsons, W.H., Homan, E.A., Maher, T., Peroni, O.D., et al., 2016. Branched Fatty Acid Esters of Hydroxy Fatty Acids Are Preferred Substrates of the MODY8 Protein Carboxyl Ester Lipase. *Biochemistry* 55(33): 4636–41, Doi: 10.1021/acs.biochem.6b00565.
- [35] Parsons, W.H., Kolar, M.J., Kamat, S.S., Cognetta, A.B. 3rd., Hulce, J.J., Saez, E., et al., 2016. AIG1 and ADTRP are atypical integral membrane hydrolases that degrade bioactive FAHFAs. *Nature Chemical Biology* 12(5): 367–72, Doi: 10.1038/nchembio.2051.
- [36] Patel, M.M., Behar, A.R., Silasi, R., Regmi, G., Sansam, C.L., Keshari, R.S., et al., 2018. Role of ADTRP (Androgen-Dependent Tissue Factor Pathway Inhibitor Regulating Protein) in Vascular Development and Function. *Journal of the American Heart Association* 7(22): e010690, Doi: 10.1161/JAHA.118.010690.
- [37] Lockyer, P., Schisler, J.C., Patterson, C., Willis, M.S., 2010. Minireview: Won't get fooled again: the nonmetabolic roles of peroxisome proliferator-activated receptors (PPARs) in the heart. *Molecular Endocrinology* (Baltimore, Md.) 24(6): 1111–9, Doi: 10.1210/me.2009-0374.
- [38] Plutzky, J., 2011. The PPAR-RXR transcriptional complex in the vasculature: energy in the balance. *Circulation Research* 108(8): 1002–16, Doi: 10.1161/CIRCRESAHA.110.226860.
- [39] Yore, M.M., Syed, I., Moraes-Vieira, P.M., Zhang, T., Herman, M.A., Homan, E.A., et al., 2014. Discovery of a class of endogenous mammalian lipids with anti-diabetic and anti-inflammatory effects. *Cell* 159(2): 318–32, Doi: 10.1016/j.cell.2014.09.035.
- [40] Kuda, O., Brezinova, M., Rombaldova, M., Slavikova, B., Posta, M., Beier, P., et al., 2016. Docosahexaenoic Acid-Derived Fatty Acid Esters of Hydroxy Fatty Acids (FAHFAs) With Anti-inflammatory Properties. *Diabetes* 65(9): 2580–90, Doi: 10.2337/db16-0385.
- [41] Kuda, O., 2017. Bioactive metabolites of docosahexaenoic acid. *Biochimie* 136: 12–20, Doi: 10.1016/j.biochi.2017.01.002.

- [42] Zhang, T., Chen, S., Syed, I., Ståhlman, M., Kolar, M.J., Homan, E.A., et al., 2016. A LC-MS-based workflow for measurement of branched fatty acid esters of hydroxy fatty acids. *Nature Protocols* 11(4): 747–63, Doi: 10.1038/nprot.2016.040.
- [43] Syed, I., Lee, J., Moraes-Vieira, P.M., Donaldson, C.J., Sontheimer, A., Aryal, P., et al., 2018. Palmitic Acid Hydroxystearic Acids Activate GPR40, Which Is Involved in Their Beneficial Effects on Glucose Homeostasis. *Cell Metabolism* 27(2): 419-427.e4, Doi: <https://doi.org/10.1016/j.cmet.2018.01.001>.
- [44] Vijayakumar, A., Aryal, P., Wen, J., Syed, I., Vazirani, R.P., Moraes-Vieira, P.M., et al., 2017. Absence of Carbohydrate Response Element Binding Protein in Adipocytes Causes Systemic Insulin Resistance and Impairs Glucose Transport. *Cell Reports* 21(4): 1021–35, Doi: <https://doi.org/10.1016/j.celrep.2017.09.091>.
- [45] Paschoal, V.A., Walenta, E., Talukdar, S., Pessentheiner, A.R., Osborn, O., Hah, N., et al., 2020. Positive Reinforcing Mechanisms between GPR120 and PPAR γ Modulate Insulin Sensitivity. *Cell Metabolism* 31(6): 1173-1188.e5, Doi: <https://doi.org/10.1016/j.cmet.2020.04.020>.
- [46] Lee, J., Moraes-Vieira, P.M., Castoldi, A., Aryal, P., Yee, E.U., Vickers, C., et al., 2016. Branched Fatty Acid Esters of Hydroxy Fatty Acids (FAHFAs) Protect against Colitis by Regulating Gut Innate and Adaptive Immune Responses. *The Journal of Biological Chemistry* 291(42): 22207–17, Doi: 10.1074/jbc.M115.703835.
- [47] Syed, I., Rubin de Celis, M.F., Mohan, J.F., Moraes-Vieira, P.M., Vijayakumar, A., Nelson, A.T., et al., 2019. PAHSAs attenuate immune responses and promote β cell survival in autoimmune diabetic mice. *The Journal of Clinical Investigation* 129(9): 3717–31, Doi: 10.1172/JCI122445.
- [48] Brezinova, M., Cajka, T., Oseeva, M., Stepan, M., Dadova, K., Rossmeislova, L., et al., 2020. Exercise training induces insulin-sensitizing PAHSAs in adipose tissue of elderly women. *Biochimica et Biophysica Acta. Molecular and Cell Biology of Lipids* 1865(2): 158576, Doi: 10.1016/j.bbali.2019.158576.
- [49] Syed, I., Lee, J., Peroni, O.D., Yore, M.M., Moraes-Vieira, P.M., Santoro, A., et al., 2018. Methodological issues in studying PAHSA biology: masking PAHSA effects. *Cell Metabolism* 28(4): 543–6.
- [50] Pflimlin, E., Bielohuby, M., Korn, M., Breitschopf, K., Löhn, M., Wohlfart, P., et al., 2018. Acute and Repeated Treatment with 5-PAHSA or 9-PAHSA Isomers Does Not Improve Glucose Control in Mice. *Cell Metabolism* 28(2): 217-227.e13, Doi: <https://doi.org/10.1016/j.cmet.2018.05.028>.
- [51] Kuda, O., 2018. On the Complexity of PAHSA Research. *Cell Metabolism* 28(4): 541–2, Doi: <https://doi.org/10.1016/j.cmet.2018.09.006>.
- [52] López-Bascón, M.A., Calderón-Santiago, M., Priego-Capote, F., 2016. Confirmatory and quantitative analysis of fatty acid esters of hydroxy fatty acids in serum by solid phase extraction coupled to liquid chromatography tandem mass spectrometry. *Analytica Chimica Acta* 943: 82–8, Doi: 10.1016/j.aca.2016.09.014.
- [53] Kolar, M.J., Nelson, A.T., Chang, T., Ertunc, M.E., Christy, M.P., Ohlsson, L., et al., 2018. Faster Protocol for Endogenous Fatty Acid Esters of Hydroxy Fatty Acid (FAHFA) Measurements. *Analytical Chemistry* 90(8): 5358–65, Doi: 10.1021/acs.analchem.8b00503.

- [54] Brezinova, M., Kuda, O., Hansikova, J., Rombaldova, M., Balas, L., Bardova, K., et al., 2018. Levels of palmitic acid ester of hydroxystearic acid (PAHSA) are reduced in the breast milk of obese mothers. *Biochimica et Biophysica Acta (BBA) - Molecular and Cell Biology of Lipids* 1863(2): 126–31, Doi: <https://doi.org/10.1016/j.bbalip.2017.11.004>.
- [55] Benlebna, M., Balas, L., Bonafos, B., Pessemesse, L., Vigor, C., Grober, J., et al., 2020. Long-term high intake of 9-PAHPA or 9-OAHPA increases basal metabolism and insulin sensitivity but disrupts liver homeostasis in healthy mice. *The Journal of Nutritional Biochemistry* 79: 108361, Doi: [10.1016/j.jnutbio.2020.108361](https://doi.org/10.1016/j.jnutbio.2020.108361).
- [56] Chen, K.Y., Brychta, R.J., Linderman, J.D., Smith, S., Courville, A., Dieckmann, W., et al., 2013. Brown fat activation mediates cold-induced thermogenesis in adult humans in response to a mild decrease in ambient temperature. *The Journal of Clinical Endocrinology and Metabolism* 98(7): E1218-23, Doi: [10.1210/jc.2012-4213](https://doi.org/10.1210/jc.2012-4213).
- [57] van Marken Lichtenbelt, W.D., Vanhomerig, J.W., Smulders, N.M., Drossaerts, J.M.A.F.L., Kemerink, G.J., Bouvy, N.D., et al., 2009. Cold-activated brown adipose tissue in healthy men. *The New England Journal of Medicine* 360(15): 1500–8, Doi: [10.1056/NEJMoa0808718](https://doi.org/10.1056/NEJMoa0808718).
- [58] Fernández-Verdejo, R., Marlatt, K.L., Ravussin, E., Galgani, J.E., 2019. Contribution of brown adipose tissue to human energy metabolism. *Molecular Aspects of Medicine* 68: 82–9, Doi: [10.1016/j.mam.2019.07.003](https://doi.org/10.1016/j.mam.2019.07.003).
- [59] Remie, C.M.E., Moonen, M.P.B., Roumans, K.H.M., Nascimento, E.B.M., Gemmink, A., Havekes, B., et al., 2021. Metabolic responses to mild cold acclimation in type 2 diabetes patients. *Nature Communications* 12(1): 1516, Doi: [10.1038/s41467-021-21813-0](https://doi.org/10.1038/s41467-021-21813-0).
- [60] Araki, M., Nakagawa, Y., Oishi, A., Han, S.-I., Wang, Y., Kumagai, K., et al., 2018. The Peroxisome Proliferator-Activated Receptor α (PPAR α) Agonist Pemaifibrate Protects against Diet-Induced Obesity in Mice. *International Journal of Molecular Sciences* 19(7), Doi: [10.3390/ijms19072148](https://doi.org/10.3390/ijms19072148).
- [61] Bargut, T.C.L., Aguila, M.B., Mandarim-de-Lacerda, C.A., 2016. Brown adipose tissue: Updates in cellular and molecular biology. *Tissue & Cell* 48(5): 452–60, Doi: [10.1016/j.tice.2016.08.001](https://doi.org/10.1016/j.tice.2016.08.001).
- [62] Rachid, T.L., Penna-de-Carvalho, A., Bringhamti, I., Aguila, M.B., Mandarim-de-Lacerda, C.A., Souza-Mello, V., 2015. Fenofibrate (PPAR α agonist) induces beige cell formation in subcutaneous white adipose tissue from diet-induced male obese mice. *Molecular and Cellular Endocrinology* 402: 86–94, Doi: [10.1016/j.mce.2014.12.027](https://doi.org/10.1016/j.mce.2014.12.027).
- [63] Rachid, T.L., Penna-de-Carvalho, A., Bringhamti, I., Aguila, M.B., Mandarim-de-Lacerda, C.A., Souza-Mello, V., 2015. PPAR- α agonist elicits metabolically active brown adipocytes and weight loss in diet-induced obese mice. *Cell Biochemistry and Function* 33(4): 249–56, Doi: [10.1002/cbf.3111](https://doi.org/10.1002/cbf.3111).
- [64] Rachid, T.L., Silva-Veiga, F.M., Graus-Nunes, F., Bringhamti, I., Mandarim-de-Lacerda, C.A., Souza-Mello, V., 2018. Differential actions of PPAR- α and PPAR- β/δ on beige adipocyte formation: A study in the subcutaneous white adipose tissue of obese male mice. *PloS One* 13(1): e0191365, Doi: [10.1371/journal.pone.0191365](https://doi.org/10.1371/journal.pone.0191365).
- [65] Marucci, A., Mangiacotti, D., Trischitta, V., Di Paola, R., 2015. GALNT2 mRNA levels are associated with serum triglycerides in humans. *Endocrine*: 8–11, Doi: [10.1007/s12020-015-0705-8](https://doi.org/10.1007/s12020-015-0705-8).

- [66] Li, P., Zhu, Z., Lu, Y., Granneman, J.G., 2005. Metabolic and cellular plasticity in white adipose tissue II: role of peroxisome proliferator-activated receptor- α . *American Journal of Physiology. Endocrinology and Metabolism* 289(4): E617–26, Doi: 10.1152/ajpendo.00010.2005.
- [67] Barquissau, V., Beuzelin, D., Pisani, D.F., Beranger, G.E., Mairal, A., Montagner, A., et al., 2016. White-to-brite conversion in human adipocytes promotes metabolic reprogramming towards fatty acid anabolic and catabolic pathways. *Molecular Metabolism* 5(5): 352–65, Doi: 10.1016/j.molmet.2016.03.002.
- [68] Klusóczyki, Á., Veréb, Z., Vámos, A., Fischer-Posovszky, P., Wabitsch, M., Bacso, Z., et al., 2019. Differentiating SGBS adipocytes respond to PPAR γ stimulation, irisin and BMP7 by functional browning and beige characteristics. *Scientific Reports* 9(1): 5823, Doi: 10.1038/s41598-019-42256-0.
- [69] Jeremic, N., Chatuverdi, P., Tyagi, S.C., 2016. Browning of White Fat: Novel Insight into Factors, Mechanisms and Therapeutics. *Journal of Cellular Physiology* (June): 1–8, Doi: 10.1002/jcp.25450.
- [70] Koppen, A., Kalkhoven, E., 2010. Brown vs white adipocytes: the PPAR γ coregulator story. *FEBS Letters* 584(15): 3250–9, Doi: 10.1016/j.febslet.2010.06.035.
- [71] Kroon, T., Harms, M., Maurer, S., Bonnet, L., Alexandersson, I., Lindblom, A., et al., 2020. PPAR γ and PPAR α synergize to induce robust browning of white fat in vivo. *Molecular Metabolism* 36: 100964, Doi: 10.1016/j.molmet.2020.02.007.
- [72] Carrière, A., Jeanson, Y., Berger-Müller, S., André, M., Chenouard, V., Arnaud, E., et al., 2014. Browning of white adipose cells by intermediate metabolites: an adaptive mechanism to alleviate redox pressure. *Diabetes* 63(10): 3253–65, Doi: 10.2337/db13-1885.
- [73] Netea, M.G., Quintin, J., Van Der Meer, J.W.M., 2011. Trained immunity: A memory for innate host defense. *Cell Host and Microbe* 9(5): 355–61, Doi: 10.1016/j.chom.2011.04.006.
- [74] Netea, M.G., 2013. Training innate immunity: The changing concept of immunological memory in innate host defence. *European Journal of Clinical Investigation* 43(8): 881–4, Doi: 10.1111/eci.12132.
- [75] Saeed, S., Quintin, J., Kerstens, H.H.D., Rao, N.A., Aghajani-refah, A., Matarese, F., et al., 2014. Epigenetic programming of monocyte-to-macrophage differentiation and trained innate immunity. *Science* 345(6204), Doi: 10.1126/science.1251086.
- [76] Longo, V.D., Mattson, M.P., 2014. Fasting: molecular mechanisms and clinical applications. *Cell Metabolism* 19(2): 181–92, Doi: 10.1016/j.cmet.2013.12.008.
- [77] McCue, M.D., Terblanche, J.S., Benoit, J.B., 2017. Learning to starve: impacts of food limitation beyond the stress period. *The Journal of Experimental Biology* 220(23): 4330–8, Doi: 10.1242/jeb.157867.
- [78] Penicaud, L., Le Magnen, J., 1980. Recovery of body weight following starvation or food restriction in rats. *Neuroscience and Biobehavioral Reviews* 4 Suppl 1: 47–52, Doi: 10.1016/0149-7634(80)90048-2.
- [79] Pearson, A.M., 1990. Muscle growth and exercise. *Critical Reviews in Food Science and Nutrition* 29(3): 167–96, Doi: 10.1080/10408399009527522.
- [80] Booth, F.W., Ruegsegger, G.N., Toedebusch, R.G., Yan, Z., 2015. Endurance Exercise and the Regulation of Skeletal Muscle Metabolism. *Progress in Molecular Biology and Translational Science* 135: 129–51, Doi: 10.1016/bs.pmbts.2015.07.016.

- [81] Mujika, I., Padilla, S., 2000. Detraining: loss of training-induced physiological and performance adaptations. Part I: short term insufficient training stimulus. *Sports Medicine (Auckland, N.Z.)* 30(2): 79–87, Doi: 10.2165/00007256-200030020-00002.
- [82] Mujika, I., Padilla, S., 2000. Detraining: Loss of Training-Induced Physiological and Performance Adaptations. Part II. *Sports Medicine* 30(3): 145–54, Doi: 10.2165/00007256-200030030-00001.
- [83] Psilander, N., Eftestøl, E., Cumming, K.T., Juvkam, I., Ekblom, M.M., Sunding, K., et al., 2019. Effects of training, detraining, and retraining on strength, hypertrophy, and myonuclear number in human skeletal muscle. *Journal of Applied Physiology (Bethesda, Md. : 1985)* 126(6): 1636–45, Doi: 10.1152/jappphysiol.00917.2018.
- [84] Bruusgaard, J.C., Johansen, I.B., Egner, I.M., Rana, Z.A., Gundersen, K., 2010. Myonuclei acquired by overload exercise precede hypertrophy and are not lost on detraining. *Proceedings of the National Academy of Sciences of the United States of America* 107(34): 15111–6, Doi: 10.1073/pnas.0913935107.
- [85] Egner, I.M., Bruusgaard, J.C., Eftestøl, E., Gundersen, K., 2013. A cellular memory mechanism aids overload hypertrophy in muscle long after an episodic exposure to anabolic steroids. *The Journal of Physiology* 591(24): 6221–30, Doi: 10.1113/jphysiol.2013.264457.
- [86] Lee, H., Kim, K., Kim, B., Shin, J., Rajan, S., Wu, J., et al., 2018. A cellular mechanism of muscle memory facilitates mitochondrial remodelling following resistance training. *Journal of Physiology* 596(18): 4413–26, Doi: 10.1113/JP275308.
- [87] Beyrer, C., 2015. The proper study of mankind. *The Lancet* 386(10005): 1724–5, Doi: 10.1016/S0140-6736(15)61217-X.
- [88] de la Rosa Rodriguez, M.A., Sugahara, G., Hooiveld, G.J.E.J., Ishida, Y., Tateno, C., Kersten, S., 2018. The whole transcriptome effects of the PPAR α agonist fenofibrate on livers of hepatocyte humanized mice. *BMC Genomics* 19(1): 443, Doi: 10.1186/s12864-018-4834-3.
- [89] Perel, P., Roberts, I., Sena, E., Wheble, P., Briscoe, C., Sandercock, P., et al., 2007. Comparison of treatment effects between animal experiments and clinical trials: systematic review. *BMJ* 334(7586): 197, Doi: 10.1136/bmj.39048.407928.BE.
- [90] Garner, J.P., Gaskill, B.N., Weber, E.M., Ahloy-Dallaire, J., Pritchett-Corning, K.R., 2017. Introducing Therioepistemology: the study of how knowledge is gained from animal research. *Lab Animal* 46(4): 103–13, Doi: 10.1038/labani.1224.
- [91] Bonovas, S., Nikolopoulos, G.K., Bagos, P.G., 2012. Use of fibrates and cancer risk: a systematic review and meta-analysis of 17 long-term randomized placebo-controlled trials. *PloS One* 7(9): e45259, Doi: 10.1371/journal.pone.0045259.
- [92] Corton, J.C., Peters, J.M., Klaunig, J.E., 2018. The PPAR α -dependent rodent liver tumor response is not relevant to humans: addressing misconceptions. *Archives of Toxicology* 92(1): 83–119, Doi: 10.1007/s00204-017-2094-7.
- [93] Peters, J.M., Cheung, C., Gonzalez, F.J., 2005. Peroxisome proliferator-activated receptor-alpha and liver cancer: where do we stand? *Journal of Molecular Medicine (Berlin, Germany)* 83(10): 774–85, Doi: 10.1007/s00109-005-0678-9.
- [94] Rosshart, S.P., Herz, J., Vassallo, B.G., Hunter, A., Wall, M.K., Badger, J.H., et al., 2019. Laboratory mice born to wild mice have natural microbiota and model human immune responses. *Science (New York, N.Y.)* 365(6452), Doi: 10.1126/science.aaw4361.

- [95] van Vlijmen, B.J., van 't Hof, H.B., Mol, M.J., van der Boom, H., van der Zee, A., Frants, R.R., et al., 1996. Modulation of very low density lipoprotein production and clearance contributes to age- and gender- dependent hyperlipoproteinemia in apolipoprotein E3-Leiden transgenic mice. *The Journal of Clinical Investigation* 97(5): 1184–92, Doi: 10.1172/JCI118532.
- [96] Hofker, M.H., van Vlijmen, B.J., Havekes, L.M., 1998. Transgenic mouse models to study the role of APOE in hyperlipidemia and atherosclerosis. *Atherosclerosis* 137(1): 1–11, Doi: 10.1016/s0021-9150(97)00266-9.
- [97] Reitman, M.L., 2018. Of mice and men - environmental temperature, body temperature, and treatment of obesity. *FEBS Letters* 592(12): 2098–107, Doi: 10.1002/1873-3468.13070.
- [98] Small, L., Gong, H., Yassmin, C., Cooney, G.J., Brandon, A.E., 2018. Thermoneutral housing does not influence fat mass or glucose homeostasis in C57BL/6 mice. *The Journal of Endocrinology* 239(3): 313–24, Doi: 10.1530/JOE-18-0279.
- [99] Rabearivony, A., Li, H., Zhang, S., Chen, S., An, X., Liu, C., 2020. Housing temperature affects the circadian rhythm of hepatic metabolism and clock genes. *The Journal of Endocrinology* 247(2): 183–95, Doi: 10.1530/JOE-20-0100.
- [100] Stemmer, K., Kotzbeck, P., Zani, F., Bauer, M., Neff, C., Müller, T.D., et al., 2015. Thermoneutral housing is a critical factor for immune function and diet-induced obesity in C57BL/6 nude mice. *International Journal of Obesity (2005)* 39(5): 791–7, Doi: 10.1038/ijo.2014.187.
- [101] Tian, X.Y., Ganeshan, K., Hong, C., Nguyen, K.D., Qiu, Y., Kim, J., et al., 2016. Thermoneutral Housing Accelerates Metabolic Inflammation to Potentiate Atherosclerosis but Not Insulin Resistance. *Cell Metabolism* 23(1): 165–78, Doi: 10.1016/j.cmet.2015.10.003.
- [102] Clayton, Z.S., McCurdy, C.E., 2018. Short-term thermoneutral housing alters glucose metabolism and markers of adipose tissue browning in response to a high-fat diet in lean mice. *American Journal of Physiology. Regulatory, Integrative and Comparative Physiology* 315(4): R627–37, Doi: 10.1152/ajpregu.00364.2017.
- [103] McKie, G.L., Medak, K.D., Knuth, C.M., Shamshoum, H., Townsend, L.K., Peppler, W.T., et al., 2019. Housing temperature affects the acute and chronic metabolic adaptations to exercise in mice. *The Journal of Physiology* 597(17): 4581–600, Doi: 10.1113/JP278221.
- [104] Giles, D.A., Moreno-Fernandez, M.E., Stankiewicz, T.E., Graspeuntner, S., Cappelletti, M., Wu, D., et al., 2017. Thermoneutral housing exacerbates nonalcoholic fatty liver disease in mice and allows for sex-independent disease modeling. *Nature Medicine* 23(7): 829–38, Doi: 10.1038/nm.4346.
- [105] Keijer, J., Li, M., Speakman, J.R., 2019. What is the best housing temperature to translate mouse experiments to humans? *Molecular Metabolism* 25: 168–76, Doi: 10.1016/j.molmet.2019.04.001.
- [106] Genzel, L., Adan, R., Berns, A., van den Beucken, J.J.J.P., Blokland, A., Boddeke, E.H.W.G.M., et al., 2020. How the COVID-19 pandemic highlights the necessity of animal research. *Current Biology* 30(18): R1014–8, Doi: <https://doi.org/10.1016/j.cub.2020.08.030>.

Summary

Over the past decades, an immense pandemic of obesity has been developing across the world, in part due to an overabundance of food that is available 24/7. While in ancient history a major need existed to store spare energy for times when food was scarce, the energy-conserving and -storing mechanisms that humans evolved with can now be considered counterproductive, as they interfere with the maintenance of a healthy homeostatic state. Chronic overfeeding results in the well-known diseases of affluence such as obesity, non-alcoholic fatty liver disease, and type 2 diabetes mellitus. These conditions are rooted in disturbances in energy metabolism related to chronic overconsumption of foods.

Energy metabolism is carefully regulated at multiple levels via the coordinated action of thousands of genes and proteins. An important group of transcription factors involved in the regulation of many pathways involved in energy metabolism are the peroxisome proliferator-activated receptors (PPARs). These nuclear receptors play a pivotal role in different aspects of glucose and lipid metabolism and inflammation. Three PPAR isoforms have been identified: PPAR α (*Nrc1*), PPAR γ (*Nrc3*) and PPAR δ (*Nrc2*). Due to their marked impact on metabolism, different therapeutic strategies towards cardiovascular diseases and diabetes mellitus type 2 targeting PPAR have been developed.

PPARs are involved in many metabolic pathways via their capacity to activate transcription of a large number of target genes. In order to get a better understanding of the regulation of lipid metabolism, in the first part of this thesis we aimed to look at novel putative target genes of PPAR. By using “regulation via PPAR” as a screening tool to identify novel genes involved in lipid and glucose metabolism, we identified Androgen Dependent TFPI Regulating Protein (ADTRP) (**chapter 2**) and Transmembrane P24 Trafficking Protein 5 (TMED5) (**chapter 3**) as genes of high interest. ADTRP encodes a serine hydrolase enzyme that was reported to catalyse the hydrolysis of fatty acid esters of hydroxy fatty acids (FAHFAs). FAHFAs have recently been identified as a potential insulin-sensitizing class of lipids. Based on the current literature and the data presented in this thesis, we could not support a major role for ADTRP in glucose or lipid metabolism in the liver since neither hepatic overexpression nor deficiency of ADTRP resulted in a clear metabolic phenotype in the liver. Additionally, upon overexpression of ADTRP, no changes in FAHFA concentrations were found in liver or plasma, questioning the role of ADTRP in FAHFA hydrolysis in the liver. For TMED5, we could not detect alterations in metabolic phenotype following overexpression of *Tmed5* in mice fed a high fat diet or subjected to fasting. Taken together, in this thesis we clearly show that ADTRP and TMED5 are targets of PPAR. However, based on the current data, we were not able to support a major role of hepatic ADTRP or TMED5 in glucose or lipid metabolism.

In the second part of this thesis, we had a deeper look into different stressors of metabolism. First in **chapter 4**, we studied the role of PPAR α during cold-induced

browning. Exposing male mice for 10 days to 5 degrees compared to a thermoneutral environment resulted in increased food intake and a decrease in adipose tissue weight independent of PPAR α . Browning, as shown by histology and by elevated expression of typical thermogenic genes such as *Ucp1*, *Elovl3* and *Cidea*, occurred to a similar extent in both genotypes. Genes and pathways involved in energy metabolism were activated to the same extent upon cold-exposure in both groups. With this work, we showed that PPAR α is dispensable for cold-induced browning, contrary to the literature showing a diminished thermogenic response in PPAR α ^{-/-} mice upon β 3-adrenergic receptor activation.

Another important stressor of metabolism is fasting. During fasting, stored energy becomes available in order for the organism to survive. Two major organs involved in the response to fasting are the liver and the adipose tissue. In the adipose tissue, which is the principal energy depot, fasting activates intracellular lipolysis, thereby releasing free fatty acids and glycerol into the circulation. Simultaneously, fasting represses extracellular lipolysis, leading to reduced uptake and storage of circulating triglycerides. Although the general response to fasting in different mammals is very similar, we carefully studied the transcriptional response to fasting in human adipose tissue and compared these data to the fasting response of mouse adipose tissue in **chapter 5**. A large number of metabolic pathways were commonly downregulated in mouse and human adipose tissue upon fasting, including triglyceride and fatty acid synthesis, glycolysis and glycogen synthesis, TCA cycle, oxidative phosphorylation, mitochondrial translation, and insulin signaling, even though the magnitude of the effect was much smaller in humans compared to mice. However, we also showed that many genes have a very distinct response to fasting in humans as compared to mice. These differentially regulated genes include genes involved in insulin signaling, PPAR signaling, glycogen metabolism, and lipid droplets. With this data we provide a useful resource for the study of the response to fasting in human adipose tissue and at the same time raise awareness for the need for caution when extrapolating findings from mice to humans.

The hepatic fasting response, which is mainly driven by PPAR α , has been studied extensively over the past decades. In line with the relatively novel idea of innate immune memory, where macrophages are believed to have an altered response to a previously encountered inflammatory compound such as LPS, we looked into a possible memory effect of fasting in the liver in **chapter 6**. However, our data do not provide evidence in favor of a lasting footprint of fasting on liver gene expression in mice. We found that previous exposure to fasting did not influence the metabolic phenotype of mice and did not influence the liver transcriptome and metabolome. Since we were the first to study the effect of an episode of fasting on the hepatic levels of numerous polar metabolites, including amino acids, other organic acids, and nucleotides, we do provide a useful resource for the study of liver metabolism during fasting.

In conclusion, with this thesis we aimed to find novel genes or pathways involved in the regulation of lipid and glucose metabolism, with the premise that these genes and pathways may be suitable candidates for therapeutic targeting. Our studies provide important new insights into the regulation of metabolism in liver and adipose tissue in response to cold, fasting, and PPAR α activation.

Acknowledgements/Dankwoord



En zo blijkt maar weer dat cliché's vaak kloppen, van de laatste loodjes zijn het zwaarst tot "it always seems impossible until it is done". Maar nu is het dan echt zover, de laatste woorden van mijn proefschrift. Misschien wel de belangrijkste, toch als je zou tellen in aantal keren gelezen ;)

Allereerst wil ik graag mijn promotor **Prof. Sander Kersten** bedanken. Sander, heel erg bedankt voor de mooie kans die ik heb gekregen om na mijn master thesis mijn PhD traject te kunnen beginnen in ons lab. Ik bewonder heel erg je gedrevenheid en kennis maar ook je optimisme en perfectionisme (zowel inhoudelijk als taaltechnisch ;)). Ik ben erg blij dat ik zoveel over onderzoek van je heb mogen leren de voorbije jaren en hoop de komende jaren ook van je onderwijs-skills een graantje te kunnen meepikken. Bedankt voor de fijne samenwerking.

Daarnaast wil mijn commissie leden, **Renger Witkamp, Ko Willems van Dijk, Erik Kalkhoven** en **Joris Hoeks** bedanken voor het lezen en beoordelen van mijn thesis, en voor hun aanwezigheid tijdens mijn verdediging.

Daarna is het de beurt aan mijn paranimfen, en hoewel een paranimf een symbolische titel is, zou er zonder hun aanwezigheid, steun en peptalks hier waarschijnlijk geen thesis liggen. Lieve **Charlotte**, ik durf het bijna niet op te schrijven, maar 7 jaar geleden begon ons avontuur in het kantoortje in de valk! Onze vriendschap begon met veel (luid krakende) wortels, thee en tijd verspillen aan beslissen welke bagels we zouden eten. De voorbije jaren was je er voor mij, op goede en slechte momenten. Dankjewel dat ik alles met je kon delen, en als het even tegen zat je met je enthousiasme mij sowieso weer aan het lachen kreeg! Ik had dit niet zonder je gekund en vind het echt een hele eer dat je vandaag naast mij staat. Ik kijk er naar uit om nog een beetje langer collega's te zijn! **Benthe**, nadat ik enkele weken geleden jou mocht bijstaan tijdens je verdediging, ben ik heel blij dat je dit nu ook voor mij doet! Eventjes 's morgens een koffie drinken om op te starten bleek de ideale manier om een dag op het lab te beginnen. Ik wil je heel erg bedanken voor je altijd-blijvende steun, het luisterend oor als het even tegen zat en de vele hulp tijdens muizen-secties! We hebben bewezen dat we een top-team zijn en er, indien nodig, een mooie carrière als team-uitjes planner in onze toekomst ligt! Hoewel we ons beter niet meer wagen aan samen buffers maken ;).

Ook wil ik **Sophie** bedanken! Je bent nu al een tijdje weg, maar ik denk nog heel vaak aan jouw goede raad. Je zorgde ervoor dat ik mij heel erg welkom voelde op mijn nieuwe plekje op kantoor. Af en toe even bij je mogen zeuren over begeleiders, schrijven en onderwijs maakte dat ik er daarna weer met frisse moed tegenaan ging. Nu lijkt het alsof we heel vaak zeurden, maar eigenlijk is het je eerlijkheid over hoe het soms niet loopt zoals je denkt en je enthousiaste persoonlijkheid die er zeker voor hebben gezorgd dat ik kon doorzetten als het minder ging en er nu uiteindelijk dit boekje ligt! Hopelijk komen we elkaar nog vaak tegen, want je bent echt een

hele fijne vriendin! **Xanthe**, wat was het fijn dat jij net voor mij klaar was en ik bij je terecht kon met al mijn afrondvragen! Maar uiteraard is dat verre van het enige waar ik je voor moet bedanken. Toen ik net begon en jij je MSc thesis afrondde was ik heel erg onder de indruk van je kennis, en dat is altijd zo gebleven! Maar ik heb je tijdens de jaren als collega vooral een hele lieve, behulpzame meid leren kennen die keihard kon werken als het nodig was, maar ook perfect aanvoelde als ik haar even nodig had en daar dan alles voor liet wijken. Bedankt voor de voorbije jaren, de gezellige praatjes op het lab, de peritoneale macrofagen die helaas nog steeds in de vriezer zitten (:) en de leuke feestjes tijdens de ADDRm. Je was een top-reisgenoot voor congressen! :D **Mara**, ook jij hoort in het rijtje van degene in de laatste fase van je PhD. Je positiviteit en nuchtere kijk op ons werk en de wetenschap hebben mij heel vaak geholpen om een situatie anders te kunnen bekijken. Het was altijd erg leuk om richting mijn kantoor te stappen en even snel bij jou binnen te springen om het te hebben over katten, nagels lakken, jouw spannende vakanties die mij altijd deden wegdromen of gewoon een beetje sparren over wetenschap. Bedankt voor de voorbije jaren, ik ben erg blij dat jij er ook nog eventjes bij bent!

Mijn gezellige corner-office heeft zeker ook bijgedragen aan dit eindresultaat! **Lisa**, bedankt voor de fijne gesprekken op de leuke kussentjes in de vensterbank! Ook al had jij echt het koudste hoekje, het was er altijd erg gezellig! **Mieke**, het is niet de eerste en zeker niet de laatste keer dat je deze titel krijgt, maar bedankt voor je rol als lab-mama! Naast goede raad over experimenten en onderzoek, stond je ook altijd klaar met koffie/thee en een luisterend oor voor alle andere problemen! Ik vind het erg fijn om nu ook op onderwijsvlak met je samen te werken! **Montse**, I cannot thank you enough! You have kept me sane with your super-chill vision on (work-) life sooo many times! Without you, a lot more tears would have been shed! Thank you for your advice, your positive mindset and your never-ending smile! I am happy to have had you around my entire PhD! It was fun working with you on the Tmed5-Adtrp-SLC project! **Tessa**, bedankt voor de gezellige gesprekjes. Over de beste woon-locatie van Wageningen, over tomatoes en potatoes, over zingen in een koortje,... Het was erg fijn om met jou op kantoor te zitten. **Wout**, bedankt voor je bemoedigende woorden. Jij wist altijd precies het goede te zeggen op het goede moment. En natuurlijk ook heel erg bedankt om onze persoonlijke spoed-dierenarts te zijn! **Ilse**, hoewel we niet vaak tegelijk op kantoor zaten, wil ik je zeker ook bedanken voor de fijne samenwerking. Ik had mij mij geen betere concurrent kunnen indenken ;) Veel succes in Nijmegen en hopelijk komen we elkaar nog tegen! **Fleur**, je bent er nog maar net, maar ik wil je heel erg veel succes wensen met je PhD. Je gaat het super doen!

Anouk, ik bewonder al van in het begin je doorzettingsvermogen en positiviteit! Ook al gaat het even niet zoals gepland, jij zet je schouders er onder en gaat er weer voor! Heel veel succes de komende jaren, ik ben zeker dat je het fantastisch gaat afronden! **Miranda**, ook jij bent bezig met die zware laatste loodjes! Het was

altijd erg fijn jouw kampeer verhalen te horen. Deed mij altijd dromen van zelf een weekendje weg te zijn! Succes met afronden, het komt helemaal goed! **Brecht**, je bent een erg gezellige en hardwerkende aanwinst voor de groep! Ik ben zeker dat je het erg goed gaat doen de komende jaren! **Danny**, thank you for sharing your culture with me, for being a really funny and sweet teammate and for opening your door to Meggie – the cat – when she was intruding in your apartment! You are almost at the end as well, I am sure you will do a very good job! Good luck! **Mingjuan, Monique and Kirsten**, you only recently joined the lab. I am sure you will do a great job, good luck!

Af en toe voelt een afdeling een beetje als een duivenkot. Elke 4 jaar vliegen er nieuwe AIOs in, die dan onder de vleugels van de “oude” AIOs wegwijs worden gemaakt. Dus ook al zijn jullie al een tijdje weg, ik moet jullie zeker ook heel hard bedanken! **Inge**, nadat je een heel fijn begeleider voor mijn master thesis was, werd je een nog veel fijner kantoorgenootje. Kletsen over (en foto’s delen van) onze lieve Beer en Megatron was een erg fijn tijdverdrijf! Ook toen we niet meer samen op kantoor zaten liep ik graag even binnen om te delen hoe het er mee ging en het over van-alles-en-nog-wat te hebben. Ik vind het erg fijn dat we contact zijn blijven houden! **Wieneke**, ik kan me heel goed voorstellen dat je af en toe gek werd van mijn vragen, maar dankzij jou heb ik het eerste jaar overleefd! Bedankt om de tijd te nemen om mij alles te laten zien en uit te leggen, mij wegwijs te maken in het CKP en mijn eerste muizenproeven met mij te doen. Ook heel erg bedankt om mij de iv-injecties te leren! Ik vond het erg jammer dat je weg ging, maar probeer nu ook mijn kennis aan de “nieuwe generatie” over te dragen, zoals jij ook bij mij hebt gedaan :) **Aafke**, wat is het steeds fantastisch om jouw oude labjournal open te slaan en perfect terug te vinden wat ik nodig heb. Naast dat je een erg goede wetenschapper bent, ben ik ook heel erg onder de indruk van je organisatorische skills! Gezellig dat we af en toe nog kunnen lunchen op de campus en ik je nog kan bestoken met labvragen! Dankjewel! **Lily**, hoewel ik in het begin vooral heel erg onder de indruk was van jou, heb ik je mettertijd leren kennen als een heel lief en betrokken persoon. Hoewel ik af en toe toch nog steeds twijfelde of je grapjes echt wel grapjes waren, haha! Heel erg bedankt voor de fijne tijd op het lab! Of course, I should not forget my ENERGISE-labmates. Antwi and Philip. **Antwi**, I could always come to you to think about PPAR-targets and if I needed primers you would have them on your secret list, haha! Thanks a lot for your scientific advice and nice talks! I wish you all the best. **Philip**, thank you for being a nice colleague. We started on the same project but we took it in a completely different direction! Thanks for the fun meetings and for sharing your passion for science! Good luck in your future career. I hope to visit the Ruppert-lab some day!

Naast mijn mede-AIOs, zijn er nog een hele groep mensen die ik zeker ook moet bedanken voor hun hulp tijdens de voorbije 6 jaar. **Rinke**, bedankt voor je kritische blik tijdens de maandag-meetings. Je wist vaak precies de vinger op de zere plek

te leggen :) , maar je kwam dan ook met een voorstel om mijn onderzoek toch weer een stapje verder te krijgen. **Guido**, heel erg bedankt voor je veeeeele vragen tijdens de donderdagmeetingen. Ik vond het vooral heel erg fijn dat je achteraf altijd nog even kwam napraten en mij op de kleine details wees die ik anders kon aanpakken. **Wilma**, jij ook heel erg bedankt voor je kritische blik, maar vooral voor je tips en advies in verband met onderwijs! Ik hoop nog veel van je te kunnen opsteken. **Lydia**, tijdens mijn master thesis bij jou begon het te kriebelen om verder te gaan in de wetenschap. Heel erg bedankt voor je begeleiding toen en de fijne gesprekken en betrokkenheid in de afgelopen jaren. **Bryan**, you only recently joined the group, but I look forward to working together. Always nice to have “nen echten Belg” around! Also all the other colleagues “of the second floor”: **Renger, Klaske, Jocelij, Frank, Xiaolin, Rieneke, Ian, Dieuwertje, Michiel, Shauna, Mark, Paulien, Judith, Iris, Suzanne, Nhien, Marlies, Susanne, Pieter** en **Marco**, ook jullie zijn heel erg bedankt voor de gesprekken over wetenschap, maar ook over koetjes en kalfjes aan de koffiemachine!

The next group of people I would like to thank were of major, if not vital, importance! Without the technicians, there would have been no lab and thus no experiments presented in this thesis! So a very big thanks in general to Mieke, Mechteld, **Jenny, Karin, Nhien**, Shohreh, Marlies, **Susanne** and **Pieter** for keeping our lab up and running. **Mechteld**, jou moet ik toch zeker nog even extra bedanken om mij als masterstudent wegwijs te maken op het lab: mijn eerste verdunningsreeksjes met mij te maken en mij de kneepjes van het qPCR'en te leren! Ook bedankt voor de fijne gesprekken tijdens de lunch en het vak in Januari! Also a special thanks to **Shohreh**, for saving my histology samples, making the perfect pictures and for crisis management from time to time! Always fun to walk into your office for a nice chat and a “healthy” snack!

Ook had dit boekje er niet gelegen zonder Wilma, Rene en Bert van het CKP. **Wilma**, bedankt voor je vele hulp bij de secties, je flexibiliteit als het weer anders moest, en de fijne kat-gesprekken! **Rene**, bedankt voor de hulp bij de staartinjecties. De tip van het eerst met de witte muizen te proberen heeft er voor gezorgd dat ik niet vroegtijdig heb opgegeven, haha! En last but not least **Bert**, het is mij gelukt om mijn PhD door te komen zonder gebeten te worden (victory!). Heel erg bedankt om mij te komen redden als er weer een muisje uit de weegschaal was gesprongen en achter een tafelpoot zat verstopt, de hulp bij het wegen als ik weer het programma liet vastlopen en de gezellige gesprekjes tijdens de secties!

Bijna aan het einde gekomen wil ik graag nog iedereen binnen het ENERGISE project bedanken. De gezellige meetings, de fijne samenwerkingen die tijdens het lekkere eten werden besproken en de leuke workshops hebben mijn PhD tijd zeker gezelliger gemaakt. Specifiek moet ik zeker **Carlijn** nog vermelden. Bedankt voor de fijne tijd samen tijdens de master. Onze wekelijkse etentjes samen hebben naar het buitenland verhuizen een stuk minder eenzaam gemaakt! Ik ben erg blij dat je

vanuit Maastricht op hetzelfde project bent beginnen werken. Het was erg fijn om meerdere keren per jaar weer bij te kunnen kletsen tijdens de ENERGISE-meetings, de NUGO week in Newcastle, de ADDRDM meetings in Oosterbeek en vooral samen de Papendal cursus door te komen! ;)

Natuurlijk moet ik ook mijn familie bedanken voor hun eeuwig-blijvende steun. **Lore**, heel dikke merci voor al de moeite die je hebt gedaan voor mijn cover. Ik vind hem echt fantastisch mooi geworden! **Mama** en **papa**, zonder dat jullie mij niet 1 maar 2 keer naar de open-master day hadden gebracht was mijn avontuur in Wageningen zelfs nooit gestart! Ik wil jullie super hard bedanken voor alle kansen, niet alleen op opleidingsvlak maar op alle vlakken, die ik van jullie gekregen heb. Jullie liefde en steun hebben er voor gezorgd dat ik hier vandaag sta. De hulp bij het zoeken en verhuizen naar de verschillende koten/appartement/huis hier in Wageningen, het luisterend oor als ik moest uitzagen over wat er niet goed liep op het lab (ook al was het echt Chinees af en toe) en recenter de vele weekenden waarop jullie Tristan en mij kwamen ophalen zodat ik mijn thesis kon afwerken terwijl jullie oppastten. Dankjulliewel voor alles! Ook mijn schoonfamilie: dank jullie wel voor jullie interesse en de pogingen om mijn artikels te lezen :)

Natuurlijk moet ik mijn gezinnetje bedanken ♥. Lieve **Tristan**, hoewel de eerste weken en maanden met een kleine baby niet altijd gemakkelijk zijn, en de vermoeidheid af en toe eerder een stoorzender was bij het afwerken van mijn thesis, zorgde jij met je schattige lach en je blijde "Aaah"-geluidjes dat ik de stress en druk van het afmaken even helemaal vergat. **Ingmar**, mijn lieve Ingmar. Zonder dat jij het aandurfde om mij te volgen naar het "hol van Pluto"-Wageningen was er natuurlijk helemaal niets van mijn PhD in huis gekomen. Bedankt dat je het aandurfde om hier opnieuw te beginnen en samen ons leven op te bouwen. Jij was er om de grote dingen met mij te vieren (met een bosje bloemen:), de tegenslagen snel achter mij te laten (met een bosje bloemen en een reep chocolade :), en de momenten dat ik het echt niet meer zag zitten mij af te leiden, op te vrolijken en te doen geloven dat er morgen weer een dag kwam om het op te lossen (met een bosje bloemen, een reep chocolade en SUSHI!). Dankjewel dat je mijn steun en toeverlaat was de voorbije jaren. Ik kijk heel erg uit naar onze toekomst hier in Wageningen, of waar dan ook in de wereld, want zolang wij elkaar hebben kunnen wij als topteam de wereld aan! We gaan een mooie toekomst tegemoet samen met Tristan en de kleine Minitron, en ik kan niet wachten om aan het volgende hoofdstuk van ons leven samen te beginnen.



About the author

Curriculum vitae

Merel Defour was born on January 21th, 1993 in Jette, Belgium. In 2010 she started the bachelor program Nutrition and Dietetics at the KHLeuven, Belgium. After successfully completing her Bachelor's degree (*cum laude*) in 2013, Merel continued her academic career by joining the Master program in Nutrition and Health, specialising in Molecular Nutrition and Toxicology at Wageningen University. During her Master thesis, she collaborated with hospital Rijnstate in Arnhem to investigate gene expression changes upon the onset of paediatric obesity and diabetes mellitus type 2. After completion of her Master thesis, she moved back to Belgium to perform her internship at the Gene Expression Group of the department of Cellular and Molecular Medicine at the KU Leuven. During this internship, she looked into the role of zinc in the storage of insulin and its role in the development of diabetes mellitus type 2 by using zinc transporter knock out mice. This internship let her gain experience in molecular research and laboratory animal work. After obtaining her Master's degree, Merel was eager to start her academic career in the field of molecular nutrition research and decided to return to Wageningen to join the group of prof. Sander Kersten as a PhD candidate. She started her PhD project in September 2015 within the "ENERGISE" consortium funded by the Netherlands Cardiovascular Research Committee. During this project she focussed on different players of lipid metabolism and their link to metabolic health. Apart from doing research, Merel was strongly involved in teaching and supervised numerous MSc students during their thesis, which she very much enjoyed. In 2018 she got the opportunity to work as a teacher, next to her PhD trajectory. In October 2021 Merel will finish her PhD, after which she will continue her work as a teacher at the Division of Human Nutrition and Health at the Wageningen University.

List of publications

Defour M, Dijk W, Ruppert P, Nascimento EBM, Schrauwen P, Kersten S. The Peroxisome Proliferator-Activated Receptor α is dispensable for cold-induced adipose tissue browning in mice. *Mol Metab.* 2018 Apr;10:39-54. doi: 10.1016/j.molmet.2018.01.023.

Defour M, Michielsen CCJR, O'Donovan SD, Afman LA, Kersten S. Transcriptomic signature of fasting in human adipose tissue. *Physiol Genomics.* 2020 Oct 1;52(10):451-467. doi: 10.1152/physiolgenomics.00083.2020.

Defour M, Hooiveld GJEJ, van Weeghel M, Kersten S. Probing metabolic memory in the hepatic response to fasting. *Physiol Genomics.* 2020 Dec 1;52(12):602-617. doi: 10.1152/physiolgenomics.00117.2020.

Defour M, van Weeghel M, Hermans J, Kersten S. Hepatic ADTRP overexpression does not influence lipid and glucose metabolism. *Am J Physiol Cell Physiol.* 2021 Jul 21. doi: 10.1152/ajpcell.00185.2021. Epub ahead of print. PMID: 34288722.

Overview of completed training activities

Discipline specific activities

Discipline specific courses

Papendal course - Atherosclerosis and Thrombosis	DHF	Arnhem (NL)	2016
Papendal course – Vascular Biology	DHF	Arnhem (NL)	2017
NUGO course – Temperature and Metabolism	NUGO	Newcastle upon Tyne (UK)	2018
Big Data Analysis in the Life Sciences	VLAG	Wageningen (NL)	2019

Conferences and symposia

Dutch Diabetes Meeting	NVDO	Oosterbeek (NL)	2015
Dutch Diabetes Meeting	NVDO	Oosterbeek (NL)	2016
Alpro – the moment for plant based eating is now	Alpro Foundation	Brussel (BE)	2017
Dutch Diabetes Meeting (oral presentation)	NVDO	Oosterbeek (NL)	2017
Lipid meeting (poster presentation)	Leipzig University	Leipzig (DE)	2017
Dutch Diabetes Meeting	NVDO	Oosterbeek (NL)	2018
NuGO week	NuGO	Newcastle upon Tyne (UK)	2018

General courses

Interpersonal communication skills for PhD students	WGS	Wageningen (NL)	2015
VLAG PhD week	VLAG	Soest (NL)	2016
PhD carousel	WGS	Wageningen (NL)	2016
Applied Statistics	VLAG	Wageningen (NL)	2016
Project and Time Management (PTM)	WGS	Wageningen (NL)	2017
Scientific writing	WGS	Wageningen (NL)	2017
Orientation on teaching	ESD	Wageningen (NL)	2017
Teaching lab practicals	ESD	Wageningen (NL)	2018
Reviewing a scientific paper	WGS	Wageningen (NL)	2018
Carreer orientation	WGS	Wageningen (NL)	2019
Supervising BSc & MSc thesis students	ESD	Wageningen (NL)	2019

Optional activities

- Preparation of research proposal
- PhD tour to the United Kingdom
- Weekly scientific meetings / journal clubs
- Management board ENERGISE
- Young talent board ENERGISE
- CVON meetings

The research described in this thesis was supported by a grant of the Dutch Heart Foundation (CVON2014-02 ENERGISE).

Financial support of the Dutch Heart Foundation and Wageningen University for the publication of this thesis is gratefully acknowledged.

Cover design: Lore Defour

Lay-out: ProefschriftMaken | [Proefschriftmaken.nl](https://proefschriftmaken.nl)

Printed by: Digiforce | [Proefschriftmaken.nl](https://proefschriftmaken.nl)

